· U C · FCTUC FACULDADE DE CIÊNCIAS E TECNOLOGIA UNIVERSIDADE DE COIMBRA

MASTER THESIS IN CHEMICAL ENGINEERING

Thermochemical conversion of lignocellulosic biomass into biofuels with Aspen Plus simulation

Author:
Ângelo Dinis Simões Nunes

Supervisors:
António Alberto Torres Garcia Portugal
Lino de Oliveira Santos

A thesis submitted in fulfilment of the requirements for the degree of Master of Science

in the

Department of Chemical Engineering

September, 2015

"The existing scientific concepts cover always only a very limited part of reality, and the other part that has not yet been understood is infinite."

Werner Heisenberg

Resumo

Nos últimos anos, a escassez de recursos fósseis tornou-se uma realidade importante. Aliada aos efeitos ambientais negativos que advêm com a exploração destes recursos, são necessárias alternativas. Nos últimos anos, houve um foco, liderado em grande parte pela Europa em encontrar alternativas aos combustíveis fósseis que sejam verdadeiramente viáveis, especialmente no sector dos transportes. O mercado dos transportes está a crescer rapidamente, muito devido à China e outros países emergentes, o que significa que a procura ligada aos combustíveis para transportes só irá aumentar. De modo a satisfazer esta procura, alternativas ao petróleo são necessárias e os biocombustíveis surgem como um importante recurso. No entanto, ainda existem muitos problemas associados ao processamento das matérias-primas, nomeadamente a biomass, em combustíveis que possam ser usados. Há também o benefício da valorização dos recursos endógenos ao nível económico, social e ambiental.

Esta tese pretende descrever a pirólise de cinco tipos de madeira, que podem ser encontradas dentro de Portugal continental. Dois esquemas reaccionais foram testados para todas as amostras e modificações foram feitas de forma a melhor coincidir com resultados experimentais, tal levou ao estudo de um cenário optimizado. Os esquemas retirados da literatura foram usados sem modificações em simulações em Aspen Plus, e apresentaram grandes desvios em relação aos resultados experimentais, com desvios de rendimentos de açúcares e água acima de 15% em erro absoluto. Com as modificações introduzidas, a maior parte dos componentes simulados apresentaram um erro inferior a 2%, com a excepção do char, água e gás, com desvios na ordem dos 3-4%. Tendo a unidade uma capacidade de processamento de 90 ton/dia de biomass, o calor necessário para a pirólise está entre 1.6-1.8MW dependendo do tipo de biomassa, e para todos os casos há excesso de calor (entre 1.75-3MW). Uma análise de sensibilidade permitiu inferir que os esquemas reaccionais usados estão limitados tanto em termos de temperatura como tempo de residência.

Abstract

In recent years, the scarcity of fossil fuels became an important reality. Allied with the negative environment consequences that come with exploration of these resources, alternatives are needed. In the last years, there has been a focus, driven mostly by Europe into finding truly viable alternatives to fossil fuels, specially in the transportation sector. Rapidly growing transportation markets in China and other developing countries means the demand for transportation fuel will only increase. In order to provide for the ever growing demand the alternative for oil is needed and the importance of biofuels is unquestionable. However there are many problems associated with processing of the feed materials, namely biomass, into usable fuels. Also, there are benefits in the valorization of endogenous resources, at the economical, social and environmental level.

The present thesis aims at properly describing pyrolysis of five selected wood samples, that can typically be found within Portugal's continental borders. Two reaction schemes will be tested for all the samples, and some modifications to better match experimental data, leading to an optimized scenario will also be studied. The schemes retrieved from the literature, used as is in an Aspen Plus simulation environment, present high deviation to experimental data, with water and sugar deviations above 15% in absolute error. When the modification are introduced, most of the components present an absolute error below 2%, with the exception of char, water and gas, which still show deviations in the 3-4% range. With a biomass processing capacity of 90 tons/day, the pyrolysis duty is around 1.6-1.8MW depending on the feedstock, and in all cases there is a heat surplus (between 1.75-3MW). Sensibility analysis shows that the used reaction schemes are limited both in temperature that can be used and residence time.

Acknowledgements

I would like to thank my supervisor, Dr. *António Portugal* for firstly captivating my interest in the subject, throughout the Energy and Biofuels classes lectured and thereafter, and secondly, in allowing me to purse this topic as my thesis, which allies two of my favourite subjects in chemical engineering: energy and numerical simulation.

I would like to thank my other supervisor, Dr. *Lino Santos*, for his promptness in solving any student's simulation problems, even if not at all related to the subject he teaches, and also for providing me with the LaTeXtemplate to put this thesis together.

To Mr. *Rui Moreira* for his help and tremendous expertise in anything Aspen Plus related, as well as lectures regarding thermochemical processes, where I could get a more deep insight of pyrolysis as well as gasification.

I want to thank the Department of Chemical Engineering for all these five years where I've felt home and to everyone that I've come across and helped me along the way, being it my fellow students, professors or employees.

I would like to acknowledge all my friends, to the ones I've met in Coimbra for sharing this wonderful experience that is the university life with me, and also helping me with my studies; the ones from Ansião, by always being there since I can remember, I'm sure there are no true friendship like yours anywhere else.

And last but not least, to my family: my parents for the motivation given, support and strength to carry on, specially in the hardest moments, and to my brother, for his support throughout my academic life and promotion in the virtues of being a chemical engineer. Without you I couldn't have done this.

Contents

List of Figures

List of Tables

Chapter 1

Introduction

Energy has proven to be a commodity absolutely essential to society and will continue to be so in the future to come. Energy consumption within a certain country has been historically tied to economic growth and well-being of the population, although more recent indexes and classifications go for a more comprehensive approach. This is a consequence of new sustainable standards that try to separate between consumption and actual economic and well-being growth. Developed countries should give the example that this is indeed a possibility and not just philosophy, and although there has been a declining trend in energy intensity for most of these countries, that has fallen short of what needs to be accomplished in order to accommodate for the emerging economies (note the U.S.A. case, where about 5% of the world's population is responsible for 20% of the world's primary energy consumption). Tying up these two parameters (see table 1.1) - energy consumption and population - reveals the social aspect of energy, or the lack thereof, meaning that the U.S. is a clear outlier (Canada's contribution is comparatively small) when it comes to energy consumption per capita, and also that the vast fossil fuel reserves have clearly shaped the Middle Eastern countries consumption profiles, in which are located all top oil and gas producers (with the exception of Russia, which explains the Eurasia share). Europe's energy share is considerable - 15,8% of the world's consumption -, although the per capita ratio is low. This might be related to the fierce environmental policy that the European Union (EU) is pursuing.

Table 1.1: 2011 world's population, energy consumption and their respective ratio (data from [1]).

Region	Population (%)	Energy (%)	Energy/Population
North America	5.0	21.3	4.29
Central & South America	8.5	6.9	0.80
Europe	8.8	15.8	1.80
Eurasia	4.2	8.6	2.07
Middle East	3.1	5.9	1.90
Africa	15.1	3.2	0.21
Asia & Oceania	55.3	38.3	0.69
Total/Mean	100.0	100.0	1.7

To get a more clear idea of the energy scenario worldwide, more data needs to be analysed, such as the energy intensity (energy consumed per GDP), although that's not the scope of this introduction, and so the following references can be consulted [2][3][4].

1.1 The transportation sector fuel problem

The use of liquid fuels is important since it is more convenient to use; are much more cheaper to store and have a higher energy content, compared to gaseous fuels. Besides, all transportation fuelling system is adapted to use liquid fuels. So it is expected that liquid fuels will still be most important type of fuel for transportation. With the increasing demand from emerging economies such as China, fossil fuel depletion is inevitable, and that's especially true for oil, where almost all of the liquid fuel originates, and will continue to be so in the future, as can be seen in figure 1.1. So in order to mitigate this fact, there are two measures one can follow, reduce in oil and fuel consumption and so the remaining reserves can last for a longer period of time, or alternatives need to be found - although these alternatives need to have a non fossil origin, otherwise the problem is not solved, just postponed.

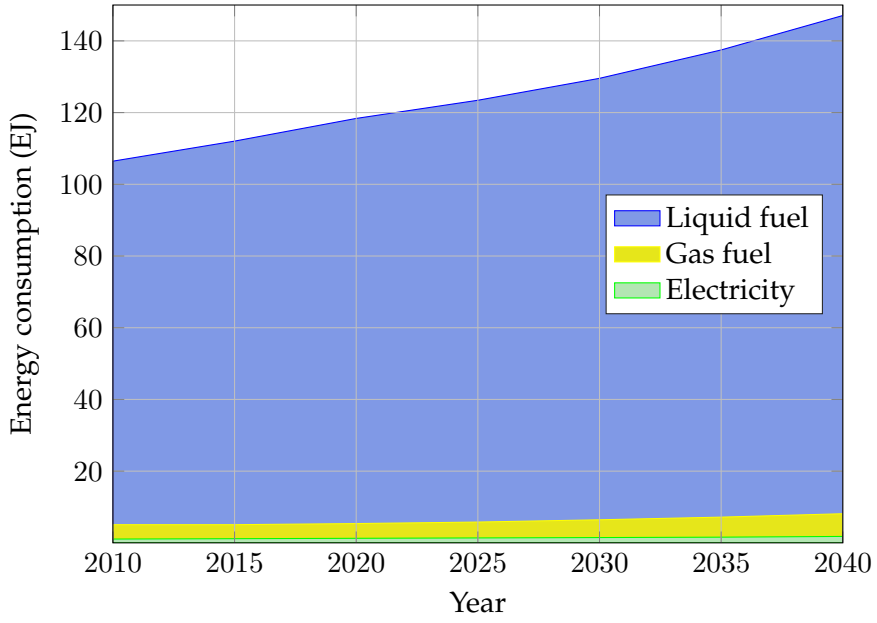

Figure 1.1: World energy consumption for transportation sector projections up to 2040 by fuel type used [5].

It is in the transportation sector where the transition to a competitive alternative, being it a renewable source of energy, or at least carbon neutral, or even a fossil fuel synthetic fuel (either from gas or coal), is proving to be quite hard to archive, both from a technological, as well as an economic point of view. No viable alternative energy sources have been found, one of the reasons being that the energy returned on energy invested (EROEI), or energy return on investment (EROI), which corresponds to a ratio between the amount of useful energy acquired from a particular source and the amount of energy expended to obtain said energy resource, is more favourable to fossil fuels than for renewable energy sources, these being used mainly for electric power. The units are normally the same so that a dimensionless value can be obtained and therefore making several energy production technologies easier to compare. Due to this fact, the EROI has become a parameter that is used without much though about what it really represents and the considerations that have been made to determine it. While the concept is simple in itself, quantify the amount of energy invested for certain sources can be a complicated and tedious task, and this is specially true

for biofuels, since water, fertilizers, agricultural machines (which consume fuel by themselves) are needed. This isn't the case for fossil fuels, where the operations involved are mostly related to extraction, since the energy used to create said resources was provided by nature during millions of years. Also, the EROI doesn't take into account the actual quality of the energy provided, and by quality, one means the form of energy at the point of use - electric energy, ethanol, gasoline, etc - and that has consequences, since for example, is possible to fuel a car with the three sources said before, but the way of accomplishing mechanical movement for each one is different. So by definition, there's an unbalance, since fossil fuels have already a vast amount of concentrated energy, due to the massive time scale required for their formation that is simply not available for any type of renewable energy sources. Plus, some authors argue that environment impacts must also be accounted for when determining the EROI of an energy source, since, again using biofuels as an example, soil erosion, or loss of biodiversity due to land exploration requires energy to revert or more energy to explore the land there after, although that seems more of an argument of those sympathetic with the oil and gas industry, with the sole goal of halting the development of any type of alternative fuels, because the negative impacts of fossil fuels, specially in the environment, are bigger, better understood and global. If buffering is considered for renewables (storage needed for excess energy produced and taking into account eventual over-capacities), then the EROI is even lower for this sources. A more comprehensive debate about these matters can be found in Murphy [6] and Weißbach [7], which is otherwise beyond the scope of this work.

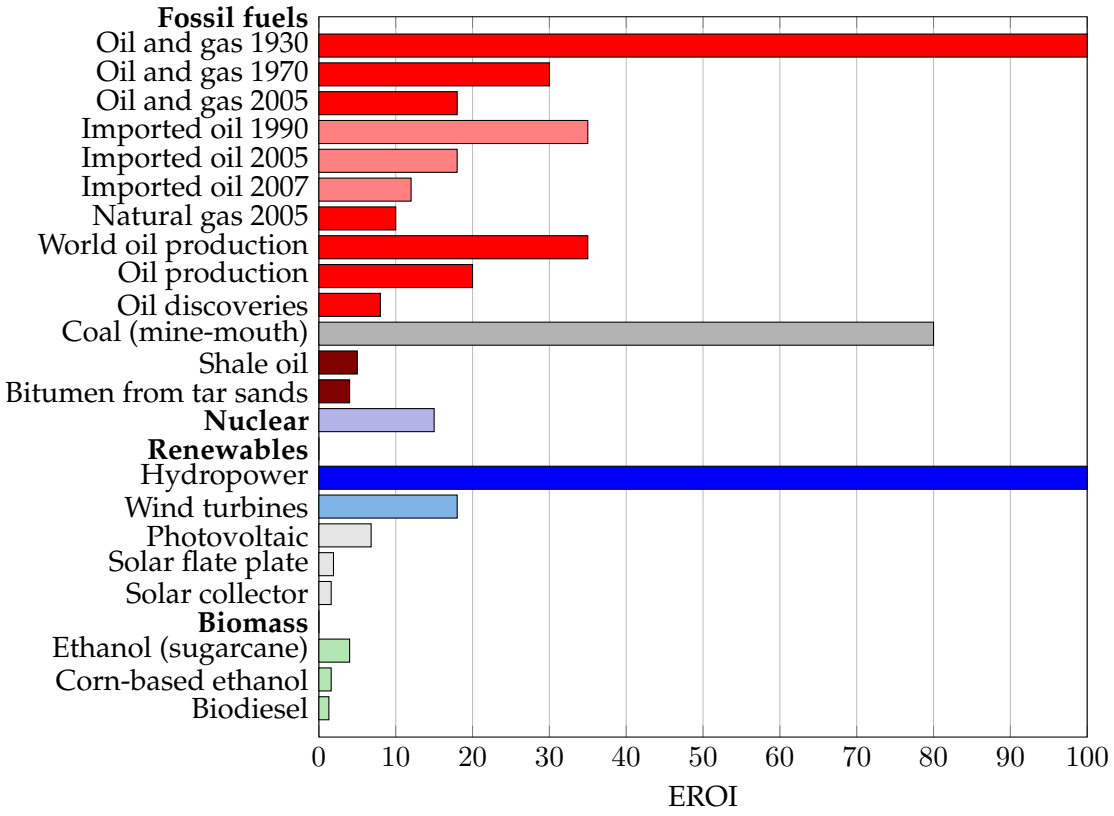

Figure 1.2: Energy Return On Investment (EROIs) for several energy sources [6].

This poses a challenge, as from a strictly capital investment point of view, it's cheaper and

less risky to use fossil fuels with current technologies than to invest in unproven concepts for renewables, category in which most biofuel projects fall into (it goes the same way for nuclear, although this is technically not a renewable energy source). That said, this has led to a dominance of the fossil fuels over the energy market since the first Industrial Revolution up to the present day (Henry Ford's famous Model T could run on ethanol, gasoline or kerosene, as well as mixtures of these components, although with the advent of cheap oil and U.S. Prohibition, the use of ethanol as fuel became unattractive).

1.2 Environmental aspects

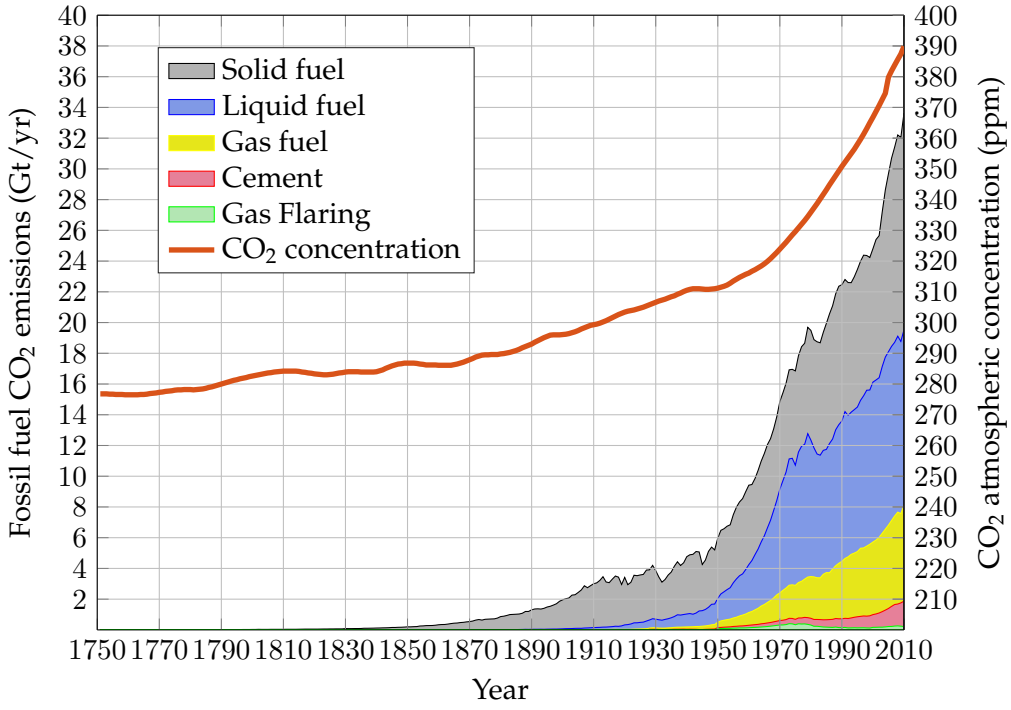

Figure 1.3: Global CO_2 atmospheric concentration and fossil fuel emissions accounted per source [8][9].

Emerging economies such as China are increasing their share in energy consumption, and will continue to do so in the near future. That alone raises concerns in several areas, although in this thesis, only the environment aspect will be given some reflection. It is known that China has large coal reserves, granting energetic self-sufficiency for the foreseeable future. And although that's a political and strategical advantage in their favour, one cannot simply ignore the negative impacts related to coal combustion, as well as other fossil fuels. The main problem with this type of resources is greenhouse gas (GHG) emissions, specially CO_2.

The effects of this type of emissions have been subject to debate even since questions started being raised regarding whether the causes for the extreme climate conditions registered for the last decades have anthropogenic origin or not. Employing statistical methods, the Intergovernmental Panel on Climate Change (IPCC) has made substantial efforts to correlate GHG emissions and global warming, and they have come to the conclusion that "it is extremely likely that more than

half of the observed increase in global average surface temperature from 1951 to 2010 was caused by the anthropogenic increase in GHG concentrations and other anthropogenic forcings together" (extremely likely meaning a > 95% probability of that being true) [4]. With that said, the fact is that the sea level is indeed rising, the mean combined ocean and land temperature is increasing and the CO_2 air concentration has increased more than 40% since 1850. Apart from the global warming effects themselves, one must be aware that high CO_2 concentrations have negative impacts on human health and well being. While the limits for CO_2 exposure tolerable by the human body are quite high (5000 ppm TWA and 30000 ppm STEL, TWA standing for Time Weighted Average and STEL for Short Term Exposure Limit), carbon dioxide is an oxygen displacer, also called asphyxiant gas, meaning that it can decrease O_2 concentration to a value lower than the breathable limit, causing asphyxiation.

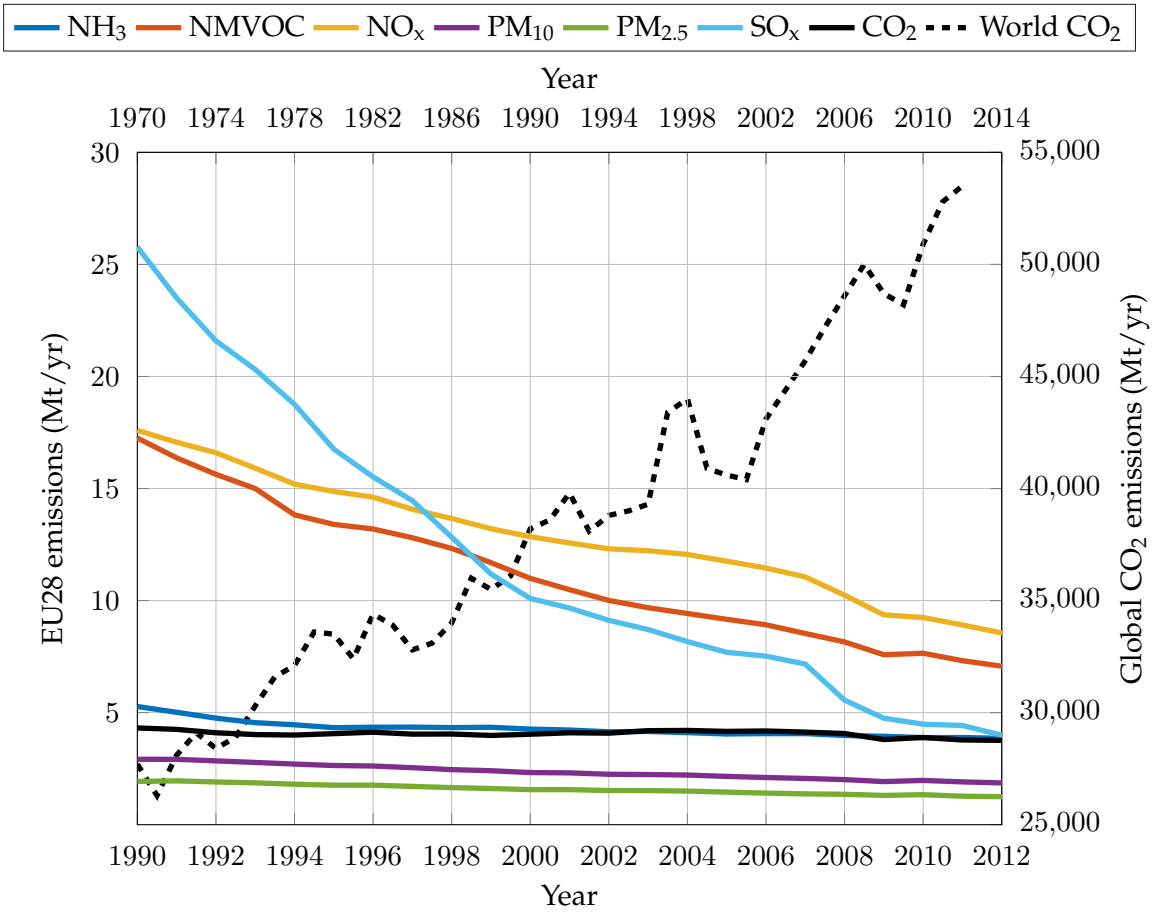

Figure 1.4: Air emissions relative to the EU28 zone and comparison with global CO_2 emissions (top and right axis are respective to the global CO_2 line) [10].

As can be seen in figure 1.4, the Euro zone making a substantial effort to lower all types of air emissions, but that has had little effect in the total world's emissions count. And again, the emerging economies will increase their emissions, regardless of the environment policies in place, because there's simply no emission-free alternatives at the moment. Therefore, it is a moral imperative to fight this trend, due to the negative consequences that come with it, although, even in light of all the scientific knowledge gathered up until now, the investments in this area tend

to follow an economic logic rather than a sustainable one. Even with governmental support, the efforts have proven to be quite scarce, and so in order to make future endeavours thrive, the economical aspect of these projects must be taken in consideration seriously, if they are to be successful.

1.3 Synthetic fuels history and developments

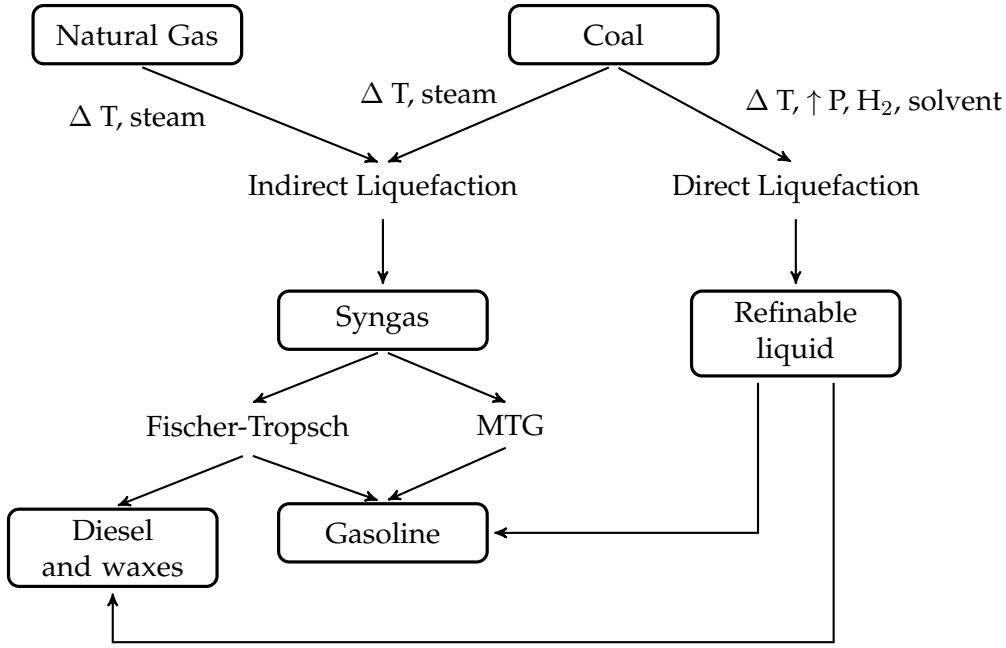

Figure 1.5: Main conversion routes for fossil synthetic fuels.

The routes to produce synthetic fuels are not very diversified per see, as can be seen in figure 1.5, either in terms of feed material used, or the technological principle itself. Most of these processes were developed for coal conversion, due to it's abundance in comparison to oil and gas, although they can also be applied to biomass and natural gas. As far as coal liquefaction goes, it can be divided in two major categories, direct and indirect. One of the first direct coal liquefaction processes was developed by Friedrich Bergius in 1913, being named after himself. It requires a temperature between 400-500 °C, hydrogen pressures between 15-30 MPa, a solvent and preferably a catalyst (although is not necessary, it promotes the desired reactions, such as cracking and hydrogenation). The solvent aids in heat and mass transfer, and serves as an hydrogen donor. Direct coal liquefaction produces a larger variety of products and it's energetically more efficient, even with the very high pressure conditions applied, when comparing to the indirect route, although there are some disadvantages, such as operating difficulties due to the abrasive nature of the slurry, hydrogen-donor solvents high cost (e.g. tetralin), and the liquid-solid separation poses some challenges. Several plants started operating after the First World War in Germany, as well as in the UK. There has been a major effort to overcome the problems related with direct coal liquefaction, in the form of a project - Cleaner Coal Technology Programme - supported by the U.S. Department of Energy (DoE) and the National Energy Technology Laboratory (NETL). Under this programme, several direct liquefaction plant configurations were devised, and can be divided

between single-stage and two-stage. What this means in practice is that there's either one or two reactors within the process. The single-stage processes were developed during the 60's and 70's, the most important being:

- Kohleoel (Ruhrkohle, Germany);
- NEDOL (NEDO, Japan);
- H-Coal (HRI, USA);
- Exxon Donor Solvent (EDS) (Exxon, USA);
- SRC-I and II (Gulf Oil, USA);
- Imhausen high-pressure (Germany);
- Conoco zinc chloride (Conoco, USA).

Only the first two were considered by their developers ready for commercialization, all the other were eventually abandoned. The two-stage processes started appearing as a response to the 1973 oil crisis. Below are listed the processes that continued development after the 80's (there were other 8 process configurations that were abandoned, and weren't listed for that same reason):

- Catalytic Two-Stage Liquefaction (CTSL) (USDOE and HRI, now HTI, USA);
- Liquid Solvent Extraction (LSE) (British Coal Corporation, UK);
- Brown Coal Liquefaction (BCL) (NEDO, Japan).

It can be seen that several novel process configurations were found, superior to older designs and able to surpass several operational problems, still the programme didn't lead to the development of new plants, apart from the demonstration plants build with the project's funds in the 80's and the Shenhua Corporation project in Erdos, Inner Mongolia, that uses licensed DoE technology - the Hydrocarbon Technologies Incorporated (HTI) process. The plant is the only one in the world that uses the direct liquefaction approach and has been operational since November 2010, producing 1,08 million ton/year of liquid products including diesel, naphtha, and liquefied petroleum gas (LPG). There are plans to expand it up to a capacity of 3 million ton/year [11].

The indirect route gasifies the feed, producing synthetic gas or syngas. There are two main paths to produce chemicals and fuels from syngas, again the direct route, which consists in a collection of chemical reactions that are commonly referred as Fischer–Tropsch (FT) synthesis, and the indirect route, in which syngas is converted to methanol, which in turn is converted to dimethyl ether (DME), and finally to gasoline - methanol-to-gasoline (MTG). The FT synthesis was first developed by Franz Fischer and Hans Tropsch at the "Kaiser-Wilhelm-Institut für Kohlenforschung" in Mülheim an der Ruhr, Germany, in 1925. The FT synthesis allows for the production of a larger range of products, depending on the operation temperature, when compared with the MTG route, being used mostly for diesel and waxes production. With the advent of Nazi Germany, this process became a commercial reality, operated by the German cartel firm Brabag. This was due to Germany's relative abundance of coal reserves (mainly lignite), when compared to oil, and these were directly or indirectly used to synthesize fuels. At the end of the 2nd World War, there were in Germany alone 9 indirect and 18 direct liquefaction plants, producing almost 4 million

tonnes/year of gasoline, 90% of German consumption. The facilities were strategically bombed by the Allies at the end of the war, thus ending the production of said fuels. The MTG route was developed by ExxonMobil in response to the 80's oil crisis, although most of the factories were shut down when the oil prices dropped [12][13][14].

More recently, other projects for synthetic liquid fuels production have been developed and are in operation. These are normally referred as XtL, with X depending on the input used - gas (GtL), coal (CtL) or biomass (BtL), with the biggest example, in terms of scale, being South Africa's Sasol and PetroSA, where coal-to-liquid (CtL) and natural gas-to-liquid (GtL) processes are used to produce most of the country's diesel, respectively (although Sasol also has GtL plants, and the company seems to be favouring this route in more recent times). Shell's MDS proprietary technology, was successfully conducted in Pearl's GTL plant, Qatar, and is the largest gas-to-liquid facility in the world. Also in Qatar, there's the Oryx GTL process, which uses Sasol's proprietary technology to convert natural gas to fuels [15].

Table 1.2: Top XtL plants ordered by production capacity [16].

Plant	Technology		Capacity (bpd)	Owner(s)	Production start
Secunda, SA	CTL	SAS	160,000	Sasol	1980/1984
Pearl, QA	GTL	Shell MDS	140,000	Shell	2011
Mossel Bay, SA	GTL	Synthol	45,000	PetroSA Statoil Lurgi	1992
Oryx, QA	GTL	SPD	34,000	Qatar Petroleum Sasol	2007
Bintulu, MY	GTL	Shell MDS	12,500	Shell	1993
Sasolburg, SA	GTL*	SPD	5,600	Sasol	1955
Ordos, CN	CTL	Synfuels China MT-FT	5,000	Shenhua	2009
Ordos, CN	CTL	Synfuels China MT-FT	4,000	Yitai	2009
Changzhi, CN	CTL	Synfuels China MT-FT	4,000	Shanxi Luan	2009

*Switched from coal to natural gas in 2005
SA - South Africa ; QA - Qatar ; MY - Malaysia ; CN - China.

Table 1.2 presents the major synthetic fuel production plants in the world and their locations. As previously discussed, most of the plants are in either South Africa or Qatar, although there's a growing interest by China to pursue this path, due to their vast coal reserves. Other smaller plants exist, but as can be seen from previous examples, all of them use non renewable, GHG emitting fossil fuels, and are located in very specific parts of the world, meaning that these were created more as a necessity than driven by market demand. Specifically, Germany's efforts in the first half of the XX century were conducted due to the conditionality of the war and South African's case is intrinsically linked with the country's former apartheid regime that isolated the country politically,

and lacking the necessary oil reserves to produce conventional transportation fuels, Sasol invested in coal gasification, building it's first plant in the 1950's and two larger ones in the 80's. The 1987 oil embargo declared by the United Nations as a measure of political pressure to end the at the time apartheid regime increased even more the need for these facilities. Qatar's GtL projects are motivated by a governmental focus on gas more than oil, and of course, due to the country's large natural gas reserves (3rd largest proven reserves, only toppled by Russia and Iran) [17].

If we consider that the two top gas producers in the world have somehow isolationist foreign policies, it's more obvious why major oil& gas companies are investing in Qatar, and vice-versa. It is important to note that similar projects, such as those planned to take advantage of the shale gas in the U.S. have been cancelled or postponed by Shell and Sasol, respectively. The oil price fall in the end of 2014 was the key factor responsible for these developments. So even when considering fossil resources as input for XtL processes, few are the projects that prosper, because these are, nonetheless, capital intensive investments that rely on unproven technology, and with so few successful cases, the risk is too high for investors and shareholders alike. This situation also holds true for renewable biomass-to-liquid (BtL) processes, where successful cases are even more scarce and exist mostly in Europe/Germany due to the political will to develop renewable energy sources. As can be seen, the technology exists, and it can be applied to biomass, but there are several problems, namely the high oxygen content of biomass, as well as logistics related to harvest and transportation, which are more severe in this case due to the lower energy density of biomass when compared to coal or oil. However, it has been proven to be economical feasible to gasify biomass, in which the syngas produced is combusted in a CHP plant, with some demonstration plants in operation, without any major problems, but the number of examples is indeed scarce. Judging by capacity alone, no BtL process is on pair with its fossil counterpart, which points out a harsh reality for any biofuel production processes based on gasification/FT - due to the high investment cost, they are not economical feasible as a stand alone project, when compared to a fossil XtL project that applies the same technology. Their feasibility increases when integrated in another industry, such as the petrochemical or pulp and paper industry, which are both in a prime position to take full advantage of these new developments to add competitiveness to the industry itself and to the countries where such facilities exist. There are other ways to increase the feasibility of these endeavours, which are going to be discussed in the next section.

1.4 Biomass potential

Producing fuels from biomass is an interesting concept, due to the benefits it brings. To name a few, most, if not all of the processes and technology described before can be applied to biomass, with the appropriate adaptations, of course; it's a less intermittent energy source when compared to other renewable alternatives and a liquid fuel is the common output when processing this kind of resource, which sets biomass aside from the other renewable energy sources, since all the others produce electricity. This means biomass can be a way to increase the renewable energy percentage in the transportation sector. On the environmental level, it's the only renewable carbon containing fuel, with a low content of sulphur, nitrogen and ash forming constituents, so it allows for a stabilization of the CO_2 emissions, and a reduction in CO, NO_x, SO_x and soot emissions. H_2S, the main compound that is responsible for rain acidity, is not formed when biomass is combusted. There's also a social and political side to this matter, since the dependence of the non producing countries on imported oil & gas raises national security issues, and the inability to regulate or retain some degree of control over the price of energy has impacts on the industry and service

sector as well, harming the economy of said countries.

Table 1.3: Several scenarios that consider the biomass potential to replace conventional fossil fuels in the near future within the Euro zone and worldwide.

		Biomass Potential (EJ/year)			
Local	Time	Residues	Crops	Total	Fossil Replacement (%)
EU25	2030	6,7	5,2	11,9	16-18
EU27	2015-2025	2,8	1,8	4,6	4-5
EU27	2025-2045	2,9	5,6	8,5	8-9
EU27	2025-2045	3,5	7,2	10,7	10-12
EU27	>2040	2,5	15,4	17,9	17-19
EU27	>2040	3,1	19,9	23	21-25
Global	2030	96	219	315	42-48
Global		96	315	411	55-62
Global	2030	87	151	238	32-36
Global	2025-2050	31	267	298	40-45
Global	2020	15	112	127	17-19
Global	2025			74	10-11
Global	2025			85	11-13
Global	2025	56	17	74	10-11
Global	2030			91	12-14
Global	2025	65	80	145	19-22

It seems infeasible to aim for total replacement of the current transportation fuels for biomass derived fuels, and the table 1.3 confirms it, a long term strategy to replace current internal combustion for electrical vehicles appears to be a better solution to this problem, since most of the renewable technologies produce electricity, novel nuclear technologies (fusion and small fission) have the potential to supply an enormous amount of energy in the future, provided that the necessary research is carried out to overcome the current problems that this concepts face, and the latest developments in the electrical car industry seem promising to increase the viability of this type of technology (e.g. Tesla Motor's battery concept, where one can switch a depleted electrical car battery at a station for a fully charged one, and the depleted battery will plug into the grid and charge until it's ready for use again, effectively eliminating the issue with the time it takes for an electric car to recharge, making the whole process very similar to filling the tank of a gasoline car). So the question arises, as why should there be a resource allocation and focus on research and development for biomass conversion routes if it's probable that in the future there will be a much better alternative, both in terms of environmental impact as well as end-user cost. And the answer is that biofuels can serve as a "bridge fuel", a way to lower emissions and carbon footprint of the transportation sector, specially considering that the technology already exists for almost a century, while for other better alternatives, a lot of research is still needed, crucial scientific understanding and engineering solutions are still lacking, and even then, it takes time for a technology to mature and become a fully fledged industry. Biofuel solutions, and therefore its importance and share within a certain country will be dependent on said country and endogenous resources. With this said, other advantages may come from developing this technology (e.g. for South European

countries, reduce the number of wildfires, by providing a financial tool to keep forestal area clean of unwanted vegetation or as a way to prevent the growth of alien plant species). In Portugal, specifically, 30% of the oil imports can be reduced if biomass conversion processes would be implemented, which would translate in about a 1500M€/year savings [18].

A lot can be done to increase the percentage of biofuels in the transportation sector, for oil importing countries specifically, a long term goal is necessary, regarding the adaptation of the current petrochemical industry to accommodate the whole bio-refinery concept, defined by the NREL as "a facility that integrates biomass conversion processes and equipment to produce fuels, power, and chemicals from biomass". An example is the introduction of pyrolysis oil (bio-oil) or pulp liquor into refinery units, which would reduce considerably the capital costs associated with building a new stand-alone plant to process these compounds, avoid engine testing and general acceptance for this type of fuels, since the characteristics of the refined product, even when co-processed with bio-oil for example, are very similar to conventional gasoline or diesel and refineries are optimized to deal with chemically complex mixtures, since oil is one of them, and so the extensive range of chemical compounds comprised within the bio-oil can represent new opportunities to produce several other products within the plant [19][20]. Blending fossil and renewable fuels, already being done, needs to continue and to be pushed beyond the current very modest limits, even if that means engine adaptation to the new blended fuels. Normally, when considering gasoline, anhydrous ethanol is used, with the name of the fuel being EX, with X standing for the percentage of ethanol added. In Europe, the most common blend is E10, and by 2020, it is predicted that about 95% of all the passenger cars and vans will be compatible with it. As for diesel, the blending designation is BX, with the X standing for the percentage of biodiesel added. As of now, all diesel vehicles are compatible with B7. If Hydrotreated Vegetable Oil (HVO) or a BtL fuel is considered, blendings are allowed to go up to 30%. Note that HVO or BtL fuels as of now are more the exception that the rule. It's technically possible to get up to B10/15 for diesel and E20 for gasoline, with the proper fuel standards. Ethanol could in theory be added to diesel, although that would change substantially the fuel's specifications. There's also the possibility of designing a stand-alone factory where the biomass is converted to fuel and chemicals and these are sold in the market, this would allow the production of an almost fully or even totally renewable fuel with similar specification as the fossil counterparts, although the high capital required and investment risk associated with this approach makes it less attractive than the other two alternatives mentioned before.

The European Union has been where most of renewable efforts are taking place, and a way to accomplish that is by creating programs that financially promote renewable energy projects, or by creating legislation and directives for the Member States to follow. The European Parliament and Council created the "Renewable Energy Directive" (RED) in 2009, in which there's an ambitious target concerning the transport sector: a 10% share of energy from renewable sources by 2020. All Member States had to submit a national renewable energy action plan (NREAP), in which they outline how they intend to meet this target. Most of the plans involve blending policies, although that might not be enough to reach the required goal. A study commissioned by the European Commission and DG Energy regarding the increase in biofuel blend percentage has reached the conclusion that the current fuel standards are a very limiting factor in archiving the 10% target and so other blending options are in need of development. Each Member State is pursuing a different blending alternative, causing fragmentation within the shareholders. Although country specific policies do need to be considered, it is also important to focus on a few good alternatives in terms of blending options, so that investment doesn't get alienated in the process. Another important aspect for a successful blending policy resides in fuel labelling. With the increase in blending

types, new fuel grades appear and the end user needs to be aware of this and know what kind of fuel is better for the vehicle.

Another major project within the EU that aims for the development of new renewable sources of energy is the Horizon 2020. This is the biggest European effort taken by the EU Research and Innovation programme in the form of a €80 short-scale billion funding available for the 2014-2020 time period. It's a project that tries to promote new technologies and getting them from lab scale to the market. Concerning some of the targets for this project, there is:

- GHG emissions reduction by 20% (or even 30%, if the conditions are right);
- 20% of energy from renewables;
- 20% increase in energy efficiency.

The EU example is being followed by countries such as U.S.A. or China, which have established various renewable national goals and targets for the next four decades. For instance, Denmark set the goal of, by 2035, having all heating and electricity covered by renewable energy [21]. Big CO_2 producers like China have targets to greatly reduce its emissions, especially from coal utilization. This energy objectives are important because they can catalyse the growth of liquid biofuels in transportation, especially in new emerging markets like India and especially China, where liquid biofuels are expected to grow due to the exponential increase in the number of sold vehicles. Taking into account the current situation of fossil fuels and all economic and environmental issues, it is expected that liquid biofuels will gain market share, since they are environmentally friendly and renewable. Currently over 50 countries have mandatory biofuel policies. Recently, new biodiesel markets are emerging, especially in Asia and Africa, since many countries like Thailand, India, Indonesia, South Africa and Zimbabwe have recently adopted B10 blending policies for road transportation fuel production. Also because of excepted price rise on fossil fuels, due to scarcity, and the green policy of maximum 2 °C rise in global temperature, the biofuel share in transportation market is expected to grow from, currently 3,5% to 27% by 2050, especially in Asia and Africa were there are developing countries with a growing transportation sector.

1.5 Motivation and objectives

When looking at the Portuguese panorama concerning raw materials for the production of liquid biofuels, most of these come from bushes, uncultivated land and agricultural wastes, and so in order to have a more sustainable liquid fuel industry, these lignocellulosic resources ought to be availed, thus reducing the energy dependency of the country. In terms of area percentage, Portugal has 22% uncultivated land, 21% of forest consisting in either pure or mixed strands of *Pinus pinaster* and *Eucalyptus globulus* and 33% of agriculture soil, consisting in mainly olive groves, vineyards and orchards. All of these areas generate lignocellulosic wastes that can and should be processed into added-value products. A very important statistic regarding this type of waste biomass is that it contributes, in a significant way, to wildfires in the country, which have an associated cost between 740–880 M€/year, as well as environmental and public safety impact. If one has a more integrated view over this subject and considers the cost reduction that implementing a process like this would bring due to wildfire prevention, the economical feasibility of it could certainly increase. Following the BioREFINA-Ter framework, a project designed to increase the value of lignocellulosic wastes in the Central Inland region of Portugal,

studies were carried out in order to access the feasibility of fast pyrolysis for certain invasive and indigenous species in the region. These species grown in uncultivated land, that has low agricultural potential, therefore, the upkeep necessary to assure a constant feed of these resources is low, most of the cost coming from logistics rather than maintenance. Nevertheless, it has a high capacity for delivering lignocellulosic biomass for bioenergy production, amounting to approximately 170,000–180,000 tons/year [18]. It is the objective of this work to simulate these results in order to determine vital design parameters for a plant and respective operation feasibility.

European environment directives and goals aim for a GHG and other air pollutants reduction, and since biomass can produce carbon neutral fuels, it is a prime candidate to replace, at least partially, conventional fossil liquid fuels. These are simpler solutions to mitigate some of the impacts of fossil fuel consumption, as well as an alternative that can actually generate profit to an activity (waste treatment) that otherwise would represent a cost. An indirect positive aspect of implementing this type of processes to treat waste biomass is the wildfire prevention, which is in concordance with environmental policies, and also provides socio-economical benefits.

A major goal of this thesis is to provide a good plant model that can realistically simulate pyrolysis behaviour for the studied biomass species to be able to correctly predict product quality and assorted characteristics as a function of operational parameters, such as temperature or residence time. This means that detailed reaction mechanisms are necessary, with dedicated kinetics, and therefore special attention and a more comprehensive approach to this aspect of the pyrolysis process was given. Specifically, a few reaction schemes were investigated and a new reaction mechanism that provides overall better results was proposed during the elaboration of this work.

By being able to correctly predict specific component yields, one can assess if it is economically viable on an industrial scale to product specific chemicals that are contained within the bio-oil. Oxygenated species are predominant, and since a lot of oxygenated chemical feedstocks have a fossil nature, adding the oxygen via a synthetic pathway, one can just separate and or purify these components from the bio-oil, which allows for an alternative, less environmental hazardous production of chemicals, since these have a biological origin, and for most cases, are also chemically identical to its oil counterparts. More reliable simulation tools, that can accurately predict product quality variations based on feedstock conditions will play a key role into the design of such processes.

Bio-oil used directly as fuel is not very attractive, having it's applicability limited to burners for the production of heat or steam. Therefore, further processing is necessary, which is normally denominated upgrading. As of now, no economically feasible bio-oil upgrading plant is in operation, due to mainly poor catalyst performance. To further study and search for suitable catalysts, bio-oil chemical composition, even if not very detailed, is necessary. For catalysis applications, kinetics need to be determined and so is not possible to represent bio-oil just with proximate and ultimate analysis in these models. Accurate pyrolysis kinetics are therefore very important, since any errors may propagate downstream, which may lead to erroneous results throughout the process chain.

There is an interesting concept to improve the economical feasibility of BtL processes, which is called BTL2, and stands for "Biomass to Liquid in Two Steps", meaning that there's a first step of biomass pre-treatment and conversion into a slurry a second one where said slurry is gasified. BTL2 consists in converting lignocellulosic material, mainly waste biomass such as bushes from

uncultivated land, straw or other types of low-grade wood without further application into either synthetic fuels or chemicals. The big difference between other BtL processes consists in the reduction of transportation costs by considering several smaller fast pyrolysis units close to the harvest locations, where the resulting slurry is then transported to a bigger gasification facility, since it has a higher energy content when compared to biomass (it's about a ten times increase in energy stored per volume). While there's only one active project using this concept, the bioliq® process, other reactor and/or process configurations for both pyrolysis and gasification haven't been tested, being a unexplored area that could prove to have great potential in the near future, and simulation tools can prove to be a valuable tool into accomplishing this.

1.6 Thesis structure

This work will be divided into a state of the art review, followed by a chapter with considerations about the kinetic parameters determination and reaction mechanisms as well as the simulations done, with respective description and problems faced. The following chapter presents the simulation results and discusses them and final chapter has some concluding remarks and suggestions for future work.

Bibliography

[1] EIA, "International energy statistics." Independent Statistics & Analysis, 2011.

[2] DOE and EIA, "International energy outlook 2013," tech. rep., U.S. Energy Information Administration, Washington, USA, 2013.

[3] EEA, "Costs of air pollution from european industrial facilities 2008–2012," tech. rep., European Environment Agency, 2014.

[4] R. K. Pachauri and L. Meyer, "Climate change 2014," tech. rep., The Intergovernmental Panel on Climate Change, 2015.

[5] EIA, "International energy statistics." Independent Statistics & Analysis, 2013.

[6] D. J. Murphy and C. A. S. Hall, "Year in review—eroi or energy return on (energy) invested," *Annals of the New York Academy of Sciences*, vol. 1185, no. 1, pp. 102–118, 2010.

[7] D. Weißbach, G. Ruprecht, A. Huke, K. Czerski, S. Gottlieb, and A. Hussein, "Energy intensities, {EROIs} (energy returned on invested), and energy payback times of electricity generating power plants," *Energy*, vol. 52, pp. 210 – 221, 2013.

[8] T. Boden and R. Andres, "Global, regional, and national fossil-fuel CO_2 emissions." Carbon Dioxide Information Analysis Center, 2015.

[9] C. MacFarling Meure, D. Etheridge, C. Trudinger, P. Steele, R. Langenfelds, T. van Ommen, A. Smith, and J. Elkins, "Law dome co2, ch4 and n2o ice core records extended to 2000 years bp," *Geophysical Research Letters*, vol. 33, no. 14, 2006.

[10] EEA, "Air pollutant emissions data viewer." LRTAP Convention, 2013.

[11] H. Shui, Z. Cai, and C. Xu, "Recent advances in direct coal liquefaction," *Energies*, vol. 3, no. 2, p. 155, 2010.

[12] R. Kamall, "Coal liquefaction," tech. rep., Cleaner Coal Technology Programme, 1999.

[13] A. N. Stranges, "Germany's synthetic fuel industry 1927-45." 4 2003.

[14] D. Leckel, "Diesel production from fischer-tropsch: The past, the present, and new concepts," *Energy & Fuels*, vol. 23, no. 5, pp. 2342–2358, 2009.

[15] A. Patel, "A new era for sasol: Sustainable development report," tech. rep., Sasol, Johannesburg, SA, 2014.

[16] B. Meyer, "Xtl: Development of synthesis fuels in europe and south africa." IEA-MOST Workshop, 2014. An optional note.

[17] B. Dudley, "Bp statistical review of world energy," tech. rep., British Petroleum, London, UK, 6 2014.

[18] M. Amutio, G. Lopez, J. Alvarez, R. Moreira, G. Duarte, J. Nunes, M. Olazar, and J. Bilbao, "Flash pyrolysis of forestry residues from the portuguese central inland region within the framework of the biorefina-ter project," *Bioresource Technology*, vol. 129, pp. 512 – 518, 2013.

[19] M. S. Talmadge, R. M. Baldwin, M. J. Biddy, R. L. McCormick, G. T. Beckham, G. A. Ferguson, S. Czernik, K. A. Magrini-Bair, T. D. Foust, P. D. Metelski, C. Hetrick, and M. R. Nimlos, "A perspective on oxygenated species in the refinery integration of pyrolysis oil," *Green Chem.*, vol. 16, pp. 407–453, 2014.

[20] J. Speight, *Synthetic Fuels Handbook: Properties, Process, and Performance*. McGraw Hill professional, McGraw-Hill Education, 2008.

[21] Danish Government, "The danish climate policy plan: Towards a low carbon societ," tech. rep., Danish Government, Copenhagen, DK, 8 2013.

Chapter 2

State of the art

The broad nature of energy and any subject that is related to it, specially biofuels, deems any state of the art review a much more crucial and necessary role, due to the complex nature of the some of the processes and techniques that are going to be mentioned, which has resulted in, for example, a lack of distinction found in the literature between the two main thermochemical processes to convert biomass - gasification and pyrolysis, although these are very different in their principle of operation (reasserting everything said before). This chapter pretends to give an overview of the main conversion paths of biomass into added value products, without becoming too exhaustive, and so special emphasis was given to new developments with promising results.

2.1 The fluidization principle

Due to the fact that this is a principle extensively used in thermochemical processes of solids, coal or biomass system alike, a brief description of this will be done. A more detailed overview on fluidization technology is given elsewhere ([1],[2]).

When fluidized, an initially stationary bed of solid particles is transformed into a fluid-like state by an upward gas or liquid stream. The volumetric flow rate of this gas or liquid stream has to exceed a certain limiting value (called minimum fluidization). In many respects, such a fluidized bed behaves like a liquid:

- The bed can be stirred like a liquid;
- Objects of greater specific gravity sink, whereas those of lower specific gravity float;
- When the vessel is tilted, the bed surface resumes a horizontal position;
- If two adjacent fluidized beds with different bed heights are connected to each other, the heights become equal;
- The fluidized bed flows out like a liquid through a lateral opening.

The fluidization principle was first used on an industrial scale in 1922 for the gasification of fine-grained coal by Winkler at BASF in Germany. Since then, fluidized beds have been applied in many industrially important processes. An extensive process application compendium exists, however, in this work, one is interested in heterogeneous, non-catalytic, gas-phase reactions. Particularly advantageous features of the fluidized bed for use as a reactor are excellent gas/solid

contact in the bed, good heating and mass transfer rate, and high bed/wall and bed/internals heat-transfer coefficients.

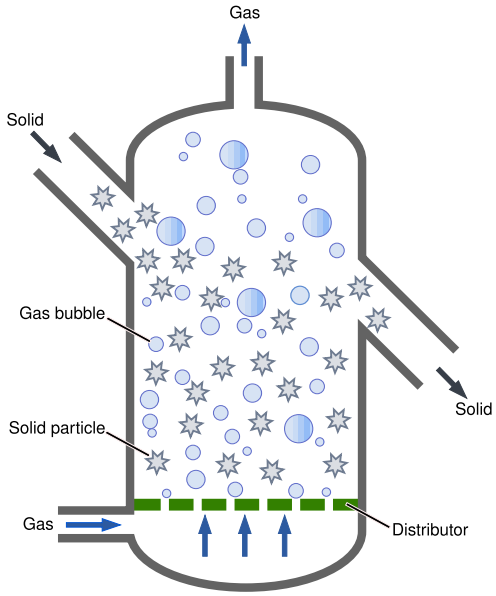

Figure 2.1: Fluidized bed reactor concept.

As the volumetric flow rate or the superficial velocity of the fluid increases beyond the value corresponding to the minimum fluidization point, one of two things happens: in fluidization with a liquid, the bed begins to expand uniformly; in fluidization with a gas - a process of greater industrial importance and the one discussed exclusively in the following sections - virtually solids-free gas bubbles begin to form. The local mean bubble size increases rapidly with increasing height above the grid because of coalescence of the bubbles. If the bed vessel is sufficiently narrow and high, the bubbles ultimately fill the entire cross section and pass through the bed as a series of gas slugs. As the gas velocity increases further, more and more solids are carried out of the bed, the original, sharply defined surface of the bed disappears, and the solids concentration comes to decrease continuously with increasing height. To achieve steady-state operation of such a "turbulent" fluidized bed, solids entrained in the fluidizing gas must be collected and returned to the bed. The simplest way to do this is with a cyclone integrated into the bed vessel and a standpipe dipping into the bed. A further increase in gas velocity finally leads to the circulating fluidized bed , which is characterized by a much lower average solids concentration than the previous systems. The high solids entrainment requires an efficient external solids recycle system with a specially designed pressure seal.

2.1.1 Advantages and disadvantages of fluidized beds

The major advantages of the (gas/solid) fluidized bed as a reaction system include:

- Easy handling and transport of solids due to liquid-like behavior of the fluidized-bed;
- Uniform temperature distribution due to intensive solids mixing (no hot spots even with strongly exothermic reactions);

- Large solid/gas exchange area by virtue of small solids grain size;
- High heat-transfer coefficients between bed and immersed heating or cooling surfaces;
- Uniform (solid) product in batchwise process because of intensive solids mixing.

Set against these advantages are the following disadvantages:

- Expensive solids separation or gas purification equipment required because of solids entrainment by fluidizing gas;
- As a consequence of high solids mixing rate, backmixing of gas and resulting lower conversion;
- In catalytic reactions, undesired bypass or broadening of residence-time distribution for reaction gas due to bubble development;
- Erosion of internals and attrition of solids (especially significant with catalysts), resulting from high solids velocities;
- Possibility of defluidization due to agglomeration of solids;
- Gas/solid countercurrent motion possible only in multistage equipment;
- Difficulty in scaling-up.

2.2 Gasification

Gasification is the conversion of an organic compound to gas, in the presence of an oxidizing agent (normally air or steam). This gas is normally called synthesis gas or just syngas, and the organic compound can be anything from fossil to non fossil resources or a mixture of both. The design goal in a gasifier is to maximize the gas yield, while avoiding char and tar formation. Therefore, the mechanisms on how this happens will be briefly discussed. In a fairly low temperature (200-500°C), primary tar is formed. When temperature is increased to 700-900°Crange, this tar reacts and forms non-condensable gases and secondary tar (reforming). The primary tar production is actually a pyrolysis process, with higher temperature reactions being the gasification ones, yielding gas and a solid residue, char. Reactor design also determines where the pyrolysis zone is, how the biomass reacts with the oxidizing agent and temperature of the reactions taking place. It is very important for the produced gas not to have a high tar content, because this will cause problems in gas engines. Proper design and operation conditions to minimize tar formation are important, but most of the cases, a gas clean-up unit is also used. This decreases the process energy generation efficiency, and these gas treatment facilities also have high capital costs. For syngas applications, tar and particles limits are very low since there poison the catalysts.

Figure2.2 shows the main gasification reactor types used. The updraft and downdraft are fixed bed reactors. All these equipments can be operated at atmospheric pressure or increased pressure. The reactor design greatly influences the tar and gas amount produced (e.g. an updraft gasifier can produce over 100g/Nm^3 of tar while a counter current moving-bed gasifier has a tar production of about 0.100g/Nm^3 - a reduction in 3 orders of magnitude). In a updraft gasifier, biomass is fed at the top and the product leaves at the top as well. The oxidizing agent is pre-heated and

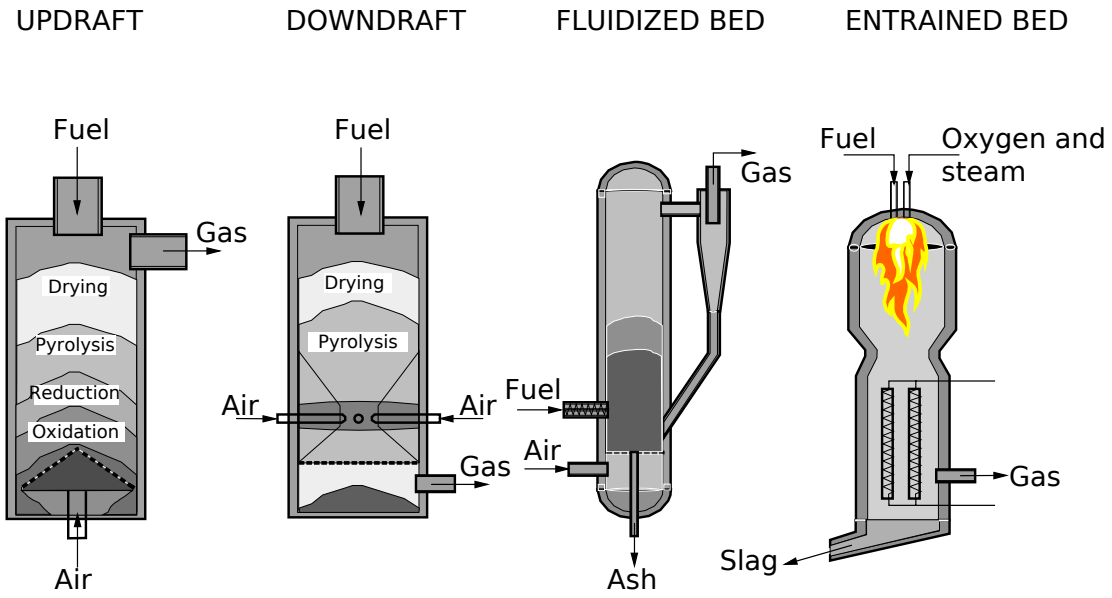

Figure 2.2: Main types of gasification reactors.

enters the reactor at the bottom, ascending through it while the fuel falls downwards. Due to high temperatures at the bottom of the reactor, ignition and combustion happens, which can be represented by reaction 2.1:

$$C + O_2 \rightarrow CO_2 - 394\ \text{kJ/mol} \tag{2.1}$$

This is a highly exothermic reaction that consumes most of the oxygen present, which eventually changes to a partial combustion reaction, releasing CO and more heat (reaction 2.2):

$$C + 1/2O_2 \rightarrow CO - 111\ \text{kJ/mol} \tag{2.2}$$

The hot gas, constituted mainly of CO_2, CO and steam rises within the reactor and enters the gasification zone, where syngas production happens (reactions 2.3 and 2.4):

$$C + CO_2 \rightarrow 2CO + 172\ \text{kJ/mol} \tag{2.3}$$

$$C + H_2O \rightarrow CO + H_2 + 131\ \text{kJ/mol} \tag{2.4}$$

Heat produced in the combustion zone supplies the energy demand for this reactions to happen. The top zone is where drying and pyrolysis of biomass happens. Vapours formed go up the reactor while the formed char goes down into the gasification zone. In downdraft reactors, the zones where described above reactions happen are different. Air or steam is fed near the bottom (see figure 2.2, while in the above zones, drying and pyrolysis happens. Gasification happens below the oxidizing agent feed, and that is where the syngas also leaves the reactor. This allows for the combustion of pyrolysis tars and so the product stream has a lower concentration of these.

In a fluidized bed reactor, biomass is fed either at the top or on the sides, and it's well mixed in the fluidizing medium which is also the oxidizing agent. The drying and reaction of the biomass

particles is relatively fast. The heat released by the oxidation of the char is quickly spread out to the entire bed. A bubbling fluidized bed cannot achieve full char conversion due to solid back mixing: while the fluidization allows for temperature uniformity, the mixing of partially and fully gasified particles hinders further reaction. Oxygen diffusion in the bed is also low, which promotes combustion and lowers gasification efficiency. In order to solve some of these problems, a circulating fluidized bed (CFB) reactor can be used. Typical temperatures employed in a fluidized bed reactor range between 800-1000°C, which is low enough to prevent ash sintering. The fuel doesn't need any pre-treatment, and so agricultural or wood wastes can be gasified without much trouble.

The entrained-flow gasifiers are the preferred reactor types in most gasification applications. They typically operate at 1400°Cand between 20-70 bar, where a slurry (or powder) containing the fuel is injected into the reactor, along with the oxidizing agent, to which pure molecular oxygen and steam is recommended for best efficiency (air is not normally used). If a slurry containing water is used, then a higher volume reactor is needed for the evaporation of said water. Plus, the energetic demand is higher when compared to dry feed systems. Due to the high temperatures employed, there are not tar or solid formation.

Regarding the industrial application of said technologies, there is a number of pilot and demonstration scale plants, but only a few industrial scale units. These are concentrated mostly in Europe, with a few in the US and Japan. The feedstock is normally of lignocellulosic nature, namelly bark, waste or forest residues, and therefore the industry has more potential in countries with a sizeable pulp and paper industry. While these facilities produce power either through co-firing or in gas turbines, there are plans to produce renewable diesel, ethanol and SNG. Table 2.1 shows the largest biomass gasifiers operational.

Table 2.1: Operational biomass gasifiers with the largest capacity [3].

No.	Company/Plant	Location	Country	Feedstock origin*	Production capacity		Biomass use
					MW_{fuel}	PJ/a	in 2012 (PJ/a)
1	Lahti Energia	Lahti	Finland	L	160	40	23
2	Vaskiluodon	Vaasa	Finland	L	140	35	05
3	Rüdersdorfer Zement	Rüdersdorf	Germany	?	65	25	12
4	Essent	Geertruidenberg	Netherlands	?	55	21	15
5	Electrabel (GDF Suez)	Ruien	Belgium	?	50	18	10
6	Metsä Fibre	Joutseno	Finland	L	30	12	05
7	Södra Cell Värö Pulp Mill	Väro	Sweden	L	25	09	07
8	Agnion Technologies	Pfaffenhofen	Germany	?	20	08	02
9	Corenso United	Varkaus	Finland	M	20	08	04
10	Skive Fjernvarme	Skive	Denmark	L	20	08	06

*L (Local), I (Import), M (Mixed), ? (Not known).

2.3 Pyrolysis

Pyrolysis is the thermal decomposition of any type of organic material, in the absence of oxygen (or any oxidizing agent). It is a irreversible chemical transformation that yields three types of products, differentiated by their state of matter: non-condensable gases, a liquid fraction referred to as tar and a solid residue, commonly defined as char. When the organic feed is lignocellulosic biomass, the tar is often denominated bio-oil, which is a dark brown liquid, with high acidity and viscosity, and a fairly complex composition (over 100 compounds). The non-condensable gases are carbon monoxide and dioxide, methane, hydrogen and a few more light compounds in trace amounts [4]. The char is very rich in carbon and retains most of the properties of the feed biomass, although the surface area normally tends to increase, which makes char good for adsorption applications (with the proper treatment). Both the gases and the char can also be burned to provide heat for the process. The yield of these three products is very sensible to process conditions.

Pyrolysis processes can be divided into slow pyrolysis (also referred to as intermediate), fast pyrolysis, carbonisation and torrefaction. Conventional pyrolysis as been used since ancient times to produce charcoal from biomass, where low heating rates and long residence times were employed, to maximize the char formation. It was in fact a torrefaction or carbonisation process. Lower temperatures and long residence times tend to favour char formation, high temperatures and moderate to long residence times favour the production of gases and moderate temperatures and short residence times increases the liquid products yield [5]. In table 2.2 is represented all these pyrolysis types as well as gasification as a term of comparison, with key information regarding each process.

Table 2.2: Various pyrolysis types, main operation characteristics and product yields.

Mode	Temperature	Residence time	Heating Rate	Liquid	Solid	Gas
Fast	∼500°C	<2 s	1,000-10,000°C/s	75%	12%	13%
Intermediate	∼500°C	10-30 s	1-100°C/min	50%*	25%	25%
Carbonisation	∼400°C	hours / days	1-10°C/min	30%	35%	35%
Torrefaction	∼290°C	10-60 min	1-10°C/min	0-5%**	80%	20%
Gasification	750-900°C	<10 s	1-100°C/s	5%	10%	85%

*In 2 phases
**If condensed can go up to 5%, otherwise, no liquid is produced.

2.3.1 Fast pyrolysis

In this work, the goal is to obtain a liquid product, bio-oil, and so a more detailed overview of fast pyrolysis deems necessary. Research started in the 80's, at the University of Waterloo, Canada, taking advantage of the fluidized bed technology for the reactor, in order to maximize the bio-oil yield, using a lignocellulosic feed. After several studies carried out by this research group [6][7][8][9], it was determined that the optimal operating temperature for maximum liquid yield is around 500°C for a fluidized bed reactor and a residence time lower that 1 second. The low residence time is thought to prevent secondary reactions, such as cracking, which produce gaseous products, and heterogeneous interaction between the pyrolysis vapours and the char, which also causes further decomposition of the liquid compounds into low molecular species.

Char and ashes act as catalysts in these last reactions [10][11]. Transport phenomena limitations increase the secondary reactions rate, particularly the vapour-solid interactions, and so it is also very important for the biomass particles to be small enough to prevent temperature gradients and consequently gas formation. A particle diameter below 2mm is recommended, to order to maximize bio-oil yield [12].

In order to perform fast pyrolysis on an industrial scale, one needs specific reactor designs, able to apply the required high heating rates to biomass and low residence time, without causing significant operational problems. As said before, the first pyrolysis reactors were fluidized beds, but since then, several other designs, very different in principle have been developed. Table 2.3 presents the most important reactor types, to which the description follows below.

Table 2.3: Several reactor types suitable for biomass pyrolysis and some of their characteristics as well as industrial development status [13].

Reactor	Liquid yield wt%	Feed size	Input gas	Complexity	Scale-up	Status*
Fluidized bed	75	Small	High	Medium	Easy	Demo
CFB	75	Medium	High	High	Easy	Pilot
Entrained gas flow	65	Small	High	High	Easy	Lab
Vaccum	60	Large	Low	High	Hard	Demo
Rotating cone	65	Very small	Low	High	Hard	Pilot
Ablative	75	Large	Low	High	Hard	Lab
Auger	65	Small	Low	Low	Easy	

*Demo scale is estimated to be 200-2000 kg/h, pilot scale is 20-200 kg/h and lab scale is <20 kg/h.

Although the reactor is not the major fraction in terms of capital investment, a lot of research as been carried out in new reactor designs, so that the desired liquid yield can be achieved. Several new reactor types appeared as a result, with the most important ones presented in table 2.3. Bridgwater [5] notes the unnecessary reinvention done at the academic level, such as fixed bed designs, which are unlikely to yield large amounts of liquid products.

Bubbling fluid beds (BFB) were first tested in the pioneer work done in Waterloo University for this kind of application, having the advantage of being well understood in terms of operation principles and is simple to construct and operate, allowing a good temperature control and high heating rates. Cyclones are required, as well as a quench cooler and a ESP for aerosol capture. Demisters can also be used but are less efficient. Pyrolysis is an endothermic process, hence, a heat source is needed. This can come from the combustion of the biomass char (typically 15% in weight of initial biomass but 25% of the energy contained in the feed) or another external fuel, with the pros and cons that come with this alternative. Heat transfer into the reactor is very important, for the BFB the fluidization gas provides the heat, with particle size limiting the achievable heating rate. The residence time is a very important design parameter as well. If too high, char and inorganic material will catalyse cracking reactions, reducing the liquid yield. Although the majority of the char leaves the reactor at low to mid height, some entrainment happens, hence the cyclones. Special attention is needed when designing and operating the heat transfer equipment due to the high gas flow required for fluidization. This also means higher capital investment due to larger equipment. Some of the industrial examples of BFB are presented in table 2.4.

Circulating fluid bed (CFB) reactors are very similar to the BFB counterpart, with the main

Table 2.4: Industrial plants using BFB reactors.

Company	Size (kg/h)	Location	Status	Reference
Fortum	10,000	Joensuu, Finland	Active	[14]
Dynamotive	8,000	Guelph, Canada	Inactive	[15]
Dynamotive	4,000	West Lorne, Canada	Inactive	[15]
Valmet	300	Joensuu, Finland	Active	[16][14]
Wellman	250	Oldbury, UK	Inactive	[17]
Biomass Engineering	250	Newton-le-Willows, UK	Inactive	[14]
Virginia Tech	250	USA	Inactive	[14]
Union Fenosa	200	Spain	Dismantled	[18]
Univ. Science & Tech of China	120	Hefei, China	Active	[14]

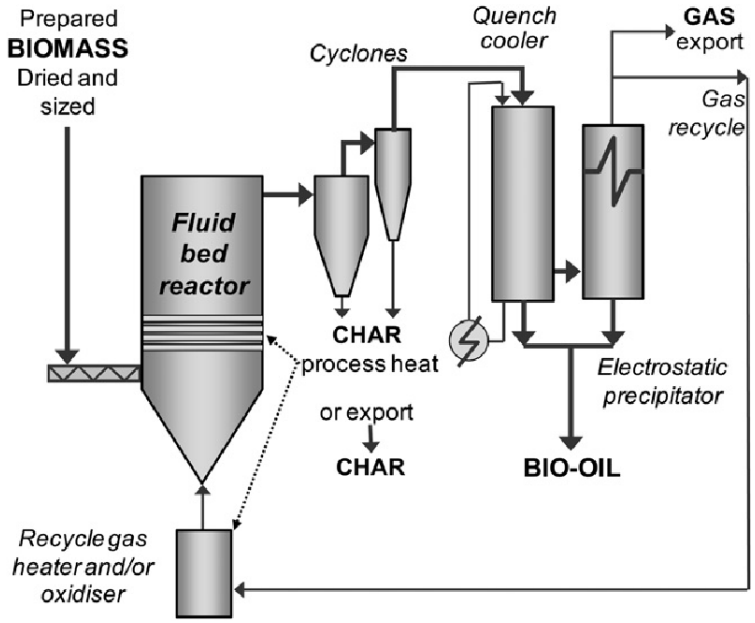

Figure 2.3: Bubbling fluidized bed reactor.

difference being the residence time for the char, which is virtually the same as for vapours and gases. This means that the char (and sand particles) also exits the reactor at the top, and collected afterwards in a cyclone. The char is then normally combusted in another fluid bed and the hot sand is returned to the main reactor. The advantages of this type of setup is the potential to process higher throughputs and the fact that hot sand is used as the heat carrier, avoiding the use of a gas heat exchangers. Higher contents of char in the bio-oil, more complex hydrodynamics and careful control of the char combustion chamber to ensure proper temperature conditions are some of the disadvantages. Industrially, Ensyn is the company that more frequently employs this technology, having built a 10 t/d plant in Bastardo, Italy [19] - not in operation for some years, food flavouring production plants in Wisconsin with a capacity up to 1700 kg/h and several plants in Renfrew,

Canada with a wood processing capacity up to 2000 kg/h and plans to increase this to 1000 t/d [20].

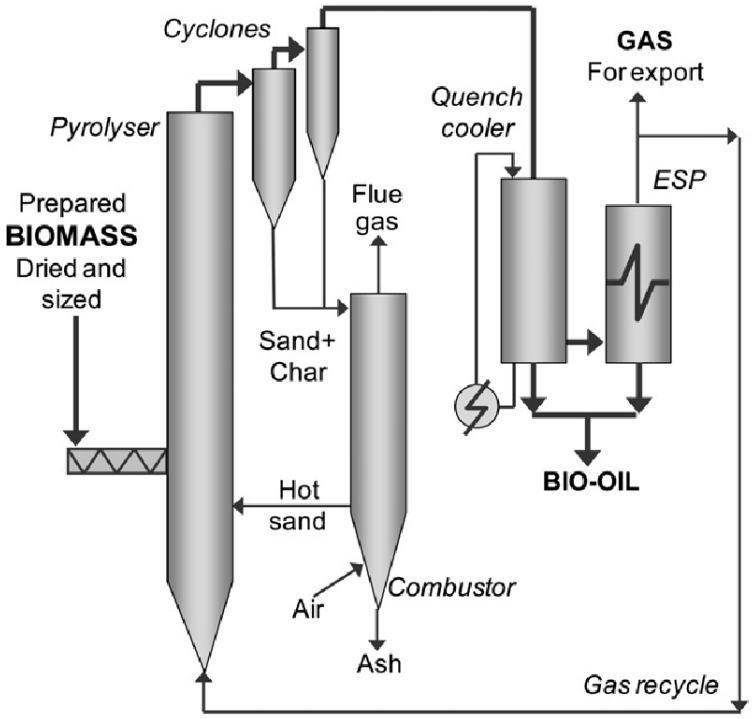

Figure 2.4: Circulating fluidized bed reactor.

Invented by the University of Twente, in the Netherlands, and later developed by the Biomass Technology Group (BTG) in close ties with the academy, the rotating cone reactor consists in a transported bed, although instead of introducing a gas to cause fluidization, a cone applies centrifugal forces (at about 10 Hz) to the solid particles that enter through an impeller at the base of the apparatus. The centrifugal forces, caused by the cone rotation, push the particles upwards, which ascend in a spiral trajectory, close to the cone wall, which in turn is heated, promoting the biomass decomposition. The vapours leave the top of the reactor and are conventionally processed, while char and sand particles fall to a fluid bed surrounding the cone and are subsequently fed into a combustion fluidized bed reactor [21]. Combustion heats the sand, which in turn is recycled into the rotating cone, providing the necessary heat for pyrolysis to take place. Liquid yields up to 70% are attainable. The major advantages of this reactor type are low carrier gas requirements, which translates in smaller equipment, both for the reactor and downstream of the process, reducing capital investment and easy to scale technology. BTG has two fast pyrolysis facilities: a small scale (1-5 kg/h) feedstock screening unit and a pilot plant unit, with a biomass processing capacity between 50-200 kg/h [22]. BTG also built an industrial scale plant with a 2 t/h capacity in Malaysia and a 5 t/h plant in Hengelo, Netherlands that just recently started operating [23][24].

Ablative pyrolysis has a different principle of operation when compared to previous reactor types, which are different forms of fluid beds. In methods that rely on the fluidization principle to thermochemically decompose biomass, the rate of reaction is heavily dependent on transport phenomena, and therefore, the particle size must be small. In ablative pyrolysis, biomass - often

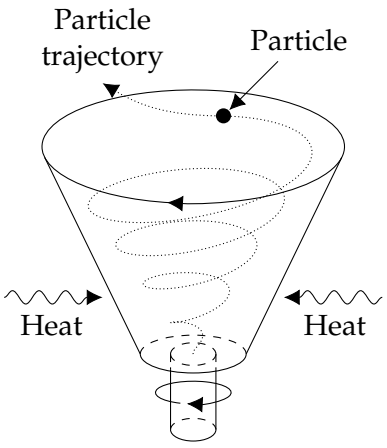

Figure 2.5: Principle of the rotating cone reactor (adapted from [21]).

designed "melt" wood - is put in contact with a hot wall under pressure. By means of either a centrifugal or a mechanical force, the biomass particle is moved away and is vaporized in a similar fashion as in a fluid bed. This provides a high and uniform heating rate, and as the biomass decomposes, a film of residual oil is formed, serving as lubrication for subsequent particles. Residence times are low and the main operational parameters for controlling the rate of reaction are the pressure applied to the wood on the hot surface, the velocity and heat exchange area of the biomass particles and the reactor's surface temperature. The main characteristics taken in consideration when designing this type of reactor are:

- How force is applied onto the particles to achieve high pressure (either mechanically or by mean of a centrifugal force);
- High relative velocity between the particles and the heated wall;
- Reactor temperature <600°C.

Theoretically, there is no upper limit in particle size. The reaction rate is dependent on the heat supply to the reactor wall rather than the heat transfer characteristics of wood. Other advantages include the absence of a carrier gas, which means that the process equipment is smaller, and also that the partial pressure for all components of interest in the pyrolysis vapours are higher, which facilitates separation, thus increasing its efficiency and also reducing size, which means a less capital intensive investment. However, scaling is difficult due to the surface area requirements and if a mechanical design is chosen, the process becomes more complex. NREL, USA tried a centrifugal force concept, however, it is no longer operational [25] and Aston University, UK opted for a mechanical design, which was described here with more detail and is presented in figure 2.6.

The ablative reactor principle and design was first studied and thoroughly tested by the CNRS laboratories, in Nancy, France. The research done was able to relate several key parameters such as pressure, motion (velocity) and temperature. The authors also concluded that in order to achieve fast pyrolysis conditions, a high heat flux is needed, as well as a way to remove the solids formed, since these would decrease the heat flow transferred to the biomass [26]. The NREL developed a ablative vortex reactor, also referred to as cyclone reactor, in which biomass particles, transported by a carrier gas, enter the reactor tangentially so that the centrifugal forces pressure the particles

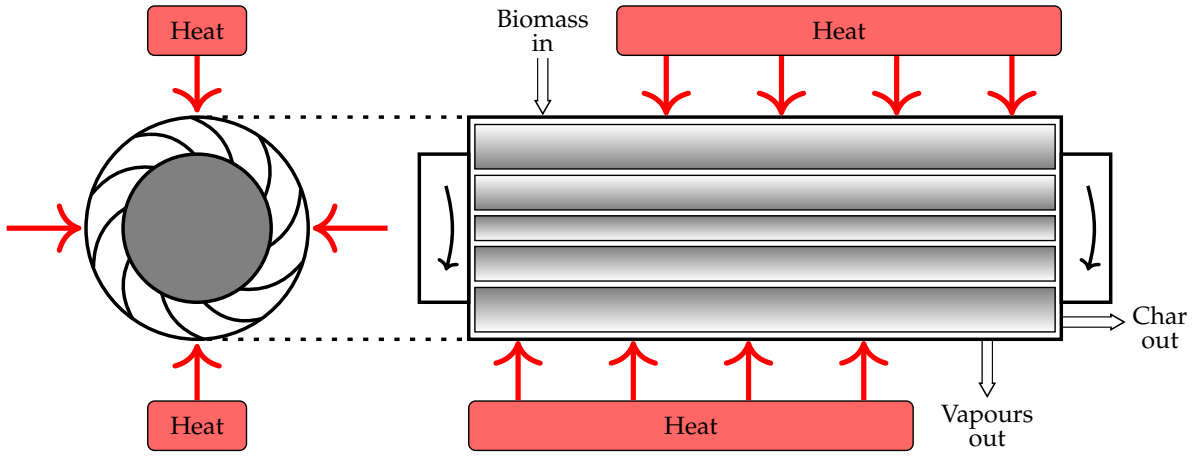

Figure 2.6: Aston University Mark 2 ablative fast pyrolysis reactor (adapted from [5]).

onto the heated reactor wall, promoting the reaction. Yields up to 70% for the pyrolysis oils can be obtained, unreacted solids are recycled and the vapours are separated from the char in a cyclone [25]. Aston University developed a ablative plate reactor, in which pressure and motions are applied to the particles mechanically, which obviates the need for a carried gas. Liquid yields of 70-75% are achievable [27]. A second generation design, shown in figure 2.6 was built and is patented [28]. A different mechanical configuration was invented by PyTec, Germany, where solid wood boards are pressed by a piston against a rotating, vertically orientated, electrically heated disk. The operational pressure is within the range of 30-50 bar and the temperature employed is 700°C. Oil yields range between 55-70%. Based on these studies, a 6 t/d was built in 2006 and further testing is being carried out to increase the capacity to 50 t/d and assess for bio-oil upgrading feasibility. In the meanwhile, the bio-oil is used in a CHP plant [29].

Screw and auger reactors rely on mechanical apparatus to move the biomass instead of using a fluid. Heating is done either with heat carriers, such as hot sand, steel or ceramic balls, or instead, the screw or auger can be heated as well, normally by means of electric resistances. The major advantage of this reactor type is the ability to process a wide range of feed materials, such as heterogeneous biomass. As disadvantages, the residence time is considerably higher than for other reactor types (5-30s), ergo the liquid yield is negatively affected, and the resulting bio-oil has a high char content, which means that applications downstream for this product are more limited and since the char is mixed with the pyrolytic oil, is not possible to burn it in order to satisfy the heat demand of the pyrolysis process, hence, an alternative heat source is needed. The Karlsruhe Institute of Technology (KIT), has done extensive work on this type of reactors, and together with Lurgi, a subsidiary of Air Liquide, developed a twin-screw reactor and built a 500kg/h fast pyrolysis plant, and have since also built an entrained flow gasifier and gasoline synthesis facility, proving the whole process to be functional in November, 2014 [30][31].

The University of Laval together with Pyrovac, Canada, developed a vacuum pyrolysis system using a multiple hearth furnace that was later upgraded into a heated horizontal moving bed. The reactor is operated at a temperature range of 400-500°Cand 2-20 kPa [32], with liquid yields ranging from 35-50% and higher char yields when comparing to other fast pyrolysis systems. Heat transfer is the reaction rate limiting step. The advantage of operating at vacuum conditions is the ability to process larger particles than other fast pyrolysis systems, less oil contamination with

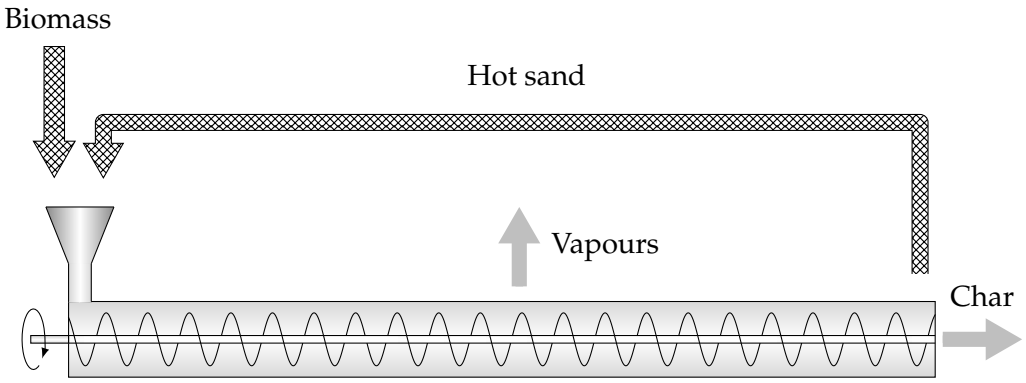

Figure 2.7: Screw/augor fast pyrolysis reactor concept.

char due to lower gas velocities and there's no need for a carrier gas. However, due to high costs related to the extreme vacuum conditions employed and complexity, the process ceased operation and no facilities using vacuum fast pyrolysis are known to be in operation. Bridgwater argues that this process, as described above, is not a true fast pyrolysis process because the heat rate applied to the biomass is much smaller than for other reactor designs, although the residence time is comparable [5].

Entrained flow reactors are well suited for gasification proposes, with the biggest suppliers of this kind of technology being Shell, GE Energy and Conoco Phillips, all used to convert coal into syngas. Nonetheless, these systems can also be used for pyrolysis, although not very successfully so far. Poor heat transfer between the biomass particles and the gas results in high gas flow demand, which in turn requires large equipment, increasing the capital cost of such installation, as well as complicating the separation processes downstream. Research done at the Georgia Tech Research Institute obtained oil yields between 30-50%, nonetheless the numerical model used for the reactor predicted a 60% maximum [33].

Microwave pyrolysis is a new concept that just recently started being developed. The way a sample is heated with microwaves is fundamentally different from all other pyrolysis processes. While in conventional heating, the exterior of the particle is heated first, and then propagates to the interior following transport phenomena laws, in microwave heating the opposite happens - heating starts in the interior of the particle and then propagates. This allows the vapours formed to escape through a lower temperature area. It requires a material with a high dielectric constant (e.g. water), and so in reality this material is the one that is responsible for the heating. The advantages of this pyrolysis type are the ability to deal with larger particles, a more uniform and selective heating, lower energy consumption and can be started and stopped immediately. As disadvantages, heat control is hard to achieve, microwaves have a penetration of about 1-2cm, which limits the particle size, although using particles in the range of centimetres is more than most technologies allow (e.g. for fluid beds, the particle size must be less than 2mm). Bio-oil yields are less than 40%.

2.3.2 Bio-oil upgrading

Pyrolysis bio-oil has some serious limitations when used directly as fuel - it can fuel burners to produce either heat or electricity via steam. Further processing is needed if a fuel with transporta-

tion quality is desired. Most of the studies in this area focus on catalytic upgrading methods, specially hydrodeoxygenation (HDO), which basically consists in using hydrogen that reacts with oxygen and converts the oxygenated components into hydrocarbons. These methods require a catalyst, and this severely limits the feasibility of these processes, since as of now, there are no catalysts that can operate for a long enough period of time to make industrial exploration possible (the benchmark is at least 4000 hours of operation without deactivating). However, a recent study conducted by Battelle in participation with DOE Bioenergy Technologies Office (BETO) managed to develop a catalyst that can operate for more than 1000 hours, which is still considerably far from the 4000 specification, however, in comparison with other studies, it's a ten fold increase in operation time, also referred to as Time On Stream (TOS) [34]. Steam reforming is another path to upgrade the bio-oil, but it suffers from the same problems as the HDO route regarding catalysts, plus high steam-to-carbon ratios and the fact that this is a highly endothermic reaction makes this route unlikely to become economically feasible in the near future.

There are also physical upgrading processes, such as filtration, solvent addition and emulsion. The filtration processes aim at reducing the ash content in the pyrolysis vapours to less than 0.01% and alkali content to 10 ppm, which is a much lower value than what can be achieved using only cyclones. This yields a higher quality bio-oil [35], since char catalyses secondary reactions, cracking the vapours which forms gaseous products, ergo reducing the liquid yield. The viscosity and average molecular weight decreases with reduction of solid particles. However, hot gas filtration long term operation has yet to be proven on an industrial scale a little work is being done in the area [5]. Solvent addition methods add a polar solvent, normally methanol, to prevent bio-oil ageing. This results in a more stable bio-oil, with as much as a 20 fold increase in storage time with 10%(wt.) methanol addition [36]. Bio-oil can also be emulsified into diesel fuels, with the aid of surfactants. Stable micro-emulsions containing between 5-30% bio-oil at CANMET and University of Florence, blends between 5-95% are being developed [37]. The drawbacks of this approach are the higher equipment corrosion, energy input and surfactant cost.

As mentioned before, catalytic upgrading is the most studied route to improve bio-oil quality. Biomass by itself has ash, which are inorganic components important to the plant's biological functions. In the highest amounts compared to other inorganics, potassium and sodium are responsible for cracking pyrolysis vapours and depending on the total ash content, this effect can b even greater than char induced cracking. Ash content can be reduced or controlled during plant's grow, however, the treatment methods available, such as washing, either with water or acid, have drawbacks that can easily make the process infeasible. Specifically, using water or acid will require a more energy intensive drying stage, hemicellulose and cellulose content can be lost if too severe conditions are used and if acid is used, it needs to be recovered and disposed of. If particularly low ash content biomass is used, levoglucosan can be produced in appreciable amount - this is promoted by vacuum conditions as well.

As for the actual upgrade into a proper biofuel there are several configurations one can use: separate pyrolysis and upgrading, most common configuration, which has advantages on its own, namely better fine tunning of each process stage, simpler unit design, operations and maintenance, and also something that is gaining momentum in the scientific community of the area and already referred in the introduction - decentralized pyrolysis with a larger scale centralized gasification plant; catalytic fast pyrolysis, where both the pyrolysis and upgrading are done in the same unit, allowing for better process economy and final product quality, although it might prove to be harder to operate, and to optimize specific parameters (since there are more process restrictions in place); partial upgrading and integration with current refinery infrastructure has potential of his own, since these units can provide the necessary scale and expertise to make a process of this

nature work in the best conditions possible, increasing its feasibility. The upgrading can also be a stand-alone project, although these represent higher investment risk, and due to the immature state of technology, is not advisable to go for a design of sorts. The upgrading can also vary in nature, that is, the fundamental principle and reactions that lead to the upgraded biofuel differ, which also results in different biofuel quality depending on process conditions employed. There are four main chemical pathways to produce biofuels:

- Hydrodeoxygenation (HDO);
- Steam reforming;
- Esterification;
- Gasification followed by Fisher-Tropsch or MTG.

As said before, HDO is the chemical removal of oxygen from the bio-oil molecules using hydrogen, which forms water. The resulting product can be used as a refinery feedstock without major equipment adaptations, if any. It employs high pressures (up to 20 MPa), moderate temperature (up to 400°C) and an hydrogen source (note that using fossil hydrogen will result in a less environment benign process). If the feedstock is fully hydrogenated, a naphta-like product is obtained, which can be conventionally refined. Using an external hydrogen supply gives a projected yield of about 25%(wt.) or 55% in terms of energy (hydrogen not included) [5]. If part of the biomass is gasified in order to supply the needed hydrogen, the yields drop to 15%(wt.) and 33% in energy. One has to note that the catalysts used when these studies started are commonly employed in the petrochemical industry, although, since oil and respective refining normally does not involve oxygenated species, specific catalysts that can process them are still lacking in development, e.g. when in comparison to sulfur-removing techniques. Nonetheless, sulfided CoMo and NiMo alumina or aluminosilicate supported catalysts spurred the development of HDO technologies in the 80's and 90's, with employed process conditions similar to desulfurisation of petroleum fractions. However, it was immediately noted that the higher water content degraded the catalyst support, as well as stripped the sulfur, requiring constant re-sulfurisation. This work was carried out by Elliot et al. at PNNL, USA and by Maggi et al. at UCL, Belgium (more information can be found elsewhere [38]). A recent design study was done by PNNL for a 2000 ton/day dry biomass capacity plant for the production of gasoline and diesel [39].

Table 2.5: Summary of important hydrotreatment studies for bio-oil upgrading.

	Country	Catalyst	Operation characteristics	Reference
PNNL	USA	Pd, Ru	Low temperature (up to 380°C)	[40]
Groningen U.	NL	Ru/C	Different levels of upgrading studied	[41]
Technical U. Munich	GER	Pd/C	"One pot" hydrogenation and hydrolysis	[42]
U. Science and Technology	China	Pd/ZrO_2 with SBA15	HDO, esterification and cracking in supercritical ethanol	[43]

All these processes require a substantial amount of hydrogen, and supplying this hydrogen is still a major shortcoming of this approach. Hydrogenation of organic fraction only allows the reforming of the aqueous phase, to which the hydrogen can be obtained. High pressures and

catalyst deactivation by coking are two major drawbacks to the implementation of these processes at a commercial scale.

Zeolite cracking consists in removing the oxygen in the bio-oil by producing CO_2 rather than water. The big advantage using this route is that there's no need for an hydrogen supply, since the bio-oil is actually reacting with an oxidizing species (normally oxygen). "The zeolite upgrading can operate on the liquid or vapours within or close coupled to the pyrolysis process, or they can be decoupled to upgrade either the liquids or re-vapourised liquids" [5]. Good liquid yields are obtained using HZSM-5 or ZSM-5 catalysts, however, these are prone to coking, acid number is too high and there are substantial formation of by-products, such as CO_2 and water.

Integrated approaches (pyrolysis and upgrading) have shown mixed results so far (there are commercial iterations that followed some of the presented studies), however, there are some studies that deserve mention, since it's a biomass treatment option that is gaining relevance, both academically and industrially. Huber and Dale developed a zeolite cracking one-step process using ZSM-5 which yielded gasoline, diesel, heating oil and aromatics [44]. High heating rates and catalyst-to-feed ratios are necessary and the residence time is about 2 min. A spin-off company was created following the success of this study, Anellotech. The upgraded fuel was branded Grassoline, and commercial feasibility has been demonstrated not only for gasoline and other biofuel related compounds but also for aromatics, such as benzene, toluene and xylene. Catalytic pyrolysis of biomass in a CFB was studied by CPERI in Greece, using zeolites and mesoporous catalysts. While upgrading was achieved, full de-oxygenation was not [45]. Agblevor (Virginia Polytechnic Institute & State University) developed a fractional pyrolysis process based on in bed catalysis, which has been patented [46]. While the concept of "one pot" processing is alluring, one must not forget that a single temperature must be used, which can limit yield optimization, and the catalyst must not suffer severe deactivation or mechanical deterioration caused by operation conditions. For zeolite catalysts, deactivation can be overcome by regeneration, and therefore it should be a key part of designing a unit of this nature.

Upgrading can be done directly to the pyrolysis vapours, which yields mostly aromatics, at a temperature around 450°Cand ambient pressure. The oxygen is removed by conversion into CO_2 and CO in a secondary oxidising reactor. The catalyst regeneration is also done in this reactor by burning out the deposited coke. A refinery FCC unit operates in a similar fashion, however, low H/C ratio limits process yield (20%(wt.) and 45% in energy) [47]. This process is attractive because it does not require hydrogen addition and can operate at ambient pressure. Plus, the coking problem can be overcome by catalyst regeneration, using a conventional FCC arrangement. However, the process is not competitive with fossil fuels [48].

Decentralized pyrolysis plants that feed into a larger central gasification plant is a concept that is getting increased attention (it has been referred before, in the introduction, BTL2 process). The goal is to increase the energy density by pyrolysis of biomass, which can then be transported much more efficiently into a large-scale gasification plant. This overcomes a serious logistics problem common to all BTL processes, and therefore allows for the use of entrained-flow gasifiers and economy of scale to greatly improve the feasibility of such processes, offsetting the small efficiency loss in not using bio-oil directly for upgrading. The possibility to use entrained flow gasifiers allows a better handling of the feed, since it's liquid and not solid biomass, costs are lower and gas quality is higher. KIT developed the bioliq® process, which is currently in operation and can produce a little under 100L/h of gasoline.

Bibliography

[1] D. Kunii and O. Levenspiel, *Fluidization Engineering*. Butterworth-Heinemann series in chemical engineering, Butterworth-Heinemann, 1991.

[2] D. Geldart, *Gas Fluidization Technology*. U.M.I., 1986.

[3] E. Vakkilainen, K. Kuparinen, and J. Heinimö, "Large industrial users of energy biomass," tech. rep., IEA Bioenergy, Lappeenranta, Finland, 9 2013.

[4] P. R. Patwardhan, *"Understanding the product distribution from biomass fast pyrolysis"*. PhD thesis, Iowa State University, Ames, Iowa, 2010.

[5] A. Bridgwater, "Review of fast pyrolysis of biomass and product upgrading," *Biomass and Bioenergy*, vol. 38, pp. 68 – 94, 2012. Overcoming Barriers to Bioenergy: Outcomes of the Bioenergy Network of Excellence 2003 – 2009.

[6] D. S. Scott and J. Piskorz, "The flash pyrolysis of aspen-poplar wood," *The Canadian Journal of Chemical Engineering*, vol. 60, no. 5, pp. 666–674, 1982.

[7] D. S. Scott and J. Piskorz, "The continuous flash pyrolysis of biomass," *The Canadian Journal of Chemical Engineering*, vol. 62, no. 3, pp. 404–412, 1984.

[8] D. S. Scott, J. Piskorz, and D. Radlein, "Liquid products from the continuous flash pyrolysis of biomass," *Industrial & Engineering Chemistry Process Design and Development*, vol. 24, no. 3, pp. 581–588, 1985.

[9] A. Liden, F. Berruti, and D. Scott, "A kinetic model for the production of liquids from the flash pyrolysis of biomass," *Chemical Engineering Communications*, vol. 65, no. 1, pp. 207–221, 1988.

[10] M. J. Antal and M. Grønli, "The art, science, and technology of charcoal production," *Industrial & Engineering Chemistry Research*, vol. 42, no. 8, pp. 1619–1640, 2003.

[11] Y. Sekiguchi and F. Shafizadeh, "The effect of inorganic additives on the formation, composition, and combustion of cellulosic char," *Journal of Applied Polymer Science*, vol. 29, no. 4, pp. 1267–1286, 1984.

[12] A. Bridgwater, "Principles and practice of biomass fast pyrolysis processes for liquids," *Journal of Analytical and Applied Pyrolysis*, vol. 51, no. 1–2, pp. 3 – 22, 1999.

[13] D. Shen, R. Xiao, S. Gu, and H. Zhang, "The overview of thermal decomposition of cellulose in lignocellulosic biomass," in *Cellulose - Biomass Conversion* (T. van de Ven and J. Kadla, eds.), pp. 193–226, InTech, 2013.

[14] A. Oasmaa, B. van de Beld, P. Saari, D. C. Elliott, and S. van Kruchten, "Update on standardisation of fast pyrolysis bio-oils from lignocellulosic biomass," *PyNe Newsletter*, no. 37, pp. 3–5, 2015.

[15] A. Robson, "Dynamotive 10 tpd facility in vancouver," *PyNe Newsletter*, pp. 1–2, May 2001.

[16] S. Gust and J. P. Nieminen, "Liquefied wood fuel could soon replace heavy oil!," *Wood Energy*, no. 6, pp. 24–25, 2002.

[17] M. R., "Wellman integrated fast pyrolysis pilot plant," *PyNe Newsletter*, no. 10, p. 12, 2000.

[18] C. A., R. C., and S. DS., eds., *Pyrolysis oil production and its perspectives*, (Espoo), Power production from biomass II, VTT, 1995.

[19] G. Trebbi, C. Rossi, and G. Pedrelli, "Plans for the production and utilization of bio-oil from biomass fast pyrolysis," in *Developments in Thermochemical Biomass Conversion* (A. Bridgwater and D. Boocock, eds.), pp. 378–387, Springer Netherlands, 1997.

[20] S. Müller, "Wellman integrated fast pyrolysis pilot plant," *PyNe Newsletter*, no. 27, pp. 11–12, 2010.

[21] B. Wagenaar, J. Kuipers, W. Prins, and W. van Swaaij, "The rotating cone flash pyrolysis reactor," in *Advances in Thermochemical Biomass Conversion* (A. Bridgwater, ed.), pp. 1122–1133, Springer Netherlands, 1993.

[22] "Fast pyrolysis test facilities." `http://www.btgworld.com/en/rtd/test-facilities/fast-pyrolysis`. Accessed: 31 August, 2015.

[23] G. Muggen, "Empyro project summary," *PyNe Newsletter*, no. 27, pp. 3–5, 2010.

[24] V. van de Beld and R. Meulenbroek, "Opening of the empyro fast pyrolysis plant," *PyNe Newsletter*, no. 37, pp. 3–5, 2015.

[25] J. Diebold and J. Scahill, *Production of Primary Pyrolysis Oils in a Vortex Reactor*, ch. 5, pp. 31–40.

[26] J. Lede, J. Panagopoulos, H. Z. Li, and J. Villermaux, "Fast pyrolysis of wood: direct measurement and study of ablation rate," *Fuel*, vol. 64, no. 11, pp. 1514 – 1520, 1985.

[27] G. Peacocke and A. Bridgwater, "Ablative plate pyrolysis of biomass for liquids," *Biomass and Bioenergy*, vol. 7, no. 1, pp. 147 – 154, 1994.

[28] A. Bridgwater, G. Peacocke, and N. Robinson, "Ablative thermolysis reactor," 2009. US Patent 7,625,532.

[29] D. Meier, S. Schoell, and H. Klaubert, "New ablative pyrolyser in operation in germany," *PyNe Newsletter*, no. 17, pp. 1,3, 2004.

[30] N. Dahmen, E. Henrich, E. Dinjus, and F. Weirich, "The bioliq® bioslurry gasification process for the production of biosynfuels, organic chemicals, and energy," *Energy, Sustainability and Society*, vol. 2, no. 1, 2012.

[31] Karlsruhe Institute of Technology, *bioliq®: Complete Process Chain Is Running*. 2014.

[32] C. Roy, B. Labrecque, and B. de Caumia, "Recycling of scrap tires to oil and carbon black by vacuum pyrolysis," *Resources, Conservation and Recycling*, vol. 4, no. 3, pp. 203 – 213, 1990.

[33] C. Gorton, R. Kovac, J. Knight, and T. Nygaard, "Modeling pyrolysis oil production in an entrained-flow reactor," *Biomass*, vol. 21, no. 1, pp. 1 – 10, 1990.

[34] Z. Abdullah, "Upgrading of biomass fast pyrolysis oil (bio-oil)," tech. rep., Battelle Memorial Institute, The address of the publisher, 3 2015.

[35] J. Diebold, J. W. Scahill, S. Czernik, S. Phillips, and C. Feik, "Progress in the production of hot-gas filtered biocrude oil at nrel," tech. rep., NREL, Springfield, Virginia, 5 1995.

[36] J. P. Diebold, , and S. Czernik, "Additives to lower and stabilize the viscosity of pyrolysis oils during storage," *Energy & Fuels*, vol. 11, no. 5, pp. 1081–1091, 1997.

[37] M. Ikura, S. Mirmiran, M. Stanciulescu, and H. Sawatzky, "Pyrolysis liquid-in-diesel oil microemulsions," Oct. 13 1998. US Patent 5,820,640.

[38] J. Blin, G. Volle, P. Girard, T. Bridgwater, and D. Meier, "Biodegradability of biomass pyrolysis oils: Comparison to conventional petroleum fuels and alternatives fuels in current use," *Fuel*, vol. 86, no. 17–18, pp. 2679 – 2686, 2007.

[39] S. Jones, J. Holladay, C. Valkenburg, D. Stevens, C. Walton, C. Kinchin, D. Elliott, and S. Czernik, "Production of gasoline and diesel from biomass via fast pyrolysis, hydrotreating and hydrocracking: A design case," tech. rep., PNNL, Springfield, Virginia, 2 2009.

[40] D. C. Elliott and T. R. Hart, "Catalytic hydroprocessing of chemical models for bio-oil," *Energy & Fuels*, vol. 23, no. 2, pp. 631–637, 2009.

[41] J. Wildschut, J. Arentz, C. Rasrendra, R. Venderbosch, and H. Heeres, "Catalytic hydrotreatment of fast pyrolysis oil: Model studies on reaction pathways for the carbohydrate fraction," *Environmental Progress & Sustainable Energy*, vol. 28, no. 3, pp. 450–460, 2009.

[42] C. Zhao, Y. Kou, A. Lemonidou, X. Li, and J. Lercher, "Highly selective catalytic conversion of phenolic bio-oil to alkanes," *Angewandte Chemie International Edition*, vol. 48, no. 22, pp. 3987–3990, 2009.

[43] Z. Tang, Q. Lu, Y. Zhang, X. Zhu, and Q. Guo, "One step bio-oil upgrading through hydrotreatment, esterification, and cracking," *Industrial & Engineering Chemistry Research*, vol. 48, no. 15, pp. 6923–6929, 2009.

[44] G. W. Huber and B. E. Dale, "Biofuels: Grassoline at the pump," vol. 301, pp. 52–59, July 2009.

[45] E. Iliopoulou, E. Antonakou, S. Karakoulia, I. Vasalos, A. Lappas, and K. Triantafyllidis, "Catalytic conversion of biomass pyrolysis products by mesoporous materials: Effect of steam stability and acidity of al-mcm-41 catalysts," *Chemical Engineering Journal*, vol. 134, no. 1–3, pp. 51 – 57, 2007.

[46] T. Carlson, G. Tompsett, W. Conner, and G. Huber, "Aromatic production from catalytic fast pyrolysis of biomass-derived feedstocks," *Topics in Catalysis*, vol. 52, no. 3, pp. 241–252, 2009.

[47] C. D. Chang, W. H. Lang, and A. J. Silvestri, "Synthesis gas conversion to aromatic hydrocarbons," *Journal of Catalysis*, vol. 56, no. 2, pp. 268 – 273, 1979.

[48] A. V. Bridgwater and M. L. Cottam, "Opportunities for biomass pyrolysis liquids production and upgrading," *Energy & Fuels*, vol. 6, no. 2, pp. 113–120, 1992.

Chapter 3

Simulation

In any simulation work, is it absolutely necessary to assess the hypothesis done to arrive at the results. Kinetic data is not without errors and deviations from reality, mostly due to the fact that there are also hypothesis and considerations being made to determine these experimental values, and so a reflection about the impact that these assumptions have on the accuracy of the provided data needs to take place, even if only for awareness sake. One has to notice that the underlying principles of the common employed techniques are relatively simple, and so prone to error. If on top of that, assumptions start being made to describe which in most of the cases are complex phenomenon, not at all well understood, which is the case of biomass pyrolysis, then it is almost mandatory to have a certain knowledge about the underlying principles of the techniques employed to retrieve the data used. After these considerations, a detailed description of the selected reaction schemes follows, as well as a description of the simulations carried out and respective objectives.

3.1 Kinetic parameters determination

The most employed technique used to determine kinetic data falls into the thermal analysis domain, since the rate of reaction is a function of temperature. Thermal analysis was formally initiated by Le Chatelier in 1887, although other scientists already had reported work that could be classified as a form of thermal analysis [1]. The definition of thermal analysis is quite controversial, the International Confederation for Thermal Analysis and Calorimetry (ICTAC) defines it as "the study of the relationship between a sample property and its temperature as the sample is heated or cooled in a controlled manner" [2] and the Handbook of Thermal Analysis and Calorimetry as "the measurement of a change in a sample property, which is the result of an imposed temperature alteration" [3]. The specific technique used for biomass pyrolysis kinetic data determination and suited for general solid-phase thermal degradation studies is thermogravimetric analysis (TGA). It consists in measuring the mass loss of a sample that is being subject of a temperature variation, and so it's adequate for thermal degradation processes like pyrolysis. This mass loss is monitored and plotted as a function of temperature or time (knowing the heating rate and considering that it is constant, these are interchangeable). If the derivative of mass loss as a function of time is used, then the technique is referred to as differential thermogravimetry (DTG), which provides the maximum reaction rate. More recently, these methods started being coupled with other methods to improve the results, specially qualitatively, such as mass spectrometry (MS), chromatography methods, mainly gas chromatography (GC) and high performance liquid chromatography (HPLC)

as well as Fourier transform infrared spectroscopy (FTIR) [4].

In order to associate any of the thermoanalytic data with kinetic data, a mathematical expression is needed, being the Arrhenius rate law almost exclusively used in the literature:

$$k(T) = A \exp\left(\frac{-E_a}{RT}\right) \tag{3.1}$$

where $k(T)$ is the reaction rate constant, T is the temperature in Kelvin, A is the frequency or pre-exponential factor, E_a is the activation energy and R is the universal gas constant. When considering an homogeneous medium, such as a gaseous reaction, both of the equation's constants have a physical correspondence that can be interpreted by the molecular collision theory. The activation energy, E_a can be interpreted as the energetic threshold necessary to overcome for the molecules to be close enough and therefore the reaction to happen. According to the transition state theory, the activation energy can be regarded as the difference between the energy of the molecules undergoing reaction and the mean energy contained in the reactants. The frequency factor represents, as the name suggests, the frequency to which the molecules collide with each other, and it's independent of the energy level of said molecules. And so, the exponential term in the equation 3.1 can be interpreted as the amount of collisions with sufficient energy to cause a reaction. Hence, the k(T) term can be regarded as the fraction of successful collisions, by successful, one means a collision that leads to reaction [4][5].

A pertinent question arises from this interpretation: is the Arrhenius equation adequate to model solid state reactions? In fact, it doesn't seem correct to apply an expression derived for homogeneous reactions to heterogeneous reactions. It was stated by Garn [6] that the deviations in kinetic data obtained for solid state thermal decomposition, such as biomass pyrolysis, may be caused exactly by an inadequacy in the used model, either for it not being applicable at all to solids, or due to rate expression not considering any solid parameters. Consequently, there is a chance that all of this data is just a consequence of force-fitting experimental data into a not at all adequate model and so, these parameters must be considered an approximation, at best, of the real phenomena that takes place when biomass is thermally decomposed. That said, and despite that there are other expressions to model processes that depend on temperature, there isn't an expression with the universal acceptance and physical correspondence that the Arrhenius rate law has. Also, if a different expression would be adopted, a recalculation of all the kinetic data pertaining heterogeneous reactions would have to be done, which would prove to be a tremendous effort. Ergo, as far as temperature dependent phenomena goes, the Arrhenius equation is the only one capable of modelling this type of behaviour and so, will probably continued to be used in the future for this propose, up until a better alternative is devised, if there's any [7].

In order to determine biomass pyrolysis kinetics under isothermal condition, the following expression is used:

$$\frac{d\alpha}{dt} = k(T)f(\alpha) = A \exp\left(\frac{-E_a}{RT}\right) f(\alpha) \tag{3.2}$$

where α represents the conversion or reaction extent, t the time, $\frac{d\alpha}{dt}$ the rate at which the isothermal process takes place, and $f(\alpha)$ is a function that is used to model the reaction and relates it to the controlling mechanism. The extent of reaction, which is the ratio of biomass decomposition, or volatiles produced, can be defined as:

$$\alpha = \frac{w_0 - w}{w_0 - w_f} = \frac{v}{v_f} \tag{3.3}$$

where w_0 is the initial sample mass, w is the sample mass at the instant t, w_f is the sample final mass, v is the volatiles mass at instant t and v_f is the final volatiles mass. The combination of A, E_a and $f(\alpha)$ is called the kinetic triplet, and is used to characterize biomass pyrolysis kinetics [8][9].

For non-isothermal conditions, with a linear heating rate, β, the following expression is used:

$$\frac{d\alpha}{dT} = \frac{d\alpha}{dt}\frac{dt}{dT} = \frac{1}{\beta}\frac{d\alpha}{dt} = \frac{1}{\beta}A\exp\left(\frac{-E_a}{RT}\right)f(\alpha) \tag{3.4}$$

With the basic equations introduced, an expression for $f(\alpha)$ is still lacking. For biomass pyrolysis specifically, it's normally assumed a first order reaction, which leads to power law type kinetics. Mathematically, it can be expressed as:

$$f(\alpha) = (1-\alpha)^n \tag{3.5}$$

with $n = 1$ for the first order case. The equation 3.2 or 3.4 is then integrated using a 4th order Range-Kutta method, and a non-linear regression is performed using the least square method to fit experimental data, in order to verify the predicted Arrhenius parameters.

It has been common practice to use isothermal methods to obtain kinetic data from solid state pyrolysis. In these methods, and as the name implies, the temperature is kept constant and several experiments are carried out, and this may repeated for other temperature values. One should note that in the initial steps of the experiment, the isothermal condition is not true, but degradation processes may already be taking place, which compromises the results and doesn't allow for high temperatures experiments, since it would imply a non negligible thermal decomposition period up to the point when the experiment temperature is reached [10]. Also due to the fact that these type of analysis require a substantial amount of effort to perform (several experiments to obtain different temperature data, necessary to keep the temperature constant at the specified value and minimize the non-isothermal period), non-isothermal methods started gaining relevance [9]. The advantage of the non-isothermal methods over the isothermal counterpart is the convenience in execution, since that with just a single experiment, one can obtain data that is temperature dependent, and varies continuously within the temperature range selected, while in isothermal techniques, a discrete set of temperature values must be selected. Non-isothermal methods are not without disadvantages though, proving to be more sensible to experimental noise, and more dependent on the model chosen, resulting in data of questionable quality if obtained from a single heating rate, which was common practice when this type of methodologies appeared. So, applying multiple heating rates is advised in order to bypass this shortcoming in accuracy [11]. The dependency of the reaction model is quite severe for non-isothermal methods because there's a force fitting of the data to the chosen model, and since temperature, T, and extension of reaction, α, vary simultaneously, it's virtually impossible to have a Arrhenius constant, $k(T)$, that is not heavily dependent on the model, $f(\alpha)$. This is normally referred to as "kinetic compensation effect", which means that regardless of the reaction model chosen, due to force-fitting, the Arrhenius equation's parameters will adjust to the experimental data, since these are the only degree of freedom in the equation, rendering the whole exercise a mathematical problem, that may not have any kind of physical meaning. Pursuant to this, the Arrhenius parameters obtained by these model-fitting approached tend to have a high degree of uncertainty [12].

In light of all said before, and as far as model-fitting techniques go, there are the isothermal methods, which provide quality data, independent of the kinetic model used, but with the major shortcoming that only a single global kinetic triplet can be obtained this way, which is a very

gross simplification of the reality, and severely limits the applicability of said methodology to describe biomass pyrolysis and non-isothermal methods, which are more prone to experimental noise and more dependent on the kinetic model used. Using different heating rates can reduce this dependency [10], and consequently increase the reliability of said methods, however, other temperature dependent processes can overlap in the thermogravimetric curves, which are hard to deconvolute [13]. In order to overcome the problems mentioned before, new methodologies started being developed.

This gave rise to what is called isoconversional methods, also referred to as "model-free" methods, due to the fact that the kinetic parameters, or rather the activation energy only, E_a, can be calculated without any model considerations, although that's not a very correct definition, because the kinetic model must be defined at some point. These methods all have the non-isothermal expression (equation 3.4) as a starting point, which renders these techniques non-isothermal as well, and as the name implies, assume that the conversion or extent of reaction, α, is constant and so, the reaction rate, $k(T)$ is a function of temperature only, not being necessary to delve into any *a priori* considerations regarding the kinetic model, $f(\alpha)$. Within isoconversional approaches, these can be divided into differential and integral, depending on how the thermogravimetric data is treated.

Friedman developed a differential isoconversional method in the 1964, which has much applicability still today and it will be the only differential method here described. Mathematically, the expression can be derived by applying natural logarithms to equation 3.4 [14]:

$$\ln\left(\frac{d\alpha}{dt}\right) = \ln\left[\beta\left(\frac{d\alpha}{dT}\right)\right] = \ln[Af(\alpha)] - \frac{E_a}{RT} \tag{3.6}$$

The conversion function, $f(\alpha)$, is considered to remain constant, which makes equation 3.6 effectively a linear expression of $\ln[d\alpha/dt]$ as a function of $1/T$. One is therefore able to determine the activation energy directly, since the slope of the plot equals to $-E_a/R$.

Ozawa in 1965 and Flynn and Wall in 1966 developed an integral isoconversional method that is known as Flynn–Wall–Ozawa (FWO) method where is assumed that the apparent activation energy remains constant throughout the reaction extension. Starting from equation 3.4 and integrating between zero and α for the first member of the equation and between zero and T_α (the temperature at conversion α) for the second member yields [15][16]:

$$g(\alpha) = \int_0^\alpha \frac{d\alpha}{f(\alpha)} = \frac{A}{\beta}\int_0^{T_\alpha} \exp\left(\frac{-E_a}{RT}\right) dT \tag{3.7}$$

If one defines $x = E_a/RT$, equation 3.7 becomes:

$$g(\alpha) = \frac{AE_a}{\beta R}\int_\alpha^\infty \frac{\exp^{-x}}{x^2} = \frac{AE_a}{\beta R}p(x) \tag{3.8}$$

where $p(x)$ represents what is referred as the temperature integral. This integral does not have an analytical solution, hence Doyle proposed an empirical interpolation of the expression [17][18][19]:

$$\log p(x) \approx -2.315 - 0.4567x, \text{ for } 20 \leq x \leq 60 \tag{3.9}$$

Substitution of Eq. 3.9 into Eq. 3.8 and applying logarithms yields:

$$\log \beta = \log \left(A \frac{E_a}{Rg(\alpha)} \right) - 2.315 - 0.4567 \left(\frac{-E_a}{RT} \right) \tag{3.10}$$

which is the integrated FWO expression. By plotting $\log \beta$ as a function of $1/T$, one gets parallel lines in accordance with the heating rate, for a fixed reaction extent. The activation energy, E_a can be determined by the slope of line and $\log A$ can be obtained by the interception with the y-axis. Yet another integral isoconversional method, called Kissinger–Akahira–Sunose (KAS) method is also commonly used, and it's similar to the FWO, but uses a different Doyle approximation for the temperature integral [20][21]:

$$\log(x) = \frac{\exp^{-x}}{x^2} \tag{3.11}$$

Substituting Eq. 3.11 into Eq. 3.8 and applying logarithms yields:

$$\ln \left(\frac{\beta}{{T_m}^2} \right) \approx -\frac{E_a}{R} \left(\frac{1}{T_m} \right) - \ln \left[\left(\frac{E_a}{AR} \right) \int_0^\alpha \frac{d\alpha}{f(\alpha)} \right] \tag{3.12}$$

where T_m is the temperature when the reaction reaches its maximum rate. The activation energy is determined by plotting $\ln(\beta/{T_m}^2)$ versus $1/T_m$.

The Coats and Redfern (CR) method falls within the non-isothermal model-fitting class, although some refer to it as a integral method, but an assumption about the kinetic model must take place to determine any type of data, and so, the first definition seems more correct. Starting from Eq. 3.8, the $p(x)$ term is approximated using a Taylor series expansion, resulting in the following expression [22][23]:

$$\ln \left(\frac{g(\alpha)}{T^2} \right) = \ln \left[\frac{AR}{\beta E_a} \left(1 - \frac{2RT}{E_a} \right) \right] - \frac{E_a}{RT} \tag{3.13}$$

For most cases, the reaction activation energy is between 80-260 kJ/mol, and so the term $2RT/E_a$ can be approximated to zero:

$$\ln \left(\frac{g(\alpha)}{T^2} \right) = \ln \left(\frac{AR}{\beta E_a} \right) - \frac{E_a}{RT} \tag{3.14}$$

By plotting $\ln[g(\alpha)/T^2]$ versus $1/T$, one can determine the E_a by the slope and the pre-exponential factor, A, by the intercept of the line with the y-axis. Although this method offers the simplicity of determining E_a and A with a single heating rate, it suffers from the same problems as any other model-fitting techniques: an assumption regarding the reaction model is necessary, and using a single thermogravimetric curve will result in convolution from other degradation phenomena, tainting the analysis. Owing to this disadvantage, a Modified Coats–Redfern (CR*) was created, which, like FWO and KAS, is a fully integral isoconversional technique. In order to archive this, a rearrangement of Eq. 3.13 is needed [24]:

$$\ln \left[\frac{\beta}{T^2(1 - 2RT/E_a)} \right] = -\frac{E_a}{RT} + \ln \left(\frac{AR}{g(\alpha)E_a} \right) \tag{3.15}$$

The left member is plotted versus $1/T$, with the slope being $-E_a/R$, and A is determined by substituting $-E_a/R$ in the intercept. Due to the fact that the left member is slightly dependent on E_a, an iterative approach is needed, by defining an initial value for the activation energy and then check for convergence.

The Vyazovkin (V) method, introduced by Vyazovkin and Dollimore, is a isoconversional non-linear technique, and uses a different expression for $p(x)$ [25]:

$$p(x) = I(E_a, T_\alpha) = \int_0^{T_\alpha} \exp\left(\frac{-E_a}{RT}\right) dT \tag{3.16}$$

The V method a set of n experiments at different heating rates is carried out, from β_i to β_j:

$$\sum_{i=1}^{n} \sum_{j \neq i}^{n} \frac{\beta_j I(E_a, T_{\alpha,i})}{\beta_i I(E_a, T_{\alpha,j})} = \Gamma(E_a) \tag{3.17}$$

where $I(E_a, T_{\alpha,i})$ and $I(E_a, T_{\alpha,j})$ are temperature integrals corresponding to heating rate β_i and β_j, respectively. By minimizing Eq. 3.17, is possible to determine the apparent activation energy, E_a. Alternatively, the Senum–Yang approximation to $p(x)$ can be used [26]:

$$p(x) = \left(\frac{\exp^{-x}}{x}\right)\left(\frac{x^3 + 18x^2 + 88x + 96}{x^4 + 20x^3 + 120x^2 + 240x + 120}\right) \tag{3.18}$$

All these integral methods have common shortcomings, however. The integral calculations are prone to errors due to necessary approximations to arrive at usable value, iterative methods are also sometimes needed, which increases the margin of error even more and the integral boundaries definition will temper with the results, specially if these are ill defined. Perhaps, the biggest shortcoming of isoconversional techniques is inability to directly determine the pre-exponential factor, A and the kinetic function $f(\alpha)$, which still requires the assumption of a reaction model. Flynn developed a methodology to separately calculate the frequency factor and the $f(\alpha)$ function, although it's only applicable to "nth order" expressions, $f(\alpha) = (1-\alpha)^n$, and other expressions that pass through the origin point (0,0), in a $\ln f(\alpha)$ vs. $\ln(1-\alpha)$ plot [27]. Flynn used a differential isoconversional method, and these seem to yield better results when compared to other integral counterparts. The differential technique approach is more susceptible to data noise, although with the computational capacities, smoothing and fitting tools of nowadays, together with a fast enough data collection rate, this issue can be minimized.

Despite all of what was said before, there are still problems that are transversal to all isoconversional methods. They are not suitable to describe either competing or concurrent reactions, which translates in a severe limitation, specially when trying to model complex reaction scheme such as biomass pyrolysis [28].

Other models do exist, although they are not as widespread as the ones described before. Balci et al. developed a deactivation model in which the frequency factor is multiplied by an activity factor, z, which in turn is a function of deactivation rate,γ, that is suitable to model lignocellulosic material pyrolysis, because it takes into consideration the heterogeneous nature of biomass by considering a variation in the active surface area that is reacting [29]:

$$k_{app} = z(\gamma)\left[A_i \exp\left(\frac{E_a}{RT}\right)\right] \tag{3.19}$$

A very interesting new type of models emerged and has been applying to fossil and biomass pyrolysis with promising results, referred to as distribution activation energy models (DAEM). This model assumes that there's a series of nth-order parallel reactions with different activation energies, which in turn constitute a continuous distribution function, $f(E)$. This difference should reflect the variations in the physicochemical properties that are common in a heterogeneous species

like biomass. The activation energy function, $f(E)$, is commonly approximated by the Gaussian distribution function. Although, this distribution is symmetrical, and the reactivity distributions tend to be asymmetrical, which is why Cai et al. suggests the use of the Weibull distribution to account for this. This procedure also allows for TGA curve deconvolution, although it requires the determination of parameters that are specific of the Weibull distribution itself [30].

3.2 Reaction mechanism developments

A sizeable effort has been made to describe pyrolysis at the microscopic level, which resulted in several publications describing reaction mechanisms and respective kinetics, that can be found in the area's literature. A brief review of these mechanisms follows, with special focus on innovative models that give good product predictions and somehow reflect the heterogeneous nature of biomass and consequently are more flexible and can be applied to various lignocellulosic materials. In order to characterize biomass, most of the devolatilization schemes divide it into three "pseudo-components": cellulose, hemicellulose and lignin. Pyrolysis models can be classified into three categories: global single-step, semi-global and multi-step [31][32][33][34]. With the exception of the global models, these categories can be further divided into concurrent (set of independent parallel reactions) or consecutive (also referred to as sequential) [35][36]. Combinations of these two approaches also exist [37][38][39][40]. Global single-step schemes, as the name implies, describe biomass decomposition with an overall reaction, which means that only one set of kinetic parameters is employed. These type of models can fit reasonable well experimental data, although they are specific to each biomass type and rely on a fixed mass ratio assumption between pyrolysis product classes (e.g. tar and char), hence, they are of limited application, since is not possible to predict product yield variations with process conditions. Besides, pyrolysis processes are complex mechanisms and therefore, a global description of these phenomena is oversimplifying [41][42]. Semi-global mechanisms try to counter some of the shortcomings of the global models by assigning different kinetics to the "lumped species", normally gas, tar and char. These may also include distinction between primary and secondary reactions, and be coupled with transport phenomena equations, which allows for good product yield prediction, specially for larger particles, where heat and mass transport limitations have a bigger impact on the reaction rate and good assessment of the influence of operation conditions on the process which allows for a better reactor design and comparison of different biomass species under the same conditions [43][44]. They are by far the most used and studied mechanism in literature. Multi-step models try to describe the pyrolysis process with several reactions, normally with concurrent and sequential combinations, that represent the various steps and mechanisms occurring during the biomass degradation. It is the most complex approach to the problem, but also the only way to predict single component yields, instead of lumped species, which is currently still lacking in the literature. The shallow understanding of the actual steps that take place during thermal degradation of biomass render the effort of obtaining models with good prediction value quite substantial.

One of the first attempts to obtain a comprehensive description of cellulose pyrolysis kinetics was carried out by Broido's research group, in 1971, in a 1000 hours experiment in vacuum conditions with high-purity cellulose at 226°C. The model accounts for an initial depolymerization of cellulose, where there's no weight loss, and consequently, the intermediate compound that results from this first step branches out and either is converted into volatiles (tar) or char, which undergoes a series of decomposition steps, also with volatiles release (see figure 3.1). The authors noted however that this mechanism contradicts other observations and fitting attempts for higher

temperatures were unsuccessful [45]. Despite all of this, it was the first model that clarified the existence of an activation step, previous to weight-losing reactions in cellulose pyrolysis.

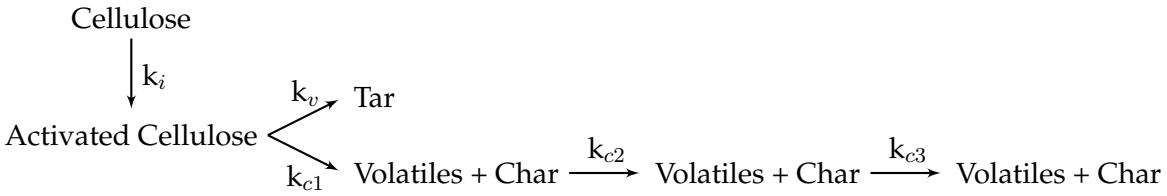

Figure 3.1: Broido's multi-step cellulose pyrolysis scheme (1971) [45].

Due to the limitations of the scheme in figure 3.1, Broido and Nelson proposed a more simple, two reaction, single-step, cellulose decomposition mechanism, where in one reaction, predominant at lower temperatures (<250°C) char and gas is produced, while at higher temperatures (>280°C), the second reaction is predominant [46]. This scheme was adapted from a likewise two reaction single-step mechanism for thermal degradation and ignition of paper sheets [47]. A later work by Suuberg et al. confirmed this hypothesis, specifying that an endothermic tar evaporation reaction happens at high heating rates (538J/g of volatiles) and an exothermic char formation reaction takes place at lower heating rates (2 kJ/g of char), although the determined temperature where the transition between the two reactions was higher (320°C), when compared to Broido and Nelson's work.

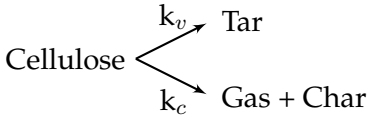

Figure 3.2: Broido and Nelson cellulose pyrolysis scheme (1975) [46].

Shafizadeh et al. noticed that for lower temperatures (259-295°C), the degradation of cellulose takes a significant amount of time, when compared to same experiments carried out at higher temperatures. In light of this evidence, it was concluded that a non weight loss, high activation energy step was taking place, and so the mechanism presented in figure 3.2 was modified to include an initial depolymerization step for cellulose, yielding a anhydro fragment, defined as "active cellulose" (similarly to Broido's scheme in figure 3.1. This mechanism is presented in figure 3.3 and is often referred to as Broido-Shafizadeh (B-S) model [48]. A similar mechanism with pseudo-zero-order kinetics for the activation step was theorized before [49].

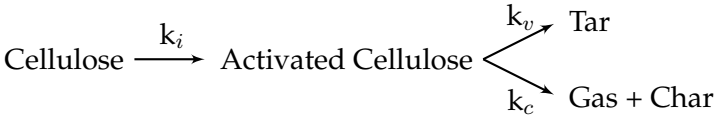

Figure 3.3: Broido-Shafizadeh (B-S) cellulose pyrolysis scheme (1979) [48].

Cooley and Antal argued that the sample size used in previous experiments was large enough to allow for heat and mass transfer limitations, and so TGA was performed to ash-free cellulose

with a sample size small enough to prevent transport phenomena influence, and the conclusion was that, under these conditions, a single-step reaction producing volatiles describes sufficiently well cellulose pyrolysis, which means that ash and heat and mass transfer limitations promote the creation of gas and char [50].

Thurner and Mann opted for a competing, parallel three reaction scheme, where primary and secondary reactions are all included, and that yield gas, tar and char separately [31]. Note that the authors applied this scheme to the whole biomass, and not to cellulose only:

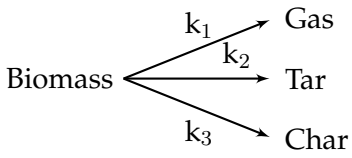

Figure 3.4: Thurner-Mann biomass pyrolysis scheme (1981) [31].

In an attempt to create a more generalized mechanism for biomass pyrolysis, Koufopanos et al. applied the (B-S) model to all three biomass "pseudo-components", cellulose, hemicellulose and lignin (all the "pseudo-components" follow the same reaction pathway) and added a secondary reaction step, where the char and volatiles produced in the primary steps react to give more volatiles and char. The global reaction rate is therefore the sum of the rates for these three components, assuming that there is no interaction between them. The hemicellulose reaction rate was considered equal to xylan decomposition rate, due to difficulties in isolating hemicellulose [39][51]:

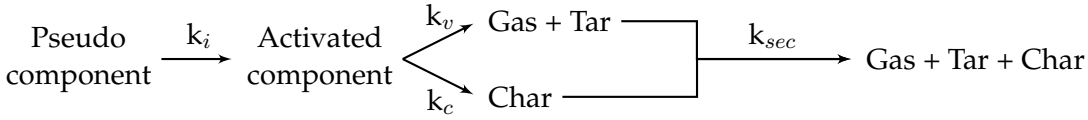

Figure 3.5: Koufopanos biomass pyrolysis scheme (1991) [51].

Miller and Bellan developed a mechanism very similar to Koufopanos, although, they modified the secondary reaction, where the tar decomposes without interaction with char [40]:

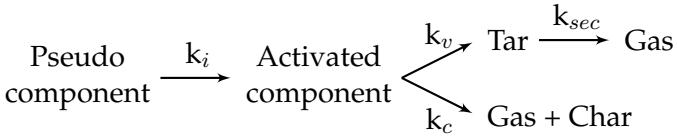

Figure 3.6: Miller-Bellan biomass pyrolysis scheme (1997) [40].

It can be seen that most of these schemes a few steps in common, namely the activation step, and that the later schemes tried to include secondary reactions, which involves tar decomposition into char and gases. Despite the progress done in the area, schemes with actual compounds as products are still scarce in the literature. These will be detailed in the next section.

3.3 Selected reaction schemes

Throughout the literature review carried out in the previous chapter, one can see that as far as kinetic models for biomass pyrolysis go, the knowledge of the actual reaction steps involved in this process are quite limited, with the bio-oil being classified in broad categories, such as gas, volatiles and char, also called "lumped species". While this knowledge is useful and paved the way for the development of new reactor designs, since the main interest in these studies was the maximization of the bio-oil yield, which in turn is dependent mostly on transport phenomena, specially heat transfer, there are drawbacks such as the inability to predict product yield variation and the fact that these models need to be derived for each biomass feedstock, and so a more detailed approach is needed when developing a process that makes use of the bio-oil downstream. The chemical composition of the bio-oil needs to be known in order to design any process downstream, being it upgrading or gasification. In the literature, the most accurate model that could be found was a competitive, multi-step and multi-component lumped kinetic scheme proposed by Ranzi et al. [52], in which the products are detailed in terms of chemical species rather than more broad categories such as gas, tar and char. The reason it is referred as lumped comes from the fact that the biomass composition is considered as a sum of cellulose, hemicellulose and lignin, which in turn are lumped components, representing a much larger variety of polymeric compounds. Although there are other more elaborated schemes, consisting in elemental reactions, such as the ones proposed by Zhou et al. [53][54], Seshadri et al. [55] or Faravelli et al. [56], these are specific to cellulose only, with the exception of the last one, which consists in a lignin de-volatilization scheme, also from the same research group as the biomass kinetic scheme proposed by Ranzi et al.. So, despite these schemes being more detailed, there's no scheme in the same level of detail for hemicellulose (none could be found in the literature), and each scheme consists in hundreds of reactions and dozens of compounds, which is overcomplicated for the purpose of the simulations carried out - the existing models for the processing done to the bio-oil downstream of the pyrolysis section are not as detailed and so it would require lumping some of the components modelled, effectively rendering the effort in characterizing the bio-oil pointless.

Due to the reasons stated above, the base kinetic scheme that is going to be used is the one proposed by Ranzi et al. in 2008, and so a brief description of the actual reactions and components involved follows. It's a multi-step de-volatilization model where the pseudo-components cellulose and hemicellulose are converted into activated species (coherent with what previous literature reported) which in turn react to form tar, char and gas; decompose into water and char or form saccharides (levoglucosan for cellulose and xylan for hemicellulose). Lignin, represented by a mixture of three reference components, named LIG-C, LIG-H and LIG-O, which are lignin monomers or building blocks rich in carbon, hydrogen and oxygen, respectively, has a more complex reaction scheme involving other three intermediate species, LIG-OH, LIG-CC and LIG. A schematic representation of the reaction scheme is presented in figures 3.7, 3.7 and 3.9.

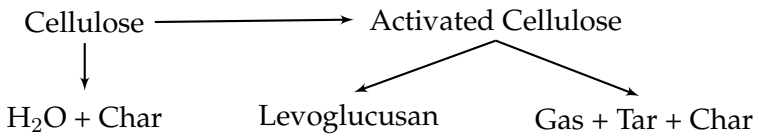

Figure 3.7: General reaction scheme for cellulose, as presented by Ranzi et al. [52].

Similarly to other schemes, no interaction between cellulose, hemicellulose or lignin is consid-

Table 3.1: Nomenclature used for the Ranzi et al. and Anca-Couce et al. reaction schemes, as presented in [57].

Abbreviation	Name	Atomic composition	CAS number
Solids			
CELL	Cellulose	$C_6H_{10}O_5$	9004-34-6
CELLA	Activated cellulose	$C_6H_{10}O_5$	
HCE	Hemicellulose	$C_5H_8O_4$	9014-63-5
HCEA1	Activated hemicellulose 1	$C_5H_8O_4$	
HCEA2	Activated hemicellulose 2	$C_5H_8O_4$	
LIG-C	Carbon-rich lignin	$C_{15}H_{14}O_4$	
LIG-H	Hydrogen-rich lignin	$C_{22}H_{28}O_9$	
LIG-O	Oxygen-rich lignin	$C_{20}H_{22}O_{10}$	
LIG-CC	Carbon-rich lignin 2	$C_{15}H_{14}O_4$	
LIG-OH	OH-rich lignin	$C_{19}H_{22}O_8$	
LIG	Lignin	$C_{11}H_{12}O_4$	
G{CO_2}	Trapped CO_2	CO_2	
G{CO}	Trapped CO	CO	
G{COH_2}	Trapped COH_2	COH_2	
G{H_2}	Trapped H_2	H_2	
Char	Char	C	7440-44-0
Tars			
HAA	Hydroxyacetaldehyde	$C_2H_4O_2$	141-46-8
GLYOX	Glyoxal	$C_2H_2O_2$	107-22-2
PROPNAL	Propanal	C_3H_6O	123-38-6
$C_3H_4O_2$	Propanedial	$C_3H_4O_2$	542-78-9
HMF	5-hydroxymethyl-furfural	$C_6H_6O_3$	67-47-0
LVG	Levoglucosan	$C_6H_{10}O_5$	498-07-7
XYL	Xylose monomer	$C_5H_8O_4$	
pCOUMARYL	Paracoumaryl alcohol	$C_9H_10O_2$	3690-05-9
PHENOL	Phenol	C_6H_6O	108-95-2
FE2MACR	Sinapaldehyde	$C_{11}H_{12}O_4$	4206-58-0
Gases			
H_2	Hydrogen	H_2	1333-74-0
CO	Carbon monoxide	CO	630-08-0
CO_2	Carbon dioxide	CO_2	124-38-9
CH_4	Methane	CH_4	74-82-8
CH_2O	Formaldehyde	CH_2O	50-00-0
MeOH	Methanol	CH_4O	67-56-1
C_2H_4	Ethylene	C_2H_4	74-85-1
CH_3CHO	Acetaldehyde	C_2H_4O	75-07-0
EtOH	Ethanol	C_2H_6O	64-17-5
H_2O	Water vapour	H_2O	7732-18-5

ered, although some authors argue that these interactions do occur, specially at high temperatures [58]. Five permanent gaseous species and 15 species that constitute the tar were selected to model the product distribution of the pyrolysis reaction. It is to note that there's no heterogeneous

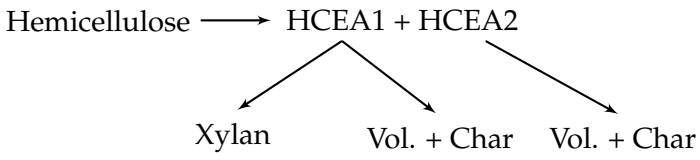

Figure 3.8: General reaction scheme for hemicellulose, as presented by Ranzi et al. [52].

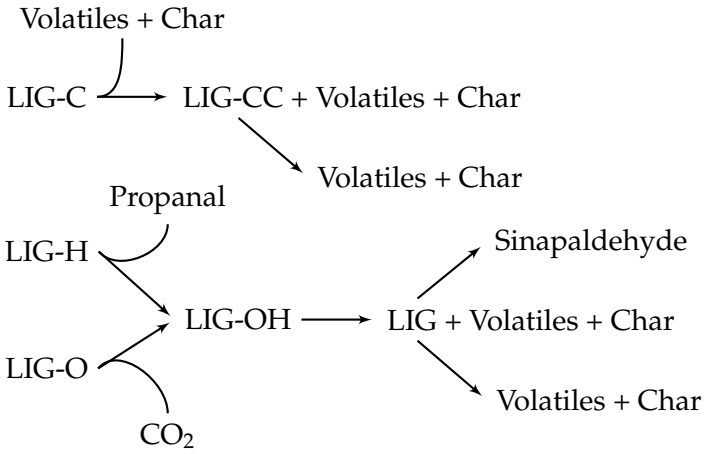

Figure 3.9: General reaction scheme for lignins, as presented by Ranzi et al. [52].

reactions in this scheme. Table 3.2 details all the reactions, plus their respective kinetic parameters.

Although Ranzi et al. kinetic scheme is the most detailed available in terms of individual components prediction, it may prove insufficient to describe the pyrolysis of certain lignocellulosic material. Also, one needs a term of comparison, not just with experimental data, but with other similar schemes, and so, a modified version of the original scheme, developed by Anca-Couce et al. was also considered [59]. The major differences in the modified mechanism consist the elimination of some activated species or intermediate compounds (activated cellulose, one of the two activated hemicelluloses and LIG - see table 3.2), the inclusion of a variable parameter, x, that modifies stoichiometric coefficients, and it represents the extent of secondary reactions taking place, and the elimination of sugar producing reactions, due to disparities with experimental values versus original model predictions. Is important to note that the data regarding saccharides yield is very variable in the literature. Levoglucosan (LVG), which is by far the sugar produced in largest amount, has reported yields that can go from 20% to 60% in weight, for pure cellulose at low temperature and vacuum conditions [60]. Although, when using wood or other lignocellulosic substrate, the yields decrease considerably, being less than 5% for pyrolysis in similar conditions and between 1% and 2% for fast pyrolysis [61]. The reason this disparity happens is related to operation conditions as well as inorganic content of the pyrolysis substrate. Richards et al. performed a very thorough study on the influence of metal ions and salts on the pyrolysis product yields, and concluded that alkali and Ca^{2+} ions hindered LVG formation, while transition metals, specially Fe^{3+} and Cu^{2+} promoted the saccharide yield [62]. In the same study, a wood sample, pretreated with acid and adsorbed in a $FeSO_4$ solution, subjected to atmospheric pyrolysis yielded 1.4% LVG, which corroborates Piskorz et al. [61] findings. Piskorz et al. also denoted a major

Table 3.2: Reaction scheme for biomass pyrolysis proposed by Ranzi et al.. G{CO_2}, G{CO}, G{COH_2} and G{H_2} are gas species trapped in the metaplast.

	Reaction			A (s^{-1})	E_a (kJ mol^{-1})
1	CELL	→	CELLA	8x10^{13}	192.5
2	CELLA	→	0.95HAA + 0.25GLYOX + 0.2CH_3CHO + 0.2PROPNAL + 0.25HMF + 0.16CO_2 + 0.23CO + 0.9H_2O + 0.1CH_4 + 0.61Char	1x10^9	125.5
3	CELLA	→	LVG	4T	41.8
4	CELL	→	5H_2O + 6Char	8x10^7	133.9
5	HCE	→	0.4HCEA1 + 0.6HCEA2	1x10^{10}	129.7
6	HCEA1	→	0.75G{H_2 + 0.8CO_2 + 1.4CO + 0.5CH_2O + 0.25MeOH + 0.125EtOH + 0.125H_2O + 0.625CH_4 + 0.25C_2H_4 + 0.675Char	3x10^9	113.0
7	HCEA1	→	XYL	3T	46.0
8	HCEA2	→	0.2CO_2 + 0.5CH_4 + 0.25C_2H_4 + 0.8G{CO_2} + 0.8G{COH_2} + 0.7CH_2O + 0.25MeOH + 0.125EtOH + 0.125H_2O + Char	1x10^{10}	138.1
9	LIG-C	→	0.35LIG-CC + 0.1pCOUMARYL + 0.08PHENOL + 0.41C_2H_4 + H_2O + 0.495CH_4 + 0.32CO + G{COH_2} + 5.735Char	4x10^{15}	202.9
10	LIG-H	→	LIG-OH + PROPNAL	2x10^{13}	156.9
11	LIG-O	→	LIG-OH + CO_2	1x10^9	106.7
12	LIG-CC	→	0.3pCOUMARYL + 0.2PHENOL + 0.35$C_3H_4O_2$ + 0.7H_2O + 0.65CH_4 + 0.6C_2H_4 + G{COH_2} + 0.8G{CO} + 6.4Char	5x10^6	131.8
13	LIG-OH	→	LIG + H_2O + MeOH + 0.45CH_4 + 0.2C_2H_4 + 1.4G{CO} + 0.6G{COH_2} + 0.1G{H_2} + 4.15Char	3x10^8	125.5
14	LIG	→	FE2MACR	8T	50.2
15	LIG	→	0.2PROPNAL + 0.2CH_2O + 0.4MeOH + 0.2CH_3CHO + H_2O + 0.5CO + 0.6CH_4 + 0.65C_2H_4 + G{CO} + 0.5G{COH_2} + 5.5Char	1.2x10^9	125.5
16	G{CO_2}	→	CO_2	1x10^5	100.4
17	G{CO}	→	CO	1x10^{13}	209.2
18	G{COH_2}	→	CO + H_2	5x10^{11}	272.0
19	G{H_2}	→	H_2	5x10^{11}	313.8

increase in LVG yield (more than 30%) when pre-treating cellulose with a sulphuric acid wash [63]. Van der Kaaden studied the effect of the matrix pH of amylase on the types of products obtained by Curie-point pyrolysis. He concluded that alkaline matrices favour the production of carbonyl compounds, acids and lactones, while acidic matrices promote the yield of anhydrosugars, such as LVG, and other hexoses [64]. Radlein et al. conducted a study where it was determined that LVG yield has a maximum at around 530°C[65], which is in agreement with Shen et al. work [66] while Liao reported a higher maximum yield (580°C) [67].

The main conclusion that can be taken from these studies is that levoglucosan is an important compound in cellulose pyrolysis, and that despite its production being hindered by fast pyrolysis conditions and substrate interactions, it doesn't necessarily means that is not an important intermediate compound in cellulose pyrolysis (and virtually all studies referenced earlier point towards this conclusion as well). Consequently, the removal of the saccharide producing reactions by Anca-Couce et al., while a practical solution to arrive at results that match experimental data,

may be overlooking the true nature of these type of phenomena. The same can be said about the removal of the activated cellulose, since there's plenty of evidence, given in previous section, that corroborate the existence of a no-weight-loss step for cellulose pyrolysis. The interesting modification is therefore in the x parameter, which can be used to account for inorganic material influence, which is a degree of freedom that does not exist in other models, and can have a major impact on the results, ergo the model will be tested in this work. Details of Anca-Couce's reaction mechanism follows.

Table 3.3: Reaction scheme for biomass pyrolysis proposed by Anca-Couce et al. [59].

	Reaction			A (s^{-1})	E_a (kJ mol^{-1})
1	CELL	→	(1 - x_1) * (0.95HAA + 0.25GLYOX + 0.2CH_3CHO + 0.2PROPNAL + 0.25HMF + 0.16CO_2 + 0.23CO + 0.9H_2O + 0.1CH_4 + 0.61Char) + x_1 * (5.5Char + 4H_2O + 0.5CO_2 + H_2)	8x10^{13}	192.5
5	HCE	→	0.4 * [(1 - x_5) * (0.75G{H_2 + 0.8CO_2 + 1.4CO + 0.5CH_2O + 0.25MeOH + 0.125EtOH + 0.125H_2O + 0.625CH_4 + 0.25C_2H_4 + 0.675Char) + x_5 * (4.5Char + 3H_2O + 0.5CO_2 + H_2)] + 0.6HCEA2	1x10^{10}	129.7
8	HCEA2	→	(1 - x_8) * (0.2CO_2 + 0.5CH_4 + 0.25C_2H_4 + 0.8G{CO_2} + 0.8G{COH_2} + 0.7CH_2O + 0.25MeOH + 0.125EtOH + 0.125H_2O + Char) + x_8 * (4.5Char + 3H_2O + 0.5CO_2 + H_2)	1x10^{10}	138.1
9	LIG-C	→	0.35LIG-CC + 0.1pCOUMARYL + 0.08PHENOL + 0.41C_2H_4 + H_2O + 0.495CH_4 + 0.32CO + G{COH_2} + 5.735Char	4x10^{15}	202.9
10	LIG-H	→	LIG-OH + PROPNAL	2x10^{13}	156.9
11	LIG-O	→	LIG-OH + CO_2	1x10^{9}	106.7
12	LIG-CC	→	(1 - x_{12}) * (0.3pCOUMARYL + 0.2PHENOL + 0.35$C_3H_4O_2$ + 0.7H_2O + 0.65CH_4 + 0.6C_2H_4 + G{COH_2} + 0.8G{CO} + 6.4Char) + x_{12} * (14.5 Char + 3H_2O + 0.5CO_2 + 4H_2)	5x10^{6}	131.8
13	LIG-OH	→	H_2O + MeOH + 0.45CH_4 + 0.2C_2H_4 + 1.4G{CO} + 0.6G{COH_2} + 0.1G{H_2} + 4.15Char + [(1 - x_{13}) * (y_{13} * FE2MACR + (1 - y_{13}) * (0.2PROPNAL + 0.2CH_2O + 0.4MeOH + 0.2CH_3CHO + H_2O + 0.5CO + 0.6CH_4 + 0.65C_2H_4 + G{CO} + 0.5G{COH_2} + 5.5Char)) + x_{13} * (10.5Char + 3H_2O + 0.5CO_2 + 3H_2)]	3x10^{8}	125.5
			y_{13} = 3.6800E-11 * T^5 + 8.2619E-8 * T^4 + 6.8901E-5 * T^3 + 2.6124E-2 * T^2 + 4.5911 * T + 4.0398E2; T in (°C)		
16	G{CO_2}	→	CO_2	1x10^{5}	100.4
17	GCO	→	CO	1x10^{13}	209.2
18	G{COH_2}	→	CO + H_2	5x10^{11}	272.0
19	G{H_2}	→	H_2	5x10^{11}	313.8

One notices in table 3.3 that in the reaction 13, relative to the decomposition of LIG-OH, there's a parameter, y_{13}, which hasn't been referenced before. This is due to the fact that is not possible in Aspen Plus to have stoichiometric coefficients as a function of temperature, not without a user model, as a result, the LIG component was also used in this mechanism, as well as reaction 14, where LIG is decomposed into sinapaldehyde (FE2MACR) from Ranzi's scheme (see table 3.2). This way, the FE2MACR production is still dependent on temperature, and the scheme can be studied using only "native" Aspen Plus features.

Another aspect, present in both schemes, is the trapped species. These are gaseous species that are trapped within the biomass solid structure and are released afterwards, according to kinetics in reactions 16-19, for both schemes. Anca-Couce et al. study also involves simulation of the proposed modified mechanism, and the authors of said work classify the unreacted trapped species as the char, as well as the intermediate compound LIG-CC. While this seems a reasonable assumption, and will be simulated for comparison sake, considering the unreacted solid compounds as char is also a valid approach, and will also be considered. In this last case, there's no trapped species - these are assumed to be in gaseous phase immediately after being formed - and consequently there are no reactions 16-19 either.

Both mechanisms use an identical lignin reaction pathway, and it has been specified by Ranzi et al. how to determine the amounts of each lignin reference component - LIG-C, LIG-H and LIG-O [68]. This methodology is based on an atom balance for carbon, hydrogen and oxygen, meant to be used when no other information about the biomass sample is available, namely the cellulose, hemicellulose and lignin contents. Since there are only three elemental balance equations, there can only be determined three unknowns, ergo, three mixtures of the five pseudo-components is used to make up for this shortcoming, and the biomass is then classified in terms of a linear combinations of these five compounds. The molar ratios used for each mixture are 60% cellulose plus 40% hemicellulose (M1), 20% LIG-C plus 80% LIG-O (M2), and 20% LIG-C plus 80% LIG-H (M3). The mixture ratios can be altered if the sample has unusual contents of hydrogen, carbon or oxygen, but even so, there is the possibility of the balance not having a solution, as it is the case of Amutio et al. biomass types [69]. As explained in the introduction, valorization through pyrolysis of these forest resources presents several advantages, and so it is important to be able to represent these lignocellulosic substrates somehow. With that in mind, the lignin reference components and subsequent products were taken in consideration and compared to experimental data in order to determine which compound is more suitable to represent a specific type of biomass (e.g. hardwoods, softwoods). LIG-C reaction leads to the formation of LIG-CC, which in turn leads to paracoumaryl alcohol formation, as well as phenol, while both LIG-H and LIG-O produce LIG-OH, which decomposes into LIG, which in turn forms sinapaldehyde. These three components - paracoumaryl alcohol, phenol and sinapaldehyde - represent the "phenolic share" within bio-oil composition.

Faravelli's study has a sizeable compendium of lignin ultimate analysis and respective reference component molar composition in terms of LIG-C, LIG-H and LIG-O sorted by wood type [56], which is presented in table 3.4. In said work, one can see that the amount of LIG-C has a trend to go progressively down, this coincides with biomass samples that are classified as softwood, which archive the highest content in LIG-C and hardwoods reporting a lower or even non existent LIG-C content (LIG-O content is the highest for hardwoods, LIG-H has a somehow high variability, and so is not possible to state with a good degree of certainty that is dependent on the wood type). Lignin is a complex polymer that is often described by the constituent monolignols (phytochemicals used by the plants to biosynthesize lignin), which are different according to wood type. One can try to assume that the variation in LIG-C/LIG-O reflects this difference in the nature of the wood samples. Following this line of thought, it is known that softwood lignin is mainly composed of guaiacyl units, while hardwood lignin also has syringyl units [70]. One could assume that LIG-C is an equivalent of the monolignol coniferyl alcohol (prevalent in softwoods and responsible for the guaiacyl units), LIG-O is the equivalent of the sinapyl alcohol (responsible for the syringyl units), commonly found in hardwoods, and LIG-H is paracoumaryl alcohol, the last monolignols that comprises almost exclusively grass lignin [71]. However, LIG-C eventually leads to the formation of paracoumaryl alcohol (see tables 3.2 and 3.3), while both LIG-H and

Table 3.4: Elemental analysis of lignins from different wood species and respective composition in terms of reference components [56].

	C (wt.)	H (wt.)	O (wt.)	LIG-C (mol)	LIG-H (mol)	LIG-O (mol)	Wood type
Pseudotsuga	0.648	0.058	0.294	0.7447	0.1376	0.1177	Softwood
Picea sylvestris	0.640	0.060	0.300	0.6372	0.2670	0.0958	Softwood
Thuja plicata	0.638	0.061	0.301	0.5993	0.3296	0.0711	Softwood
Picea mariana	0.637	0.063	0.300	0.5504	0.4494	0.0002	Softwood
Larix occidentalis	0.637	0.061	0.302	0.5896	0.3329	0.0775	Softwood
Tsuga heterophylla	0.634	0.063	0.303	0.5198	0.4609	0.0193	Softwood
Picea abies	0.634	0.060	0.306	0.5794	0.2856	0.1350	Softwood
Arachis hypogaea	0.631	0.057	0.312	0.6075	0.1272	0.2653	Hardwood
Metasequoia	0.629	0.059	0.312	0.5494	0.2442	0.2064	Softwood
Dalbergia melanoxylon	0.627	0.058	0.315	0.5491	0.1934	0.2574	Hardwood
Dalbergia granadillo	0.625	0.060	0.315	0.4881	0.3149	0.1970	Hardwood
Pinus ponderosa	0.625	0.060	0.315	0.4881	0.3149	0.1970	Softwood
Millettia laurentii	0.623	0.057	0.320	0.5288	0.1483	0.3229	Hardwood
Afzelia sp.	0.623	0.056	0.321	0.5486	0.0926	0.3588	Hardwood
Tieghemella heckelii	0.611	0.058	0.331	0.3797	0.2418	0.3785	Hardwood
Manilcara sp.	0.607	0.059	0.334	0.3106	0.3166	0.3728	Hardwood
Entandrophragma cylindricum	0.606	0.058	0.336	0.3226	0.2581	0.4194	Hardwood
Acer macrophyllum	0.604	0.057	0.339	0.3228	0.2034	0.4738	Hardwood
Fagus sylvatica	0.603	0.063	0.334	0.1600	0.5959	0.2441	Hardwood
Juglans regia L.	0.604	0.059	0.337	0.2749	0.3274	0.3977	Hardwood
Miscanthus	0.602	0.058	0.340	0.2753	0.2716	0.4532	Hardwood
Olea sp.	0.601	0.059	0.340	0.2384	0.3384	0.4232	Hardwood
Populus tremuloides	0.600	0.061	0.339	0.1743	0.4737	0.3520	Hardwood
Caesaeia paecox	0.600	0.059	0.341	0.2260	0.3422	0.4318	Hardwood
Prunus serotina	0.597	0.059	0.344	0.1883	0.3536	0.4580	Hardwood
Eucalyptus	0.592	0.063	0.345	0.0098	0.6522	0.3380	Hardwood
Liriodendrum tulipifera	0.584	0.058	0.358	0.0432	0.3378	0.6190	Hardwood
Liquidambar styraciflua	0.576	0.056	0.368	0.0000	0.2299	0.7701	Hardwood

LIG-O lead to sinapaldehyde formation. So there is no guaiacol production, even though this is a product resulting from lignin guaiacyl units, present in all wood types. Also, according to this mechanism, one would get high amounts of sinapaldehyde for hardwoods, which is reasonable, but no guaiacol, since there's no component of sorts in the scheme, and softwoods would register an abnormal high amount of paracoumaryl alcohol, which is not at all expected. Therefore, this scheme fails to represent the true nature of the lignin polymer. Table 3.4 presents Faravelli's table, adding the classification of wood types in terms of softwood or hardwood, where it's clear that the reference components don't relate to guaiacyl, sinapyl or coumaryl units of lignin, specially in the case of *Dalbergia granadillo* and *Pinus ponderosa*, that have the same ultimate composition, and therefore have the same molar content in reference lignin components, despite de fact that one is a hardwood and the other a softwood. In light of this fact, one can see that the methodology proposed to determine the reference lignin components is merely solution to a mathematical problem, hence it begs the question: is it necessary to use such a complex scheme to model lignin pyrolysis? The author of the mechanism doesn't delve very deeply into detailing why this mechanism for lignin was adopted, perhaps because there's little information and experimental

data to really understand the pyrolysis of this complex polymer.

3.4 Aspen Plus considerations

This section intends to detail on how exactly the simulations were performed, presenting some problems encountered while introducing the necessary data (e.g. component properties, unit operation specifications or convergence parameters), and providing the solutions to overcome these difficulties. The solutions found may not be the best, since they may and probably will influence the obtained results negatively, hence, all the "workarounds" need to be clearly stated, so that an eventual source of error can be expeditiously identified. This section is also intended to shed some light on specific procedures needed to carry a simulation of this nature, since the only work that could be found in literature employing a fast pyrolysis operation unit, on this level of detail in an Aspen Plus simulation was a study carried out by Shemfe et al. [72], which consists in a techno-economic assessment of both the pyrolysis plant, as well as a bio-oil upgrading plant, and the authors are oblivious about quite a few aspects regarding the simulation. While in the future, better models will undoubtedly be developed, a common ground, a simulation backbone is needed for there to be more progress in this area, which has a substantial potential unexplored.

3.4.1 Properties

Choosing an appropriate thermodynamic property method is crucial to obtain good and meaningful results. The physical property method selected will influence both thermodynamic properties of the considered components, as well as any transport phenomena modelled in the unit operations. The criteria contemplated to select any particular method are process conditions (e.g. state variables, such as temperature and pressure) and components involved in the simulation. Unfortunately, up until the making of this study, no Aspen Plus property method specifically designed for thermochemical processing of lignocellulosic material has been developed. NREL developed a biofuels property database, where some key biomass pseudo-components are represented (namely cellulose, hemicellulose and lignin, as well as various saccharides) [73]. However, this database seems to be more adequate for biochemical processing of biomass rather then thermochemical conversion due to the high number of saccharides represented, as well as enzymes. Nonetheless, hemicellulose (xylan) properties from this database were used in this work.

Property methods can be classified as activity coefficient or equation of state based. Due to the complex nature of the bio-oil, which results in highly non-linear behaviour of the simulated components and interactions between component classes, Onarheim et al. argues that an activity coefficient method is better suited, since it can account for mixture deviations to ideal state (fugacity higher than one - $\gamma > 1$) and it can also handle supercritical components such as the gases involved in the process by adaptation of Henry's law [74]. Aspen Physical Property System help also recommends the use of an activity-coefficient-based method if polar and non polar components at low pressures are present, which is the case. The UNIQUAC model fits this description, since it can describe virtually any polar and non-polar combination of compounds up to strongly nonideal liquid solutions such as bio-oil. On top of this method, equations of state (EOS) can be used to correct vapour phase phenomena (Poynting correction is applied - dimerization degree is evaluated based on the compressibility factor, Z). Available EOS to use with this method include Redlich-Kwong, Hayden-O'Connell and Nothnagel. The later (UNIQ-NTH) can model dimerization in the vapour phase, such as acetic acid gas-phase association that happens

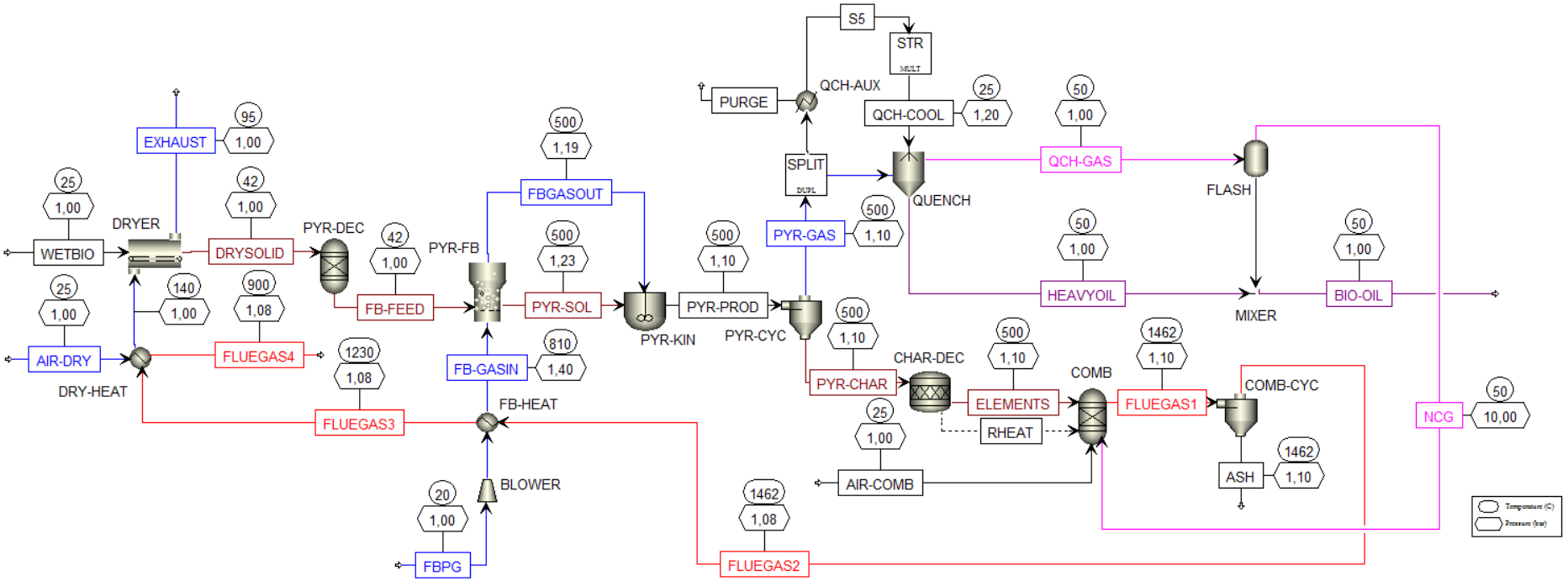

Figure 3.10: Process flow diagram as seen in Aspen Plus.

at high temperatures (this affects vapour-liquid equilibrium). However, UNIQ-NTH method requires several additional input specifications that simple are not possible to determine or retrieve from literature, therefore, other method was considered. Peng-Robinson with Boston-Mathias modification method (PR-BM) is adequate in moderate to high temperatures, and often used to model oil & gas processing, which fast pyrolysis process approximates to. One must note that this is an equation of state method, not an activity coefficient method, but despite this, this was the chosen method, because is more flexible in the applicable temperature range, and does not require additional inputs. A study conducted by the NREL and PNNL also used this method for their fast pyrolysis techno-economical assessment [75]. The binary interaction parameters were estimated using the UNIFAC-DMD method, in which all conventional components were included. The Dortmund databank (DMD) was used because is the most complete available within Aspen Plus.

Biomass and ash was modelled as a non-conventional solid, with the methods used to determine heat capacity and molar volume being HCOALGEN and DCOALIGT, respectively. The trapped species were represented as regular solid components (details on how key properties were determined is below). The NREL database was used to retrieve properties of hemicellulose and respective sugar, xylan [73]. Other details regarding the components are presented in table 3.5.

When introducing new solid components in Aspen Plus, there are two required properties that need to be defined (other than molecular formula/weight) - heat capacity and molar volume. This can prove to be a difficult task if one does not have any information about said compound, which is the case for all the lignin reference components and reaction intermediates as well as trapped species. Blondeau and Jeanmart provided key information regarding this aspect of the kinetic scheme, namely the molecular formula for the intermediates LIG-OH, LIG-CC and LIG, as well as an expression for the heat capacity of biomass, char, tar, gas and air (see table 7 from [57]). The char correlation was used to estimate the heat capacity of the trapped species, since these are considered as char anyway, and is presented in equation 3.20.

$$C_{p,char} = 1430 + 0.355T - 7.3210^{7}T^{-2} \tag{3.20}$$

Equation 3.20 was introduced as an Aspen solid heat capacity polynomial (CPSPO1), for which the full mathematical expression is (one can see by comparison between Eqs. 3.20 and 3.21 that only $C_{1,i}$, $C_{2,i}$ and $C_{5,i}$ are non-zero elements):

$$C_{p,i}^{*,s} = C_{1,i} + C_{2,i}\,T + C_{3,i}\,T^2 + \frac{C_{4,i}}{T} + \frac{C_{5,i}}{T^2} + \frac{C_{6,i}}{\sqrt{T}} \text{ for } C_{7,i} \geq T \geq C_{8,i} \tag{3.21}$$

Regarding the lignin components, using the biomass relation would be the most correct approach (see equation 3.22, although Aspen Plus built-in property models don't have any expression to calculate solids heat capacity which involves exponentials, hence for the lignin components the heat capacity expression was calculated outside of Aspen environment, and introduced in Property Setup as a data set (Data>New>PURE-COMP), creating a dedicated, discrete set of heat capacity values for each lignin component.

$$C_{p,biomass} = 2300 - 1150\exp(-0.0055T) \tag{3.22}$$

To determine molar volumes, there are two approaches that vary according to the component in question: the lignin segments can be considered polymers and so a polymer contribution group for molar volume can be used - the one used in this work is presented in van Krevelen's work [76]:

Table 3.5: Aspen Plus component table for Ranzi et al. and Anca-Couce et al. simulations.

Component ID	Type	Component Name	Alias
SIO2	Solid	SILICON-DIOXIDE	SIO2
N2	Conventional	NITROGEN	N2
O2	Conventional	OXYGEN	O2
DRYBIO	Nonconventional		
ASH	Nonconventional		
CELLULOS	Solid	CELLULOSE	CELLULOSE
HCE	Solid	XYLAN	C5H8O4-U
HCEA2	Solid	XYLAN	C5H8O4-U
LIG-C	Solid		C17H17O5
LIG-O	Solid		C20H23O10
LIG-H	Solid		C22H29O9
LIG-CC	Solid		C15H15O4
LIG-OH	Solid		C19H23O8
LIG	Solid		C11H12O4
C	Solid	CARBON-GRAPHITE	C
HAA	Conventional	GLYCOL-ALDEHYDE	C2H4O2-D1
GLYOXAL	Conventional	GLYOXAL	C2H2O2
PROPNAL	Conventional	N-PROPIONALDEHYDE	C3H6O-3
C3H4O2	Conventional	PROPANEDIAL	C3H4O2
CH3CHO	Conventional	ACETALDEHYDE	C2H4O-1
CH2O	Conventional	FORMALDEHYDE	CH2O
MEOH	Conventional	METHANOL	CH4O
ETOH	Conventional	ETHANOL	C2H6O-2
COUMARYL	Conventional	ETHYL-BENZOATE	C9H10O2
PHENOL	Conventional	PHENOL	C6H6O
FE2MACR	Conventional	SINAPALDEHYDE	C11H12O4-2
HMF	Conventional	5-HYDROXYMETHYLFURFURAL	C20H23O10
LVG	Conventional	LEVOGLUCOSAN	C6H10O5-N1
XYL	Conventional	XYLAN	C5H8O4-U
H2O	Conventional	WATER	C22H29O9
CO2	Conventional	CARBON-DIOXIDE	C15H15O4
CO	Conventional	CARBON-MONOXIDE	C19H23O8
CH4	Conventional	METHANE	C11H12O4
C2H4	Conventional	ETHYLENE	C2H4
H2	Conventional	HYDROGEN	H2
NO2	Conventional	NITROGEN-DIOXIDE	NO2
NO	Conventional	NITRIC-OXIDE	NO
S	Conventional	SULFUR	S
SO2	Conventional	SULFUR-DIOXIDE	O2S
SO3	Conventional	SULFUR-TRIOXIDE	O3S
CL2	Conventional	CHLORINE	CL2
HCL	Conventional	HYDROGEN-CHLORIDE	HCL

$$V_m(298) = \sum_i n_i \, V_i(298) \tag{3.23}$$

with n_i being the number of times the functional group i is present in the molecule and V_i is the respective molar volume of said functional group.

The trapped species however require a less straightforward method, since in literature there aren't any mathematical expressions that determine this kind of information (these are in fact hypothetical species that serve the propose of better modelling the reaction kinetics rather than being an actual component). Ergo, a built-in Aspen Plus model to determine density of non-conventional components (e.g. HCOALGEN & DCOALIGT) was applied to these components, since is possible to determine the elemental composition of each lignin components as if it was in pure state, and if one assumes the proximate analysis of said compounds to be 100 % volatile matter - which is a reasonable assumption, key properties such as density and heat capacity can be determined for these compounds (however, only density is needed in this case, since a correlation for heat capacity is already used).

Regarding actual non-conventional components, such as biomass and ash, HCOALGEN and DCOALIGT methods were used to determine enthalpy and density, respectively. Although biomass is only considered as a non-conventional component in one unit (the dryer), correct properties are needed to perform mass and heat balances. Specifically, the heat capacity was determined using the Kirov correlation, which takes into account proximate analysis data (see eqs. 3.243.25).

$$C_{p,i} = \sum_{j=1}^{ncn} w_j C_{p,ij} \tag{3.24}$$

$$C_{p,ij} = a_{ij1} + a_{ij2}T + a_{ij3}T^2 + a_{ij4}T^3 \tag{3.25}$$

3.4.2 Simulation

3750 kg/h of wet biomass (50% moisture) enter the process through the WETBIO stream at 25°Cand 1 bar, being subject to a drying process in the DRYER unit (modelled as a convective dryer), which reduces the moisture below 10% (9.2 to 9.5% depending on the sample). To accomplish this, a 61250-61750 kg/h (depending on the sample) of air at 140°Center the dryer in a cross-flow direction. The solids are considered to be in plug flow, the length of the dryer is set to 5 meters and the residence time to 1 minute. A drying process is considered to have three phases, an initial period of heating, a constant rate period, where the free water is evaporated (mainly moisture in the solid's surface) and a falling rate period, where the moisture in the solid matrix is removed. In order to properly describe this phenomena, a drying curve is needed, or a way to estimate the critical and equilibrium moisture content (Aspen Plus allows from curve data introduction or it can generate the curve, given these two key parameters). However, this type of data is not available for all the biomass samples covered in this study, therefore, a critical moisture value of 10% was defined. Since the critical moisture parameter marks the end of the first drying phase, and final moisture contents around 10% are desired, one can assume that the falling rate period is negligible, and since the first period has a constant drying rate, obtained simulated results shouldn't differ much from reality.

After leaving the DRYER unit, the DRYSOLID stream, which is constituted by the remaining water and 2500 kg/h of a non-conventional component that represents biomass (DRYBIO), enters

the PYR-DEC (RYield) reactor, which decomposes the DRYBIO into 6 different compounds: cellulose, hemicellulose (modelled as xylan), carbon, oxygen and hydrogen rich lignin (LIG-C, LIG-O and LIG-H respectively) and ash (the respective yields are based on atom balances considering ultimate analysis data). The PYR-DEC unit operates at 42 to 49°C, depending on sample (since each has a different moisture specification), and 1 bar. As valid phases, Solid-Only option was chosen and the PSD from DRYBIO was kept. This is an artificial operation done in order to overcome the software limitations to properly model biomass, since reaction kinetics are defined for the "pseudo-components" and not for biomass as a whole. This way one can have correct biomass properties for any pre-treatment operations, such as milling and drying, which only involves physical phenomena and not any type of chemical reactions or treatment. The decomposed "pseudo-components" (FB-FEED), enter the fluidized bed unit (PYR-FB), to which a more detailed description follows.

Fluidized bed model description

The Aspen Plus FLUIDBED model was introduced recently, in the 8.X series, hence is important to make a brief description of it, for major source of design uncertainty will originate here, ergo any less valid assumptions made will propagate error into downstream units of the process. FLUIDBED is an one-dimensional model regarding fluid mechanics, able to describe isothermal fluidized beds as well as entrainment of particles. This allows determination of key operational parameters, which are important for the design of an industrial-size plant and also make it possible to assess the economical feasibility of such an endeavour. Specifically, the model considers:

- Particle size and density/terminal velocity;
- Geometry of the vessel;
- Additional gas supply;
- Impact of heat exchangers on bed temperature and fluid mechanics;
- Chemical reactions and their impact on the fluid-mechanics and vice-versa.

Regarding the available input options, there are mathematical expressions/correlations to determine:

- Minimum fluidization velocity;
- Transport disengagement height;
- Entrainment of solids from the bed;
- Distributor pressure drop (porous plate / bubble caps).

Model of the fluidized bed considers two zones.
Bottom zone:

- High solids concentration;
- Fluid mechanics according to Werther and Wein;

- Considers growth and splitting of bubbles.

Freeboard:

- Comparable low solids concentration;
- Fluid mechanics according to Kunii and Levenspiel;
- User defines bed inventory by specifying the pressure drop or the solids hold-up;
- Height of the bottom zone and the freeboard can be determined;
- Bubble related profiles (e.g. bubble diameter, bubble rise velocity etc.), interstitial gas velocity, pressure and solids volume concentration profile can be calculated;
- By use of selected entrainment correlation the solids mass flow and PSD at the outlets can be calculated

Model allows to consider chemical reactions with the following assumptions:

- Gas in plug flow;
- Solids ideally mixed;
- Each balance cell is considered as CSTR.

Considers:

- Impact of volume production/reduction on the fluid mechanics;
- Change in particle size distribution due to reaction.

Table 3.6 presents the input parameters for the FLUIDBED unit. This was introduced in the simulation for design proposes only - no reaction sets were directly introduced into the FLUIDBED unit. Therefore, determination of key design parameters to maintain the reactor in bubbling fluidization regime is the only reason to that this unit is modelled. The reactions sets are introduced in a separate CSTR (PYR-REAC), downstream of the FLUIDBED (PYR-FB), where the solid components (PYR-SOL) and vapours (FBGASOUT) are the inputs. This is again a fictitious unit because introducing reaction sets directly into the PYR-FB unit would make mass balances convergence much harder. The actual cause for this to happen can be subject to debate, due to the fact that Aspen Plus models are somehow a black box, and therefore make the task of linking result variation with physicochemical phenomena taking place in the simulated environment much harder. Nonetheless, likely causes can be related to heat transfer limitations, which may not exist at higher heating rates, because as discussed in the beginning of this chapter, the treatment of thermogravimetric data to determine reaction kinetics also has physical limitations which taint the validity of these parameters. Namely, the heat rate conducted in TGA routines is much lower than an industrial-scale fluidized bed, and so the effective pre-exponential factor may be higher than the apparent factor, which is the one actually determined experimentally. To test if this hypothesis is true, an alternative kinetic data, retrieved from Miller and Bellan reaction scheme is used [40], a methodology also tried by Blondeau and Jeanmart [57].

Reaction products exit the CSTR through the PYR-PROD stream, and are fed into a cyclone (PYR-CYC), which separates most of the solids, that exit through PYR-CHAR stream, from the

Table 3.6: FLUIDBED model input specifications

Bed characteristics and model inputs		Geometry	
Bed mass	1000 kg	Height	7.5 m
Voidage at V_{mf}	0.5	Solids discharge location	0.05
Geldard classification	Geldard B	Cross-section	Circular
Minimum fluidization velocity (V_{mf})	Wen & Yu correlation	Diameter	1.5 m
Transport disengagement height	George & Grace	Gas distributor	
$dC_v/dh\|_{max}$	10^{-6}	Type	Perforated plate
Elutriation model	Tasirin & Geldart	Number of orifices	6000
Convergence tolerance	0.01%	Orifice diameter	2 mm
Flash tolerance	0.01%	Orifice discharge coefficient	0.8

vapours (PYR-GAS). It is important to note that in an actual BFB reactor, most of the char exits the fluidized bed at mid height, by-passing the cyclone, however, due to the fact that the reactions happen in a separate CSTR and that the fluidization medium is needed for the reaction calculations to converge, even when using a CSTR, the PYR-CYC cyclone is actually separating a substantial higher amount of solids than in reality. As for the input parameters, design mode was selected, with Leith-Licht calculation method and Stairmand-HT type. The desired separation efficiency was set at 99%.

With the vapours separated from the solids (PYR-GAS), this stream enters a manipulator block (SPLIT), that divides the inlet stream into two outlet streams with equal flow, one entering a quench cooler directly (QUENCH), while the second is passed through a heat exchanger to correct temperature and pressure, and another manipulator block (this time, a multiplication block - STR), which increases the stream flow by a factor of 25 and is also fed into QUENCH unit (QCH-COOL stream). This represents bio-oil that is in storage and is cycled back into the process so that in can cool the newly produced oil. In reality, there's either a bio-oil recycle stream or a storage with enough buffer capacity to provide fresh bio-oil stream at ambient conditions, with a much higher mass flow than the outlet stream. If the recycle stream is used, a heat exchanger is necessary, to cool down the bio-oil leaving the quench at 50°Cto cooling water temperature. The cooled stream re-enters the quench cooler at the top (QCH-COOL), cooling the incoming pyrolysis vapours and so forth. However, since it was not possible to make the recycle configuration work properly, using manipulators proved to be a simpler and working alternative. Note that the addition of the manipulator block STR does not mean that there's a 25:1 mass ratio of cooling liquid to vapours, this ratio is lower because the stream that suffers the flow increase had the gases removed (PURGE stream).

Regarding the quench unit itself, it was modelled as a spray tower in simulation mode, with the Calvert calculation method and a relative gas velocity of 1 m/s. The diameter of the droplets was calculated by Aspen Plus, the pressure drop was set to 0.1 bar, nozzle diameter to 50 μm, with a 30°spray angle and with 100 nozzles.

The vapours that leave the quench system go into a flash tank (FLASH), to remove aerosols suspended in the gas phase. Using an ESP as an alternative was considered, but was ruled out due to the flash tank more simple design and better separation efficiency. The liquid phase is mixed with the bio-oil from the quench cooler (HEAVYOIL) and exits the process as the sole product stream. The gas stream leaving the FLASH unit (NCG), constituted mostly by non condensable gases is burned in the COMB reactor (RGibbs).

The char stream (PYR-CHAR) that leaves the PYR-CYC unit is decomposed into its elemental composition in the CHAR-DEC reactor (RStoic). Stoichiometric reactions yielding H_2, C, N_2 and O_2 to all solid components were implemented in this reactor, similarly to the procedure done with the RYield reactor and non-conventional components such as coal to model its combustion (see Aspen Plus manual for more information). The considered operation temperature was 500°Cand pressure 1 bar. In table 3.7, it's possible to see the stoichiometric reactions used in this unit to decompose the various solid components into molecular elements. Expressing a stream of solids this way still allows for correct enthalpy prediction of the combustion process via Gibbs energy minimization.

Table 3.7: RStoic reactions specification tab

Specification type	Stoichiometry		
Frac. conversion	CELLULOS(CIPSD)	–>	6 C(CIPSD) + 5 H2(MIXED) + 2,5 O2(MIXED)
Frac. conversion	CELLA(CIPSD)	–>	6 C(CIPSD) + 5 H2(MIXED) + 2,5 O2(MIXED)
Frac. conversion	HCE(CIPSD)	–>	5 C(CIPSD) + 4 H2(MIXED) + 2 O2(MIXED)
Frac. conversion	HCEA1(CIPSD)	–>	5 C(CIPSD) + 4 H2(MIXED) + 2 O2(MIXED)
Frac. conversion	HCEA2(CIPSD)	–>	5 C(CIPSD) + 4 H2(MIXED) + 2 O2(MIXED)
Frac. conversion	LIG-C(CIPSD)	–>	15 C(CIPSD) + 7 H2(MIXED) + 2 O2(MIXED)
Frac. conversion	LIG-O(CIPSD)	–>	20 C(CIPSD) + 11,5 H2(MIXED) + 5 O2(MIXED)
Frac. conversion	LIG-H(CIPSD)	–>	22 C(CIPSD) + 14,5 H2(MIXED) + 4,5 O2(MIXED)
Frac. conversion	LIG-CC(CIPSD)	–>	15 C(CIPSD) + 7 H2(MIXED) + 2 O2(MIXED)
Frac. conversion	LIG-OH(CIPSD)	–>	19 C(CIPSD) + 11,5 H2(MIXED) + 4 O2(MIXED)
Frac. conversion	LIG(CIPSD)	–>	11 C(CIPSD) + 6 H2(MIXED) + 2 O2(MIXED)

The stream that exits CHAR-DEC, ELEMENTS, enters a RGibbs reactor (COMB) in which combustion calculations are performed. Due to the workaround done before to enable Aspen Plus to determine combustion key parameters (the solid decomposition into elements), a heat stream between CHAR-DEC and COMB needs to be added (RHeat stream) in order to have correct enthalpy calculations. In the combustion reactor, possible reaction products were identified and the yields were determined by minimizing Gibbs energy.

Table 3.8: RGibbs possible products considered.

Component	N2	O2	H2O	NO2	NO	H2	CO	CO2	C
Valid phases	Mixed	Mixed	Mixed	Mixed	Mixed	Mixed	Mixed	Mixed	PureSolid

The required inputs were pressure (1.1 bar), phases - where vapour phase was included, and calculation option - phase and chemical equilibrium were determined. Table 3.8 presents the possible products that were considered by the thermodynamic calculations. The flue gases leaving the combustion reactor enter another cyclone for ash removal and are used for the heat needs of the process, namely providing heat for the pyrolysis reactor and for the drying pre-treatment. An important note regarding the pyrolysis heat duty considered in this work, it considers both the energy necessary to heat the streams to the desired temperature and to the actual thermal decomposition of the lignocellulosic material.

There's one last parameter that needs to be set in order to proceed with the simulations, the air flow into the combustion reactor (AIR-COMB stream). In order the determine the proper air flow, since it will influence the combustion process - heat produced and flue gas composition - a sensitivity block was created (S-COMB), where the air flow is varied and gas composition, air to fuel ratio and outlet temperature are determined (the results are shown in the appendix).

Bibliography

[1] H. L. Chatelier, "De l'action de la chaleur sur les argiles," *Bulletin de la Societe Francaise de Mineralogie et de Cristallographie*, vol. 10, pp. 204–207, 1887.

[2] T. Lever, P. Haines, J. Rouquerol, E. L. Charsley, P. V. Eckeren, and D. J. Burlett, "Ictac nomenclature of thermal analysis (iupac recommendations 2014)," *Pure and Applied Chemistry*, vol. 86, no. 4, pp. 545–553, 2014.

[3] W. Hemminger and S. Sarge, "Chapter 1 - definitions, nomenclature, terms and literature," in *Principles and Practice* (M. E. Brown, ed.), vol. 1 of *Handbook of Thermal Analysis and Calorimetry*, pp. 1–73, Elsevier Science B.V., 1998.

[4] J. E. White, W. J. Catallo, and B. L. Legendre, "Biomass pyrolysis kinetics: A comparative critical review with relevant agricultural residue case studies," *Journal of Analytical and Applied Pyrolysis*, vol. 91, no. 1, pp. 1 – 33, 2011.

[5] A. K. Galwey and M. E. Brown, "Application of the arrhenius equation to solid state kinetics: can this be justified?," *Thermochimica Acta*, vol. 386, no. 1, pp. 91 – 98, 2002.

[6] P. Garn, "Kinetic parameters," *Journal of thermal analysis*, vol. 13, no. 3, pp. 581–593, 1978.

[7] J. H. Flynn, "The 'temperature integral' - its use and abuse," *Thermochimica Acta*, vol. 300, no. 1-2, pp. 83–92, 1997. A Collection of Invited Papers in Celebration of Volume 300.

[8] S. Kim and Y. Eom, "Estimation of kinetic triplet of cellulose pyrolysis reaction from isothermal kinetic results," *Korean Journal of Chemical Engineering*, vol. 23, no. 3, pp. 409–414, 2006.

[9] S. Vyazovkin and C. A. Wight, "Model-free and model-fitting approaches to kinetic analysis of isothermal and nonisothermal data," *Thermochimica Acta*, vol. 340-341, pp. 53–68, 1999.

[10] S. Vyazovkin and C. A. Wight, "Isothermal and non-isothermal kinetics of thermally stimulated reactions of solids," *International Reviews in Physical Chemistry*, vol. 17, no. 3, pp. 407–433, 1998.

[11] M. Starink, "The determination of activation energy from linear heating rate experiments: a comparison of the accuracy of isoconversion methods," *Thermochimica Acta*, vol. 404, no. 1-2, pp. 163–176, 2003.

[12] S. Vyazovkin, "Modification of the integral isoconversional method to account for variation in the activation energy," *Journal of Computational Chemistry*, vol. 22, no. 2, pp. 178–183, 2001.

[13] R. Cao, S. Naya, R. Artiaga, A. García, and A. Varela, "Logistic approach to polymer degradation in dynamic {TGA}," *Polymer Degradation and Stability*, vol. 85, no. 1, pp. 667–674, 2004.

[14] H. L. Friedman, "Kinetics of thermal degradation of char-forming plastics from thermogravimetry. application to a phenolic plastic," *Journal of Polymer Science Part C: Polymer Symposia*, vol. 6, no. 1, pp. 183–195, 1964.

[15] T. Ozawa, "A new method of analyzing thermogravimetric data," *Bulletin of the Chemical Society of Japan*, vol. 38, no. 11, pp. 1881–1886, 1965.

[16] J. H. Flynn and L. A. Wall, "A quick, direct method for the determination of activation energy from thermogravimetric data," *Journal of Polymer Science Part B: Polymer Letters*, vol. 4, no. 5, pp. 323–328, 1966.

[17] T. Tang and M. Chaudhri, "Analysis of dynamic kinetic data from solid-state reactions," *Journal of thermal analysis*, vol. 18, no. 2, pp. 247–261, 1980.

[18] C. D. Doyle, "Kinetic analysis of thermogravimetric data," *Journal of Applied Polymer Science*, vol. 5, no. 15, pp. 285–292, 1961.

[19] C. D. Doyle, "Estimating isothermal life from thermogravimetric data," *Journal of Applied Polymer Science*, vol. 6, no. 24, pp. 639–642, 1962.

[20] H. E. Kissinger, "Reaction kinetics in differential thermal analysis," *Analytical Chemistry*, vol. 29, no. 11, pp. 1702–1706, 1957.

[21] T. Akahira and T. Sunose, "Method of determining activation deterioration constant of electrical insulating materials," *Res. Rep. Chiba Inst. Technol.(Sci. Technol.)*, vol. 16, pp. 22–31, 1971.

[22] A. W. Coats and J. P. Redfern, "Kinetic parameters from thermogravimetric data," *Nature*, vol. 201, no. 4914, pp. 68–69, 1964.

[23] A. W. Coats and J. P. Redfern, "Kinetic parameters from thermogravimetric data. ii.," *Journal of Polymer Science Part B: Polymer Letters*, vol. 3, no. 11, pp. 917–920, 1965.

[24] A. K. Burnham and R. L. Braun, "Global kinetic analysis of complex materials," *Energy & Fuels*, vol. 13, no. 1, pp. 1–22, 1999.

[25] S. Vyazovkin and D. Dollimore, "Linear and nonlinear procedures in isoconversional computations of the activation energy of nonisothermal reactions in solids," *Journal of Chemical Information and Computer Sciences*, vol. 36, no. 1, pp. 42–45, 1996.

[26] G. Senum and R. Yang, "Rational approximations of the integral of the arrhenius function," *Journal of thermal analysis*, vol. 11, no. 3, pp. 445–447, 1977.

[27] J. Flynn, "A general differential technique for the determination of parameters for d(α)/dt=f(α) a exp(-e/rt)," *Journal of thermal analysis*, vol. 37, no. 2, pp. 293–305, 1991.

[28] A. Burnham and L. Dinh, "A comparison of isoconversional and model-fitting approaches to kinetic parameter estimation and application predictions," *Journal of Thermal Analysis and Calorimetry*, vol. 89, no. 2, pp. 479–490, 2007.

[29] S. Balci, T. Dogu, and H. Yucel, "Pyrolysis kinetics of lignocellulosic materials," *Industrial & Engineering Chemistry Research*, vol. 32, no. 11, pp. 2573–2579, 1993.

[30] J. Cai, W. Wu, and R. Liu, "An overview of distributed activation energy model and its application in the pyrolysis of lignocellulosic biomass," *Renewable and Sustainable Energy Reviews*, vol. 36, pp. 236–246, 2014.

[31] F. Thurner and U. Mann, "Kinetic investigation of wood pyrolysis," *Industrial & Engineering Chemistry Process Design and Development*, vol. 20, no. 3, pp. 482–488, 1981.

[32] M. R. Hajaligol, J. B. Howard, J. P. Longwell, and W. A. Peters, "Product compositions and kinetics for rapid pyrolysis of cellulose," *Industrial & Engineering Chemistry Process Design and Development*, vol. 21, no. 3, pp. 457–465, 1982.

[33] R. K. Agrawal, "Kinetics of reactions involved in pyrolysis of cellulose i. the three reaction model," *The Canadian Journal of Chemical Engineering*, vol. 66, no. 3, pp. 403–412, 1988.

[34] A. J. Tsamba, W. Yang, and W. Blasiak, "Pyrolysis characteristics and global kinetics of coconut and cashew nut shells," *Fuel Processing Technology*, vol. 87, no. 6, pp. 523 – 530, 2006.

[35] S. Alves and J. Figueiredo, "Kinetics of cellulose pyrolysis modelled by three consecutive first-order reactions," *Journal of Analytical and Applied Pyrolysis*, vol. 17, no. 1, pp. 37 – 46, 1989.

[36] M. Lanzetta and C. D. Blasi, "Pyrolysis kinetics of wheat and corn straw," *Journal of Analytical and Applied Pyrolysis*, vol. 44, no. 2, pp. 181 – 192, 1998.

[37] R. K. Agrawal, "Kinetics of reactions involved in pvrolvsis of cellulose ii. the modified kilzer-bioid model," *The Canadian Journal of Chemical Engineering*, vol. 66, no. 3, pp. 413–418, 1988.

[38] M. L. Boroson, J. B. Howard, J. P. Longwell, and W. A. Peters, "Product yields and kinetics from the vapor phase cracking of wood pyrolysis tars," *AIChE Journal*, vol. 35, no. 1, pp. 120–128, 1989.

[39] C. A. Koufopanos, A. Lucchesi, and G. Maschio, "Kinetic modelling of the pyrolysis of biomass and biomass components," *The Canadian Journal of Chemical Engineering*, vol. 67, no. 1, pp. 75–84, 1989.

[40] R. Miller and J. Bellan, "A generalized biomass pyrolysis model based on superimposed cellulose, hemicellulose and lignin kinetics," *Combustion Science and Technology*, vol. 126, no. 1-6, pp. 97–137, 1997.

[41] C. D. Blasi, "Comparison of semi-global mechanisms for primary pyrolysis of lignocellulosic fuels," *Journal of Analytical and Applied Pyrolysis*, vol. 47, no. 1, pp. 43 – 64, 1998.

[42] J. Flynn, "Thermal analysis kinetics-problems, pitfalls and how to deal with them," *Journal of thermal analysis*, vol. 34, no. 1, pp. 367–381, 1988.

[43] M. Lapuerta, J. J. Hernández, and J. Rodríguez, "Comparison between the kinetics of devolatilisation of forestry and agricultural wastes from the middle-south regions of spain," *Biomass and Bioenergy*, vol. 31, no. 1, pp. 13 – 19, 2007.

[44] T. R. Nunn, J. B. Howard, J. P. Longwell, and W. A. Peters, "Product compositions and kinetics in the rapid pyrolysis of sweet gum hardwood," *Industrial & Engineering Chemistry Process Design and Development*, vol. 24, no. 3, pp. 836–844, 1985.

[45] A. Broido, "Kinetics of solid-phase cellulose pyrolysis," in *Thermal Uses and Properties of Carbohydrates and Lignins* (F. Shafizadeh, K. V. Sarkanen, and D. A. Tillman, eds.), ch. 2, pp. 19–36, 111 Fifth Avenue, New York, New York 10003: Academic Press, Inc., 1976.

[46] A. Broido and M. A. Nelson, "Char yield on pyrolysis of cellulose," *Combustion and Flame*, vol. 24, pp. 263 – 268, 1975.

[47] U. K. Shivadev and H. W. Emmons, "Thermal degradation and spontaneous ignition of paper sheets in air by irradiation," *Combustion and Flame*, vol. 22, no. 2, pp. 223 – 236, 1974.

[48] A. G. W. Bradbury, Y. Sakai, and F. Shafizadeh, "A kinetic model for pyrolysis of cellulose," *Journal of Applied Polymer Science*, vol. 23, no. 11, pp. 3271–3280, 1979.

[49] W. K. Tang and W. K. Neill, "Effect of flame retardants on pyrolysis and combustion of α-cellulose," *Journal of Polymer Science Part C: Polymer Symposia*, vol. 6, no. 1, pp. 65–81, 1964.

[50] S. Cooley and M. J. Antal, "Kinetics of cellulose pyrolysis in the presence of nitric oxide," *Journal of Analytical and Applied Pyrolysis*, vol. 14, no. 2, pp. 149 – 161, 1988.

[51] C. A. Koufopanos, N. Papayannakos, G. Maschio, and A. Lucchesi, "Modelling of the pyrolysis of biomass particles. studies on kinetics, thermal and heat transfer effects," *The Canadian Journal of Chemical Engineering*, vol. 69, no. 4, pp. 907–915, 1991.

[52] E. Ranzi, A. Cuoci, T. Faravelli, A. Frassoldati, G. Migliavacca, S. Pierucci, and S. Sommariva, "Chemical kinetics of biomass pyrolysis," *Energy & Fuels*, vol. 22, no. 6, pp. 4292–4300, 2008.

[53] X. Zhou, M. W. Nolte, H. B. Mayes, B. H. Shanks, and L. J. Broadbelt, "Experimental and mechanistic modeling of fast pyrolysis of neat glucose-based carbohydrates. 1. experiments and development of a detailed mechanistic model," *Industrial & Engineering Chemistry Research*, vol. 53, no. 34, pp. 13274–13289, 2014.

[54] X. Zhou, M. W. Nolte, B. H. Shanks, and L. J. Broadbelt, "Experimental and mechanistic modeling of fast pyrolysis of neat glucose-based carbohydrates. 2. validation and evaluation of the mechanistic model," *Industrial & Engineering Chemistry Research*, vol. 53, no. 34, pp. 13290–13301, 2014.

[55] V. Seshadri and P. R. Westmoreland, "Concerted reactions and mechanism of glucose pyrolysis and implications for cellulose kinetics," *The Journal of Physical Chemistry A*, vol. 116, no. 49, pp. 11997–12013, 2012. PMID: 23082925.

[56] T. Faravelli, A. Frassoldati, G. Migliavacca, and E. Ranzi, "Detailed kinetic modeling of the thermal degradation of lignins," *Biomass and Bioenergy*, vol. 34, no. 3, pp. 290 – 301, 2010.

[57] J. Blondeau and H. Jeanmart, "Biomass pyrolysis at high temperatures: Prediction of gaseous species yields from an anisotropic particle," *Biomass and Bioenergy*, vol. 41, pp. 107 – 121, 2012.

[58] T. Hosoya, H. Kawamoto, and S. Saka, "Cellulose–hemicellulose and cellulose–lignin interactions in wood pyrolysis at gasification temperature," *Journal of Analytical and Applied Pyrolysis*, vol. 80, no. 1, pp. 118 – 125, 2007.

[59] A. Anca-Couce, R. Mehrabian, R. Scharler, and I. Obernberger, "Kinetic scheme of biomass pyrolysis considering secondary charring reactions," *Energy Conversion and Management*, vol. 87, pp. 687 – 696, 2014.

[60] F. Shafizadeh, R. H. Furneaux, T. G. Cochran, J. P. Scholl, and Y. Sakai, "Production of levoglucosan and glucose from pyrolysis of cellulosic materials," *Journal of Applied Polymer Science*, vol. 23, no. 12, pp. 3525–3539, 1979.

[61] J. Piskorz, D. Radlein, and D. S. Scott, "On the mechanism of the rapid pyrolysis of cellulose," *Journal of Analytical and Applied Pyrolysis*, vol. 9, no. 2, pp. 121 – 137, 1986.

[62] G. N. Richards and G. Zheng, "Influence of metal ions and of salts on products from pyrolysis of wood: Applications to thermochemical processing of newsprint and biomass," *Journal of Analytical and Applied Pyrolysis*, vol. 21, no. 1–2, pp. 133 – 146, 1991.

[63] J. Piskorz, D. S. Radlein, D. S. Scott, and S. Czernik, "Pretreatment of wood and cellulose for production of sugars by fast pyrolysis," *Journal of Analytical and Applied Pyrolysis*, vol. 16, no. 2, pp. 127 – 142, 1989.

[64] A. van Der Kaaden, J. Haverkamp, J. J. Boon, and J. W. D. Leeuw, "Analytical pyrolysis of carbohydrates," *Journal of Analytical and Applied Pyrolysis*, vol. 5, no. 3, pp. 199 – 220, 1983.

[65] D. Radlein, J. Piskorz, and D. Scott, "Proceedings of the 9th international conference on fundamentals aspects, analytical techniques, processes and applications of pyrolysis fast pyrolysis of natural polysaccharides as a potential industrial process," *Journal of Analytical and Applied Pyrolysis*, vol. 19, pp. 41 – 63, 1991.

[66] D. Shen and S. Gu, "The mechanism for thermal decomposition of cellulose and its main products," *Bioresource Technology*, vol. 100, no. 24, pp. 6496 – 6504, 2009.

[67] D. Shen, R. Xiao, S. Gu, and H. Zhang, "The overview of thermal decomposition of cellulose in lignocellulosic biomass," in *Cellulose - Biomass Conversion* (T. van de Ven and J. Kadla, eds.), pp. 193–226, InTech, 2013.

[68] E. Ranzi, M. Corbetta, F. Manenti, and S. Pierucci, "Kinetic modeling of the thermal degradation and combustion of biomass," *Chemical Engineering Science*, vol. 110, pp. 2 – 12, 2014. Mackie-2013 "Pushing the boundaries".

[69] M. Amutio, G. Lopez, J. Alvarez, R. Moreira, G. Duarte, J. Nunes, M. Olazar, and J. Bilbao, "Flash pyrolysis of forestry residues from the portuguese central inland region within the framework of the biorefina-ter project," *Bioresource Technology*, vol. 129, pp. 512 – 518, 2013.

[70] D. Fengel and G. Wegener, *Wood: chemistry, ultrastructure, reactions*. Berlin, Germany: Walter de Gruyter & Co., 1983.

[71] D. Lee, V. N. Owens, A. Boe, and P. Jeranyama, "Composition of herbaceous biomass feedstocks," tech. rep., North Central Sun Grant Center, South Dakota State University, Box 2140C, Brookings, SD 57007, 2007.

[72] M. B. Shemfe, S. Gu, and P. Ranganathan, "Techno-economic performance analysis of biofuel production and miniature electric power generation from biomass fast pyrolysis and bio-oil upgrading," *Fuel*, vol. 143, pp. 361 – 372, 2015.

[73] R. J. Wooley and V. Putsche, "Development of an aspen plus physical property database for biofuels components," tech. rep., National Renewable Energy Laboratory (NREL), Colorado, USA, 4 1996.

[74] K. Onarheim, Y. Solantausta, and J. Lehto, "Process simulation development of fast pyrolysis of wood using aspen plus," *Energy & Fuels*, vol. 29, no. 1, pp. 205–217, 2015.

[75] A. Dutta, A. Sahir, E. Tan, D. Humbird, L. J. Snowden-Swan, P. Meyer, J. Ross, D. Sexton, R. Yap, and J. Lukas, "Process design and economics for the conversion of lignocellulosic biomass to hydrocarbon fuels: Thermochemical research pathways with in situ and ex situ upgrading of fast pyrolysis vapors," tech. rep., NREL and PNNL, Colorado and Washington, USA, 3 2015.

[76] D. van Krevelen and K. te Nijenhuis, *Properties of Polymers: Their Correlation with Chemical Structure; their Numerical Estimation and Prediction from Additive Group Contributions*. Elsevier Science, 2009.

Chapter 4

Results and Discussion

In this chapter the results from the simulations described before are presented, as well as a discussion about said results consistency with experimental data and possible reasons why these deviate, keeping in mind the considerations and hypothesis done while running the simulations.

Five types of wood species were simulated, three biomass samples characterized by Amutio et al. [1], *Pinus insignis* [2] and *Eucalyptus globulus* [3] (Bio1 to 5, respectively). The criteria used prioritized wood species that have the highest expression in the Portuguese forest biome, and specially in the country's Central region, and therefore constitute the native fabric of the respective ecosystems and a endogenous resource that is often under-exploited. The reason for the use of this particular criteria lies on the fact that assuring a sizeable and constant supply of waste lignocellulosic material is crucial to a facility of this nature. A few important notes regarding the chosen biomass types: there's only one softwood species (*Pinus insignis*), and so different pyrolysis oil product distribution is expected, the pinewood species here studied is not the predominant one in Portugal (*Pinus pinaster*), although data to characterize the later proved hard to obtain and hence *Pinus insignis* was chosen. Still, it's pinewood and therefore, the expected results shouldn't be much different. The species reported in Amutio's work are either native species in the region or invading species (e.g. Acacia) [1], and due to the fact that optimization of the reaction scheme is to be performed, a generalized scheme for softwoods and another for hardwoods is presented in the end of this chapter. This way this study does not render itself too specific, however, these are invading species in other regions of the globe, hence, this could prove to be a good solution to that particular problem, which improves the applicability of this work. Composition for the various biomass samples considered expressed in terms of pseudo-components is presented in table 4.1.

Table 4.1: Pseudo-component composition for the five biomass types used throughout the simulations.

	First set (S1 to S6)					Second set (SX)				
Sample	Bio1	Bio2	Bio3	Bio4	Bio5	Bio1	Bio2	Bio3	Bio4	Bio5
Cellulose	41.13	36.56	41.58	39.11	50.96	41.19	37.58	41.58	37.31	48.82
Hemicellulose	20.52	15.97	17.59	24.25	29.22	19.74	15.92	17.59	23.13	19.20
LIG-C	20.28	11.91	1.49	15.80	1.75	4.50	5.59	1.49	3.01	0.78
LIG-O	13.15	0.00	20.88	8.88	4.93	21.09	19.63	20.88	34.95	19.78
LIG-H	4.53	34.57	17.26	11.47	12.73	13.07	20.28	17.26	1.09	10.22
Ash	0.40	1.00	1.20	0.50	1.20	0.40	1.00	1.20	0.50	1.20

Table 4.2: Simulations planning.

Simulation	S1	S2	S3	S4	S5	S6	SX
Kinetic scheme	Ranzi		Anca-Couce				Ranzi*
Trapped species	Yes	-	Yes	-	Yes	Yes	Yes
Variable x	NA	NA	-	-	Yes	-	NA
In FLUIDBED	-	-	-	-	-	Yes	-
Subject to optimization	Yes	-	-	-	Yes	Yes	Yes

To allow a better understanding on how the various variables that differ between simulations influence the results, table 4.2 was compiled and presents the simulations planning, with terminology used for each scenario as well as key parameters varied. The main goal of this set of simulations is exploratory, that is, the focus is on gaining a good perception of the reaction mechanisms ability to match experimental data, and identify potential strengths and limitations. A more rigorous approach using optimization algorithms in order to match experimental data was contemplated, but later discarded as it would turn an already complex system to model into a pure mathematical problem, which could lead to results that are only the result of a minimization of error instead of actually relating biomass characteristics with product yield. As can be seen in table 4.2, previous mentioned kinetic schemes proposed by Ranzi et al. [4] and Anca-Couce et al [5] were tested (S1 and S2), the inclusion or not of trapped species in both schemes (S1 to S4), impact of varying the x in the Anca-Couce reaction set (S5) and a final simulation were the reactions are introduced in the FLUIDBED unit instead of a separated CSTR (S6). While this first approach is exploratory, some basic optimization is attempted throughout this chapter. Modified versions of this simulations will be identified with an asterisk (e.g. S5*). A second set of simulations that attempt to optimize these reaction mechanisms for the biomass samples studied follows (SX). At the end of the chapter, design parameters for the important process units are presented.

4.1 Exploratory analysis

Starting with S1, since it's the original scheme, with no additional simplifications, table 4.3 summarises the yield results. Bio1 to 3 have similar cellulose and hemicellulose contents and its in noticeable acids, aldehydes, furans and sugar yield, which tend to remain constant (acids and furans are only formed through the cellulose reaction). LIG-H content appears to be responsible for sinapaldehyde formation, translated in higher phenolics yield - this could be a suitable pseudo-component to model hardwood then (these have higher monolignol content in sinapyl alcohol, which decomposes in sinapaldehyde). The alcohol and phenolic yield increase is most likely due to higher LIG-O and LIG-H content, since these two decompose into LIG-OH. Again, the lignin reaction pathway used is not adequate to reflect different wood types (see previous chapter), so it's likely that other results using the same or a modified version of this scheme will show phenolics also as a major source of yield error (see [5] [6]). Char and gas contents are for almost all cases over-predicted.

Figure 4.1 shows the actual absolute simulation errors compared to real data. Water, sugars and gas show a systematic and very pronounced deviation, with sugar and gas content over-predicted and water content under-predicted. It is a first evidence that this scheme is not optimized for fast

Table 4.3: PYR-KIN yield results for the S1 simulation.

	Simulation					Experimental*				
Sample	Bio1	Bio2	Bio3	Bio4	Bio5	Bio1	Bio2	Bio3	Bio4	Bio5
Acids	5.95	5.28	5.55	5.65	7.37	7.60	7.20	3.20	2.73	3.65
Aldehydes	5.65	5.08	5.43	6.10	7.43	1.70	2.10	1.60	1.93	1.69
Alcohols	3.72	4.71	5.49	4.32	4.58	0.80	1.30	1.00	2.00	0.75
Ketones	2.24	6.29	6.67	3.11	3.48	15.00	8.50	6.10	6.37	8.04
Phenolic	5.36	7.43	7.77	5.34	3.37	12.70	13.30	18.80	16.49	19.79
Furans	3.29	2.92	3.07	3.12	4.07	6.80	4.50	2.80	3.32	4.46
Sugars	23.81	21.14	22.20	22.69	29.54	1.40	1.50	4.80	4.46	2.45
Water	4.89	5.06	4.91	4.70	4.12	27.00	28.90	29.20	25.36	26.95
Bio-oil	54.90	57.92	61.09	55.04	63.98	79.50	72.10	75.10	75.33	75.39
Char	27.02	25.01	20.52	25.74	16.89	16.56	23.05	20.72	17.67	18.46
Gas	17.69	16.08	17.19	18.71	18.73	3.94	4.85	4.18	7.00	6.15

*Unidentified compounds: Bio1 - 5.8%; Bio2 - 4.4%; Bio3 - 7.5%; Bio4 - 12.61%; Bio5 - 6.60%.

pyrolysis conditions. Phenolics, ketones and char yields also show a considerable deviation. For pinewood (Bio4), the biggest difference is in the phenolic and ketone content decrease, which can be attributed to the different make up of lignin monomers when compared to the first three samples. The eucalyptus sample shows a significant different product distribution than other samples. Specifically, acids, aldehyde and furan content is higher, which is attributed to the higher cellulose and hemicellulose content. Due to this, phenolic content is the lowest of all samples. Ketones have a similar yield when compared to Bio4, which is the only softwood sample. Analysing the absolute error allows identification of specially ill-formulated reaction mechanisms, and therefore will prove to be a valuable methodology in further optimization and refinement of the studied kinetic schemes.

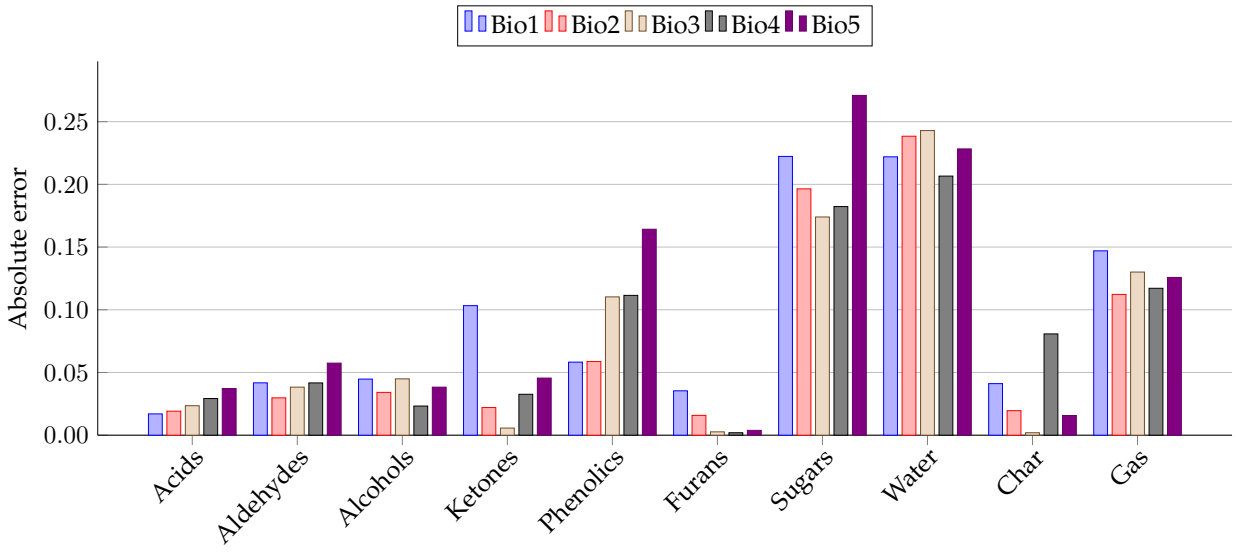

Figure 4.1: Absolute error for the five biomass samples (S1 simulation).

Table 4.4 presents the results for simulation using Ranzi's scheme without considering trapped species. Most of the results are similar or even the same compared to S1 simulation values. The only major differences are higher gas absolute error as well as char. Both approaches (considering trapped species or not) seemed reasonable, although the non trapped species results have higher deviation from experimental data, and so they will not be considered for further optimization. Despite this, a simulation also not considering trapped species with the Anca-Couce will still be performed (S4). Generally speaking, the model over-predicts by a fair margin sugar content (>15% yield deviation in all cases); water and phenolic content is under-predicted, although the error magnitude for water is on pair with sugar, while the phenolic yield deviation is lower when compared; alcohol is over-predicted, with a fairly constant deviation of about 4%; acids, aldehyde and ketone content has deviations of about 2% in relation to experimental yields except for the eucalyptus sample, leaving furans, which are the component class that is better predicted by the model, with <0.5% deviations for Bio 3, 4 and 5.

Table 4.4: Simulated yields for several biomass samples using Ranzi reaction scheme (S2).

	Simulation					Experimental*				
Sample	Bio1	Bio2	Bio3	Bio4	Bio5	Bio1	Bio2	Bio3	Bio4	Bio5
Acids	5.95	5.29	5.55	5.67	7.37	7.60	7.20	3.20	2.73	3.65
Aldehydes	5.65	5.08	5.44	6.11	7.44	1.70	2.10	1.60	1.93	1.69
Alcohols	3.72	4.72	5.50	4.34	4.59	0.80	1.30	1.00	2.00	0.75
Ketones	2.25	6.30	6.67	3.15	3.49	15.00	8.50	6.10	6.37	8.04
Phenolic	5.40	7.47	7.80	5.48	3.38	12.70	13.30	18.80	16.49	19.79
Furans	3.29	2.92	3.07	3.13	4.07	6.80	4.50	2.80	3.32	4.46
Sugars	23.83	21.16	22.21	22.74	29.56	1.40	1.50	4.80	4.46	2.45
Water	4.91	5.07	4.92	4.74	4.13	27.00	28.90	29.20	25.36	26.95
Bio-oil	55.00	58.02	61.17	55.36	64.04	79.50	72.10	75.10	75.33	75.39
Char	18.29	16.73	12.71	16.22	8.79	16.56	23.05	20.72	17.67	18.46
Gas	26.31	24.26	24.92	27.93	26.77	3.94	4.85	4.18	7.00	6.15

*Unidentified compounds: Bio1 - 5.8%; Bio2 - 4.4%; Bio3 - 7.5%; Bio4 - 12.61%; Bio5 - 6.60%.

By analysis of table 4.4 above, it's clear that the Ranzi et al. model has some serious shortcomings, namely the gross over-prediction of levoglucusan and under-prediction of water yield. At this point, one has to define the acceptable deviation for the yield obtained via simulation. There isn't any type of standards for this in the literature, although Gopakumar et al. [7] determined yield deviation of ketones, sugars, furans and phenols for switchgrass and pinewood, which can be used as a reference. Apart from sugars, which present high yield variability (an issue already discussed in previous chapter), the yield deviation stays below 2% for the component classes of interest, also the models themselves are not accurate enough to allow for a rigorous characterization of the bio-oil composition, and so a <2% deviation was considered. A more accurate approach would be to consider different acceptable deviations according to the component class, although there aren't deviation values to all component classes in the simulation and the model is already close to 2% deviation for a few classes, and so if stoichiometric coefficient modifications are needed, it won't prove to be such a radical change, when compared to tighter tolerance values.

In order to try and overcome some of the problems encountered using Ranzi et al. reaction scheme, the reaction responsible for levoglucosan formation was modified: the temperature

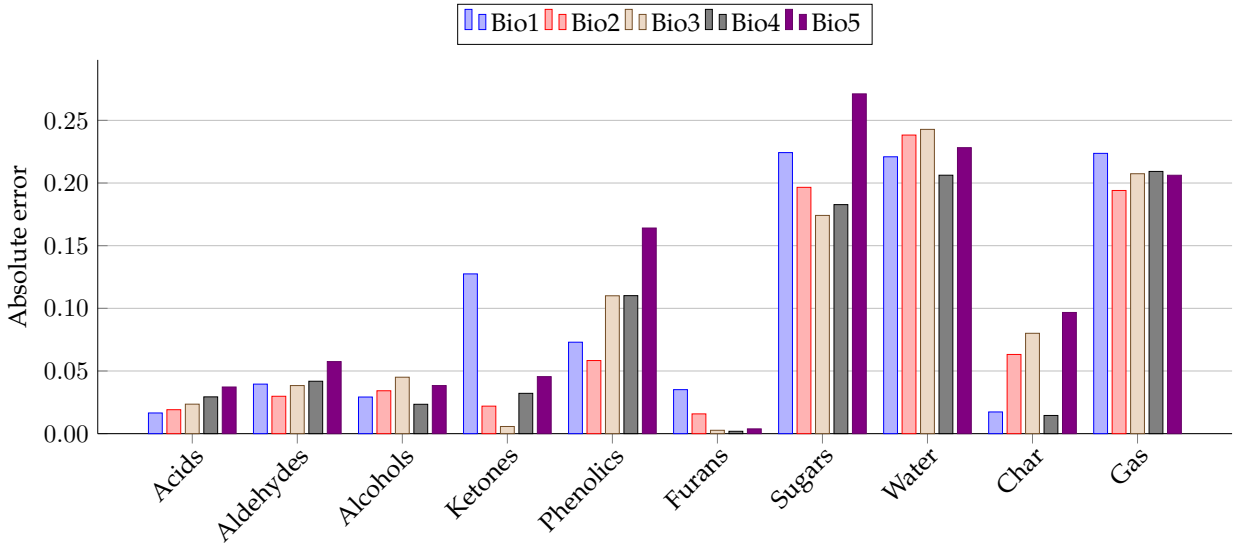

Figure 4.2: Absolute error for the five biomass samples (S2 simulation).

exponent in the pre-exponential factor was altered from 1 to 0.5. Results for this simulation are presented in table 4.5.

Table 4.5: Results for the PYR-KIN reactor when the n exponent in reaction 3 is changed from 1 to 0.5 (conversion of activated cellulose into LVG).

	Simulation					Experimental*				
Sample	Bio1	Bio2	Bio3	Bio4	Bio5	Bio1	Bio2	Bio3	Bio4	Bio5
Acids	13.51	12.01	12.61	12.85	16.75	7.60	7.20	3.20	2.73	3.65
Aldehydes	8.74	7.83	8.32	9.04	11.27	1.70	2.10	1.60	1.93	1.69
Alcohols	3.72	4.71	5.49	4.32	4.58	0.80	1.30	1.00	2.00	0.75
Ketones	3.78	7.66	8.11	4.57	5.39	15.00	8.50	6.10	6.37	8.04
Phenolic	5.36	7.43	7.77	5.34	3.37	12.70	13.30	18.80	16.49	19.79
Furans	7.47	6.64	6.97	7.10	9.25	6.80	4.50	2.80	3.32	4.46
Sugars	2.14	1.88	1.97	2.08	2.69	1.40	1.50	4.80	4.46	2.45
Water	7.05	6.97	6.92	6.75	6.79	27.00	28.90	29.20	25.36	26.95
Bio-oil	51.76	55.13	58.16	52.06	60.09	79.50	72.10	75.10	75.33	75.39
Char	28.15	26.01	21.58	26.82	18.30	16.56	23.05	20.72	17.67	18.46
Gas	19.69	17.86	19.06	20.62	21.21	3.94	4.85	4.18	7.00	6.15

*Unidentified compounds: Bio1 - 5.8%; Bio2 - 4.4%; Bio3 - 7.5%; Bio4 - 12.61%; Bio5 - 6.60%.

The change in component yields is quite significant, given that only one parameter in one particular reaction was changed. Acids and furans yield suffers an approximately two fold increase, while aldehydes and ketones yield increases by about 50%. Alcohols and phenolics yield remains constant and water yield increases by about 75%. Char and gas yield also increase, which means that the error for these component classes will be higher. Sugar yield dropped to about 2% in all biomass samples. It's not hard to hypothesize a probable reason why other

component yield increases with this modification - given that the pre-exponential factor of the LVG formation reaction was lowered, thus slowing the reaction rate for this particular reaction meant more activated cellulose available to react. Since there is only one other reaction specified for activated cellulose (reaction 2), the products of said reaction must be the ones which yield is favoured, which is indeed the case, validating this hypothesis (neither alcohols or phenolics are in this reaction, and their yield remains constant, which also confirms this).

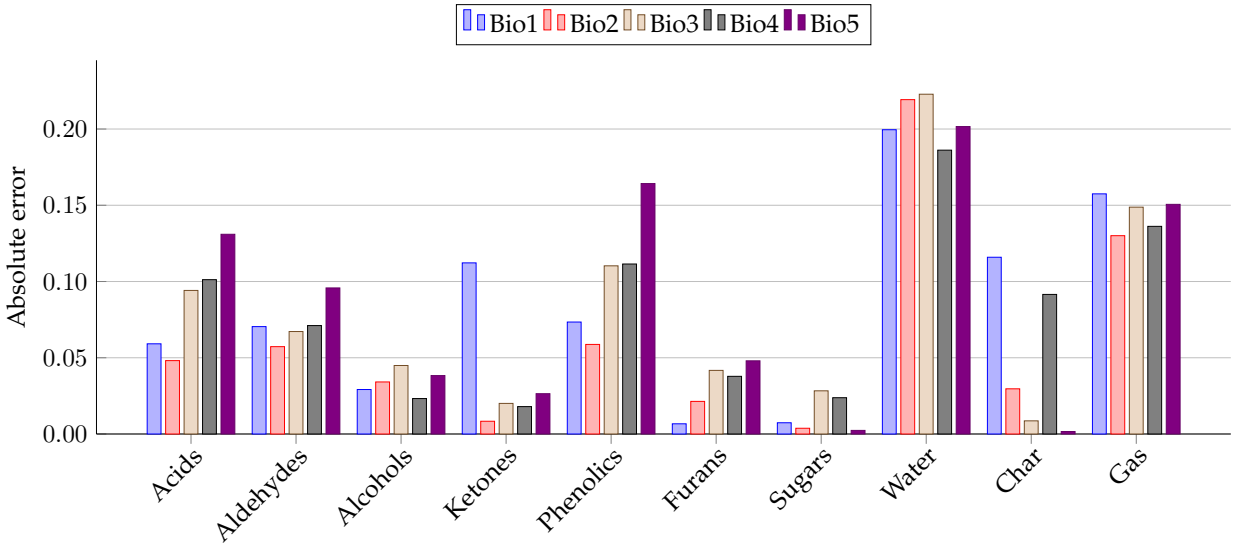

Figure 4.3: Absolute error for the five biomass samples, reaction 2 with $n = 0.5$ (S1* simulation).

Analysing figure 4.3, one can see that the acids, aldehydes and furans show an higher deviation than previous simulations, this is due to the yield increase caused by reaction 2 modification. So in order to at the same time keep the sugar and other organics errors low, a modification to the stoichiometric coefficients of reaction 2 may be needed.

Simulations S3 and S4 use Anca-Couce's mechanism. The non trapped species scenario is still considered in S4. Regarding S3, since there is an additional freedom degree, the x parameter, so S3 results had to be obtained using different values for this new variable. Therefore, three values were set: 0.3, 0.5 and 0.8. The best between the three (x = 0.3) was chosen to be presented here, while the others can be consulted in the appendix.

By analysing table 4.6, one can see that the acid content is substantially higher (roughly double), as well all other liquid components, with the exception of alcohols, when compared to Ranzi's scheme. This general yield increase may be justified by the removal of saccharides from the reaction mechanism. Due to the inclusion of secondary reaction terms, which originate CO_2, water and solid carbon, the yields for these components are considerably higher. While that is desirable for water, which is still under-predicted (simulation results determine the yield to be about half of the actual experimental results), char (mainly composed of solid carbon) seems to have a constant yield rounding 30 wt.%, while experimental data rounds about 20 wt.%. As far as CO_2 yield is concerned, a slight increase was observed, although the global gas yield remained fairly the same in both schemes. It is important to note that while in Anca-Couce's scheme, char is indeed mainly composed by solid carbon, that is not the case for Ranzi's scheme, where more than half of the char yield actually originates from the trapped species. Therefore, biomass that has a more heterogeneous char ultimate composition may be better modelled by Ranzi's scheme.

Table 4.6: Simulation results using Anca-Couce et al. reaction scheme, with x = 0.3 (S3).

	Simulation					Experimental*				
Sample	Bio1	Bio2	Bio3	Bio4	Bio5	Bio1	Bio2	Bio3	Bio4	Bio5
Acids	10.10	8.98	9.43	9.60	12.51	7.60	7.20	3.20	2.73	3.65
Aldehydes	6.79	6.47	7.00	7.04	8.62	1.70	2.10	1.60	1.93	1.69
Alcohols	3.09	4.21	4.97	3.58	3.70	0.80	1.30	1.00	2.00	0.75
Ketones	3.26	7.44	7.97	4.13	4.75	15.00	8.50	6.10	6.37	8.04
Phenolic	4.04	5.04	4.90	3.87	2.16	12.70	13.30	18.80	16.49	19.79
Furans	5.58	4.96	5.21	5.31	6.91	6.80	4.50	2.80	3.32	4.46
Water	13.99	13.05	13.30	13.93	15.71	27.00	28.90	29.20	25.36	26.95
Bio-oil	46.84	50.15	52.77	47.47	54.36	79.50	72.10	75.10	75.33	75.39
Char	33.00	33.12	31.00	32.39	26.42	16.56	23.05	20.72	17.67	18.46
Gas	19.76	15.74	15.03	19.64	18.82	3.94	4.85	4.18	7.00	6.15

*Unidentified compounds: Bio1 - 5.8%; Bio2 - 4.4%; Bio3 - 7.5%; Bio4 - 12.61%; Bio5 - 6.60%.

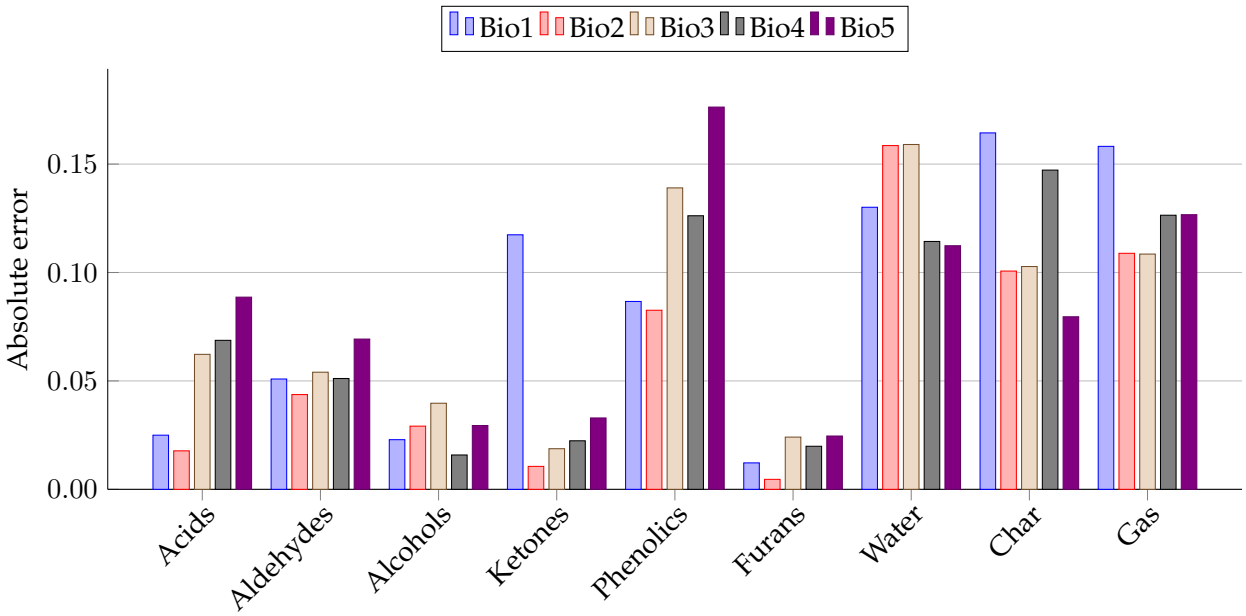

Figure 4.4: Absolute error for the five biomass samples, $x = 0.3$ (S3 simulation).

Since acid yield suffered a two fold increase, the absolute errors are also much higher than for S1 and S2, as can be seen in figure 4.4. Water error decreased but is still quite high, with phenolics still under-predicted with almost unaltered absolute errors compared to S1 (as with other components classes). So, the major differences between schemes are water, char and acids content increase.

Table 4.7 shows the yields for all the components in simulation S4. Similarly to S2, were no trapped species are considered either, the yield for gas products increases, and char yield decreases. Phenolic yield also decreases slightly comparing to S3.

Figure 4.5 shows the absolute errors for S4, in which the major differences are only in the char

Table 4.7: Yield results using Anca-Couce scheme without trapped species, $x = 0.3$ (S4).

	Simulation					Experimental*				
Sample	Bio1	Bio2	Bio3	Bio4	Bio5	Bio1	Bio2	Bio3	Bio4	Bio5
Acids	10.10	8.98	9.43	9.60	12.51	7.60	7.20	3.20	2.73	3.65
Aldehydes	6.76	6.41	6.93	7.01	8.59	1.70	2.10	1.60	1.93	1.69
Alcohols	3.06	4.16	4.91	3.55	3.67	0.80	1.30	1.00	2.00	0.75
Ketones	3.24	7.39	7.91	4.10	4.72	15.00	8.50	6.10	6.37	8.04
Phenolic	3.75	4.50	4.23	3.55	1.88	12.70	13.30	18.80	16.49	19.79
Furans	5.58	4.96	5.21	5.31	6.91	6.80	4.50	2.80	3.32	4.46
Water	13.95	12.97	13.20	13.88	15.67	27.00	28.90	29.20	25.36	26.95
Bio-oil	46.44	49.37	51.81	47.00	53.96	79.50	72.10	75.10	75.33	75.39
Char	26.15	23.70	19.97	24.54	18.54	16.56	23.05	20.72	17.67	18.46
Gas	27.01	25.93	27.01	27.96	27.09	3.94	4.85	4.18	7.00	6.15

*Unidentified compounds: Bio1 - 5.8%; Bio2 - 4.4%; Bio3 - 7.5%; Bio4 - 12.61%; Bio5 - 6.60%.

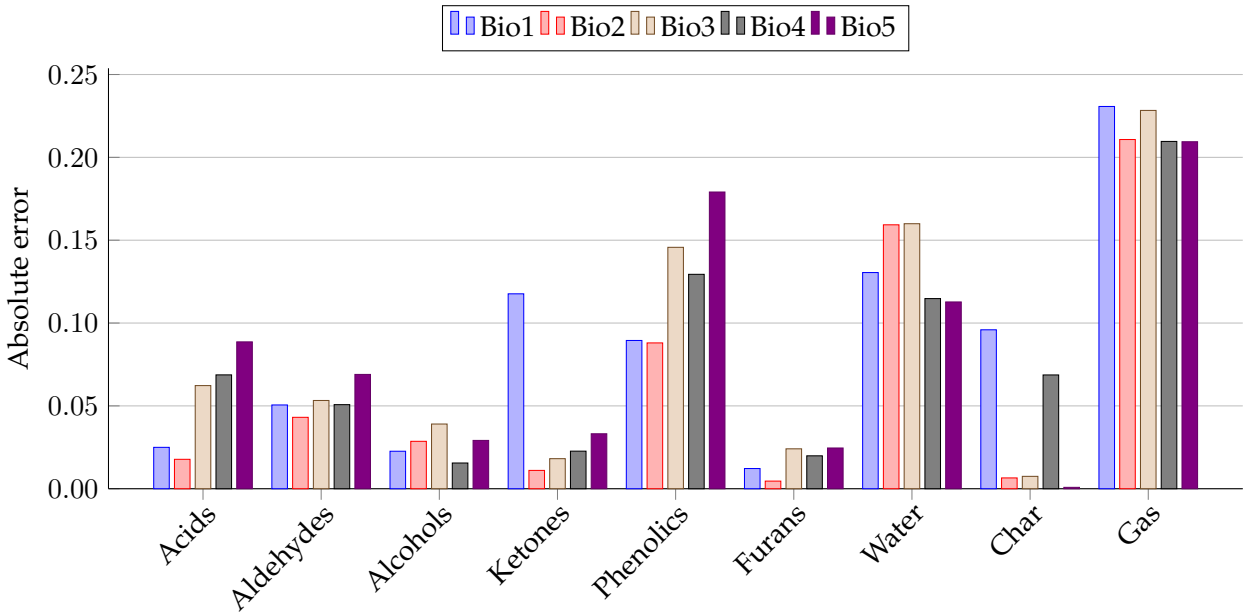

Figure 4.5: Absolute error for the five biomass samples, $x = 0.3$ (S4 simulation).

and gas content. This is due to the fact that no trapped species were considered, which translates into higher gas contents. Char content decreased, but that was also due to the fact that there are no trapped species, and so their yield doesn't add up. While the char absolute error is lower than the trapped species case, the underlying cause for such high char contents remains unsolved (the mechanistic modifications proposed by Anca-Couce). Since the x parameter is related to the extent of secondary reactions happening, considering char yield only, lower values are preferred. Next simulation will detail into the impact of this parameter in the results.

Considering trapped species proved to be a better approach in both schemes overall, despite the fact that the absolute error for char alone as well as summing the gas fraction in S4 is lower

(solid carbon yield remains fairly constant in both S3 and S4 scenarios). This has to do with a tendency for the Anca-Couce scheme to yield more gas and char due to secondary reaction considerations. However, trapped species "inhibit" high gas yields, which are not consistent with fast pyrolysis empirical data, also the manipulation of the kinetic parameters for the gas release reactions could be used as a way to control gas and char ratios. It's important to note that the kinetics for these reactions, in the reaction conditions studied, are relatively slow, which means that almost all of the trapped species don't react. This is a problem that arises from the determination conditions of the kinetic data, due to the restrictive heating rates allowed. It is likely that the real kinetic triplet favours faster reaction rates.

Table 4.8: Simulated yields for *Pinus insignis* (Bio4) as a function of the x parameter using Anca-Couce reaction scheme.

x	0.3	0.35	0.4	0.45	0.5	0.55	0.6	0.65	0.7	0.75	0.8
Acids	9.60	8.92	8.23	7.54	6.86	6.17	5.49	4.80	4.11	3.43	2.74
Aldehydes	7.04	6.55	6.06	5.57	5.08	4.58	4.09	3.60	3.10	2.61	2.11
Alcohols	3.58	3.46	3.34	3.21	3.08	2.95	2.81	2.67	2.52	2.37	2.22
Ketones	4.13	3.95	3.78	3.60	3.42	3.24	3.07	2.89	2.71	2.53	2.34
Phenolic	3.87	3.81	3.74	3.66	3.58	3.49	3.40	3.29	3.19	3.07	2.95
Furans	5.31	4.93	4.55	4.17	3.79	3.41	3.03	2.65	2.27	1.90	1.52
Water	13.93	15.17	16.42	17.68	18.94	20.21	21.49	22.78	24.07	25.37	26.68
Bio-oil	47.47	46.79	46.11	45.43	44.75	44.06	43.37	42.67	41.98	41.27	40.57
Char	32.39	33.22	34.06	34.90	35.76	36.62	37.49	38.38	39.26	40.16	41.07
Gas	19.64	19.49	19.33	19.16	18.99	18.82	18.64	18.45	18.26	18.06	17.86

With a deviation limit defined, the Anca-Couce scheme was tested varying globally the x value. For simplicity sake, the results shown in table 4.8 are only for one species, the same simulation for the other species can be consulted in the appendix. The selected species to present here was *Pinus insignis* (Bio4) due to the fact that the elemental balances and respective cellulose, hemicellulose and lignin content were better matched (the equation system to determine the lignin representative components didn't converge for all the samples). By analysing table 4.8, where the x parameter is varied, one can see that bio-oil and gas yield tend to decrease while water and char content increases with higher x. This is most likely due to secondary reactions, to which the contribution is increased with x, therefore promoting char, water and gas formation. Despite this gas content decreases, so there's other mechanism that offsets the effect of the x parameter for gas formation. Acids are the most sensitive to x variation, while phenolics are the less sensitive. This may be due to the fact that acids are only formed in one reaction (cellulose decomposition), which has the stoichiometric coefficients as a function of x, while for reactions the involve phenolic formation, only two are reported as a function of x. This decreases the effect of the variation in this parameter, therefore translating in less sensitive yield results.

In order to have a better perception of the deviation to experimental data for each compound category, an absolute error plot vs variable x is presented in figure 4.6. One can see that at $x = 0.8$, most of the bio-oil components are under the tolerance value, with the exception of ketones and phenolics. Gas and char deviation are quite high, and if one tries to minimize error for bio-oil components, then the char error is increased.

With the notion on how the product yields vary with x, some modifications to the reaction scheme were made to match experimental data. The first optimization (Opt1) consisted in increas-

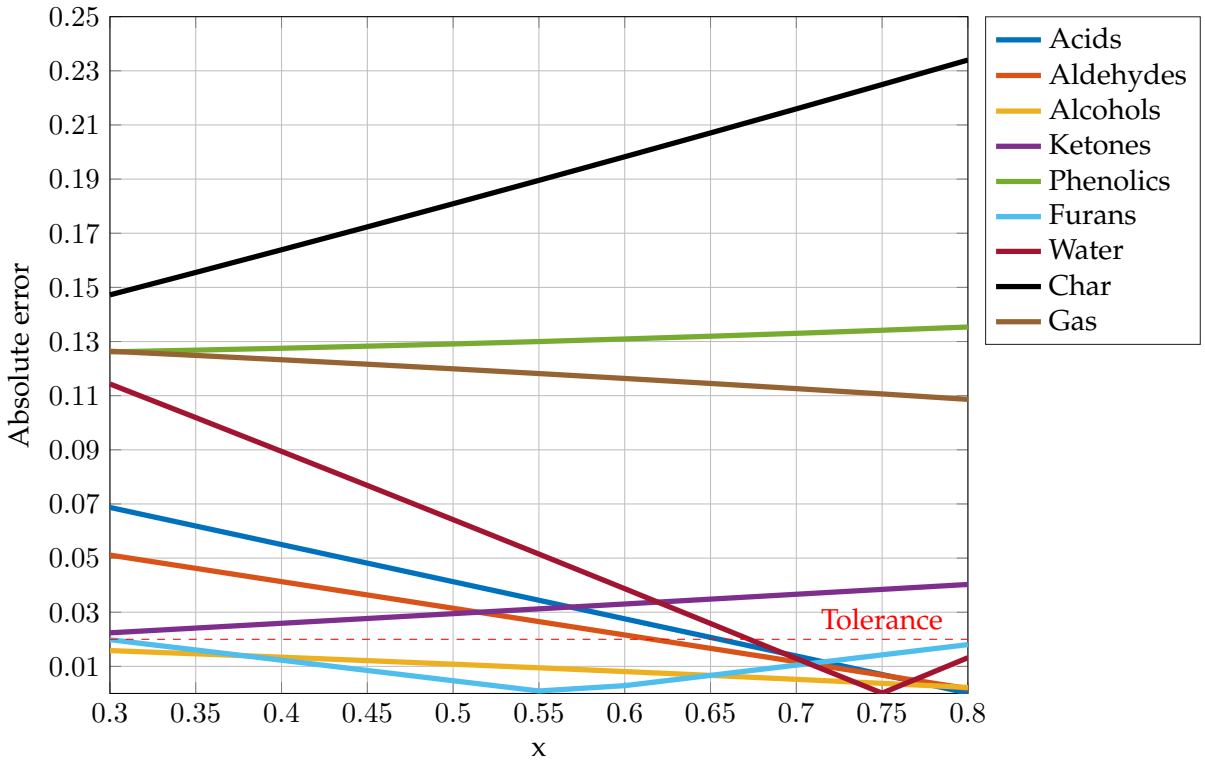

Figure 4.6: Absolute error as a function of x parameter for *Pinus insignis* (S5).

ing the pre-exponential factor of reaction 12 (LIG-CC decomposition) by two orders of magnitude, with $x = 0.3$ (this modification was kept throughout the other optimization simulations). The x parameter was maintained for the reactions involving lignin, and was set to 0.8 for all the other (Opt2). The last optimization (Opt3) consisted in setting the x parameter to zero in the lignin reaction coefficients, which is equivalent to revert the coefficients back to the ones used in Ranzi's mechanism.

Figure 4.7 shows the results for the optimized scenarios. One can see that the modifications allowed a considerable decrease in the absolute error of most of the component classes, the exceptions being ketones, phenolics, char and gas. For these, yields are still far from a 2% deviation. A more profound modification of the scheme is therefore required.

The last exploratory scenario studied (S6) used the relatively new feature of the FLUIDBED unit that allows introduction of chemical reactions, and so fluid dynamics of the bed are taken into consideration when determining reaction yields. Unfortunately, the calculations proved to be cumbersome and any increase in the kinetic parameters led to convergence problems, therefore, no further attempts were made to arrive at a working version of this simulation with appreciable conversion (table 4.9 presents the almost non existent yields that resulted with this simulation).

However, in the Aspen Plus description of the fluidized bed model, one can see how it considers chemical reactions, and an alternative way of reaching to similar results of those that would result from the FLUIDBED model calculations is to use a battery of CSTRs, which is the approach used by the model itself. So each CSTR is a "cell", where the solid and gas are considered perfectly mixed. The only question that remains is the number for cells that should be considered.

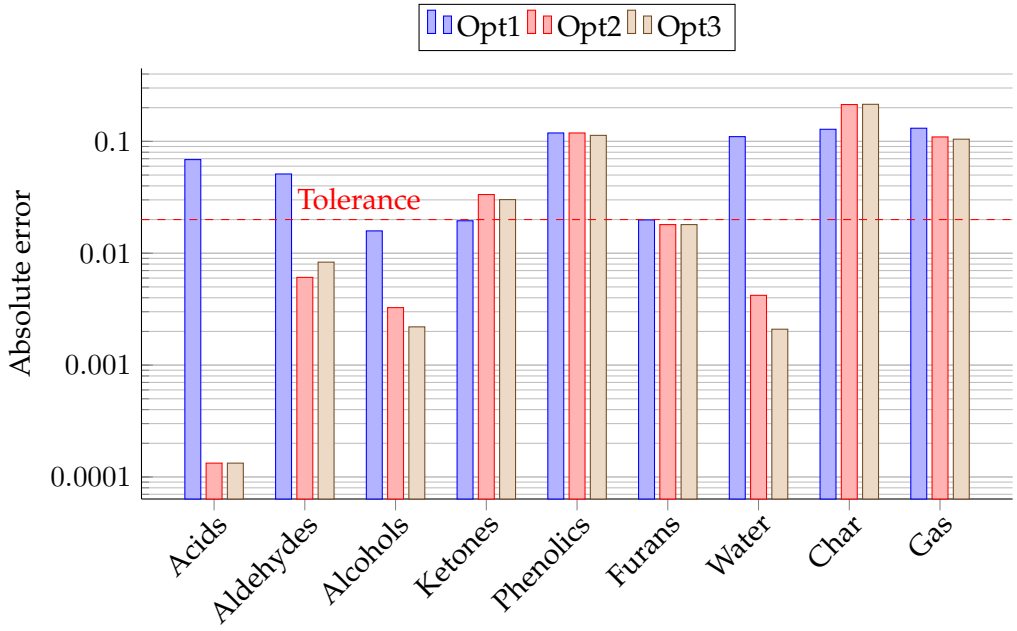

Figure 4.7: Absolute error in log scale for the different component classes and optimization scenarios (S5*).

Table 4.9: Component yields as a function of temperature for scenario S6, Bio4 sample, with reactions introduced directly into the FLUIDBED unit (S6).

Temperature (°C)	450	460	470	480	490	500	510	Exp.
Acids	0.29	0.41	0.56	0.75	0.98	1.23	1.52	2.73
Aldehydes	0.27	0.39	0.54	0.73	0.95	1.19	1.47	1.93
Alcohols	0.31	0.40	0.52	0.65	0.80	0.96	1.14	2.00
Ketones	0.09	0.12	0.15	0.18	0.21	0.25	0.29	6.37
Phenolic	1.16	1.43	1.73	2.07	2.46	2.87	3.33	16.49
Furans	0.05	0.07	0.08	0.10	0.12	0.15	0.18	3.32
Water	0.03	0.04	0.05	0.06	0.07	0.08	0.09	25.36
Bio-oil	2.21	2.86	3.64	4.54	5.60	6.74	8.02	75.33
Char	95.48	94.27	92.82	91.15	89.20	87.09	84.74	17.67
Gas	1.37	1.80	2.32	2.91	3.61	4.37	5.21	7.00

Most likely, for a proper simulation, a high number of cell would be advisable, although it's not practical to implement in Aspen Plus, and so as a proof of concept, only 5 CSTR in series were simulated, however with much more significant results.

It can be seen in figure 4.8 that yields are sensitive to reactor temperature, although the results themselves show significant difference with previous simulations. A myriad of reasons could be causing this difference, although investigating these reasons fall out of the scope of this work. However, using several CSTRs as numerical cells could prove to be a insightful approach to these type of systems in Aspen Plus and surely deserves further studies.

An important aspect of this work that has not been mentioned yet is the required energy to

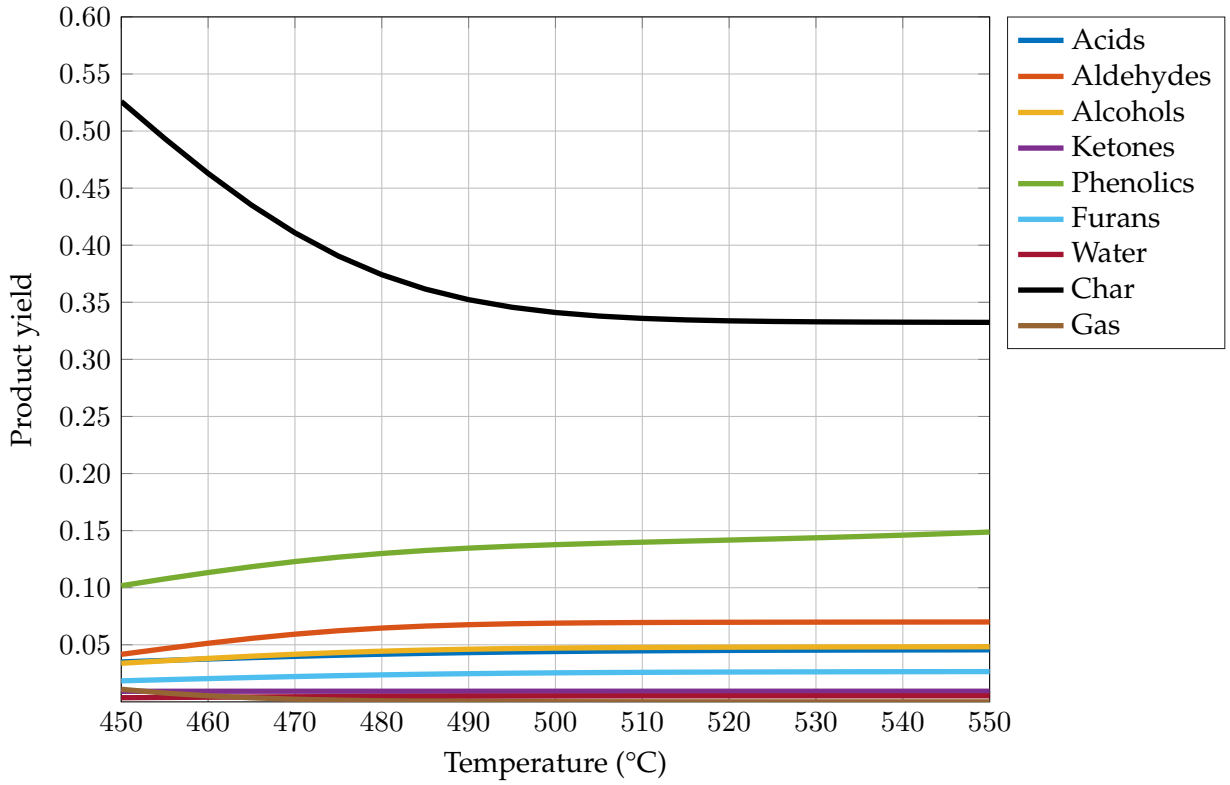

Figure 4.8: Product yield for the 5 CSTR in series as a function of temperature (S6*, Bio4).

meet process demands. There are two energy-requiring operations within the process: drying and pyrolysis. In order to efficiently pyrolyse the lignocellulosic material, that has to be a moisture of <10%, achievable only by a drying operation, since using natural convection only makes possible to reduce the wood's water content to about 25% (from about 50% when harvested) and there are security concerns as well for solid combustible materials that unadvise against storing these in low moisture conditions. While drying is a necessary pre-treatment, the pyrolysis reactor is the core of the process, and where the most energy intensive operations take place. It is therefore necessary to cautiously consider heat balances, since these will dictate process viability and profitability.

So far in the simulations done, a rather high residence time (τ) for the CSTR has been used ($\approx$ 10 secs), this is due to the fact yields tend to stabilize at about this time. This is shown in figure 4.9, using Bio4 sample from optimized scenario three (Opt3).

In previous chapters, as well as throughout the literature, the optimal residence times for fast pyrolysis are within a 1-2 second range, and so the question arises as to why such a high residence time was used. The kinetic parameters used in Ranzi et al. scheme, specifically the pre-exponential factor, result in a slower than expected reaction rate, probably because this is a scheme that also allows for slow pyrolysis modelling (and seems more adequate for it as well given the yield predictions obtained so far). Blondeau and Jeanmart also noted this and replaced Ranzi's kinetic parameters by those obtained in the work of Miller and Bellan [8]. Hence, there are two ways to compensate for this fact in order to have a similar product distribution with lower residence times: increase the kinetic parameters (pre-exponential factor is preferred, since is subject to higher error than activation energy, due to kinetic model assumptions when analysing TGA data) or an

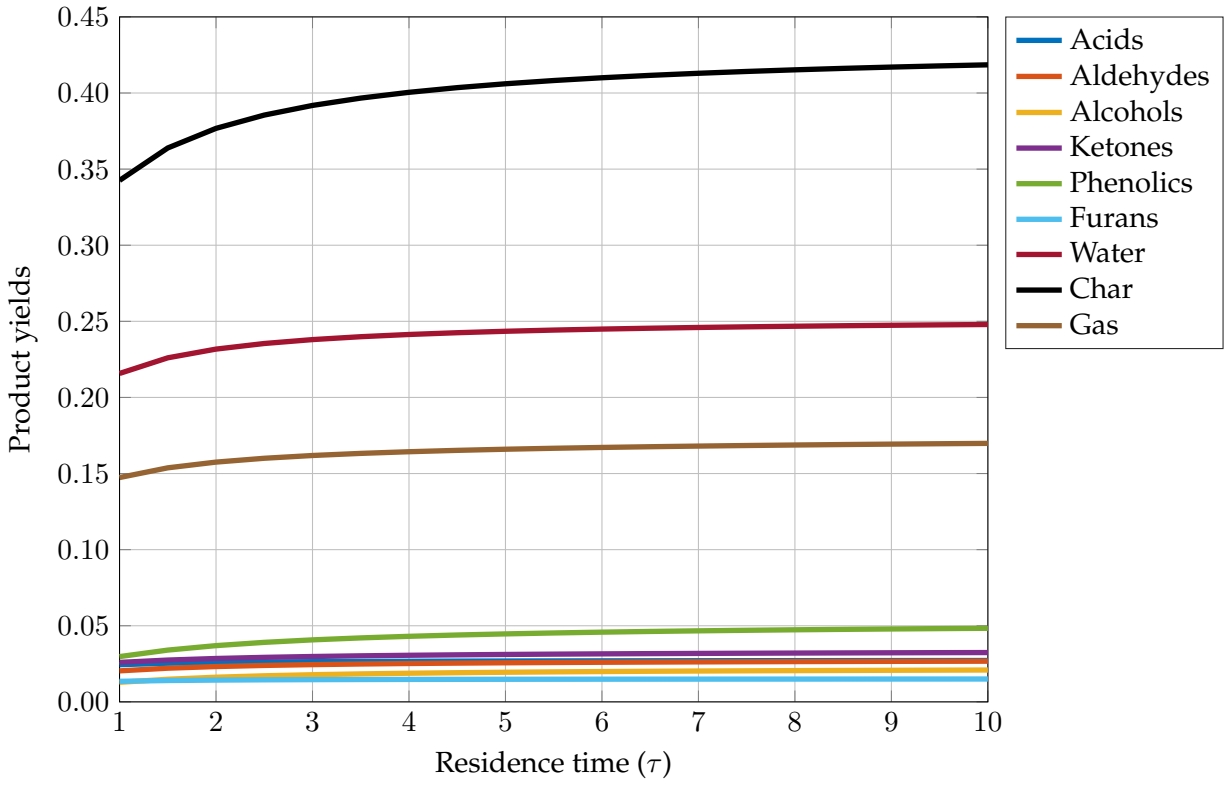

Figure 4.9: Pyrolysis products yields as a function of reactor PYR-KIN residence time (Opt3 scenario from S5*).

increase in residence time. The later approach was chosen for previous simulations due to the fact that it's easier to implement than kinetic parameter modification, however, it's validity is subject to greater debate. Nonetheless, since these simulations were conducted more as a exploratory tool to understand how and what to optimize, it seems more adequate to use simpler and less intensive modifications for this purpose. This is not the case for all following simulations.

Residence time and heat duty of the reactor are intrinsically linked, and so energy balance considerations need also to be accounted for when defining a value for the residence time. Higher residence times result in higher heat duty required, up to the point of unrealistic energy requirements: if residence time is kept at 10 sec, Aspen Plus point towards heat duties in the order of 100 MW, while if using 1 sec, this drops to about 60 MW. The exception is the eucalyptus sample (Bio5), where these values are about 70 MW and 30 MW, respectively. The likely cause that result in lower heat duties for this sample may be due the higher cellulose and hemicellulose content, when compared to the other considered species. One can deduce from this that lignin decomposition is more energy intensive, which is consistent with thermogravimetric data (lignin has a wider decomposition temperature range). However, even when using proper fast pyrolysis residence times, the energetic demand is still unrealistic high. This remains unchanged when using different property methods or parameters (e.g. heat capacity). So, in order to arrive at heat inputs comparable to other works (see Onarheim et al. [9]), one has to pin down the cause of this infeasible heat duties. These are reaction 9 and 13, responsible for LIG-C and LIG-OH decomposition, respectively. This also explains why simulations using the Bio5 sample, with

higher cellulose and hemicellulose content, present lower heat duties. In Aspen Plus environment, if one goes to solid options regarding calculation of the denominator term of concentration (select said reaction, go to Kinetics tab, select Solids options and in the "For the solid component" section, is possible to select either "Solid phase only" or "Solid and fluid phase"), one can see that these have a great impact over the resulting heat duty calculations, e.g. selecting the "Solid phase only" option results in even higher heat duties (an approximate 30 MW increase), while "Solid and fluid phase" option for these two particular reactions still give unusual heat requirements (if one does not consider these reactions, the global heat balance results drop from an energetic demand of about 60 MW to a surplus of about -1 MW, in other words, the process shifts to exothermic). The true reason why these reactions are causing these results is likely related to poorly calculated heat of formation for these components, since these are not in any Aspen Plus databases, and so their properties had to be determined using either contribution group methods or correlations considered adequate. The contribution group method used to specifically determine solid heat of formation within Aspen Plus - Mostafa - does not seem to properly determine the heat of formation for these components. Therefore, another contribution method was used, Van Krevelen [10], which resulted in much more adequate heat requirements (the parameters were externally calculated and introduced as DHSFRM in Properties> Parameters> Pure Components>PCES-1).

4.2 Reaction parameters optimization

In order to optimize the reaction schemes presented before, a new set of simulations (referred from now on as SX) was carried out where reactions pre-exponential factors and stoichiometric coefficients were varied. For the stoichiometric coefficients, the Simplex algorithm was used to assure correct atom balance in all the chemical reactions (Aspen Plus doesn't allow reaction that are not in atom balance either). Restrictions were applied to all the reactions in order to arrive at close to experimental yield values. An important note regarding the optimizations done concerns the cellulose and lignin reactions. Two new components were added into the modified schemes, furfural and guaiacol. Furfural is a furan that is typically found in pyrolysis oil, and it's existence has been detected and confirmed by several works, while 5-(Hydroxymethyl)furfural is not as common reported, and always in lower quantities. Other "cosmetic" changes were done as well, such as replacement of propanal by acetone, since the atomic composition is the same for both components, it doesn't cause any yield variation. This was done due to experimental reports, where acetone shows up in high quantities, while propanal does not, and so it's a more suitable reference component for this class. Hydroacetaldehyde is lumped together with acetic acid in the original scheme, and since both have the same atomic composition, acetid acid was not introduced into the optimized scheme. Acetol is a component that is produced in appreciable quantities, although, due to difficulties in maintaining the atomic balance for the modified reactions, it was not introduced either. Reaction 11 (LIG-O decomposition), was completely reworked, since it was redundant (both LIG-H and LIG-O lead to the formation of LIG-OH, which further decomposes into other volatiles and synapaldehyde). The new decomposition reaction for LIG-O forms guaiacol, which compasses a wide range of products typically found in pyrolysis oil and are the resulting product of the thermal decomposition of the coniferyl alcohol monolignol (predominant in softwoods) [6][1][2][3]. Hardwoods also have sinapyl alcohol and derived components, which were modelled as synapaldehyde (LIG-H decomposition - reactions 10, 13, 14 and 15). LIG-C decomposition, following the original scheme, yields para-coumaryl alcohol, which is the monolignol typically found in grasses. Phenol is also a product of LIG-C decomposition, and of

para-coumaryl alcohol pyrolysis as well. Therefore, with the modifications introduced, is possible to model differences in pyrolysis oil quality as a function of the wood nature.

Table 4.10: Mass yields for the pyrolysis products and respective absolute errors with optimized schemes (SX).

	Component yields (wt.%)					Absolute error (%)				
	Bio1	Bio2	Bio3	Bio4	Bio5	Bio1	Bio2	Bio3	Bio4	Bio5
Acids	8.49	7.49	3.69	4.56	4.53	0.89	0.29	0.49	1.83	0.88
Aldehydes	2.41	2.54	2.23	2.92	2.71	0.71	0.44	0.63	0.99	1.02
Alcohols	2.24	2.30	1.96	1.95	1.85	1.44	1.00	0.96	0.05	1.10
Ketones	12.29	7.69	7.10	8.23	8.63	2.71	0.81	1.00	1.86	0.60
Phenolic	13.69	14.71	18.92	18.27	18.36	0.99	1.41	0.12	1.78	1.43
Furans	4.78	3.84	2.93	5.13	5.59	2.02	0.66	0.13	1.81	1.13
Sugars	0.52	1.19	4.40	3.18	3.54	0.88	0.31	0.40	1.28	1.09
Water	22.54	25.69	27.19	23.35	26.16	4.46	3.21	2.01	2.01	0.79
Bio-oil	66.96	65.46	68.43	67.60	71.38	-	-	-	-	-
Char	22.89	25.43	22.72	20.46	19.40	6.33	2.38	2.00	2.79	0.94
Gas	9.79	8.20	7.76	11.48	8.13	5.85	3.35	3.58	4.48	1.98

Table 4.10 shows the optimized yields for the various considered components on the left and respective error in relation to experimental data on the right. Unfortunately, is was not possible to lower the deviation for all product classes to a value below 2%, specifically, char and gas yields are over-predicted and water yield under-predicted, which was already the case for other simulations. The deviation is more severe for gaseous products, in the 3-6% range, except for Bio5 sample, in which all the component classes are actually below the tolerance limit, while for char and water, deviations around 3% or below were achieved, with the exception of Bio1 sample, which is the one presenting larger errors in general. So, despite the efforts to correct the main issues with the studied reaction mechanisms, they persist, even if less pronounced. It was stated before that the reaction schemes appear to be more adequate for slow pyrolysis conditions, and that might be a very limiting factor in obtaining good data, since per default slow pyrolysis has higher gas and char yields.

Figure 4.10 plots the absolute errors for the various component classes and biomass samples. As previously stated, it was not possible to lower the errors for certain components below the tolerance established, still, a significant improvement was done in comparison to all other simulations tested. Bio1 seems to present higher deviations compared to other biomass samples, with water, char, gas and ketones yield going above the tolerance limit by about 2.5%, 4.3%, 4.9% and 0.7% respectively. Product yields for Bio1 proved to be harder to approximate to experimental results due to the abnormally high ketone yield. This constrained the optimization of the stoichiometric coefficients formulated as a linear problem even further, hence, for it to converge, the Simplex algorithm increased the char and gas coefficients, which can be seen by the higher deviation when compared to the other samples. It can be seen more easily in figure 4.10 that Bio5 is under the tolerance limit in all component classes. The difficulty in matching the simulated yields with actual experimental evidence, specifically water, char and gas, is a convergence issue, a mathematical problem, rather than caused by any physical constrains, although the actual reaction pathways were created based on experimental evidence retrieved from thermogravimetric data. Since char, gaseous components and water are simple molecules, the optimization algorithm prioritizes this over other more

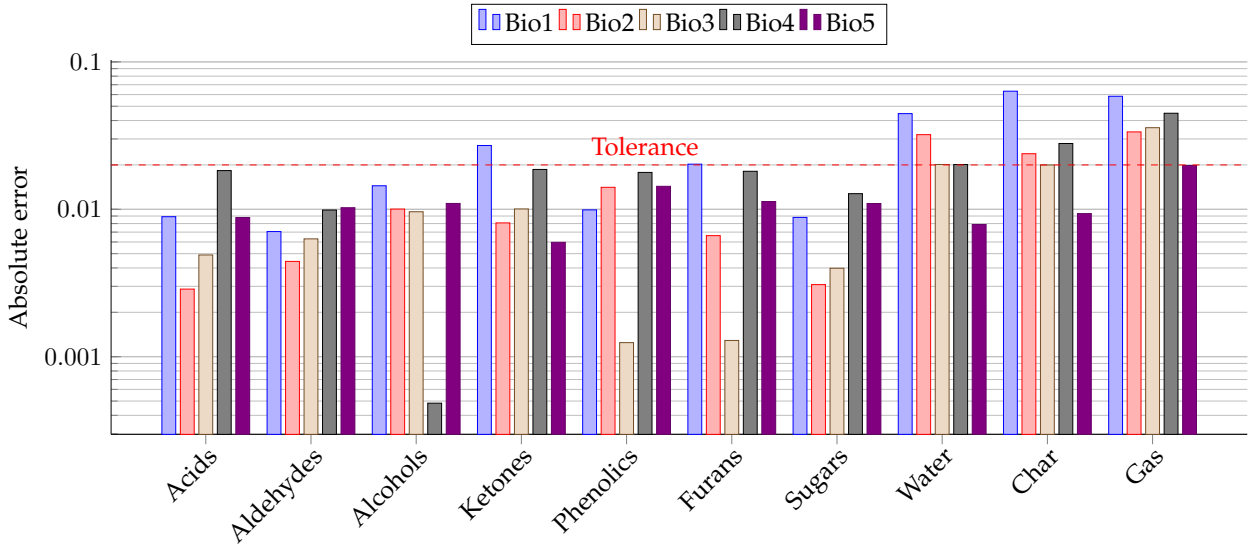

Figure 4.10: Absolute error for the five biomass types used in the simulation (SX).

complex species, since for some cases it's the only way to actually arrive at a reaction with proper atom balance.

So far, the results presented grouped the components into classes, for easier understanding and comparison with experimental results, and since the reaction products are model components, supposed to represent a wide class of molecules with similar structure and properties, this seems to be a reasonable simplification. However, there are substantial differences within grouped component classes, e.g. the phenolics yield is the sum of guaiacol, synapaldehyde, p-coumaryl alcohol and phenol and these present different yields according to the biomass sample used. This was done on propose to somehow represent the differences between wood types and respective lignin structures. As previously discussed, the pyrolysis products that originate from lignin differ according the the biomass monolignol make-up, and the optimized scenario (SX) attempted to model this by considering each lignin model component representative of a monolignol (LIG-C as p-coumaryl alcohol, predominant in grassy biomass; LIG-O as coniferyl alcohol, common is most biomass types, however in softwoods this is virtually the sole monolignol present; and LIG-H as sinapyl alcohol, which can be found in hardwood, along with coniferyl alcohol as well). While Faravelli et al. proposed a method to determine each representative lignin component based on ultimate analysis of lignin, it has been discussed before that this is a purely mathematical exercise, and it fails to represent the true nature of the complex polymer that is lignin. Also, applying the proposed method wasn't successful for all the biomass samples studied in this work (based on the cellulose, hemicellulose and lignin contents, as well as ultimate analysis retrieved from the literature, only *Pinus insignis* (Bio4) was able to arrive at lignin compositions expressed in terms of LIG-C, LIG-O and LIG-H and that simultaneously fulfilled the condition of having the same ultimate composition of sample's lignin fraction and experimental determined cellulose, hemicellulose and lignin content). With this said, the differences in elemental composition experimentally determined and the one that results from the combination of the five pseudo-components used to describe biomass are not very significant (below 2%), and therefore, and for the sake for being able to actually perform the simulations, this inconsistency was allowed.

Table 4.11 presents the yields for various components grouped in the "phenolics" class. Due to

Table 4.11: Yield (wt.%) variation for the considered phenolic products in the SX simulation according to biomass sample.

	Bio1	Bio2	Bio3	Bio4	Bio5
Guaiacol	7.05	6.56	7.26	12.15	8.99
p-Coumaryl alcohol	1.61	1.99	0.53	1.08	0.28
Phenol	2.74	2.67	2.67	4.51	4.08
Sinapaldehyde	2.30	3.49	8.47	0.54	5.01

the overall high phenolic yield that is reported throughout the literature regarding lignocellulosic biomass fast pyrolysis, substantial variations in specific component yield can occur without this translating in a drastic change in the overall phenolics yield. That is noticeable in table 4.11, specially for sinapaldehyde, which has a low yield for Bio4 sample, since this is a softwood, while for hardwoods (all the remaining samples), the yields range between 2.3 to about 8.5%. The reason why there's such a high variability in wood samples that are the same type is related to the atomic balances done in order to determine the pseudo-component composition - this had to be recalculated for the SX scenario, so that it could account for the changes done in the reactions mechanisms (the changes are mostly in lignin components). In order to match as close as possible the ultimate analysis data and pseudo-component composition, it proved easier to alter the LIG-H content, which is responsible for the sinapaldehyde formation and therefore, it greatly influences the yield of this component. Since the only expected major difference between biomass samples is indeed synapyl alcohol, it makes sense to adjust the content of this pseudo-component rather than others in order to match simulation data with experimental results.

Table 4.12 presents the optimized reaction scheme for Bio5 sample, where one can see substantial differences when in comparison to the other used reaction sets. Stoichiometric coefficients differ for most of the reactions, as well as the pre-exponential factors. Reaction 11, where LIG-O decomposition happens, was completely reworked to account for guaiacol formation, a product that originates from coniferyl alcohol decomposition and was considered the model component for all other products that also result from this monolignol pyrolysis. One other major difference in the SX reaction scheme is the amount of trapped species that are formed in the reactions. Most of the CO_2 and CO that were directly formed in the thermal decomposition of the various pseudo-components are now converted into trapped species and only after released. This allows for a better control in the amount of gas formed, with the added disadvantage that it will directly affect char yield, since the trapped species are considered as char, and if they don't react, they will count towards solid yield. One can also see that reaction 14, that leads to the formation of sinapaldehyde, has a rather high exponent in the temperature dependent pre-exponential term. This means that if LIG-H is present in enough quantity, it will likely form sinapaldehyde in high amounts, which is indeed the case. Branca et al. results [6] show that for hardwoods, the syringol and guaiacol yield is equivalent, and so the optimization carried out attempted to match this, however, not with much success, as can be seen in table 4.11.

Table 4.13 presents the energy balance results for all the studied biomass samples using the optimized schemes (SX). It is to note that pyrolysis duty includes the energy necessary to heat both the fluidization gas and solid biomass up to the reaction temperature as well as the energy required for the chemical reactions. Bio-oil energy efficiency was calculated using equation 4.1,

Table 4.12: Reaction scheme with optimized stoichiometric coefficients and kinetic parameters for Bio5 sample (SX).

	Reaction			A (s^{-1})	E_a (kJ mol^{-1})
1	CELL	$\rightarrow$	CELLA	8x10^{15}	192.5
2	CELLA	$\rightarrow$	0.3HAA + 0.05GLYOX + 0.05CH_3CHO + 0.3ACETONE + 0.1HMF + 0.1FURFURAL + 2.85H_2O + 2.9Char + 0.3G{CO}$_2$	5x10^{10}	125.5
3	CELLA	$\rightarrow$	LVG	$4T^{1.17}$	41.8
4	CELL	$\rightarrow$	5H_2O + 6Char	8x10^{7}	133.9
5	HCE	$\rightarrow$	0.4HCEA1 + 0.6HCEA2	1x10^{12}	129.7
6	HCEA1	$\rightarrow$	0.15CH_2O + 0.2MeOH + 0.05EtOH + 0.3ACETONE + 2H_2O + 2.7Char + 0.65G{CO_2}+ 0.1CH_4 + 0.1C_2H_4	3x10^{10}	113.0
7	HCEA2	$\rightarrow$	XYL	$3T$	46.0
8	HCEA2	$\rightarrow$	0.5CH_2O + 0.15MeOH + 0.15EtOH + 0.45ACETONE + 0.5H_2O + 1.025Char + 0.875G{CO_2} + 0.5G{COH_2}+ 0.1CH_4 + 0.1C_2H_4	1x10^{12}	138.1
9	LIG-C	$\rightarrow$	0.35LIG-CC + 0.59pCOUMARYL + 0.2PHENOL + H_2O + 3.02Char + 0.22CO	4x10^{15}	202.9
10	LIG-H	$\rightarrow$	LIG-OH + ACETONE	2x10^{13}	156.9
11	LIG-O	$\rightarrow$	1.7GUAIACOL + PHENOL + 0.1MeOH + 1.5H_2O + 2G{CO_2}	1x10^{10}	106.7
12	LIG-CC	$\rightarrow$	0.3pCOUMARYL + 0.2PHENOL + 0.35$C_3H_4O_2$ + 0.7H_2O + 0.65CH_4 + 0.6C_2H_4 + G{COH_2} + 0.8G{CO} + 6.4Char	5x10^{9}	131.8
13	LIG-OH	$\rightarrow$	0.5MeOH + 2.1H_2O + 3.9Char + 1.2LIG + 0.6G{CO} + 0.4CH_4 + 0.2C_2H_4	5x10^{9}	125.5
14	LIG	$\rightarrow$	FE2MACR	$8T^2$	50.2
15	LIG	$\rightarrow$	0.2ACETONE + 0.2CH_2O + 0.4MeOH + 0.2CH_3CHO + H_2O + 0.5CO + 0.6CH_4 + 0.65C_2H_4 + G{CO} + 0.5G{COH_2} + 5.5Char	1.2x10^{8}	125.5
16	G{CO_2}	$\rightarrow$	CO_2	1x10^{7}	100.4
17	G{CO}	$\rightarrow$	CO	1x10^{13}	209.2
18	G{COH_2}	$\rightarrow$	CO + H_2	5x10^{11}	272.0
19	G{H_2}	$\rightarrow$	H_2	5x10^{11}	313.8

$$\eta_{\text{bio-oil}} = \frac{Q_{\text{bio-oil}}}{Q_{\text{feed}} + 2.5P} \tag{4.1}$$

where $Q_{\text{bio-oil}}$ and Q_{feed} are the enthalpies of the bio-oil stream and feed stream, respectively and P is the electricity input (by means of grinding, pumps, compressors and the dryer belt).

It can be seen that the heat duty for pyrolysis is more or less constant for all the samples, with Bio4 and Bio5 having higher duties. This may be due to the fact that these two biomass types are different than the first three samples (and therefore have different elemental and pseudo-component composition). The efficiency values are consistent with literature [11][9], with the exception of Bio1 and Bio5, which present higher than expected values (7-12% difference in efficiency). The heat surplus ranges between 0.59 to 2.05MW with sample type, and so all these samples are adequate for an energetic self-sufficient process, although the quality of the bio-oil varies and so it could prove to be more beneficial to have an energy deficit if this would translate in higher bio-oil quality and energy efficiency. There seems to be a tendency for the heat surplus to

Table 4.13: Energy balance to the pyrolysis plant for the five biomass types.

	Bio1	Bio2	Bio3	Bio4	Bio5
Pyrolysis duty (MW)	1.64	1.65	1.66	1.77	1.79
Bio-oil energy efficiency (%)	66.26	60.91	60.73	66.15	67.55
Excess heat (MW)	1.95	2.48	2.97	2.47	1.75
Feed					
Mass flow (kg/h)	3750	3750	3750	3750	3750
Enthalpy (MW)	11.16	11.03	11.93	12.38	11.22
Dryer					
Air flow (kg/h)	61700	61500	61500	61500	61250
Dryer duty (MW)	2.00	2.00	2.00	2.00	1.99
Bio-oil					
Mass flow (kg/h)	1220.2	1519.9	1324.6	1200.3	1305.7
Enthalpy (MW)	8.72	6.87	7.40	8.35	7.75
Water (wt.%)	22.54	25.69	27.19	23.35	26.16
Heating value (MJ/kg)	21.95	16.27	20.11	25.06	21.37
Char					
Mass flow (kg/h)	626.43	696.08	621.78	560.12	530.84
Enthalpy (MW)	4.32	5.32	5.39	4.73	4.08
Heating value (MJ/kg)	24.8	27.5	31.2	30.4	27.7

decrease with bio-oil energy efficiency increase, which makes sense - the energy that isn't converted into bio-oil goes to either the gas or the char stream, which are both combusted in the COMB unit, and turned into heat for the process, so higher char yield (and to a less extent gas) translates into more available heat for the process. In order to determine the dryer gas flow and heat duty, two operational parameters were fixed: outlet solid stream moisture and inlet temperature of the drying gas (air). The outlet biomass moisture was matched to the moisture content determined in the proximate analysis for each sample and the temperature was set to 140°C. The difference in air flow that can be seen in table 4.13 is due to the different outlet moisture contents for each biomass type (these range from 9.2 wt.% (Bio1) to 9.5 wt.% (Bio5)). The mass flow differs within a 200 kg/h range, since the global bio-oil yield differs between biomass samples as well. The energy density or heating value of the bio-oil is between 19-22 MJ/kg, which is in agreement with literature [12]. Water content must not be higher than 30 % to avoid formation of separated phases [9], a requirement that all the biomass samples meet. Char enthalpy was determined using heating values from the literature, with the proper adjustments done in Aspen Plus. An alternative way of determining enthalpy consists in expressing all the char components in terms of C, H and O content so that heat capacity can be determined by Aspen Plus, considering char as a non conventional component, which allows for the consequent determination of the stream enthalpy. However, since experimental data is available, is was favoured over the mentioned alternative approach.

Important unit calculated parameters are presented below. Table 4.14 shows fluidized bed design parameters obtained by Aspen Plus. The pressure drop is relatively low, and the minimum fluidization velocity is also low, which means that relatively low fluidization gas flows can be used without negative fluidization performance.

Table 4.14: Fluidized bed calculated specification (Bio5 sample, SX simulation).

Parameter	Value	Units
Height of bottom zone	0.950	meters
Height of freeboard	6.550	meters
TDH*	5.782 4.520	meters
Solids holdup	1000	kg
Pressure drop	0.208	bar
Minimum fluidization velocity	0.039	m/s
Temperature	500	°C

*First value obtain via correlation and second by solids volume fraction profile.

In figure 4.12 is possible to see the pressure drop, solid fraction and superficial velocity inside the fluidized bed. The limit between the bottom zone and the freeboard as also been identified, being coincident with the solid fraction decrease (the amount of solids exiting through the top should be minimal, since this fluidized bed was designed as a bubbling fluidized bed). Pressure drop only happens in the bottom zone, as well as most of the increase in superficial velocity. Since the solids are all concentrated in the bottom zone, where they behave as a fluid, it's natural that there's pressure drop here, while the remaining height of the reactor contain mostly vapours and so the pressure tends to remain constant.

Regarding the cyclone, figure 4.11 presents the separation efficiency as function of particle diameter. The medium size of the particles is about 500 μm (a normal distribution function with a standard deviation of 50μm and a mean of 500 μm was defined as the PSD for biomass), and so it can be seen that the desired efficiency (99%) is achieved.

In order to determine the air flow needed in the combustion chamber, this was varied and a few important parameters were determined, with the chosen flow being the one that maximize outlet flue gases temperature. This was done for each biomass sample, because there is a fraction of bio-oil that is contained in the non-condensable gases stream, and the char itself does not have the same composition either.

4.3 Sensibility analysis

In this section, a sensibility analysis using the SX reaction parameters and Bio5 sample was performed (the same analysis for other biomass types can be found in the appendix). Reactor residence time and temperature was varied and the correspondent yields determined, with the results presented in figures 4.14 and 4.15, respectively.

As can be seen in figure 4.14, char and gas yields are the component classes that are more sensible to this operation parameter than the bio-oil components. If one was to consider higher residence times, mass balance convergence fails (above approximately 5 secs), and the char yield remains at about 17%. This points out to an inadequacy in properly modelling slow pyrolysis conditions (or any other than fast pyrolysis), since the char yield is suppose to increase with residence time. Gas yield increase is consistent with experimental evidence though. The bio-oil components remains pretty much unchanged (a less than 2% increase in yield from 0.1 to 1 sec).

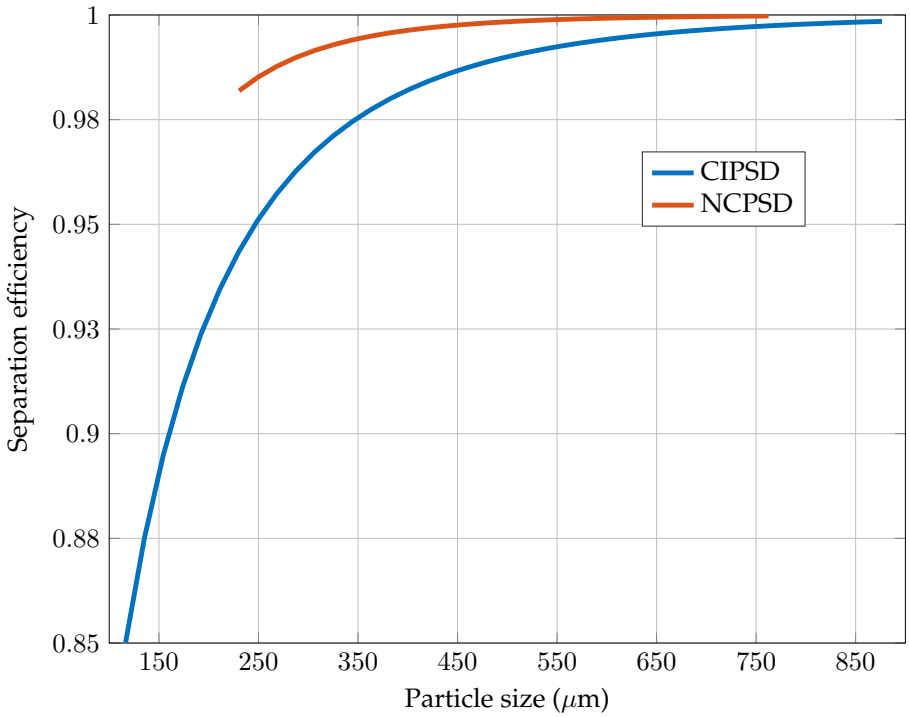

Figure 4.11: Separation efficiency of the PYR-CYC unit as a function of the particle diameter for conventional (CIPSD) and non conventional solids (NCPSD).

It seems that the applicability of the modified reaction mechanisms is limited in residence time range, and by consequence, are not applicable to other types of pyrolysis.

In figure 4.15, one can see the variation in component yields as a function of reactor temperature, and is noticeable that generally speaking, all components are more sensitive to this operation parameter when compared to residence time. All bio-oil components tend to increase with temperature, with the exception of sugars, this is probably due to the sugar formation kinetics, both for levoglucosan and xylan, where the pre-exponential factor is a function of temperature. However, this would in principle cause yield of this compounds to increase, which is not the case. Since these reactions compete with others that have the same reactant, the temperature increase effect is more pronounced in the other reactions, as less substrate is available to be converted into sugars. Similarly to the residence time case, char yield decreases and gas yield increases, however, at least for gas, the increase is not in the same fashion as with residence time. Looking at the respective gas yield curve, it suggests that there's a second order dependency with temperature, at least for the range considered. The decrease in char yield with temperature is consistent with experimental data, however, applicability of the reaction scheme is still limited by the residence time.

An important aspect of a plant of this nature is the utilities used, which is this case are the air used for drying, air for combustion, fluidization gas and cooling liquid in the quench tower. The flows of the first two, and how they were determined can be found above, however, for the fluidization gas and cooling liquid, no explanation has been given on how the flows were determined and which selection parameters were used to accomplish this. Figure 4.16 shows the variation in cooling liquid/pyrolysis vapours ratio in the quench tower as a function of the

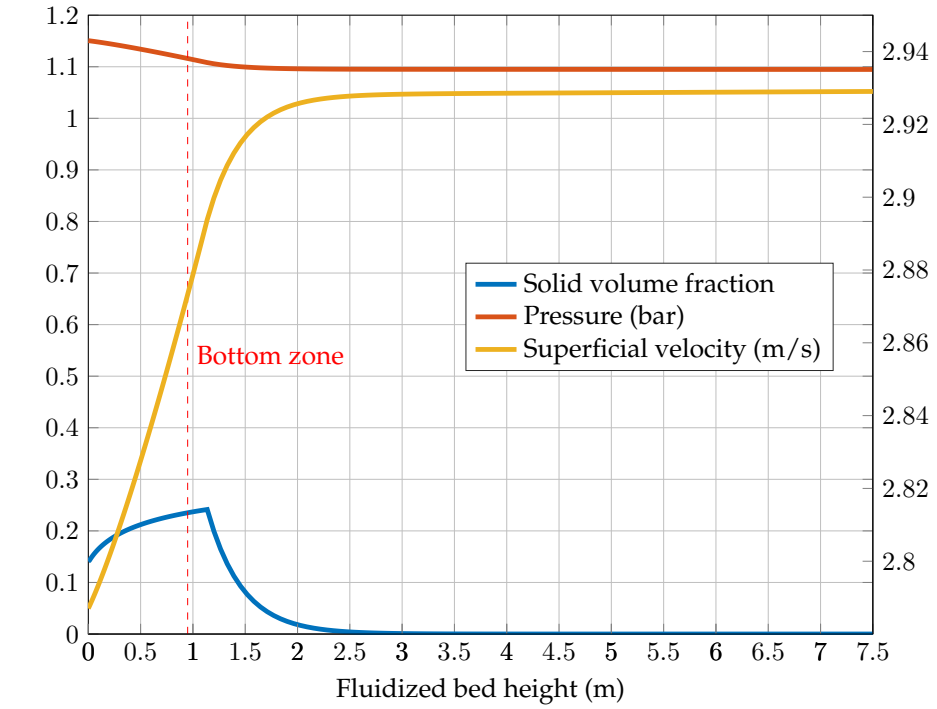

Figure 4.12: Important operation parameters variation with fluidized bed height (Bio5 sample, SX simulation).

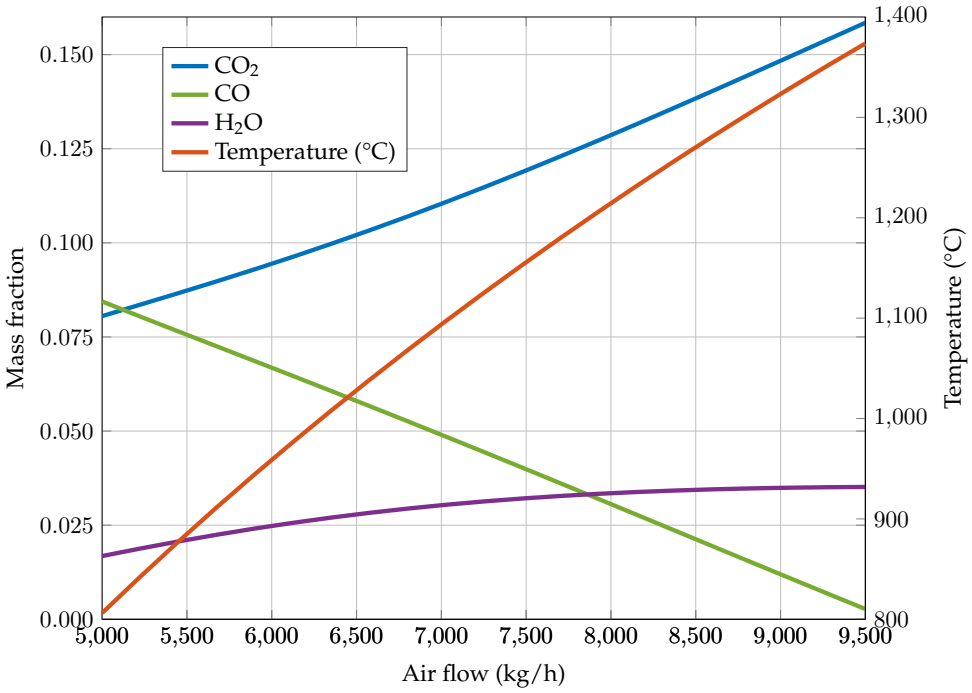

Figure 4.13: Main products and temperature variation of the combustion unit with air mass flow (Bio5 sample, SX simulation).

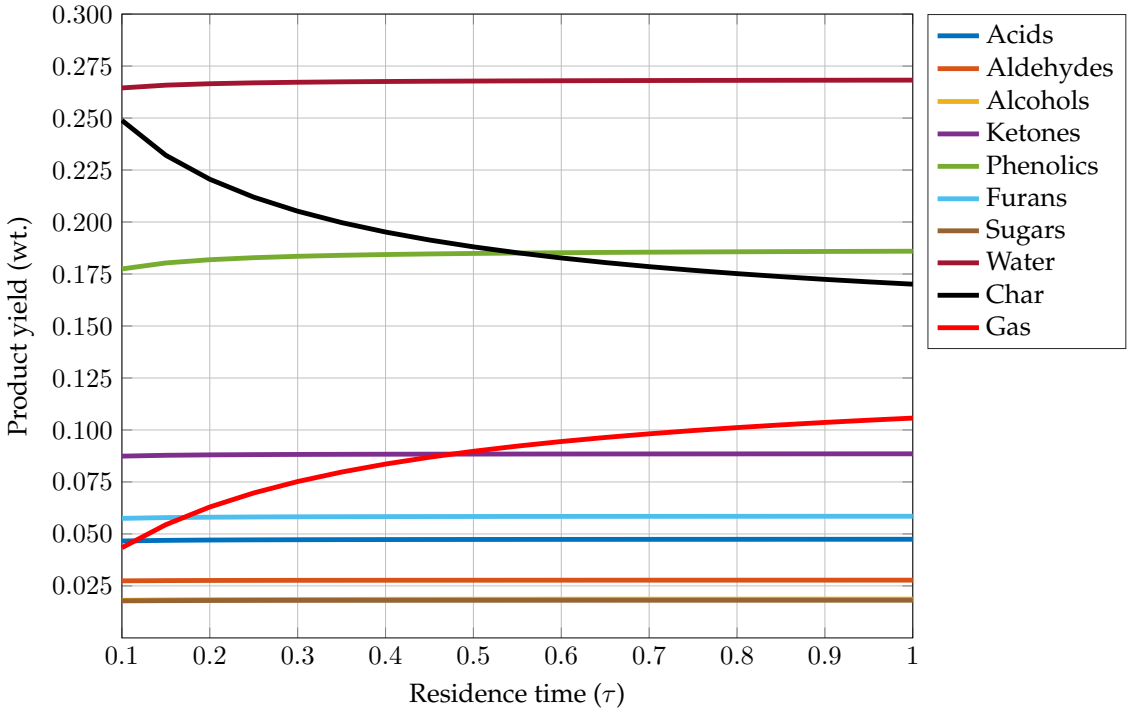

Figure 4.14: Yield variation as a function of reactor residence time (τ) (Bio5 sample, simulation SX).

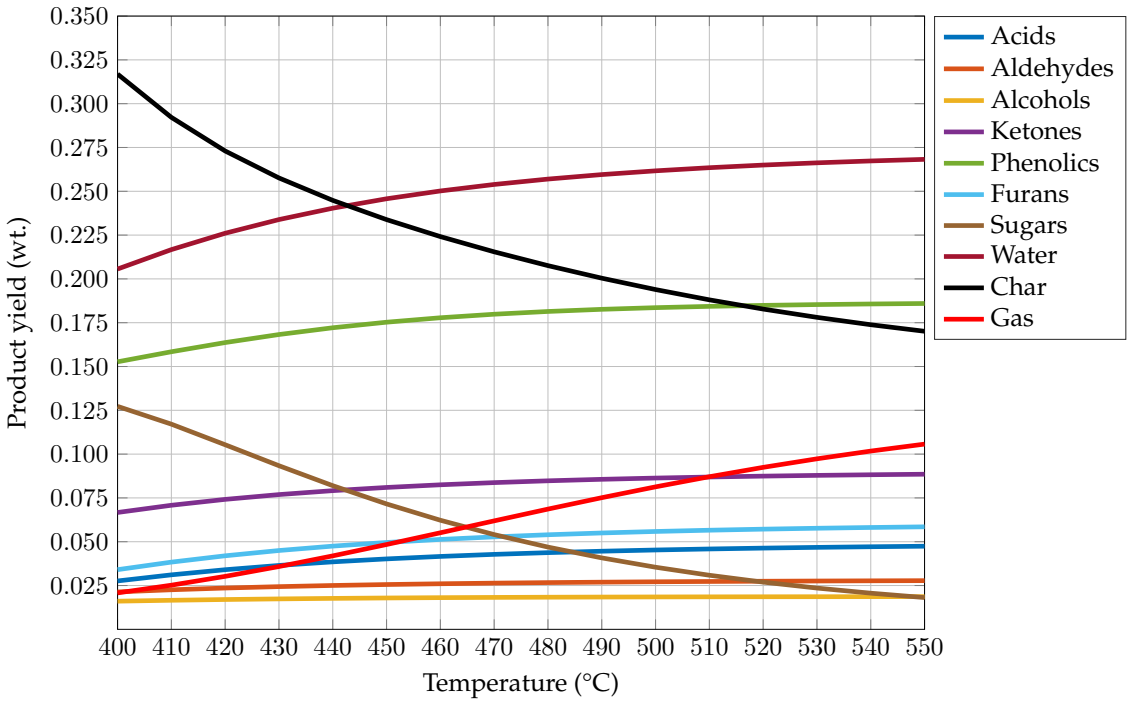

Figure 4.15: Yield variation as a function of reactor residence temperature (in °C) (Bio5 sample, simulation SX).

fluidization gas that enters the fluidized bed reactor. These two streams seem unrelated at first glance, since they are utilities in different unit operations, however, the higher fluidization gas flow used in the BFB reactor is, the higher the pyrolysis vapours flow will be, since the fluidization gas is present along with the vapours until quenching. This means that there's an optimal point, where the fluidization gas and cooling liquid flows are minimized so that the overall cost of using these utilities is the lowest. Unfortunately, is was not possible to retrieve information to allow for an optimization to be carried out. There's also another aspect still related to the utilities flow, specifically the fluidization gas - higher flows will mean larger equipment and harder and more costly separation operations (since the partial pressure of the components of interest is low due to dilution in the inert gas used for fluidization).

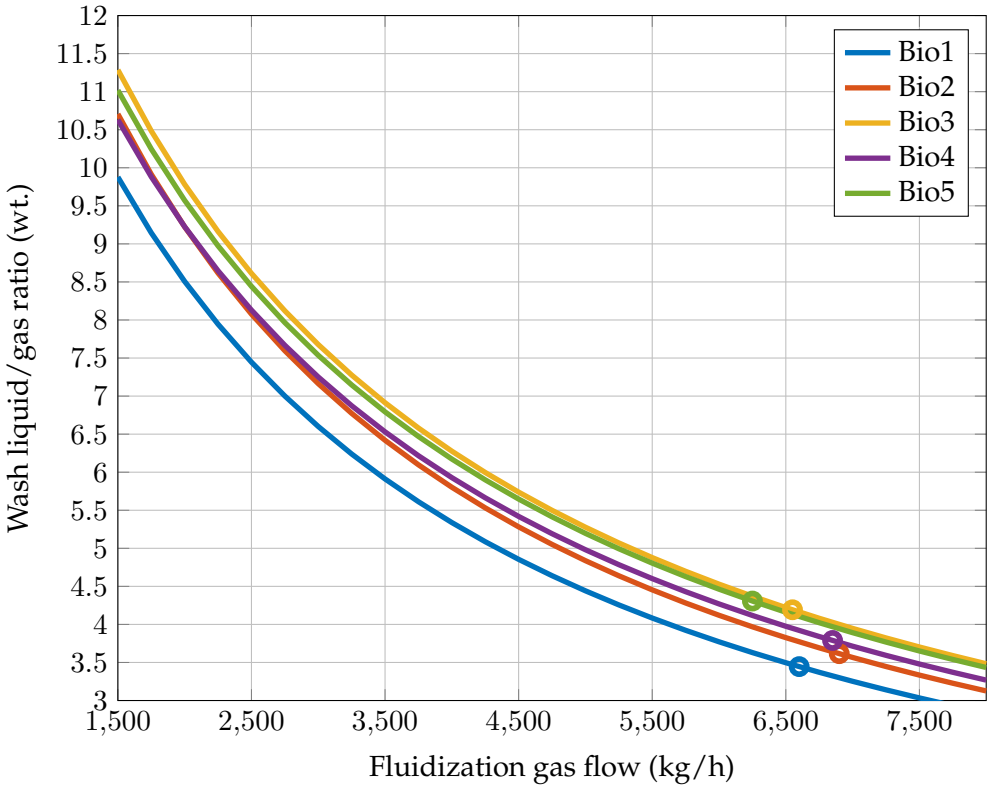

Figure 4.16: Wash liquid (from storage) gas mass flow ratio in the quench cooler (QUENCH) as a function of fluidizing gas, with actual calculated ratios from the simulations marked as dots.

Bibliography

[1] M. Amutio, G. Lopez, J. Alvarez, R. Moreira, G. Duarte, J. Nunes, M. Olazar, and J. Bilbao, "Flash pyrolysis of forestry residues from the portuguese central inland region within the framework of the biorefina-ter project," *Bioresource Technology*, vol. 129, pp. 512 – 518, 2013.

[2] M. Amutio, G. Lopez, M. Artetxe, G. Elordi, M. Olazar, and J. Bilbao, "Influence of temperature on biomass pyrolysis in a conical spouted bed reactor," *Resources, Conservation and Recycling*, vol. 59, pp. 23 – 31, 2012. Biomass valorization to energy and value added chemicals6th European Meeting on Chemical Industry and Environment.

[3] M. Amutio, G. Lopez, J. Alvarez, M. Olazar, and J. Bilbao, "Fast pyrolysis of eucalyptus waste in a conical spouted bed reactor," *Bioresource Technology*, vol. 194, pp. 225 – 232, 2015.

[4] E. Ranzi, A. Cuoci, T. Faravelli, A. Frassoldati, G. Migliavacca, S. Pierucci, and S. Sommariva, "Chemical kinetics of biomass pyrolysis," *Energy & Fuels*, vol. 22, no. 6, pp. 4292–4300, 2008.

[5] A. Anca-Couce, R. Mehrabian, R. Scharler, and I. Obernberger, "Kinetic scheme of biomass pyrolysis considering secondary charring reactions," *Energy Conversion and Management*, vol. 87, pp. 687 – 696, 2014.

[6] C. Branca, P. Giudicianni, and C. D. Blasi, "Gc/ms characterization of liquids generated from low-temperature pyrolysis of wood," *Industrial & Engineering Chemistry Research*, vol. 42, no. 14, pp. 3190–3202, 2003.

[7] S. Thangalazhy-Gopakumar, S. Adhikari, R. B. Gupta, and S. D. Fernando, "Influence of pyrolysis operating conditions on bio-oil components: A microscale study in a pyroprobe," *Energy & Fuels*, vol. 25, no. 3, pp. 1191–1199, 2011.

[8] J. Blondeau and H. Jeanmart, "Biomass pyrolysis at high temperatures: Prediction of gaseous species yields from an anisotropic particle," *Biomass and Bioenergy*, vol. 41, pp. 107 – 121, 2012.

[9] K. Onarheim, Y. Solantausta, and J. Lehto, "Process simulation development of fast pyrolysis of wood using aspen plus," *Energy & Fuels*, vol. 29, no. 1, pp. 205–217, 2015.

[10] D. van Krevelen and K. te Nijenhuis, *Properties of Polymers: Their Correlation with Chemical Structure; their Numerical Estimation and Prediction from Additive Group Contributions*. Elsevier Science, 2009.

[11] M. B. Shemfe, S. Gu, and P. Ranganathan, "Techno-economic performance analysis of biofuel production and miniature electric power generation from biomass fast pyrolysis and bio-oil upgrading," *Fuel*, vol. 143, pp. 361 – 372, 2015.

[12] A. J. Ragauskas, "Heating values for pyrolysis oil and char." Technical Reviews, 2010.

Chapter 5

Conclusion and future work

The energy paradigm is changing, specially in the European Union, where most of the focus towards sustainable alternatives is being made. Biofuels can and will have to play a more important role in this aspect, since these are good "bridge fuels", due to being technologically easier and more feasible to implement than other alternatives regarding the transportation sector. This will allow a smother transition to other more viable renewable alternatives that are still facing technological or other development problems. It is also important to note the biorefinery concept and its benefits, which surpass the transportation sector and could prove its potential delivering other added-value products, such as polymers or speciality chemicals. While a full replacement of conventional fossil fuels by biofuels is unlikely, if not impossible, an increase in total fuel share can certainly be achieved. Specially if other factors come into play, such as alien wood species eradication or wildfires. Therefore one can see that the biofuels thematic is wide and has far reaching implications, such as economical, social and environmental, forming a truly sustainable triangle.

A lot of research has been done in pyrolysis for the last three to four decades, during which the fast pyrolysis concept was created and thoroughly developed into an already commercial reality. Projects such as BTG's BTL rotating cone reactor that provide the community (both residential and industrial) in Hengelo, the Netherlands with renewable electricity, process steam, and pyrolysis oil to replace diesel used in the burners of a nearby industrial installation or KIT's bioliq® process, in Germany, that can produce chemically identical to fossil gasoline exclusively from biomass prove that this industry is thriving at the moment, and may continue to do so, with tighter environmental restrictions and oil price increase. Other reactor designs or new process concepts will certainly aid in the further development of this area and respective technology, however, the focus should be on bio-oil upgrading, which is still lacking viable alternatives to produce fully fledged hydrocarbons that can be used as fuel (DOE catalyst study that determined a TOS of 1200 hours, which is indeed very promising).

Regarding pyrolysis kinetic schemes, there is still a lot of work to do, since there's only one kinetic scheme in the literature with sufficiently detailed reaction mechanisms to actually being applicable in Aspen Plus. Some authors used DFT calculations to determine reaction pathways which is an interesting approach, without the limitations of the thermogravimetric analysis data, typically used to arrive at mechanisms that match thermal degradation curves, which is subject to substantial errors. Combination of these two approaches could prove beneficial. New kinetic models that represent activation energy as a distribution function are also very promising, due to the fact that these can account for biomass heterogeneity.

A standardization in methodologies used is needed, specifically for model components used

to carry out experiments and simulations, and specially for pyrolysis product distribution, since each author groups components and families of components differently.

Aspen Plus introduction of solid modelling units in the 8.X iteration of the software shows potential, however, some issues were encountered that somehow limited this work results, specifically, the inability for the FLUIDBED unit to cope with the pyrolysis reaction mechanism and the quench cooler recycle stream difficulty in converging that forced the use of manipulators (which is not a major issue, since it's assumed that the bio-oil that enters the cooler comes from storage, but still). The solid modelling units used also proved to slightly increase the computational time, without causing much performance issues. However, stacking units that process solids may prove to be a cumbersome task if proper optimization is not done. The non database component introduction also proven to be not so straightforward, with the only solid property estimation method not providing good data, hence, a wider choice in contribution methods is necessary.

The studied reaction mechanisms proved to have high deviations from experimental values, specially regarding water, gas, char, sugars and phenolics. Ranzi's reaction scheme favours levoglucosan formation in excess, which is only true for very low ash content biomass, preferably at vacuum conditions, which is not the case for fast pyrolysis. Anca-Couce scheme registered too high char content, likely due to modifications done to the original scheme (Ranzi et al.), which consisted in adding to some reactions a secondary term containing water, solid carbon and hydrogen to which the stoichiometric coefficients were multiplied by a factor that accounted for secondary reactions (if equal to zero, the original scheme is obtained, if equal to 1, all the reactant is converted into water, solid carbon and hydrogen). The lignin reaction scheme did not reflect the lignin nature in terms of monolignols and was modified to account for this. However, more information about coniferyl/sinapyl ratios for studied biomass species is necessary for a proper representation of lignin pyrolysis. Modifying the stoichiometric coefficients and pre-exponential factors for some reactions proved to be enough to reduce deviation to experimental data considerably, however, the reaction scheme do have limitations, and better reaction kinetics are needed. The limitations of the approach used can be seen in the sensibility analysis, where the liquid components yield didn't vary according to residence time and for temperature it only varied slightly. The heat balances proved to be favourable, with excess heat being generated in all cases and a bio-oil with heating values consistent with experimental data.

These type of studies help paving the way for better understanding of pyrolysis and to develop tools that can help in eventual techno-economical assessments and other assorted works. Allied with experimental verification, these simulation tools may prove to very valuable into designing new pyrolysis facilities, provided that the issues discussed above are resolved.

Appendices

Appendix A

Component yields

Table A.1: Component yields for simulation S1 and S1*.

	S1					S1*				
Sample	Bio1	Bio2	Bio3	Bio4	Bio5	Bio1	Bio2	Bio3	Bio4	Bio5
HAA	0.05946	0.05285	0.05550	0.05654	0.07368	0.13515	0.12012	0.12615	0.12851	0.16747
GLYOXAL	0.01512	0.01344	0.01411	0.01438	0.01874	0.03437	0.03055	0.03208	0.03268	0.04259
CH3CHO	0.01136	0.01231	0.01369	0.01121	0.01352	0.02305	0.02270	0.02460	0.02232	0.02800
CH2O	0.03001	0.02503	0.02651	0.03540	0.04209	0.03001	0.02503	0.02651	0.03540	0.04209
MEOH	0.02836	0.04028	0.04781	0.03283	0.03330	0.02836	0.04028	0.04781	0.03283	0.03330
ETOH	0.00881	0.00686	0.00711	0.01041	0.01255	0.00881	0.00686	0.00711	0.01041	0.01255
PROPANAL	0.02099	0.06213	0.06658	0.03001	0.03473	0.03640	0.07583	0.08097	0.04466	0.05382
PROPDIAL	0.00138	0.00081	0.00010	0.00108	0.00012	0.00138	0.00081	0.00010	0.00108	0.00012
COUMARYL	0.01426	0.00837	0.00098	0.01111	0.00123	0.01426	0.00837	0.00098	0.01111	0.00123
PHENOL	0.00694	0.00408	0.00048	0.00541	0.00060	0.00694	0.00408	0.00048	0.00541	0.00060
FE2MACR	0.03238	0.06181	0.07625	0.03690	0.03187	0.03238	0.06181	0.07625	0.03690	0.03187
HMF	0.03286	0.02921	0.03067	0.03124	0.04072	0.07469	0.06639	0.06971	0.07102	0.09255
LVG	0.23604	0.20980	0.22032	0.22444	0.29249	0.01930	0.01715	0.01801	0.01835	0.02391
XYL	0.00208	0.00162	0.00168	0.00245	0.00296	0.00208	0.00162	0.00168	0.00245	0.00296
H2O	0.04895	0.05061	0.04909	0.04701	0.04121	0.07046	0.06973	0.06917	0.06746	0.06787
TOTAL	0.54897	0.57919	0.61089	0.55041	0.63978	0.51761	0.55132	0.58162	0.52059	0.60092
CO2	0.06337	0.03950	0.04717	0.06627	0.07456	0.07271	0.04780	0.05589	0.07516	0.08614
CO	0.05880	0.06808	0.07406	0.06387	0.06287	0.06734	0.07568	0.08203	0.07200	0.07346
CH4	0.02725	0.02607	0.02537	0.02885	0.02707	0.02938	0.02797	0.02736	0.03088	0.02971
C2H4	0.02745	0.02711	0.02528	0.02814	0.02280	0.02745	0.02711	0.02528	0.02814	0.02280
H2	0.00000	0.00000	0.00000	0.00000	0.00000	0.00000	0.00000	0.00000	0.00000	0.00000
TOTAL	0.17686	0.16076	0.17188	0.18714	0.18730	0.19688	0.17856	0.19056	0.20617	0.21211
C	0.12000	0.12447	0.11140	0.11468	0.07520	0.12972	0.13312	0.12047	0.12392	0.08725
CELL	0.00129	0.00114	0.00120	0.00122	0.00159	0.00129	0.00114	0.00120	0.00122	0.00159
CELLA	0.00127	0.00113	0.00119	0.00121	0.00158	0.00289	0.00257	0.00270	0.00275	0.00358
HCE	0.00030	0.00023	0.00024	0.00035	0.00042	0.00030	0.00023	0.00024	0.00035	0.00042
HCEA1	0.00003	0.00002	0.00002	0.00003	0.00004	0.00003	0.00002	0.00002	0.00003	0.00004
HCEA2	0.00065	0.00051	0.00053	0.00077	0.00093	0.00065	0.00051	0.00053	0.00077	0.00093
LIGC	0.00006	0.00004	0.00000	0.00005	0.00001	0.00006	0.00004	0.00000	0.00005	0.00001
LIGO	0.00005	0.00000	0.00002	0.00004	0.00002	0.00005	0.00000	0.00002	0.00004	0.00002
LIGH	0.00000	0.00000	0.00000	0.00000	0.00000	0.00000	0.00000	0.00000	0.00000	0.00000
LIGCC	0.05680	0.03335	0.00392	0.04425	0.00491	0.05680	0.03335	0.00392	0.04425	0.00491
LIGOH	0.00385	0.00734	0.00906	0.00438	0.00378	0.00385	0.00734	0.00906	0.00438	0.00379
LIG	0.00032	0.00062	0.00076	0.00037	0.00032	0.00032	0.00062	0.00076	0.00037	0.00032
G{CO2}	0.01964	0.01529	0.01585	0.02321	0.02797	0.01964	0.01529	0.01585	0.02321	0.02797
G{CO}	0.00609	0.01121	0.01362	0.00682	0.00571	0.00609	0.01121	0.01362	0.00682	0.00571
G{COH2}	0.05842	0.05306	0.04554	0.05843	0.04465	0.05842	0.05307	0.04554	0.05843	0.04465
G{H2}	0.00140	0.00164	0.00189	0.00164	0.00178	0.00140	0.00164	0.00189	0.00164	0.00178
TOTAL	0.27017	0.25005	0.20524	0.25745	0.16892	0.28151	0.26013	0.21582	0.26824	0.18297

Table A.2: Component yields for simulation S2.

Sample	Bio1	Bio2	Bio3	Bio4	Bio5
HAA	0.05950	0.05288	0.05554	0.05665	0.07373
GLYOXAL	0.01513	0.01345	0.01412	0.01441	0.01875
CH3CHO	0.01137	0.01233	0.01371	0.01125	0.01353
CH2O	0.03003	0.02505	0.02654	0.03547	0.04211
MEOH	0.02841	0.04037	0.04792	0.03301	0.03336
ETOH	0.00881	0.00686	0.00711	0.01043	0.01255
PROPANAL	0.02100	0.06216	0.06661	0.03006	0.03474
PROPDIAL	0.00152	0.00089	0.00010	0.00147	0.00013
COUMARYL	0.01450	0.00851	0.00100	0.01181	0.00125
PHENOL	0.00704	0.00413	0.00049	0.00570	0.00061
FE2MACR	0.03249	0.06201	0.07649	0.03726	0.03197
HMF	0.03288	0.02923	0.03069	0.03131	0.04074
LVG	0.23620	0.20995	0.22047	0.22491	0.29269
XYL	0.00208	0.00162	0.00168	0.00245	0.00296
H2O	0.04906	0.05073	0.04919	0.04736	0.04127
TOTAL	0.55002	0.58016	0.61168	0.55356	0.64040
CO2	0.08305	0.05481	0.06306	0.08962	0.10259
CO	0.11978	0.12917	0.13044	0.12644	0.11039
CH4	0.02733	0.02614	0.02542	0.02910	0.02710
C2H4	0.02756	0.02720	0.02534	0.02850	0.02284
H2	0.00534	0.00522	0.00496	0.00561	0.00479
TOTAL	0.26307	0.24255	0.24921	0.27926	0.26770
C	0.12054	0.12493	0.11169	0.11629	0.07536
CELL	0.00114	0.00102	0.00107	0.00082	0.00142
CELLA	0.00113	0.00101	0.00106	0.00081	0.00140
HCE	0.00026	0.00021	0.00021	0.00023	0.00038
HCEA1	0.00003	0.00002	0.00002	0.00002	0.00004
HCEA2	0.00058	0.00045	0.00047	0.00052	0.00083
LIGC	0.00006	0.00003	0.00000	0.00003	0.00000
LIGO	0.00005	0.00000	0.00002	0.00002	0.00002
LIGH	0.00000	0.00000	0.00000	0.00000	0.00000
LIGCC	0.05541	0.03254	0.00382	0.04024	0.00479
LIGOH	0.00343	0.00654	0.00807	0.00295	0.00337
LIG	0.00029	0.00055	0.00068	0.00025	0.00028
TOTAL	0.18292	0.16730	0.12711	0.16218	0.08789

Table A.3: Component yields for simulation S3 ($x = 0.3$ and $x = 0.5$).

x	0.5					0.3				
Sample	Bio1	Bio2	Bio3	Bio4	Bio5	Bio1	Bio2	Bio3	Bio4	Bio5
HAA	0.07212	0.06411	0.06732	0.09602	0.08938	0.10097	0.08975	0.09425	0.09602	0.12513
GLYOXAL	0.01834	0.01630	0.01712	0.02442	0.02273	0.02568	0.02283	0.02397	0.02442	0.03182
CH3CHO	0.01413	0.01562	0.01745	0.01921	0.01675	0.01944	0.02121	0.02362	0.01921	0.02311
CH2O	0.01642	0.01509	0.01642	0.02678	0.02249	0.02276	0.02068	0.02243	0.02678	0.03126
MEOH	0.02219	0.03537	0.04268	0.02848	0.02457	0.02467	0.03729	0.04468	0.02848	0.02809
ETOH	0.00445	0.00346	0.00359	0.00736	0.00634	0.00623	0.00485	0.00503	0.00736	0.00887
PROPANAL	0.02465	0.06649	0.07154	0.04056	0.03899	0.03165	0.07386	0.07967	0.04056	0.04737
PROPDIAL	0.00069	0.00041	0.00005	0.00075	0.00006	0.00097	0.00057	0.00007	0.00075	0.00008
COUMARYL	0.01302	0.00765	0.00090	0.01053	0.00113	0.01351	0.00794	0.00093	0.01053	0.00117
PHENOL	0.00642	0.00377	0.00044	0.00517	0.00056	0.00663	0.00389	0.00046	0.00517	0.00057
FE2MACR	0.01811	0.03457	0.04265	0.02303	0.01782	0.02021	0.03858	0.04759	0.02303	0.01989
HMF	0.03986	0.03543	0.03721	0.05306	0.04939	0.05580	0.04960	0.05209	0.05306	0.06915
H2O	0.18811	0.17496	0.18051	0.13928	0.21841	0.13991	0.13045	0.13296	0.13928	0.15713
TOTAL	0.43854	0.47322	0.49788	0.47466	0.50861	0.46844	0.50148	0.52774	0.47466	0.54365
CO2	0.09168	0.06718	0.07673	0.08571	0.10766	0.08423	0.05898	0.06774	0.08571	0.09940
CO	0.05267	0.04013	0.02730	0.05739	0.03322	0.06079	0.04681	0.03426	0.05739	0.04418
CH4	0.02058	0.02090	0.02013	0.02510	0.01793	0.02424	0.02380	0.02309	0.02510	0.02283
C2H4	0.02153	0.02243	0.02063	0.02405	0.01506	0.02388	0.02422	0.02238	0.02405	0.01816
H2	0.00658	0.00573	0.00520	0.00417	0.00614	0.00443	0.00353	0.00282	0.00417	0.00359
TOTAL	0.19305	0.15637	0.14999	0.19641	0.18000	0.19758	0.15735	0.15030	0.19641	0.18816
C	0.25216	0.24988	0.24560	0.19573	0.23911	0.19978	0.19680	0.18770	0.19573	0.17498
CELL	0.00130	0.00115	0.00121	0.00123	0.00161	0.00130	0.00115	0.00121	0.00123	0.00161
HCE	0.00030	0.00023	0.00024	0.00035	0.00042	0.00030	0.00023	0.00024	0.00035	0.00042
HCEA2	0.00065	0.00051	0.00053	0.00077	0.00093	0.00065	0.00051	0.00053	0.00077	0.00093
LIGC	0.00006	0.00004	0.00000	0.00005	0.00001	0.00006	0.00004	0.00000	0.00005	0.00001
LIGO	0.00005	0.00000	0.00002	0.00004	0.00002	0.00005	0.00000	0.00002	0.00004	0.00002
LIGH	0.00000	0.00000	0.00000	0.00000	0.00000	0.00000	0.00000	0.00000	0.00000	0.00000
LIGCC	0.05679	0.03335	0.00392	0.04425	0.00491	0.05679	0.03335	0.00392	0.04425	0.00491
LIGOH	0.00385	0.00734	0.00906	0.00438	0.00378	0.00385	0.00734	0.00906	0.00438	0.00379
LIG	0.00018	0.00034	0.00042	0.00023	0.00018	0.00020	0.00038	0.00047	0.00023	0.00020
G{CO2}	0.00982	0.00764	0.00793	0.01625	0.01399	0.01375	0.01070	0.01110	0.01625	0.01958
G{CO}	0.01806	0.03365	0.04111	0.02725	0.01722	0.02418	0.04502	0.05497	0.02725	0.02302
G{COH2}	0.02068	0.02582	0.02961	0.03256	0.02451	0.02836	0.03502	0.04007	0.03256	0.03373
G{H2}	0.00051	0.00044	0.00047	0.00084	0.00071	0.00071	0.00062	0.00066	0.00084	0.00099
TOTAL	0.36441	0.36040	0.34013	0.32393	0.30738	0.32998	0.33116	0.30996	0.32393	0.26418

Table A.4: Component yields for simulation S3 ($x = 0.8$).

Sample	Bio1	Bio2	Bio3	Bio4	Bio5
HAA	0.02885	0.02564	0.02693	0.02743	0.03575
GLYOXAL	0.00734	0.00652	0.00685	0.00698	0.00909
CH3CHO	0.00606	0.00703	0.00794	0.00607	0.00710
CH2O	0.00685	0.00657	0.00722	0.00805	0.00927
MEOH	0.01755	0.03070	0.03749	0.02010	0.01836
ETOH	0.00178	0.00139	0.00144	0.00210	0.00254
PROPANAL	0.01401	0.05517	0.05901	0.02323	0.02627
PROPDIAL	0.00028	0.00016	0.00002	0.00022	0.00002
COUMARYL	0.01228	0.00721	0.00085	0.00957	0.00106
PHENOL	0.00612	0.00359	0.00042	0.00476	0.00053
FE2MACR	0.01335	0.02548	0.03143	0.01521	0.01313
HMF	0.01594	0.01417	0.01488	0.01516	0.01976
H2O	0.26238	0.24545	0.25645	0.26680	0.31226
TOTAL	0.39278	0.42908	0.45093	0.40568	0.45515
CO2	0.10418	0.08201	0.09335	0.10447	0.12136
CO	0.03947	0.02817	0.01446	0.03411	0.01577
CH4	0.01440	0.01519	0.01403	0.01409	0.00989
C2H4	0.01668	0.01721	0.01486	0.01578	0.00910
H2	0.01016	0.00974	0.00964	0.01018	0.01032
TOTAL	0.18490	0.15232	0.14634	0.17863	0.16643
C	0.33356	0.33489	0.33908	0.33466	0.33807
CELL	0.00130	0.00115	0.00121	0.00123	0.00161
HCE	0.00030	0.00023	0.00024	0.00035	0.00042
HCEA2	0.00065	0.00051	0.00053	0.00077	0.00093
LIGC	0.00006	0.00004	0.00000	0.00005	0.00001
LIGO	0.00005	0.00000	0.00002	0.00004	0.00002
LIGH	0.00000	0.00000	0.00000	0.00000	0.00000
LIGCC	0.05679	0.03335	0.00392	0.04425	0.00491
LIGOH	0.00385	0.00734	0.00906	0.00438	0.00378
LIG	0.00013	0.00025	0.00031	0.00015	0.00013
G{CO2}	0.00393	0.00306	0.00317	0.00464	0.00559
G{CO}	0.00852	0.01595	0.01951	0.00963	0.00817
G{COH2}	0.00897	0.01166	0.01349	0.01029	0.01049
G{H2}	0.00020	0.00018	0.00019	0.00024	0.00028
TOTAL	0.41833	0.40861	0.39074	0.41069	0.37442

Table A.5: Component yields for simulation S4 ($x = 0.3$ and $x = 0.5$).

	0.5					0.3				
Sample	Bio1	Bio2	Bio3	Bio4	Bio5	Bio1	Bio2	Bio3	Bio4	Bio5
HAA	0.07212	0.06411	0.06732	0.06858	0.08938	0.10097	0.08975	0.09425	0.09602	0.12513
GLYOXAL	0.01834	0.01630	0.01712	0.01744	0.02273	0.02568	0.02283	0.02397	0.02442	0.03182
CH3CHO	0.01382	0.01503	0.01672	0.01365	0.01645	0.01925	0.02084	0.02317	0.01900	0.02292
CH2O	0.01621	0.01469	0.01592	0.01908	0.02229	0.02263	0.02043	0.02212	0.02663	0.03113
MEOH	0.02174	0.03451	0.04162	0.02504	0.02412	0.02439	0.03676	0.04402	0.02816	0.02782
ETOH	0.00445	0.00346	0.00359	0.00526	0.00634	0.00623	0.00485	0.00503	0.00736	0.00887
PROPANAL	0.02424	0.06571	0.07058	0.03323	0.03858	0.03139	0.07338	0.07908	0.04027	0.04713
PROPDIAL	0.00069	0.00041	0.00005	0.00054	0.00006	0.00097	0.00057	0.00007	0.00075	0.00008
COUMARYL	0.01302	0.00765	0.00090	0.01015	0.00113	0.01351	0.00794	0.00093	0.01053	0.00117
PHENOL	0.00642	0.00377	0.00044	0.00501	0.00056	0.00663	0.00389	0.00046	0.00517	0.00057
FE2MACR	0.01349	0.02575	0.03177	0.01537	0.01328	0.01737	0.03316	0.04091	0.01980	0.01710
HMF	0.03986	0.03543	0.03721	0.03790	0.04939	0.05580	0.04960	0.05209	0.05306	0.06915
H2O	0.18748	0.17375	0.17902	0.18867	0.21779	0.13952	0.12971	0.13205	0.13884	0.15675
TOTAL	0.43190	0.46055	0.48225	0.43992	0.50208	0.46436	0.49371	0.51815	0.47001	0.53964
CO2	0.10150	0.07482	0.08465	0.10421	0.12164	0.09798	0.06968	0.07884	0.10196	0.11898
CO	0.09936	0.11570	0.11803	0.10168	0.08249	0.11701	0.13515	0.13975	0.12136	0.10416
CH4	0.02024	0.02025	0.01933	0.02063	0.01759	0.02403	0.02341	0.02260	0.02486	0.02262
C2H4	0.02089	0.02121	0.01912	0.02062	0.01443	0.02349	0.02347	0.02146	0.02360	0.01777
H2	0.00913	0.00916	0.00921	0.00935	0.00914	0.00761	0.00757	0.00748	0.00783	0.00740
TOTAL	0.25112	0.24114	0.25034	0.25649	0.24529	0.27011	0.25927	0.27013	0.27961	0.27093
C	0.24984	0.24544	0.24012	0.24736	0.23682	0.19835	0.19407	0.18434	0.19410	0.17358
CELL	0.00130	0.00115	0.00121	0.00123	0.00161	0.00130	0.00115	0.00121	0.00123	0.00161
HCE	0.00030	0.00023	0.00024	0.00035	0.00042	0.00030	0.00023	0.00024	0.00035	0.00042
HCEA2	0.00065	0.00051	0.00053	0.00077	0.00093	0.00065	0.00051	0.00053	0.00077	0.00093
LIGC	0.00006	0.00004	0.00000	0.00005	0.00001	0.00006	0.00004	0.00000	0.00005	0.00001
LIGO	0.00005	0.00000	0.00002	0.00004	0.00002	0.00005	0.00000	0.00002	0.00004	0.00002
LIGH	0.00000	0.00000	0.00000	0.00000	0.00000	0.00000	0.00000	0.00000	0.00000	0.00000
LIGCC	0.05679	0.03335	0.00392	0.04425	0.00491	0.05679	0.03335	0.00392	0.04425	0.00491
LIGOH	0.00385	0.00734	0.00906	0.00438	0.00378	0.00385	0.00734	0.00906	0.00438	0.00378
LIG	0.00013	0.00026	0.00032	0.00015	0.00013	0.00017	0.00033	0.00041	0.00020	0.00017
TOTAL	0.31297	0.28831	0.25541	0.29859	0.24863	0.26153	0.23702	0.19973	0.24537	0.18543

Table A.6: Component yields for simulation S4 ($x = 0.8$).

Sample	Bio1	Bio2	Bio3	Bio4	Bio5
HAA	0.02885	0.02564	0.02693	0.02743	0.03575
GLYOXAL	0.00734	0.00652	0.00685	0.00698	0.00909
CH3CHO	0.00557	0.00609	0.00679	0.00551	0.00662
CH2O	0.00651	0.00593	0.00644	0.00767	0.00894
MEOH	0.01684	0.02934	0.03581	0.01929	0.01766
ETOH	0.00178	0.00139	0.00144	0.00210	0.00254
PROPANAL	0.01336	0.05393	0.05749	0.02249	0.02563
PROPDIAL	0.00028	0.00016	0.00002	0.00022	0.00002
COUMARYL	0.01228	0.00721	0.00085	0.00957	0.00106
PHENOL	0.00612	0.00359	0.00042	0.00476	0.00053
FE2MACR	0.00604	0.01154	0.01423	0.00689	0.00595
HMF	0.01594	0.01417	0.01488	0.01516	0.01976
H2O	0.26138	0.24354	0.25409	0.26566	0.31128
TOTAL	0.38229	0.40906	0.42623	0.39373	0.44483
CO2	0.10811	0.08507	0.09652	0.10911	0.12695
CO	0.07135	0.08359	0.08183	0.07041	0.04846
CH4	0.01387	0.01417	0.01277	0.01348	0.00936
C2H4	0.01566	0.01527	0.01247	0.01462	0.00810
H2	0.01177	0.01224	0.01263	0.01203	0.01210
TOTAL	0.22076	0.21034	0.21623	0.21966	0.20497
C	0.32989	0.32787	0.33043	0.33047	0.33446
CELL	0.00130	0.00115	0.00121	0.00123	0.00161
HCE	0.00030	0.00023	0.00024	0.00035	0.00042
HCEA2	0.00065	0.00051	0.00053	0.00077	0.00093
LIGC	0.00006	0.00004	0.00000	0.00005	0.00001
LIGO	0.00005	0.00000	0.00002	0.00004	0.00002
LIGH	0.00000	0.00000	0.00000	0.00000	0.00000
LIGCC	0.05679	0.03335	0.00392	0.04425	0.00491
LIGOH	0.00385	0.00734	0.00906	0.00438	0.00378
LIG	0.00006	0.00011	0.00014	0.00007	0.00006
TOTAL	0.39295	0.37061	0.34555	0.38162	0.34620

Table A.7: Component yields for simulation S5 (Bio4 sample).

x	0.3	0.4	0.5	0.6	0.7	0.8	Opt1	Opt2	Opt3
HAA	0.09602	0.08230	0.06858	0.05487	0.04115	0.02743	0.09602	0.02743	0.02743
GLYOXAL	0.02442	0.02093	0.01744	0.01395	0.01047	0.00698	0.02442	0.00698	0.00698
CH3CHO	0.01921	0.01662	0.01401	0.01138	0.00873	0.00607	0.01921	0.00862	0.00996
CH2O	0.02678	0.02306	0.01932	0.01558	0.01182	0.00805	0.02678	0.00979	0.01070
MEOH	0.02848	0.02709	0.02556	0.02388	0.02206	0.02010	0.02848	0.02116	0.02009
ETOH	0.00736	0.00631	0.00526	0.00421	0.00316	0.00210	0.00736	0.00210	0.00210
PROPANAL	0.04056	0.03714	0.03369	0.03023	0.02674	0.02323	0.04056	0.02659	0.02835
PROPDIAL	0.00075	0.00065	0.00054	0.00043	0.00032	0.00022	0.00363	0.00363	0.00519
COUMARYL	0.01053	0.01034	0.01015	0.00995	0.00976	0.00957	0.01567	0.01567	0.01845
PHENOL	0.00517	0.00509	0.00501	0.00493	0.00485	0.00476	0.00732	0.00732	0.00848
FE2MACR	0.02303	0.02196	0.02064	0.01908	0.01727	0.01521	0.02303	0.02303	0.02477
HMF	0.05306	0.04548	0.03790	0.03032	0.02274	0.01516	0.05306	0.01516	0.01516
H2O	0.13928	0.16419	0.18939	0.21490	0.24070	0.26680	0.14336	0.25781	0.25151
TOTAL	0.47466	0.46114	0.44749	0.43369	0.41976	0.40568	0.48891	0.42530	0.42917
CO2	0.08571	0.08906	0.09261	0.09636	0.10032	0.10447	0.08679	0.09951	0.09724
CO	0.05739	0.05304	0.04854	0.04389	0.03908	0.03411	0.05739	0.03527	0.03410
CH4	0.02510	0.02311	0.02101	0.01881	0.01650	0.01409	0.02629	0.01630	0.01614
C2H4	0.02405	0.02280	0.02135	0.01969	0.01784	0.01578	0.02597	0.01957	0.01908
H2	0.00417	0.00526	0.00641	0.00761	0.00887	0.01018	0.00466	0.00893	0.00806
TOTAL	0.19641	0.19327	0.18992	0.18636	0.18260	0.17863	0.20110	0.17957	0.17462
C	0.19573	0.22265	0.25001	0.27780	0.30601	0.33466	0.21292	0.32336	0.30674
CELL	0.00123	0.00123	0.00123	0.00123	0.00123	0.00123	0.00123	0.00123	0.00123
HCE	0.00035	0.00035	0.00035	0.00035	0.00035	0.00035	0.00035	0.00035	0.00035
HCEA2	0.00077	0.00077	0.00077	0.00077	0.00077	0.00077	0.00077	0.00077	0.00077
LIGC	0.00005	0.00005	0.00005	0.00005	0.00005	0.00005	0.00005	0.00005	0.00005
LIGO	0.00004	0.00004	0.00004	0.00004	0.00004	0.00004	0.00004	0.00004	0.00004
LIGH	0.00000	0.00000	0.00000	0.00000	0.00000	0.00000	0.00000	0.00000	0.00000
LIGCC	0.04425	0.04425	0.04425	0.04425	0.04425	0.04425	0.00213	0.00213	0.00213
LIGOH	0.00438	0.00438	0.00438	0.00438	0.00438	0.00438	0.00438	0.00438	0.00438
LIG	0.00023	0.00022	0.00021	0.00019	0.00017	0.00015	0.00023	0.00023	0.00025
G{CO2}	0.01625	0.01393	0.01160	0.00928	0.00696	0.00464	0.01625	0.00464	0.00464
G{CO}	0.02725	0.02383	0.02036	0.01683	0.01326	0.00963	0.02980	0.02980	0.04084
G{COH2}	0.03256	0.02816	0.02374	0.01928	0.01480	0.01029	0.03599	0.02286	0.02947
G{H2}	0.00084	0.00072	0.00060	0.00048	0.00036	0.00024	0.00084	0.00029	0.00031
TOTAL	0.32393	0.34059	0.35759	0.37495	0.39264	0.41069	0.30499	0.39013	0.39121

Table A.8: Component yields for simulation S5 (Bio1 sample).

x	0.3	0.4	0.5	0.6	0.7	0.8
HAA	0.10097	0.08655	0.07212	0.05770	0.04327	0.04327
GLYOXAL	0.02568	0.02201	0.01834	0.01467	0.01101	0.01101
CH3CHO	0.01944	0.01680	0.01413	0.01146	0.00877	0.00877
CH2O	0.02276	0.01960	0.01642	0.01324	0.01005	0.01005
MEOH	0.02467	0.02349	0.02219	0.02077	0.01922	0.01922
ETOH	0.00623	0.00534	0.00445	0.00356	0.00267	0.00267
PROPANAL	0.03165	0.02816	0.02465	0.02112	0.01757	0.01757
PROPDIAL	0.00097	0.00083	0.00069	0.00055	0.00041	0.00041
COUMARYL	0.01351	0.01327	0.01302	0.01277	0.01253	0.01253
PHENOL	0.00663	0.00653	0.00642	0.00632	0.00622	0.00622
FE2MACR	0.02021	0.01927	0.01811	0.01674	0.01515	0.01515
HMF	0.05580	0.04783	0.03986	0.03189	0.02392	0.02392
H2O	0.13991	0.16388	0.18811	0.21261	0.23736	0.23736
TOTAL	0.46844	0.45355	0.43854	0.42341	0.40816	0.40816
CO2	0.08423	0.08787	0.09168	0.09567	0.09984	0.09984
CO	0.06079	0.05680	0.05267	0.04841	0.04401	0.04401
CH4	0.02424	0.02246	0.02058	0.01862	0.01656	0.01656
C2H4	0.02388	0.02280	0.02153	0.02009	0.01847	0.01847
H2	0.00443	0.00548	0.00658	0.00772	0.00891	0.00891
TOTAL	0.19758	0.19540	0.19305	0.19051	0.18779	0.18779
C	0.19978	0.22578	0.25216	0.27892	0.30605	0.30605
CELL	0.00130	0.00130	0.00130	0.00130	0.00130	0.00130
HCE	0.00030	0.00030	0.00030	0.00030	0.00030	0.00030
HCEA2	0.00065	0.00065	0.00065	0.00065	0.00065	0.00065
LIGC	0.00006	0.00006	0.00006	0.00006	0.00006	0.00006
LIGO	0.00005	0.00005	0.00005	0.00005	0.00005	0.00005
LIGH	0.00000	0.00000	0.00000	0.00000	0.00000	0.00000
LIGCC	0.05679	0.05679	0.05680	0.05679	0.05679	0.05679
LIGOH	0.00385	0.00385	0.00385	0.00385	0.00385	0.00385
LIG	0.00020	0.00019	0.00018	0.00017	0.00015	0.00015
G{CO2}	0.01375	0.01178	0.00982	0.00786	0.00589	0.00589
G{CO}	0.02418	0.02114	0.01806	0.01492	0.01175	0.01175
G{COH2}	0.02836	0.02453	0.02068	0.01680	0.01290	0.01290
G{H2}	0.00071	0.00061	0.00051	0.00041	0.00031	0.00031
TOTAL	0.32998	0.34705	0.36441	0.38208	0.40005	0.40005

Table A.9: Component yields for simulation S5 (Bio2 sample).

x	0.3	0.4	0.5	0.6	0.7	0.8
HAA	0.08975	0.07693	0.06411	0.05129	0.03846	0.02564
GLYOXAL	0.02283	0.01957	0.01630	0.01304	0.00978	0.00652
CH3CHO	0.02121	0.01843	0.01562	0.01278	0.00992	0.00703
CH2O	0.02068	0.01789	0.01509	0.01227	0.00943	0.00657
MEOH	0.03729	0.03645	0.03537	0.03405	0.03249	0.03070
ETOH	0.00485	0.00416	0.00346	0.00277	0.00208	0.00139
PROPANAL	0.07386	0.07019	0.06649	0.06275	0.05898	0.05517
PROPDIAL	0.00057	0.00049	0.00041	0.00032	0.00024	0.00016
COUMARYL	0.00794	0.00779	0.00765	0.00750	0.00736	0.00721
PHENOL	0.00389	0.00383	0.00377	0.00371	0.00365	0.00359
FE2MACR	0.03858	0.03678	0.03457	0.03195	0.02892	0.02548
HMF	0.04960	0.04251	0.03543	0.02834	0.02126	0.01417
H2O	0.13045	0.15246	0.17496	0.19796	0.22146	0.24545
TOTAL	0.50148	0.48747	0.47322	0.45874	0.44403	0.42908
CO2	0.05898	0.06291	0.06718	0.07178	0.07673	0.08201
CO	0.04681	0.04360	0.04013	0.03640	0.03242	0.02817
CH4	0.02380	0.02244	0.02090	0.01917	0.01727	0.01519
C2H4	0.02422	0.02350	0.02243	0.02103	0.01929	0.01721
H2	0.00353	0.00459	0.00573	0.00698	0.00831	0.00974
TOTAL	0.15735	0.15704	0.15637	0.15537	0.15402	0.15232
C	0.19680	0.22298	0.24988	0.27750	0.30583	0.33489
CELL	0.00115	0.00115	0.00115	0.00115	0.00115	0.00115
HCE	0.00023	0.00023	0.00023	0.00023	0.00023	0.00023
HCEA2	0.00051	0.00051	0.00051	0.00051	0.00051	0.00051
LIGC	0.00004	0.00004	0.00004	0.00004	0.00004	0.00004
LIGO	0.00000	0.00000	0.00000	0.00000	0.00000	0.00000
LIGH	0.00000	0.00000	0.00000	0.00000	0.00000	0.00000
LIGCC	0.03335	0.03335	0.03335	0.03335	0.03335	0.03335
LIGOH	0.00734	0.00734	0.00734	0.00734	0.00734	0.00734
LIG	0.00038	0.00037	0.00034	0.00032	0.00029	0.00025
G{CO2}	0.01070	0.00917	0.00764	0.00611	0.00459	0.00306
G{CO}	0.04502	0.03938	0.03365	0.02784	0.02194	0.01595
G{COH2}	0.03502	0.03045	0.02582	0.02115	0.01643	0.01166
G{H2}	0.00062	0.00053	0.00044	0.00035	0.00027	0.00018
TOTAL	0.33116	0.34549	0.36040	0.37589	0.39196	0.40861

Table A.10: Component yields for simulation S5 (Bio3 sample).

x	0.3	0.4	0.5	0.6	0.7	0.8
HAA	0.10209	0.08751	0.07292	0.05834	0.04375	0.02917
GLYOXAL	0.02596	0.02225	0.01855	0.01484	0.01113	0.00742
CH3CHO	0.02402	0.02086	0.01768	0.01447	0.01123	0.00795
CH2O	0.02289	0.01981	0.01671	0.01359	0.01045	0.00728
MEOH	0.04174	0.04081	0.03962	0.03816	0.03643	0.03444
ETOH	0.00534	0.00458	0.00382	0.00305	0.00229	0.00153
PROPANAL	0.05458	0.05042	0.04623	0.04199	0.03772	0.03340
PROPDIAL	0.00007	0.00006	0.00005	0.00004	0.00003	0.00002
COUMARYL	0.00099	0.00097	0.00095	0.00094	0.00092	0.00090
PHENOL	0.00049	0.00048	0.00047	0.00046	0.00046	0.00045
FE2MACR	0.04333	0.04131	0.03883	0.03589	0.03248	0.02861
HMF	0.05642	0.04836	0.04030	0.03224	0.02418	0.01612
H2O	0.13803	0.16265	0.18784	0.21358	0.23989	0.26676
TOTAL	0.51593	0.50008	0.48396	0.46759	0.45094	0.43404
CO2	0.08743	0.09183	0.09662	0.10178	0.10733	0.11326
CO	0.03543	0.03184	0.02797	0.02380	0.01934	0.01459
CH4	0.02272	0.02124	0.01956	0.01768	0.01559	0.01331
C2H4	0.02141	0.02067	0.01954	0.01804	0.01616	0.01389
H2	0.00295	0.00410	0.00536	0.00672	0.00819	0.00976
TOTAL	0.16994	0.16968	0.16904	0.16802	0.16660	0.16480
C	0.18615	0.21532	0.24531	0.27610	0.30769	0.34010
CELL	0.00131	0.00131	0.00131	0.00131	0.00131	0.00131
HCE	0.00025	0.00025	0.00025	0.00025	0.00025	0.00025
HCEA2	0.00056	0.00056	0.00056	0.00056	0.00056	0.00056
LIGC	0.00000	0.00000	0.00000	0.00000	0.00000	0.00000
LIGO	0.00008	0.00008	0.00008	0.00008	0.00008	0.00008
LIGH	0.00000	0.00000	0.00000	0.00000	0.00000	0.00000
LIGCC	0.00416	0.00416	0.00416	0.00416	0.00416	0.00416
LIGOH	0.00825	0.00825	0.00825	0.00825	0.00825	0.00825
LIG	0.00043	0.00041	0.00039	0.00036	0.00032	0.00028
G{CO2}	0.01179	0.01010	0.00842	0.00674	0.00505	0.00337
G{CO}	0.05005	0.04379	0.03744	0.03098	0.02442	0.01777
G{COH2}	0.03840	0.03339	0.02833	0.02322	0.01805	0.01283
G{H2}	0.00069	0.00059	0.00049	0.00039	0.00029	0.00020
TOTAL	0.30213	0.31824	0.33499	0.35240	0.37046	0.38916

Table A.11: Component yields for simulation S5 (Bio5 sample).

x	0.3	0.4	0.5	0.6	0.7	0.8
HAA	0.12513	0.10725	0.08938	0.07150	0.05363	0.03575
GLYOXAL	0.03182	0.02728	0.02273	0.01818	0.01364	0.00909
CH3CHO	0.02311	0.01994	0.01675	0.01355	0.01033	0.00710
CH2O	0.03126	0.02688	0.02249	0.01810	0.01369	0.00927
MEOH	0.02809	0.02639	0.02457	0.02262	0.02055	0.01836
ETOH	0.00887	0.00761	0.00634	0.00507	0.00380	0.00254
PROPANAL	0.04737	0.04319	0.03899	0.03477	0.03053	0.02627
PROPDIAL	0.00008	0.00007	0.00006	0.00005	0.00004	0.00002
COUMARYL	0.00117	0.00115	0.00113	0.00110	0.00108	0.00106
PHENOL	0.00057	0.00056	0.00056	0.00055	0.00054	0.00053
FE2MACR	0.01989	0.01896	0.01782	0.01647	0.01491	0.01313
HMF	0.06915	0.05927	0.04939	0.03951	0.02964	0.01976
H2O	0.15713	0.18764	0.21841	0.24944	0.28072	0.31226
TOTAL	0.54365	0.52619	0.50861	0.49091	0.47309	0.45515
CO2	0.09940	0.10344	0.10766	0.11205	0.11662	0.12136
CO	0.04418	0.03877	0.03322	0.02754	0.02172	0.01577
CH4	0.02283	0.02042	0.01793	0.01534	0.01266	0.00989
C2H4	0.01816	0.01670	0.01506	0.01325	0.01126	0.00910
H2	0.00359	0.00484	0.00614	0.00748	0.00888	0.01032
TOTAL	0.18816	0.18417	0.18000	0.17565	0.17113	0.16643
C	0.17498	0.20686	0.23911	0.27173	0.30472	0.33807
CELL	0.00161	0.00161	0.00161	0.00161	0.00161	0.00161
HCE	0.00042	0.00042	0.00042	0.00042	0.00042	0.00042
HCEA2	0.00093	0.00093	0.00093	0.00093	0.00093	0.00093
LIGC	0.00001	0.00001	0.00001	0.00001	0.00001	0.00001
LIGO	0.00002	0.00002	0.00002	0.00002	0.00002	0.00002
LIGH	0.00000	0.00000	0.00000	0.00000	0.00000	0.00000
LIGCC	0.00491	0.00491	0.00491	0.00491	0.00491	0.00491
LIGOH	0.00379	0.00378	0.00378	0.00378	0.00378	0.00378
LIG	0.00020	0.00019	0.00018	0.00016	0.00015	0.00013
G{CO2}	0.01958	0.01678	0.01399	0.01119	0.00839	0.00559
G{CO}	0.02302	0.02014	0.01722	0.01425	0.01123	0.00817
G{COH2}	0.03373	0.02913	0.02451	0.01986	0.01519	0.01049
G{H2}	0.00099	0.00085	0.00071	0.00057	0.00042	0.00028
TOTAL	0.26418	0.28564	0.30739	0.32943	0.35178	0.37442

Table A.12: Component yields for simulation S6* as a function of reactor temperature (Bio4 sample).

x	450	460	470	480	490	500	510	520	530	540	550
HAA	0.03497	0.03756	0.03985	0.04173	0.04313	0.04409	0.04469	0.04506	0.04529	0.04545	0.04556
GLYOXAL	0.01044	0.01293	0.01496	0.01631	0.01703	0.01734	0.01745	0.01749	0.01749	0.01750	0.01750
CH3CHO	0.00848	0.01029	0.01182	0.01290	0.01356	0.01392	0.01412	0.01424	0.01432	0.01439	0.01445
CH2O	0.02269	0.02810	0.03251	0.03545	0.03701	0.03769	0.03793	0.03800	0.03802	0.03802	0.03802
MEOH	0.01991	0.02410	0.02770	0.03039	0.03212	0.03311	0.03364	0.03392	0.03408	0.03419	0.03428
ETOH	0.01389	0.01398	0.01400	0.01401	0.01401	0.01401	0.01401	0.01401	0.01401	0.01401	0.01401
PROPANAL	0.00656	0.00661	0.00662	0.00662	0.00662	0.00662	0.00662	0.00662	0.00662	0.00662	0.00662
PROPDIAL	0.00266	0.00269	0.00270	0.00270	0.00270	0.00270	0.00270	0.00270	0.00270	0.00270	0.00270
COUMARYL	0.06308	0.07092	0.07737	0.08192	0.08469	0.08618	0.08694	0.08734	0.08757	0.08774	0.08790
PHENOL	0.02608	0.02799	0.02957	0.03081	0.03180	0.03271	0.03372	0.03498	0.03660	0.03866	0.04118
FE2MACR	0.01258	0.01437	0.01596	0.01724	0.01818	0.01880	0.01919	0.01942	0.01955	0.01963	0.01968
HMF	0.01841	0.02039	0.02218	0.02363	0.02470	0.02542	0.02586	0.02613	0.02630	0.02642	0.02652
H2O	0.00362	0.00407	0.00446	0.00477	0.00498	0.00512	0.00520	0.00525	0.00527	0.00528	0.00528
TOTAL	0.24340	0.27401	0.29970	0.31847	0.33054	0.33771	0.34207	0.34514	0.34783	0.35061	0.35370
CO2	0.13094	0.15208	0.16961	0.18196	0.18935	0.19321	0.19507	0.19596	0.19640	0.19665	0.19681
CO	0.01688	0.01832	0.01955	0.02053	0.02123	0.02169	0.02199	0.02217	0.02229	0.02238	0.02245
CH4	0.01799	0.01924	0.02035	0.02130	0.02204	0.02258	0.02295	0.02321	0.02341	0.02356	0.02368
C2H4	0.00432	0.00488	0.00535	0.00568	0.00588	0.00598	0.00603	0.00606	0.00607	0.00607	0.00607
H2	0.01801	0.01954	0.02059	0.02102	0.02081	0.02005	0.01891	0.01759	0.01622	0.01487	0.01360
TOTAL	0.18814	0.21406	0.23546	0.25049	0.25930	0.26351	0.26496	0.26499	0.26438	0.26353	0.26262
C	0.20032	0.22281	0.24165	0.25543	0.26424	0.26931	0.27210	0.27365	0.27460	0.27524	0.27574
CELL	0.15765	0.10200	0.05665	0.02649	0.01036	0.00342	0.00098	0.00025	0.00006	0.00001	0.00000
HCE	0.01101	0.00529	0.00234	0.00096	0.00037	0.00014	0.00005	0.00002	0.00001	0.00000	0.00000
HCEA2	0.06521	0.05029	0.03545	0.02282	0.01342	0.00724	0.00360	0.00166	0.00072	0.00030	0.00012
LIGC	0.00097	0.00020	0.00004	0.00001	0.00000	0.00000	0.00000	0.00000	0.00000	0.00000	0.00000
LIGO	0.00003	0.00001	0.00000	0.00000	0.00000	0.00000	0.00000	0.00000	0.00000	0.00000	0.00000
LIGH	0.04894	0.03539	0.02335	0.01390	0.00742	0.00355	0.00153	0.00060	0.00022	0.00007	0.00002
LIGCC	0.00041	0.00012	0.00003	0.00001	0.00000	0.00000	0.00000	0.00000	0.00000	0.00000	0.00000
LIGOH	0.00164	0.00125	0.00088	0.00056	0.00032	0.00016	0.00008	0.00003	0.00001	0.00000	0.00000
LIG	0.00982	0.00836	0.00670	0.00498	0.00339	0.00211	0.00120	0.00064	0.00032	0.00015	0.00007
G{CO2}	0.00978	0.01221	0.01439	0.01614	0.01739	0.01817	0.01859	0.01877	0.01879	0.01873	0.01862
G{CO}	0.00978	0.01221	0.01439	0.01614	0.01739	0.01817	0.01859	0.01877	0.01879	0.01873	0.01862
G{COH2}	0.00978	0.01221	0.01439	0.01614	0.01739	0.01817	0.01859	0.01877	0.01879	0.01873	0.01862
G{H2}	0.00057	0.00058	0.00059	0.00060	0.00060	0.00060	0.00060	0.00060	0.00060	0.00060	0.00060
TOTAL	0.52591	0.46292	0.41086	0.37419	0.35231	0.34105	0.33591	0.33375	0.33291	0.33258	0.33242

Table A.13: Component yields for simulation SX.

Sample	Bio1	Bio2	Bio3	Bio4	Bio5
HAA	0.08491	0.07487	0.03690	0.04560	0.04528
GLYOXAL	0.00513	0.00452	0.00446	0.00551	0.00729
CH3CHO	0.00170	0.00601	0.00338	0.00418	0.00554
CH2O	0.01723	0.01489	0.01446	0.01949	0.01431
MEOH	0.01554	0.01747	0.01348	0.01144	0.01179
ETOH	0.00690	0.00556	0.00614	0.00808	0.00671
PROPANAL	0.12172	0.07543	0.07065	0.08154	0.08614
PROPDIAL	0.00120	0.00148	0.00039	0.00080	0.00021
GUAIACOL	0.07049	0.06560	0.07258	0.12148	0.08991
COUMARYL	0.01607	0.01994	0.00530	0.01076	0.00279
PHENOL	0.02737	0.02666	0.02667	0.04508	0.04076
FE2MACR	0.02299	0.03490	0.08470	0.00537	0.05014
HMF	0.02229	0.01965	0.01453	0.02394	0.03170
FURFURAL	0.02547	0.01872	0.01476	0.02736	0.02415
LVG	0.00500	0.01177	0.04385	0.03162	0.03527
XYL	0.00019	0.00015	0.00017	0.00022	0.00018
H2O	0.22544	0.25691	0.27187	0.23348	0.26159
TOTAL	0.66962	0.65455	0.68429	0.67595	0.71377
CO2	0.07261	0.05279	0.06122	0.09630	0.07244
CO	0.00577	0.00642	0.00074	0.00072	0.00041
CH4	0.00986	0.01114	0.01006	0.01269	0.00350
C2H4	0.00961	0.01165	0.00557	0.00513	0.00498
H2	0.00000	0.00000	0.00000	0.00000	0.00000
TOTAL	0.09785	0.08199	0.07758	0.11484	0.08133
C	0.12855	0.17136	0.16049	0.12532	0.12553
CELL	0.00037	0.00034	0.00037	0.00043	0.00056
CELLA	0.00108	0.00254	0.00250	0.00093	0.00246
HCE	0.00010	0.00008	0.00009	0.00012	0.00010
HCEA1	0.00010	0.00008	0.00009	0.00012	0.00010
HCEA2	0.00023	0.00019	0.00021	0.00027	0.00022
LIGC	0.00052	0.00064	0.00017	0.00035	0.00009
LIGO	0.00031	0.00029	0.00031	0.00052	0.00029
LIGH	0.00024	0.00037	0.00031	0.00002	0.00019
LIGCC	0.00197	0.00244	0.00065	0.00132	0.00034
LIGOH	0.00375	0.00911	0.00775	0.00049	0.00459
LIG	0.00242	0.00368	0.00004	0.00000	0.00003
G{CO2}	0.04407	0.03204	0.03715	0.05844	0.04396
G{CO}	0.02858	0.01511	0.00564	0.00100	0.00332
G{COH2}	0.01658	0.01606	0.01140	0.01532	0.01217
G{H2}	0.00000	0.00000	0.00000	0.00000	0.00000
TOTAL	0.22887	0.25432	0.22718	0.20465	0.19395

Table A.14: Component yields for reactor temperature sensibility analysis (Bio1).

Temperature (°C)	400	420	440	450	460	470	480	490	500	510	520	530	540	550
HAA	0.04309	0.05448	0.06430	0.06862	0.07257	0.07618	0.07946	0.08243	0.08512	0.08755	0.08975	0.09173	0.09352	0.09513
GLYOXAL	0.00260	0.00329	0.00388	0.00414	0.00438	0.00460	0.00480	0.00498	0.00514	0.00529	0.00542	0.00554	0.00565	0.00575
CH3CHO	0.00033	0.00059	0.00088	0.00103	0.00118	0.00132	0.00146	0.00159	0.00171	0.00181	0.00191	0.00201	0.00209	0.00216
CH2O	0.01552	0.01611	0.01652	0.01668	0.01683	0.01696	0.01708	0.01718	0.01728	0.01736	0.01744	0.01750	0.01757	0.01762
MEOH	0.01141	0.01267	0.01369	0.01411	0.01448	0.01481	0.01510	0.01536	0.01558	0.01578	0.01596	0.01612	0.01626	0.01639
ETOH	0.00654	0.00673	0.00682	0.00685	0.00687	0.00689	0.00690	0.00691	0.00691	0.00692	0.00692	0.00692	0.00693	0.00693
PROPANAL	0.08544	0.09594	0.10451	0.10820	0.11155	0.11457	0.11731	0.11979	0.12203	0.12404	0.12586	0.12750	0.12897	0.13030
PROPDIAL	0.00013	0.00035	0.00063	0.00076	0.00088	0.00099	0.00107	0.00114	0.00120	0.00124	0.00128	0.00131	0.00133	0.00134
GUAIACOL	0.06946	0.07001	0.07032	0.07042	0.07050	0.07056	0.07060	0.07064	0.07066	0.07069	0.07070	0.07072	0.07073	0.07074
COUMARYL	0.00616	0.01013	0.01309	0.01407	0.01478	0.01529	0.01565	0.01592	0.01611	0.01625	0.01635	0.01642	0.01648	0.01652
PHENOL	0.02453	0.02563	0.02647	0.02676	0.02698	0.02715	0.02727	0.02736	0.02743	0.02749	0.02753	0.02756	0.02758	0.02760
FE2MACR	0.02147	0.02689	0.02901	0.02898	0.02839	0.02738	0.02609	0.02462	0.02305	0.02144	0.01986	0.01832	0.01686	0.01548
HMF	0.01131	0.01430	0.01688	0.01801	0.01905	0.02000	0.02086	0.02164	0.02234	0.02298	0.02356	0.02408	0.02455	0.02497
FURFURAL	0.01293	0.01634	0.01929	0.02059	0.02177	0.02285	0.02384	0.02473	0.02554	0.02627	0.02692	0.02752	0.02806	0.02854
LVG	0.01530	0.01293	0.01045	0.00931	0.00825	0.00730	0.00645	0.00569	0.00502	0.00443	0.00391	0.00345	0.00305	0.00271
XYL	0.00074	0.00055	0.00041	0.00036	0.00031	0.00027	0.00024	0.00021	0.00019	0.00017	0.00015	0.00013	0.00012	0.00011
H2O	0.25730	0.25222	0.24497	0.24110	0.23725	0.23352	0.22996	0.22661	0.22349	0.22061	0.21795	0.21551	0.21328	0.21125
TOTAL	0.58424	0.61917	0.64212	0.64999	0.65603	0.66064	0.66414	0.66679	0.66879	0.67031	0.67147	0.67234	0.67302	0.67353
CO2	0.01370	0.02224	0.03331	0.03960	0.04622	0.05301	0.05981	0.06644	0.07279	0.07875	0.08426	0.08927	0.09378	0.09780
CO	0.00094	0.00163	0.00234	0.00271	0.00311	0.00357	0.00413	0.00485	0.00579	0.00704	0.00869	0.01081	0.01343	0.01649
CH4	0.00706	0.00779	0.00847	0.00877	0.00905	0.00929	0.00952	0.00971	0.00989	0.01004	0.01018	0.01030	0.01041	0.01050
C2H4	0.00526	0.00627	0.00729	0.00777	0.00821	0.00862	0.00899	0.00933	0.00963	0.00990	0.01015	0.01036	0.01056	0.01073
H2	0.00000	0.00000	0.00000	0.00000	0.00000	0.00000	0.00000	0.00000	0.00000	0.00000	0.00000	0.00000	0.00000	0.00000
TOTAL	0.02696	0.03793	0.05140	0.05885	0.06659	0.07450	0.08244	0.09033	0.09810	0.10574	0.11328	0.12075	0.12817	0.13552
C	0.14892	0.14655	0.14253	0.14023	0.13786	0.13549	0.13318	0.13097	0.12887	0.12691	0.12508	0.12338	0.12182	0.12039
CELL	0.01847	0.00816	0.00364	0.00245	0.00166	0.00113	0.00077	0.00053	0.00037	0.00026	0.00018	0.00013	0.00009	0.00007
CELLA	0.00995	0.00659	0.00422	0.00336	0.00268	0.00213	0.00170	0.00135	0.00108	0.00087	0.00070	0.00056	0.00045	0.00037
HCE	0.00207	0.00107	0.00057	0.00042	0.00031	0.00024	0.00018	0.00014	0.00010	0.00008	0.00006	0.00005	0.00004	0.00003
HCEA1	0.00136	0.00077	0.00045	0.00035	0.00027	0.00021	0.00016	0.00013	0.00010	0.00008	0.00007	0.00005	0.00004	0.00004
HCEA2	0.00530	0.00268	0.00139	0.00101	0.00074	0.00055	0.00041	0.00031	0.00023	0.00018	0.00013	0.00010	0.00008	0.00006
LIGC	0.02397	0.01352	0.00634	0.00419	0.00275	0.00180	0.00118	0.00078	0.00052	0.00035	0.00024	0.00016	0.00011	0.00008
LIGO	0.00361	0.00210	0.00125	0.00098	0.00077	0.00061	0.00048	0.00039	0.00031	0.00025	0.00021	0.00017	0.00014	0.00011
LIGH	0.00833	0.00386	0.00183	0.00128	0.00090	0.00064	0.00045	0.00033	0.00024	0.00017	0.00013	0.00010	0.00007	0.00005
LIGCC	0.00466	0.00612	0.00579	0.00517	0.00444	0.00371	0.00304	0.00246	0.00197	0.00157	0.00125	0.00100	0.00080	0.00064
LIGOH	0.03926	0.02651	0.01666	0.01303	0.01015	0.00790	0.00615	0.00480	0.00376	0.00296	0.00233	0.00185	0.00147	0.00118
LIG	0.00852	0.00795	0.00649	0.00567	0.00488	0.00415	0.00349	0.00292	0.00243	0.00201	0.00167	0.00138	0.00114	0.00094
G{CO2}	0.08466	0.08187	0.07522	0.07076	0.06577	0.06044	0.05495	0.04948	0.04418	0.03915	0.03449	0.03023	0.02640	0.02298
G{CO}	0.01375	0.01813	0.02204	0.02375	0.02527	0.02655	0.02758	0.02830	0.02865	0.02857	0.02797	0.02680	0.02504	0.02274
G{COH2}	0.01230	0.01336	0.01438	0.01485	0.01528	0.01568	0.01603	0.01635	0.01663	0.01687	0.01709	0.01728	0.01745	0.01761
G{H2}	0.00000	0.00000	0.00000	0.00000	0.00000	0.00000	0.00000	0.00000	0.00000	0.00000	0.00000	0.00000	0.00000	0.00000
TOTAL	0.38514	0.33924	0.30281	0.28750	0.27372	0.26120	0.24976	0.23922	0.22945	0.22029	0.21160	0.20325	0.19515	0.18729

Table A.15: Component yields for residence time sensibility analysis (Bio1).

τ	0.1	0.2	0.3	0.4	0.5	0.6	0.7	0.8	0.9	1
HAA	0.09401	0.09463	0.09484	0.09494	0.09500	0.09504	0.09507	0.09510	0.09511	0.09513
GLYOXAL	0.00568	0.00572	0.00573	0.00573	0.00574	0.00574	0.00574	0.00574	0.00574	0.00575
CH3CHO	0.00174	0.00196	0.00204	0.00208	0.00211	0.00213	0.00214	0.00215	0.00216	0.00216
CH2O	0.01723	0.01743	0.01751	0.01755	0.01757	0.01759	0.01760	0.01761	0.01762	0.01762
MEOH	0.01529	0.01586	0.01607	0.01618	0.01625	0.01629	0.01633	0.01635	0.01637	0.01639
ETOH	0.00688	0.00691	0.00692	0.00692	0.00692	0.00692	0.00693	0.00693	0.00693	0.00693
PROPANAL	0.12858	0.12951	0.12984	0.13000	0.13010	0.13017	0.13022	0.13025	0.13028	0.13030
PROPDIAL	0.00095	0.00113	0.00121	0.00126	0.00129	0.00130	0.00132	0.00133	0.00134	0.00134
GUAIACOL	0.07036	0.07057	0.07064	0.07067	0.07070	0.07071	0.07072	0.07073	0.07073	0.07074
COUMARYL	0.01557	0.01604	0.01623	0.01633	0.01639	0.01643	0.01646	0.01649	0.01651	0.01652
PHENOL	0.02713	0.02736	0.02746	0.02750	0.02754	0.02756	0.02757	0.02758	0.02759	0.02760
FE2MACR	0.01243	0.01400	0.01459	0.01490	0.01509	0.01522	0.01531	0.01538	0.01544	0.01548
HMF	0.02468	0.02484	0.02489	0.02492	0.02494	0.02495	0.02496	0.02496	0.02497	0.02497
FURFURAL	0.02820	0.02839	0.02845	0.02848	0.02850	0.02851	0.02852	0.02853	0.02853	0.02854
LVG	0.00267	0.00269	0.00270	0.00270	0.00270	0.00270	0.00270	0.00271	0.00271	0.00271
XYL	0.00011	0.00011	0.00011	0.00011	0.00011	0.00011	0.00011	0.00011	0.00011	0.00011
H2O	0.20846	0.20993	0.21047	0.21074	0.21091	0.21102	0.21110	0.21117	0.21121	0.21125
TOTAL	0.65997	0.66709	0.66968	0.67102	0.67184	0.67240	0.67280	0.67310	0.67334	0.67353
CO2	0.03578	0.05534	0.06759	0.07599	0.08210	0.08674	0.09039	0.09334	0.09577	0.09780
CO	0.00536	0.00731	0.00890	0.01030	0.01157	0.01272	0.01377	0.01475	0.01565	0.01649
CH4	0.00967	0.01010	0.01026	0.01034	0.01040	0.01043	0.01046	0.01048	0.01049	0.01050
C2H4	0.00941	0.01008	0.01034	0.01047	0.01055	0.01061	0.01065	0.01068	0.01071	0.01073
H2	0.00000	0.00000	0.00000	0.00000	0.00000	0.00000	0.00000	0.00000	0.00000	0.00000
TOTAL	0.06022	0.08284	0.09709	0.10711	0.11462	0.12050	0.12528	0.12925	0.13262	0.13552
C	0.11425	0.11740	0.11859	0.11921	0.11960	0.11986	0.12005	0.12019	0.12030	0.12039
CELL	0.00066	0.00033	0.00022	0.00017	0.00013	0.00011	0.00010	0.00008	0.00007	0.00007
CELLA	0.00365	0.00184	0.00123	0.00092	0.00074	0.00061	0.00053	0.00046	0.00041	0.00037
HCE	0.00031	0.00015	0.00010	0.00008	0.00006	0.00005	0.00004	0.00004	0.00003	0.00003
HCEA1	0.00035	0.00018	0.00012	0.00009	0.00007	0.00006	0.00005	0.00004	0.00004	0.00004
HCEA2	0.00062	0.00031	0.00021	0.00016	0.00013	0.00010	0.00009	0.00008	0.00007	0.00006
LIGC	0.00076	0.00038	0.00026	0.00019	0.00015	0.00013	0.00011	0.00010	0.00009	0.00008
LIGO	0.00113	0.00057	0.00038	0.00028	0.00023	0.00019	0.00016	0.00014	0.00013	0.00011
LIGH	0.00054	0.00027	0.00018	0.00014	0.00011	0.00009	0.00008	0.00007	0.00006	0.00005
LIGCC	0.00448	0.00268	0.00191	0.00149	0.00122	0.00103	0.00089	0.00079	0.00070	0.00064
LIGOH	0.01066	0.00563	0.00383	0.00290	0.00233	0.00195	0.00168	0.00147	0.00131	0.00118
LIG	0.00756	0.00426	0.00296	0.00226	0.00183	0.00154	0.00133	0.00117	0.00104	0.00094
G{CO2}	0.08408	0.06503	0.05295	0.04464	0.03859	0.03397	0.03035	0.02742	0.02501	0.02298
G{CO}	0.03076	0.03041	0.02942	0.02833	0.02726	0.02624	0.02528	0.02438	0.02353	0.02274
G{COH2}	0.01632	0.01697	0.01722	0.01735	0.01743	0.01749	0.01753	0.01756	0.01759	0.01761
G{H2}	0.00000	0.00000	0.00000	0.00000	0.00000	0.00000	0.00000	0.00000	0.00000	0.00000
TOTAL	0.27615	0.24642	0.22957	0.21821	0.20988	0.20344	0.19826	0.19399	0.19038	0.18729

Table A.16: Component yields for reactor temperature sensibility analysis (Bio2).

Temperature (°C)	400	420	440	450	460	470	480	490	500	510	520	530	540	550
HAA	0.03415	0.04482	0.05439	0.05868	0.06263	0.06625	0.06955	0.07255	0.07526	0.07771	0.07993	0.08192	0.08372	0.08533
GLYOXAL	0.00206	0.00271	0.00329	0.00354	0.00378	0.00400	0.00420	0.00438	0.00455	0.00469	0.00483	0.00495	0.00506	0.00515
CH3CHO	0.00210	0.00299	0.00388	0.00431	0.00472	0.00510	0.00546	0.00579	0.00610	0.00638	0.00663	0.00687	0.00708	0.00727
CH2O	0.01283	0.01344	0.01392	0.01413	0.01432	0.01450	0.01466	0.01480	0.01494	0.01506	0.01517	0.01527	0.01536	0.01544
MEOH	0.01172	0.01351	0.01497	0.01558	0.01612	0.01660	0.01702	0.01740	0.01773	0.01803	0.01830	0.01853	0.01874	0.01893
ETOH	0.00526	0.00541	0.00549	0.00551	0.00553	0.00554	0.00555	0.00556	0.00556	0.00557	0.00557	0.00557	0.00557	0.00557
PROPANAL	0.05749	0.06280	0.06703	0.06884	0.07049	0.07197	0.07332	0.07453	0.07563	0.07663	0.07752	0.07832	0.07905	0.07970
PROPDIAL	0.00017	0.00043	0.00078	0.00094	0.00109	0.00122	0.00133	0.00141	0.00148	0.00154	0.00158	0.00162	0.00164	0.00166
GUAIACOL	0.06447	0.06499	0.06527	0.06537	0.06544	0.06549	0.06554	0.06557	0.06559	0.06562	0.06563	0.06564	0.06565	0.06566
COUMARYL	0.00763	0.01254	0.01620	0.01741	0.01829	0.01892	0.01938	0.01970	0.01994	0.02011	0.02023	0.02033	0.02040	0.02045
PHENOL	0.02319	0.02450	0.02550	0.02585	0.02611	0.02631	0.02646	0.02658	0.02666	0.02672	0.02677	0.02681	0.02684	0.02686
FE2MACR	0.03478	0.04286	0.04571	0.04547	0.04440	0.04272	0.04063	0.03828	0.03580	0.03328	0.03080	0.02840	0.02612	0.02398
HMF	0.00896	0.01177	0.01428	0.01540	0.01644	0.01739	0.01826	0.01904	0.01976	0.02040	0.02098	0.02150	0.02198	0.02240
FURFURAL	0.00854	0.01121	0.01360	0.01467	0.01566	0.01656	0.01739	0.01814	0.01882	0.01943	0.01998	0.02048	0.02093	0.02133
LVG	0.03219	0.02839	0.02369	0.02136	0.01916	0.01711	0.01524	0.01355	0.01203	0.01067	0.00947	0.00841	0.00747	0.00664
XYL	0.00059	0.00044	0.00033	0.00029	0.00025	0.00022	0.00019	0.00017	0.00015	0.00013	0.00012	0.00011	0.00010	0.00009
H2O	0.26600	0.26749	0.26623	0.26504	0.26367	0.26219	0.26069	0.25921	0.25777	0.25641	0.25512	0.25392	0.25280	0.25177
TOTAL	0.57214	0.61030	0.63456	0.64241	0.64810	0.65212	0.65486	0.65666	0.65777	0.65838	0.65864	0.65865	0.65850	0.65825
CO2	0.01018	0.01639	0.02440	0.02895	0.03373	0.03863	0.04351	0.04828	0.05284	0.05711	0.06105	0.06463	0.06785	0.07071
CO	0.00136	0.00232	0.00329	0.00377	0.00424	0.00472	0.00525	0.00584	0.00655	0.00741	0.00848	0.00979	0.01137	0.01319
CH4	0.00723	0.00827	0.00923	0.00967	0.01006	0.01042	0.01074	0.01103	0.01128	0.01151	0.01171	0.01189	0.01205	0.01220
C2H4	0.00552	0.00697	0.00843	0.00912	0.00976	0.01036	0.01090	0.01140	0.01184	0.01225	0.01261	0.01293	0.01322	0.01348
H2	0.00000	0.00000	0.00000	0.00000	0.00000	0.00000	0.00000	0.00000	0.00000	0.00000	0.00000	0.00000	0.00000	0.00000
TOTAL	0.02429	0.03395	0.04536	0.05150	0.05779	0.06413	0.07040	0.07655	0.08251	0.08828	0.09385	0.09925	0.10450	0.10958
C	0.16143	0.16707	0.17036	0.17133	0.17196	0.17234	0.17252	0.17258	0.17253	0.17242	0.17226	0.17207	0.17186	0.17164
CELL	0.01681	0.00743	0.00331	0.00223	0.00151	0.00103	0.00070	0.00049	0.00034	0.00024	0.00017	0.00012	0.00008	0.00006
CELLA	0.00789	0.00542	0.00357	0.00288	0.00231	0.00185	0.00148	0.00119	0.00096	0.00077	0.00062	0.00050	0.00041	0.00033
HCE	0.00167	0.00086	0.00046	0.00034	0.00025	0.00019	0.00014	0.00011	0.00008	0.00007	0.00005	0.00004	0.00003	0.00002
HCEA1	0.00109	0.00062	0.00036	0.00028	0.00022	0.00017	0.00013	0.00010	0.00008	0.00007	0.00005	0.00004	0.00004	0.00003
HCEA2	0.00427	0.00216	0.00112	0.00081	0.00060	0.00044	0.00033	0.00025	0.00019	0.00014	0.00011	0.00008	0.00006	0.00005
LIGC	0.02966	0.01673	0.00785	0.00519	0.00340	0.00223	0.00146	0.00097	0.00064	0.00043	0.00029	0.00020	0.00014	0.00010
LIGO	0.00335	0.00195	0.00116	0.00091	0.00071	0.00056	0.00045	0.00036	0.00029	0.00023	0.00019	0.00016	0.00013	0.00011
LIGH	0.01289	0.00597	0.00283	0.00197	0.00139	0.00098	0.00070	0.00051	0.00037	0.00027	0.00020	0.00015	0.00011	0.00008
LIGCC	0.00577	0.00758	0.00716	0.00639	0.00549	0.00459	0.00376	0.00304	0.00244	0.00195	0.00155	0.00124	0.00099	0.00079
LIGOH	0.05654	0.03756	0.02333	0.01817	0.01411	0.01095	0.00852	0.00664	0.00519	0.00408	0.00322	0.00255	0.00203	0.00162
LIG	0.01380	0.01268	0.01023	0.00890	0.00763	0.00647	0.00543	0.00454	0.00377	0.00312	0.00258	0.00214	0.00176	0.00146
G{CO2}	0.06288	0.06032	0.05511	0.05173	0.04800	0.04404	0.03998	0.03596	0.03207	0.02839	0.02499	0.02189	0.01910	0.01662
G{CO}	0.00596	0.00857	0.01103	0.01213	0.01312	0.01397	0.01466	0.01518	0.01547	0.01552	0.01526	0.01468	0.01376	0.01253
G{COH2}	0.01043	0.01172	0.01305	0.01369	0.01428	0.01483	0.01532	0.01577	0.01617	0.01653	0.01684	0.01713	0.01738	0.01760
G{H2}	0.00000	0.00000	0.00000	0.00000	0.00000	0.00000	0.00000	0.00000	0.00000	0.00000	0.00000	0.00000	0.00000	0.00000
TOTAL	0.39444	0.34662	0.31095	0.29696	0.28498	0.27463	0.26561	0.25766	0.25059	0.24421	0.23838	0.23297	0.22787	0.22304

Table A.17: Component yields for residence time sensibility analysis (Bio2).

τ	0.1	0.2	0.3	0.4	0.5	0.6	0.7	0.8	0.9	1
HAA	0.07227	0.07391	0.07447	0.07475	0.07492	0.07503	0.07511	0.07517	0.07522	0.07526
GLYOXAL	0.00437	0.00446	0.00450	0.00451	0.00453	0.00453	0.00454	0.00454	0.00454	0.00455
CH3CHO	0.00483	0.00542	0.00567	0.00581	0.00590	0.00597	0.00601	0.00605	0.00608	0.00610
CH2O	0.01387	0.01438	0.01459	0.01471	0.01478	0.01483	0.01487	0.01490	0.01492	0.01494
MEOH	0.01437	0.01597	0.01664	0.01700	0.01724	0.01740	0.01752	0.01761	0.01768	0.01773
ETOH	0.00543	0.00550	0.00553	0.00554	0.00555	0.00555	0.00556	0.00556	0.00556	0.00556
PROPANAL	0.07225	0.07397	0.07462	0.07497	0.07518	0.07533	0.07544	0.07552	0.07558	0.07563
PROPDIAL	0.00059	0.00091	0.00109	0.00121	0.00129	0.00135	0.00139	0.00143	0.00146	0.00148
GUAIACOL	0.06466	0.06517	0.06535	0.06544	0.06549	0.06552	0.06555	0.06557	0.06558	0.06559
COUMARYL	0.01659	0.01808	0.01874	0.01912	0.01937	0.01955	0.01968	0.01979	0.01987	0.01994
PHENOL	0.02531	0.02592	0.02618	0.02633	0.02643	0.02650	0.02656	0.02660	0.02663	0.02666
FE2MACR	0.02044	0.02740	0.03050	0.03225	0.03337	0.03415	0.03473	0.03517	0.03552	0.03580
HMF	0.01897	0.01940	0.01955	0.01962	0.01967	0.01970	0.01972	0.01973	0.01975	0.01976
FURFURAL	0.01807	0.01848	0.01862	0.01869	0.01873	0.01876	0.01878	0.01879	0.01881	0.01882
LVG	0.01155	0.01181	0.01190	0.01194	0.01197	0.01199	0.01200	0.01201	0.01202	0.01203
XYL	0.00015	0.00015	0.00015	0.00015	0.00015	0.00015	0.00015	0.00015	0.00015	0.00015
H2O	0.24758	0.25265	0.25463	0.25570	0.25637	0.25682	0.25716	0.25741	0.25761	0.25777
TOTAL	0.61129	0.63357	0.64272	0.64775	0.65094	0.65314	0.65476	0.65600	0.65698	0.65777
CO2	0.01174	0.02083	0.02792	0.03360	0.03825	0.04214	0.04543	0.04825	0.05070	0.05284
CO	0.00356	0.00456	0.00507	0.00541	0.00567	0.00588	0.00607	0.00624	0.00640	0.00655
CH4	0.00896	0.01001	0.01047	0.01074	0.01091	0.01103	0.01112	0.01118	0.01124	0.01128
C2H4	0.00828	0.00987	0.01058	0.01099	0.01126	0.01144	0.01158	0.01169	0.01177	0.01184
H2	0.00000	0.00000	0.00000	0.00000	0.00000	0.00000	0.00000	0.00000	0.00000	0.00000
TOTAL	0.03254	0.04526	0.05404	0.06073	0.06609	0.07049	0.07420	0.07736	0.08011	0.08251
C	0.15336	0.16226	0.16607	0.16819	0.16956	0.17051	0.17121	0.17175	0.17218	0.17253
CELL	0.00335	0.00168	0.00112	0.00084	0.00068	0.00056	0.00048	0.00042	0.00038	0.00034
CELLA	0.00918	0.00470	0.00315	0.00237	0.00190	0.00159	0.00136	0.00119	0.00106	0.00096
HCE	0.00084	0.00042	0.00028	0.00021	0.00017	0.00014	0.00012	0.00011	0.00009	0.00008
HCEA1	0.00082	0.00041	0.00028	0.00021	0.00017	0.00014	0.00012	0.00010	0.00009	0.00008
HCEA2	0.00182	0.00092	0.00062	0.00046	0.00037	0.00031	0.00027	0.00023	0.00021	0.00019
LIGC	0.00578	0.00306	0.00208	0.00158	0.00127	0.00106	0.00091	0.00080	0.00071	0.00064
LIGO	0.00285	0.00144	0.00096	0.00072	0.00058	0.00048	0.00041	0.00036	0.00032	0.00029
LIGH	0.00362	0.00183	0.00122	0.00092	0.00073	0.00061	0.00053	0.00046	0.00041	0.00037
LIGCC	0.00976	0.00748	0.00597	0.00496	0.00423	0.00369	0.00327	0.00294	0.00267	0.00244
LIGOH	0.03949	0.02280	0.01602	0.01234	0.01004	0.00846	0.00731	0.00643	0.00575	0.00519
LIG	0.02153	0.01443	0.01071	0.00849	0.00703	0.00600	0.00523	0.00463	0.00416	0.00377
G{CO2}	0.07123	0.06320	0.05648	0.05098	0.04643	0.04262	0.03939	0.03660	0.03419	0.03207
G{CO}	0.01049	0.01310	0.01419	0.01476	0.01508	0.01527	0.01539	0.01545	0.01547	0.01547
G{COH2}	0.01294	0.01432	0.01497	0.01535	0.01560	0.01578	0.01591	0.01602	0.01610	0.01617
G{H2}	0.00000	0.00000	0.00000	0.00000	0.00000	0.00000	0.00000	0.00000	0.00000	0.00000
TOTAL	0.34705	0.31204	0.29411	0.28239	0.27385	0.26723	0.26191	0.25751	0.25378	0.25059

Table A.18: Component yields for reactor temperature sensibility analysis (Bio3).

Temperature (°C)	400	420	440	450	460	470	480	490	500	510	520	530	540	550
HAA	0.01152	0.01698	0.02262	0.02537	0.02800	0.03049	0.03281	0.03497	0.03695	0.03876	0.04041	0.04190	0.04324	0.04446
GLYOXAL	0.00139	0.00205	0.00273	0.00306	0.00338	0.00368	0.00396	0.00422	0.00446	0.00468	0.00488	0.00506	0.00522	0.00537
CH3CHO	0.00106	0.00156	0.00207	0.00233	0.00257	0.00280	0.00301	0.00321	0.00339	0.00356	0.00371	0.00384	0.00397	0.00408
CH2O	0.01374	0.01412	0.01430	0.01436	0.01440	0.01443	0.01445	0.01447	0.01448	0.01449	0.01449	0.01450	0.01450	0.01451
MEOH	0.01028	0.01144	0.01231	0.01264	0.01290	0.01311	0.01327	0.01340	0.01350	0.01357	0.01363	0.01368	0.01372	0.01375
ETOH	0.00582	0.00599	0.00607	0.00610	0.00612	0.00613	0.00614	0.00615	0.00615	0.00616	0.00616	0.00616	0.00616	0.00617
PROPANAL	0.05255	0.05734	0.06147	0.06333	0.06507	0.06668	0.06816	0.06951	0.07075	0.07188	0.07289	0.07381	0.07464	0.07538
PROPDIAL	0.00004	0.00012	0.00021	0.00025	0.00029	0.00032	0.00035	0.00038	0.00040	0.00041	0.00042	0.00043	0.00044	0.00044
GUAIACOL	0.07144	0.07201	0.07233	0.07243	0.07251	0.07257	0.07262	0.07265	0.07268	0.07270	0.07272	0.07273	0.07275	0.07276
COUMARYL	0.00203	0.00334	0.00432	0.00464	0.00487	0.00504	0.00516	0.00525	0.00531	0.00536	0.00539	0.00541	0.00543	0.00545
PHENOL	0.02544	0.02595	0.02630	0.02642	0.02651	0.02658	0.02663	0.02667	0.02670	0.02673	0.02674	0.02676	0.02677	0.02678
FE2MACR	0.03995	0.05537	0.06762	0.07231	0.07610	0.07912	0.08150	0.08336	0.08481	0.08594	0.08681	0.08749	0.08802	0.08844
HMF	0.00453	0.00668	0.00891	0.00999	0.01102	0.01200	0.01292	0.01377	0.01455	0.01526	0.01591	0.01650	0.01703	0.01751
FURFURAL	0.00461	0.00679	0.00905	0.01015	0.01120	0.01219	0.01313	0.01399	0.01478	0.01550	0.01616	0.01676	0.01730	0.01778
LVG	0.08019	0.07954	0.07298	0.06845	0.06352	0.05844	0.05340	0.04853	0.04391	0.03962	0.03566	0.03205	0.02878	0.02583
XYL	0.00066	0.00049	0.00037	0.00032	0.00028	0.00024	0.00021	0.00019	0.00017	0.00015	0.00013	0.00012	0.00011	0.00009
H2O	0.26573	0.26822	0.26950	0.26992	0.27024	0.27049	0.27067	0.27079	0.27086	0.27088	0.27087	0.27082	0.27074	0.27065
TOTAL	0.59100	0.62797	0.65315	0.66205	0.66898	0.67432	0.67840	0.68150	0.68385	0.68564	0.68699	0.68803	0.68882	0.68943
CO2	0.01171	0.01878	0.02800	0.03326	0.03883	0.04455	0.05028	0.05591	0.06130	0.06637	0.07107	0.07535	0.07921	0.08265
CO	0.00014	0.00022	0.00030	0.00033	0.00037	0.00042	0.00049	0.00059	0.00074	0.00094	0.00121	0.00157	0.00201	0.00253
CH4	0.00858	0.00910	0.00950	0.00965	0.00978	0.00988	0.00996	0.01002	0.01007	0.01011	0.01014	0.01016	0.01018	0.01020
C2H4	0.00417	0.00464	0.00502	0.00517	0.00529	0.00539	0.00547	0.00553	0.00558	0.00561	0.00564	0.00567	0.00568	0.00570
H2	0.00000	0.00000	0.00000	0.00000	0.00000	0.00000	0.00000	0.00000	0.00000	0.00000	0.00000	0.00000	0.00000	0.00000
TOTAL	0.02460	0.03275	0.04282	0.04842	0.05427	0.06023	0.06620	0.07205	0.07768	0.08304	0.08806	0.09275	0.09708	0.10107
C	0.15675	0.15934	0.16058	0.16089	0.16104	0.16108	0.16102	0.16089	0.16071	0.16049	0.16025	0.15998	0.15972	0.15944
CELL	0.01863	0.00823	0.00367	0.00247	0.00167	0.00114	0.00078	0.00054	0.00037	0.00026	0.00018	0.00013	0.00009	0.00007
CELLA	0.01419	0.01095	0.00792	0.00663	0.00551	0.00454	0.00373	0.00306	0.00250	0.00205	0.00167	0.00137	0.00112	0.00092
HCE	0.00184	0.00095	0.00051	0.00038	0.00028	0.00021	0.00016	0.00012	0.00009	0.00007	0.00006	0.00004	0.00003	0.00003
HCEA1	0.00121	0.00069	0.00040	0.00031	0.00024	0.00019	0.00015	0.00012	0.00009	0.00007	0.00006	0.00005	0.00004	0.00003
HCEA2	0.00472	0.00239	0.00124	0.00090	0.00066	0.00049	0.00036	0.00027	0.00021	0.00016	0.00012	0.00009	0.00007	0.00006
LIGC	0.00790	0.00446	0.00209	0.00138	0.00091	0.00059	0.00039	0.00026	0.00017	0.00011	0.00008	0.00005	0.00004	0.00003
LIGO	0.00357	0.00207	0.00124	0.00097	0.00076	0.00060	0.00048	0.00038	0.00031	0.00025	0.00020	0.00017	0.00014	0.00011
LIGH	0.01099	0.00509	0.00241	0.00168	0.00118	0.00084	0.00060	0.00043	0.00031	0.00023	0.00017	0.00013	0.00009	0.00007
LIGCC	0.00154	0.00202	0.00191	0.00170	0.00146	0.00122	0.00100	0.00081	0.00065	0.00052	0.00041	0.00033	0.00026	0.00021
LIGOH	0.06658	0.04829	0.03201	0.02554	0.02022	0.01593	0.01253	0.00986	0.00776	0.00613	0.00486	0.00386	0.00308	0.00247
LIG	0.00009	0.00009	0.00008	0.00007	0.00007	0.00006	0.00005	0.00005	0.00004	0.00004	0.00003	0.00003	0.00003	0.00003
G{CO2}	0.07234	0.06914	0.06323	0.05944	0.05524	0.05078	0.04620	0.04163	0.03720	0.03300	0.02909	0.02552	0.02229	0.01942
G{CO}	0.00273	0.00383	0.00472	0.00505	0.00532	0.00551	0.00563	0.00568	0.00565	0.00554	0.00533	0.00503	0.00463	0.00415
G{COH2}	0.01036	0.01077	0.01104	0.01114	0.01122	0.01129	0.01134	0.01138	0.01141	0.01144	0.01146	0.01147	0.01148	0.01149
G{H2}	0.00000	0.00000	0.00000	0.00000	0.00000	0.00000	0.00000	0.00000	0.00000	0.00000	0.00000	0.00000	0.00000	0.00000
TOTAL	0.37344	0.32830	0.29306	0.27856	0.26578	0.25448	0.24443	0.23548	0.22749	0.22035	0.21397	0.20825	0.20312	0.19853

Table A.19: Component yields for residence time sensibility analysis (Bio3).

τ	0.1	0.2	0.3	0.4	0.5	0.6	0.7	0.8	0.9	1
HAA	0.04329	0.04393	0.04415	0.04426	0.04433	0.04437	0.04440	0.04442	0.04444	0.04446
GLYOXAL	0.00523	0.00531	0.00533	0.00535	0.00535	0.00536	0.00536	0.00537	0.00537	0.00537
CH3CHO	0.00397	0.00403	0.00405	0.00406	0.00407	0.00407	0.00407	0.00407	0.00408	0.00408
CH2O	0.01441	0.01447	0.01448	0.01449	0.01450	0.01450	0.01450	0.01450	0.01451	0.01451
MEOH	0.01288	0.01333	0.01350	0.01358	0.01364	0.01367	0.01370	0.01372	0.01373	0.01375
ETOH	0.00613	0.00615	0.00616	0.00616	0.00616	0.00616	0.00616	0.00616	0.00617	0.00617
PROPANAL	0.07441	0.07495	0.07513	0.07522	0.07527	0.07531	0.07533	0.07535	0.07537	0.07538
PROPDIAL	0.00031	0.00037	0.00040	0.00041	0.00042	0.00043	0.00043	0.00044	0.00044	0.00044
GUAIACOL	0.07237	0.07258	0.07266	0.07269	0.07271	0.07273	0.07274	0.07274	0.07275	0.07276
COUMARYL	0.00513	0.00529	0.00535	0.00538	0.00540	0.00542	0.00543	0.00543	0.00544	0.00545
PHENOL	0.02653	0.02666	0.02671	0.02673	0.02675	0.02676	0.02676	0.02677	0.02677	0.02678
FE2MACR	0.07557	0.08224	0.08472	0.08601	0.08681	0.08734	0.08773	0.08802	0.08825	0.08844
HMF	0.01705	0.01730	0.01738	0.01743	0.01745	0.01747	0.01748	0.01749	0.01750	0.01751
FURFURAL	0.01732	0.01757	0.01766	0.01770	0.01773	0.01775	0.01776	0.01777	0.01778	0.01778
LVG	0.02515	0.02552	0.02565	0.02571	0.02575	0.02578	0.02580	0.02581	0.02582	0.02583
XYL	0.00009	0.00009	0.00009	0.00009	0.00009	0.00009	0.00009	0.00009	0.00009	0.00009
H2O	0.26582	0.26841	0.26932	0.26979	0.27008	0.27027	0.27040	0.27051	0.27059	0.27065
TOTAL	0.66567	0.67820	0.68273	0.68507	0.68651	0.68747	0.68817	0.68869	0.68910	0.68943
CO2	0.03017	0.04672	0.05709	0.06419	0.06936	0.07329	0.07638	0.07887	0.08093	0.08265
CO	0.00059	0.00089	0.00116	0.00140	0.00163	0.00184	0.00203	0.00221	0.00237	0.00253
CH4	0.00977	0.00999	0.01007	0.01011	0.01014	0.01016	0.01017	0.01018	0.01019	0.01020
C2H4	0.00530	0.00550	0.00558	0.00562	0.00565	0.00566	0.00568	0.00569	0.00569	0.00570
H2	0.00000	0.00000	0.00000	0.00000	0.00000	0.00000	0.00000	0.00000	0.00000	0.00000
TOTAL	0.04583	0.06310	0.07390	0.08133	0.08678	0.09095	0.09426	0.09695	0.09918	0.10107
C	0.15454	0.15713	0.15806	0.15855	0.15884	0.15904	0.15918	0.15929	0.15938	0.15944
CELL	0.00067	0.00034	0.00022	0.00017	0.00013	0.00011	0.00010	0.00008	0.00007	0.00007
CELLA	0.00896	0.00455	0.00305	0.00229	0.00184	0.00153	0.00131	0.00115	0.00102	0.00092
HCE	0.00027	0.00014	0.00009	0.00007	0.00005	0.00005	0.00004	0.00003	0.00003	0.00003
HCEA1	0.00032	0.00016	0.00011	0.00008	0.00006	0.00005	0.00005	0.00004	0.00004	0.00003
HCEA2	0.00056	0.00028	0.00019	0.00014	0.00011	0.00009	0.00008	0.00007	0.00006	0.00006
LIGC	0.00025	0.00013	0.00008	0.00006	0.00005	0.00004	0.00004	0.00003	0.00003	0.00003
LIGO	0.00112	0.00056	0.00037	0.00028	0.00023	0.00019	0.00016	0.00014	0.00013	0.00011
LIGH	0.00071	0.00036	0.00024	0.00018	0.00014	0.00012	0.00010	0.00009	0.00008	0.00007
LIGCC	0.00148	0.00088	0.00063	0.00049	0.00040	0.00034	0.00029	0.00026	0.00023	0.00021
LIGOH	0.02118	0.01151	0.00790	0.00601	0.00486	0.00407	0.00350	0.00308	0.00274	0.00247
LIG	0.00021	0.00012	0.00008	0.00006	0.00005	0.00004	0.00004	0.00003	0.00003	0.00003
G{CO2}	0.07089	0.05490	0.04472	0.03771	0.03260	0.02871	0.02564	0.02317	0.02113	0.01942
G{CO}	0.00511	0.00531	0.00523	0.00508	0.00492	0.00475	0.00459	0.00444	0.00429	0.00415
G{COH2}	0.01126	0.01138	0.01142	0.01145	0.01146	0.01147	0.01148	0.01148	0.01149	0.01149
G{H2}	0.00000	0.00000	0.00000	0.00000	0.00000	0.00000	0.00000	0.00000	0.00000	0.00000
TOTAL	0.27753	0.24773	0.23240	0.22262	0.21574	0.21061	0.20660	0.20339	0.20074	0.19853

Table A.20: Component yields for reactor temperature sensibility analysis (Bio4).

Temperature (°C)	400	420	440	450	460	470	480	490	500	510	520	530	540	550
HAA	0.02423	0.03061	0.03550	0.03747	0.03919	0.04067	0.04195	0.04306	0.04401	0.04484	0.04555	0.04616	0.04669	0.04715
GLYOXAL	0.00293	0.00370	0.00429	0.00453	0.00473	0.00491	0.00507	0.00520	0.00532	0.00542	0.00550	0.00558	0.00564	0.00570
CH3CHO	0.00222	0.00281	0.00325	0.00344	0.00359	0.00373	0.00385	0.00395	0.00404	0.00411	0.00418	0.00423	0.00428	0.00432
CH2O	0.01855	0.01904	0.01929	0.01936	0.01942	0.01946	0.01949	0.01951	0.01952	0.01953	0.01954	0.01955	0.01956	0.01956
MEOH	0.01082	0.01110	0.01127	0.01132	0.01136	0.01140	0.01142	0.01144	0.01145	0.01146	0.01147	0.01148	0.01148	0.01149
ETOH	0.00766	0.00788	0.00799	0.00802	0.00804	0.00806	0.00807	0.00808	0.00809	0.00810	0.00810	0.00810	0.00811	0.00811
PROPANAL	0.05898	0.06613	0.07135	0.07341	0.07517	0.07668	0.07798	0.07910	0.08005	0.08087	0.08158	0.08219	0.08271	0.08316
PROPDIAL	0.00009	0.00023	0.00042	0.00051	0.00059	0.00066	0.00072	0.00076	0.00080	0.00083	0.00086	0.00087	0.00089	0.00090
GUAIACOL	0.11957	0.12052	0.12105	0.12123	0.12136	0.12146	0.12154	0.12160	0.12165	0.12168	0.12171	0.12174	0.12176	0.12177
COUMARYL	0.00412	0.00678	0.00876	0.00941	0.00988	0.01022	0.01047	0.01065	0.01077	0.01087	0.01093	0.01098	0.01102	0.01105
PHENOL	0.04275	0.04370	0.04437	0.04460	0.04478	0.04491	0.04501	0.04509	0.04515	0.04519	0.04522	0.04525	0.04527	0.04529
FE2MACR	0.00253	0.00351	0.00429	0.00458	0.00482	0.00502	0.00517	0.00529	0.00538	0.00545	0.00550	0.00555	0.00558	0.00561
HMF	0.01272	0.01607	0.01864	0.01967	0.02057	0.02135	0.02203	0.02261	0.02311	0.02354	0.02391	0.02423	0.02451	0.02475
FURFURAL	0.01454	0.01837	0.02130	0.02248	0.02351	0.02440	0.02517	0.02584	0.02641	0.02690	0.02733	0.02770	0.02801	0.02829
LVG	0.13445	0.11476	0.09203	0.08144	0.07176	0.06305	0.05532	0.04851	0.04255	0.03735	0.03282	0.02889	0.02547	0.02249
XYL	0.00086	0.00064	0.00048	0.00042	0.00036	0.00032	0.00028	0.00025	0.00022	0.00019	0.00017	0.00015	0.00014	0.00012
H2O	0.19302	0.20527	0.21445	0.21808	0.22120	0.22387	0.22615	0.22811	0.22978	0.23122	0.23245	0.23351	0.23443	0.23521
TOTAL	0.65004	0.67111	0.67870	0.67998	0.68035	0.68018	0.67969	0.67903	0.67830	0.67756	0.67684	0.67617	0.67554	0.67497
CO2	0.01886	0.03032	0.04496	0.05320	0.06180	0.07056	0.07925	0.08768	0.09568	0.10314	0.10996	0.11613	0.12164	0.12650
CO	0.00028	0.00044	0.00056	0.00060	0.00062	0.00065	0.00067	0.00069	0.00072	0.00076	0.00082	0.00088	0.00097	0.00106
CH4	0.01205	0.01227	0.01244	0.01251	0.01257	0.01261	0.01265	0.01268	0.01270	0.01272	0.01274	0.01275	0.01276	0.01277
C2H4	0.00437	0.00460	0.00480	0.00488	0.00495	0.00501	0.00506	0.00510	0.00513	0.00516	0.00518	0.00519	0.00520	0.00521
H2	0.00000	0.00000	0.00000	0.00000	0.00000	0.00000	0.00000	0.00000	0.00000	0.00000	0.00000	0.00000	0.00000	0.00000
TOTAL	0.03555	0.04763	0.06276	0.07119	0.07995	0.08883	0.09763	0.10615	0.11424	0.12178	0.12870	0.13496	0.14057	0.14555
C	0.09701	0.10604	0.11288	0.11557	0.11785	0.11978	0.12140	0.12278	0.12394	0.12492	0.12576	0.12647	0.12707	0.12759
CELL	0.03323	0.01313	0.00527	0.00339	0.00220	0.00144	0.00095	0.00064	0.00043	0.00029	0.00020	0.00014	0.00010	0.00007
CELLA	0.00896	0.00592	0.00373	0.00294	0.00231	0.00182	0.00143	0.00113	0.00089	0.00071	0.00057	0.00045	0.00036	0.00029
HCE	0.00243	0.00125	0.00067	0.00049	0.00037	0.00028	0.00021	0.00016	0.00012	0.00009	0.00007	0.00006	0.00005	0.00004
HCEA1	0.00159	0.00090	0.00053	0.00040	0.00031	0.00025	0.00019	0.00015	0.00012	0.00010	0.00008	0.00006	0.00005	0.00004
HCEA2	0.00621	0.00314	0.00163	0.00119	0.00087	0.00064	0.00048	0.00036	0.00027	0.00021	0.00016	0.00012	0.00009	0.00007
LIGC	0.01603	0.00904	0.00424	0.00280	0.00184	0.00120	0.00079	0.00052	0.00035	0.00023	0.00016	0.00011	0.00007	0.00005
LIGO	0.00597	0.00347	0.00208	0.00162	0.00127	0.00101	0.00080	0.00064	0.00052	0.00042	0.00034	0.00028	0.00023	0.00019
LIGH	0.00070	0.00032	0.00015	0.00011	0.00007	0.00005	0.00004	0.00003	0.00002	0.00001	0.00001	0.00001	0.00001	0.00000
LIGCC	0.00312	0.00409	0.00387	0.00346	0.00297	0.00248	0.00203	0.00164	0.00132	0.00105	0.00084	0.00067	0.00053	0.00043
LIGOH	0.00422	0.00306	0.00203	0.00162	0.00128	0.00101	0.00079	0.00062	0.00049	0.00039	0.00031	0.00024	0.00020	0.00016
LIG	0.00001	0.00001	0.00001	0.00000	0.00000	0.00000	0.00000	0.00000	0.00000	0.00000	0.00000	0.00000	0.00000	0.00000
G{CO2}	0.11647	0.11160	0.10154	0.09506	0.08794	0.08044	0.07282	0.06529	0.05807	0.05127	0.04501	0.03933	0.03424	0.02973
G{CO}	0.00025	0.00044	0.00066	0.00076	0.00084	0.00091	0.00096	0.00099	0.00100	0.00100	0.00097	0.00092	0.00085	0.00077
G{COH2}	0.01366	0.01426	0.01470	0.01486	0.01500	0.01512	0.01521	0.01528	0.01534	0.01539	0.01542	0.01545	0.01547	0.01549
G{H2}	0.00000	0.00000	0.00000	0.00000	0.00000	0.00000	0.00000	0.00000	0.00000	0.00000	0.00000	0.00000	0.00000	0.00000
TOTAL	0.30984	0.27669	0.25397	0.24427	0.23513	0.22642	0.21811	0.21024	0.20288	0.19609	0.18989	0.18431	0.17932	0.17491

Table A.21: Component yields for residence time sensibility analysis (Bio4).

τ	0.1	0.2	0.3	0.4	0.5	0.6	0.7	0.8	0.9	1
HAA	0.04670	0.04695	0.04703	0.04707	0.04710	0.04711	0.04713	0.04714	0.04714	0.04715
GLYOXAL	0.00564	0.00567	0.00568	0.00569	0.00569	0.00569	0.00569	0.00569	0.00569	0.00570
CH3CHO	0.00428	0.00431	0.00431	0.00432	0.00432	0.00432	0.00432	0.00432	0.00432	0.00432
CH2O	0.01943	0.01950	0.01953	0.01954	0.01955	0.01955	0.01955	0.01956	0.01956	0.01956
MEOH	0.01137	0.01143	0.01146	0.01147	0.01147	0.01148	0.01148	0.01149	0.01149	0.01149
ETOH	0.00805	0.00808	0.00809	0.00810	0.00810	0.00810	0.00811	0.00811	0.00811	0.00811
PROPANAL	0.08249	0.08286	0.08299	0.08305	0.08309	0.08311	0.08313	0.08314	0.08315	0.08316
PROPDIAL	0.00063	0.00076	0.00081	0.00084	0.00086	0.00087	0.00088	0.00089	0.00089	0.00090
GUAIACOL	0.12113	0.12149	0.12160	0.12166	0.12170	0.12172	0.12174	0.12175	0.12176	0.12177
COUMARYL	0.01042	0.01073	0.01085	0.01092	0.01096	0.01099	0.01101	0.01103	0.01104	0.01105
PHENOL	0.04483	0.04507	0.04515	0.04520	0.04523	0.04525	0.04526	0.04527	0.04528	0.04529
FE2MACR	0.00479	0.00521	0.00537	0.00545	0.00550	0.00554	0.00556	0.00558	0.00560	0.00561
HMF	0.02452	0.02465	0.02469	0.02471	0.02473	0.02474	0.02474	0.02475	0.02475	0.02475
FURFURAL	0.02802	0.02817	0.02822	0.02824	0.02826	0.02827	0.02828	0.02828	0.02829	0.02829
LVG	0.02228	0.02240	0.02244	0.02246	0.02247	0.02248	0.02248	0.02249	0.02249	0.02249
XYL	0.00012	0.00012	0.00012	0.00012	0.00012	0.00012	0.00012	0.00012	0.00012	0.00012
H2O	0.23379	0.23456	0.23483	0.23496	0.23505	0.23510	0.23514	0.23517	0.23519	0.23521
TOTAL	0.66850	0.67196	0.67318	0.67381	0.67419	0.67445	0.67463	0.67477	0.67488	0.67497
CO2	0.04633	0.07162	0.08745	0.09830	0.10620	0.11220	0.11692	0.12073	0.12387	0.12650
CO	0.00069	0.00075	0.00080	0.00085	0.00089	0.00093	0.00097	0.00100	0.00104	0.00106
CH4	0.01257	0.01267	0.01271	0.01273	0.01274	0.01275	0.01275	0.01276	0.01276	0.01277
C2H4	0.00499	0.00510	0.00514	0.00517	0.00518	0.00519	0.00520	0.00521	0.00521	0.00521
H2	0.00000	0.00000	0.00000	0.00000	0.00000	0.00000	0.00000	0.00000	0.00000	0.00000
TOTAL	0.06457	0.09013	0.10611	0.11705	0.12501	0.13108	0.13585	0.13970	0.14288	0.14555
C	0.12569	0.12667	0.12704	0.12723	0.12734	0.12742	0.12748	0.12753	0.12756	0.12759
CELL	0.00070	0.00035	0.00023	0.00017	0.00014	0.00012	0.00010	0.00009	0.00008	0.00007
CELLA	0.00290	0.00146	0.00097	0.00073	0.00059	0.00049	0.00042	0.00037	0.00033	0.00029
HCE	0.00036	0.00018	0.00012	0.00009	0.00007	0.00006	0.00005	0.00004	0.00004	0.00004
HCEA1	0.00041	0.00021	0.00014	0.00010	0.00008	0.00007	0.00006	0.00005	0.00005	0.00004
HCEA2	0.00073	0.00037	0.00024	0.00018	0.00015	0.00012	0.00011	0.00009	0.00008	0.00007
LIGC	0.00051	0.00026	0.00017	0.00013	0.00010	0.00009	0.00007	0.00006	0.00006	0.00005
LIGO	0.00187	0.00094	0.00063	0.00047	0.00038	0.00031	0.00027	0.00024	0.00021	0.00019
LIGH	0.00005	0.00002	0.00002	0.00001	0.00001	0.00001	0.00001	0.00001	0.00001	0.00000
LIGCC	0.00299	0.00179	0.00128	0.00099	0.00081	0.00069	0.00060	0.00053	0.00047	0.00043
LIGOH	0.00134	0.00073	0.00050	0.00038	0.00031	0.00026	0.00022	0.00020	0.00017	0.00016
LIG	0.00001	0.00001	0.00001	0.00000	0.00000	0.00000	0.00000	0.00000	0.00000	0.00000
G{CO2}	0.10887	0.08415	0.06851	0.05775	0.04991	0.04395	0.03926	0.03547	0.03235	0.02973
G{CO}	0.00084	0.00093	0.00093	0.00092	0.00090	0.00087	0.00084	0.00082	0.00079	0.00077
G{COH2}	0.01507	0.01528	0.01536	0.01540	0.01543	0.01545	0.01546	0.01547	0.01548	0.01549
G{H2}	0.00000	0.00000	0.00000	0.00000	0.00000	0.00000	0.00000	0.00000	0.00000	0.00000
TOTAL	0.26236	0.23334	0.21614	0.20457	0.19622	0.18991	0.18495	0.18095	0.17767	0.17491

Table A.22: Component yields for reactor temperature sensibility analysis (Bio5).

Temperature (°C)	400	420	440	450	460	470	480	490	500	510	520	530	540	550
HAA	0.02761	0.03403	0.03851	0.04020	0.04161	0.04278	0.04377	0.04459	0.04528	0.04587	0.04636	0.04678	0.04713	0.04744
GLYOXAL	0.00445	0.00548	0.00620	0.00647	0.00670	0.00689	0.00705	0.00718	0.00729	0.00739	0.00747	0.00753	0.00759	0.00764
CH3CHO	0.00338	0.00416	0.00471	0.00491	0.00509	0.00523	0.00535	0.00545	0.00554	0.00561	0.00567	0.00572	0.00576	0.00580
CH2O	0.01353	0.01392	0.01412	0.01418	0.01422	0.01425	0.01428	0.01429	0.01431	0.01431	0.01432	0.01433	0.01433	0.01434
MEOH	0.00972	0.01049	0.01104	0.01125	0.01141	0.01154	0.01165	0.01173	0.01179	0.01184	0.01187	0.01190	0.01192	0.01194
ETOH	0.00635	0.00653	0.00662	0.00665	0.00667	0.00668	0.00669	0.00670	0.00671	0.00671	0.00671	0.00672	0.00672	0.00672
PROPANAL	0.06667	0.07411	0.07904	0.08085	0.08234	0.08356	0.08458	0.08542	0.08613	0.08672	0.08722	0.08764	0.08799	0.08830
PROPDIAL	0.00002	0.00006	0.00011	0.00013	0.00015	0.00017	0.00019	0.00020	0.00021	0.00022	0.00022	0.00023	0.00023	0.00023
GUAIACOL	0.08836	0.08907	0.08946	0.08959	0.08968	0.08976	0.08982	0.08986	0.08990	0.08993	0.08995	0.08997	0.08998	0.08999
COUMARYL	0.00107	0.00176	0.00227	0.00244	0.00256	0.00265	0.00271	0.00276	0.00279	0.00281	0.00283	0.00284	0.00285	0.00286
PHENOL	0.03964	0.04011	0.04042	0.04052	0.04060	0.04065	0.04070	0.04073	0.04076	0.04078	0.04080	0.04081	0.04082	0.04083
FE2MACR	0.02362	0.03273	0.03997	0.04274	0.04499	0.04677	0.04818	0.04928	0.05014	0.05080	0.05132	0.05172	0.05204	0.05228
HMF	0.01933	0.02382	0.02695	0.02814	0.02912	0.02995	0.03064	0.03121	0.03170	0.03211	0.03245	0.03275	0.03299	0.03321
FURFURAL	0.01473	0.01815	0.02054	0.02144	0.02219	0.02282	0.02334	0.02378	0.02415	0.02446	0.02473	0.02495	0.02514	0.02530
LVG	0.12654	0.10481	0.08159	0.07122	0.06196	0.05381	0.04671	0.04056	0.03527	0.03071	0.02679	0.02342	0.02052	0.01803
XYL	0.00072	0.00053	0.00040	0.00035	0.00030	0.00026	0.00023	0.00021	0.00018	0.00016	0.00014	0.00013	0.00011	0.00010
H2O	0.20563	0.22605	0.24035	0.24573	0.25019	0.25389	0.25697	0.25953	0.26167	0.26347	0.26497	0.26624	0.26732	0.26823
TOTAL	0.65136	0.68581	0.70229	0.70681	0.70978	0.71169	0.71285	0.71350	0.71381	0.71389	0.71382	0.71367	0.71346	0.71322
CO2	0.01400	0.02278	0.03396	0.04024	0.04678	0.05342	0.06001	0.06639	0.07243	0.07805	0.08320	0.08784	0.09197	0.09563
CO	0.00007	0.00012	0.00016	0.00018	0.00020	0.00023	0.00027	0.00033	0.00041	0.00053	0.00069	0.00090	0.00116	0.00146
CH4	0.00264	0.00294	0.00317	0.00326	0.00333	0.00339	0.00343	0.00347	0.00350	0.00352	0.00354	0.00355	0.00356	0.00357
C2H4	0.00408	0.00440	0.00464	0.00473	0.00480	0.00486	0.00491	0.00495	0.00498	0.00500	0.00502	0.00503	0.00504	0.00505
H2	0.00000	0.00000	0.00000	0.00000	0.00000	0.00000	0.00000	0.00000	0.00000	0.00000	0.00000	0.00000	0.00000	0.00000
TOTAL	0.02078	0.03023	0.04193	0.04840	0.05511	0.06190	0.06862	0.07513	0.08132	0.08710	0.09244	0.09732	0.10174	0.10571
C	0.08405	0.09910	0.10974	0.11375	0.11706	0.11980	0.12206	0.12394	0.12550	0.12680	0.12789	0.12880	0.12957	0.13022
CELL	0.04354	0.01720	0.00690	0.00443	0.00287	0.00188	0.00125	0.00083	0.00056	0.00038	0.00027	0.00018	0.00013	0.00009
CELLA	0.02722	0.01756	0.01079	0.00841	0.00655	0.00510	0.00399	0.00312	0.00246	0.00194	0.00154	0.00122	0.00098	0.00079
HCE	0.00201	0.00104	0.00055	0.00041	0.00030	0.00023	0.00017	0.00013	0.00010	0.00008	0.00006	0.00005	0.00004	0.00003
HCEA1	0.00132	0.00075	0.00044	0.00034	0.00026	0.00020	0.00016	0.00013	0.00010	0.00008	0.00006	0.00005	0.00004	0.00003
HCEA2	0.00514	0.00260	0.00135	0.00098	0.00072	0.00053	0.00040	0.00030	0.00022	0.00017	0.00013	0.00010	0.00008	0.00006
LIGC	0.00415	0.00234	0.00110	0.00073	0.00048	0.00031	0.00020	0.00014	0.00009	0.00006	0.00004	0.00003	0.00002	0.00001
LIGO	0.00338	0.00196	0.00117	0.00092	0.00072	0.00057	0.00045	0.00036	0.00029	0.00024	0.00019	0.00016	0.00013	0.00011
LIGH	0.00650	0.00301	0.00143	0.00099	0.00070	0.00050	0.00035	0.00026	0.00019	0.00014	0.00010	0.00007	0.00006	0.00004
LIGCC	0.00081	0.00106	0.00100	0.00089	0.00077	0.00064	0.00053	0.00043	0.00034	0.00027	0.00022	0.00017	0.00014	0.00011
LIGOH	0.03936	0.02855	0.01892	0.01510	0.01195	0.00942	0.00741	0.00583	0.00459	0.00362	0.00287	0.00228	0.00182	0.00146
LIG	0.00005	0.00005	0.00005	0.00004	0.00004	0.00004	0.00003	0.00003	0.00003	0.00002	0.00002	0.00002	0.00002	0.00001
G{CO2}	0.08648	0.08386	0.07671	0.07190	0.06657	0.06091	0.05514	0.04944	0.04396	0.03880	0.03405	0.02974	0.02589	0.02247
G{CO}	0.00161	0.00226	0.00278	0.00297	0.00313	0.00324	0.00331	0.00333	0.00332	0.00325	0.00313	0.00295	0.00272	0.00244
G{COH2}	0.01126	0.01166	0.01190	0.01197	0.01204	0.01208	0.01212	0.01215	0.01217	0.01219	0.01220	0.01221	0.01222	0.01223
G{H2}	0.00000	0.00000	0.00000	0.00000	0.00000	0.00000	0.00000	0.00000	0.00000	0.00000	0.00000	0.00000	0.00000	0.00000
TOTAL	0.31689	0.27300	0.24482	0.23383	0.22415	0.21545	0.20757	0.20041	0.19392	0.18805	0.18278	0.17805	0.17384	0.17011

Table A.23: Component yields for residence time sensibility analysis (Bio5).

τ	0.1	0.2	0.3	0.4	0.5	0.6	0.7	0.8	0.9	1
HAA	0.04661	0.04691	0.04707	0.04716	0.04722	0.04726	0.04730	0.04732	0.04734	0.04736
GLYOXAL	0.00751	0.00756	0.00758	0.00760	0.00761	0.00761	0.00762	0.00762	0.00763	0.00763
CH3CHO	0.00570	0.00574	0.00576	0.00577	0.00577	0.00578	0.00578	0.00579	0.00579	0.00579
CH2O	0.01424	0.01428	0.01429	0.01430	0.01431	0.01432	0.01432	0.01432	0.01432	0.01433
MEOH	0.01141	0.01159	0.01169	0.01175	0.01179	0.01182	0.01184	0.01186	0.01188	0.01189
ETOH	0.00668	0.00669	0.00670	0.00671	0.00671	0.00671	0.00671	0.00671	0.00672	0.00672
PROPANAL	0.08725	0.08764	0.08783	0.08795	0.08802	0.08808	0.08812	0.08815	0.08818	0.08820
PROPDIAL	0.00016	0.00018	0.00020	0.00020	0.00021	0.00021	0.00022	0.00022	0.00022	0.00022
GUAIACOL	0.08952	0.08969	0.08978	0.08983	0.08987	0.08989	0.08991	0.08993	0.08994	0.08995
COUMARYL	0.00270	0.00275	0.00278	0.00280	0.00281	0.00282	0.00283	0.00283	0.00284	0.00284
PHENOL	0.04055	0.04065	0.04070	0.04073	0.04075	0.04077	0.04078	0.04079	0.04079	0.04080
FE2MACR	0.04467	0.04723	0.04861	0.04948	0.05008	0.05052	0.05085	0.05111	0.05132	0.05149
HMF	0.03263	0.03284	0.03295	0.03301	0.03305	0.03309	0.03311	0.03313	0.03314	0.03315
FURFURAL	0.02486	0.02502	0.02510	0.02515	0.02518	0.02521	0.02523	0.02524	0.02525	0.02526
LVG	0.01771	0.01783	0.01788	0.01792	0.01794	0.01796	0.01797	0.01798	0.01799	0.01800
XYL	0.00010	0.00010	0.00010	0.00010	0.00010	0.00010	0.00010	0.00010	0.00010	0.00010
H2O	0.26447	0.26581	0.26650	0.26692	0.26721	0.26741	0.26757	0.26769	0.26779	0.26787
TOTAL	0.69677	0.70250	0.70552	0.70738	0.70864	0.70956	0.71025	0.71079	0.71123	0.71159
CO2	0.03492	0.04574	0.05407	0.06069	0.06606	0.07052	0.07428	0.07748	0.08025	0.08267
CO	0.00033	0.00042	0.00050	0.00058	0.00066	0.00073	0.00080	0.00087	0.00094	0.00100
CH4	0.00333	0.00341	0.00345	0.00348	0.00350	0.00351	0.00352	0.00353	0.00354	0.00354
C2H4	0.00481	0.00489	0.00493	0.00496	0.00498	0.00499	0.00501	0.00501	0.00502	0.00503
H2	0.00000	0.00000	0.00000	0.00000	0.00000	0.00000	0.00000	0.00000	0.00000	0.00000
TOTAL	0.04340	0.05446	0.06296	0.06971	0.07520	0.07976	0.08361	0.08690	0.08975	0.09224
C	0.12682	0.12801	0.12863	0.12902	0.12928	0.12946	0.12961	0.12972	0.12981	0.12988
CELL	0.00091	0.00061	0.00046	0.00037	0.00030	0.00026	0.00023	0.00020	0.00018	0.00017
CELLA	0.00772	0.00518	0.00390	0.00312	0.00261	0.00224	0.00196	0.00174	0.00157	0.00143
HCE	0.00030	0.00020	0.00015	0.00012	0.00010	0.00009	0.00007	0.00007	0.00006	0.00005
HCEA1	0.00034	0.00023	0.00017	0.00014	0.00012	0.00010	0.00009	0.00008	0.00007	0.00006
HCEA2	0.00061	0.00040	0.00030	0.00024	0.00020	0.00017	0.00015	0.00014	0.00012	0.00011
LIGC	0.00013	0.00009	0.00007	0.00005	0.00004	0.00004	0.00003	0.00003	0.00003	0.00002
LIGO	0.00106	0.00071	0.00053	0.00043	0.00035	0.00030	0.00027	0.00024	0.00021	0.00019
LIGH	0.00042	0.00028	0.00021	0.00017	0.00014	0.00012	0.00011	0.00009	0.00008	0.00008
LIGCC	0.00078	0.00058	0.00046	0.00039	0.00033	0.00029	0.00026	0.00023	0.00021	0.00019
LIGOH	0.01252	0.00882	0.00680	0.00554	0.00467	0.00404	0.00356	0.00318	0.00287	0.00262
LIG	0.00013	0.00009	0.00007	0.00006	0.00005	0.00004	0.00004	0.00003	0.00003	0.00003
G{CO2}	0.08208	0.07166	0.06354	0.05705	0.05175	0.04735	0.04364	0.04047	0.03772	0.03533
G{CO}	0.00300	0.00310	0.00312	0.00311	0.00307	0.00303	0.00299	0.00294	0.00289	0.00284
G{COH2}	0.01206	0.01212	0.01215	0.01217	0.01218	0.01219	0.01220	0.01220	0.01221	0.01221
G{H2}	0.00000	0.00000	0.00000	0.00000	0.00000	0.00000	0.00000	0.00000	0.00000	0.00000
TOTAL	0.24888	0.23208	0.22056	0.21195	0.20520	0.19972	0.19518	0.19135	0.18806	0.18521

Appendix B

Mass balances

Table B.1: Mass balance for SX simulation using Bio1 sample (Part 1 of 2).

	AIR-COMB	AIR-DRY	BIO-OIL	DRYSOLID	ELEMENTS	EXHAUST	FB-FEED	FB-GASIN	FBGASOUT	FBPG	FLUEGAS1	FLUEGAS2
Temperature °C	25	25	50.2	49.3	500	94.8	49	810	500.7	25	1519.4	1519.4
Pressure bar	1	1	1	1	1.1	1	1	1.2	0.9	1	1.1	1.1
Mass Flow kg/hr	10200	61700	31346.1	2730.2	630.1	62719.8	2730.3	6600	7850.8	6600	18303.7	18293.7
N2	7824.2	47329	0.4	0	0	47329	0	6600	6600	6600	14422.4	14422.4
O2	2375.8	14371	0	0	10.2	14371	0	0	0	0	9.5	9.5
HAA	0	0	4137.2	0	0	0	0	0	0	0	0	0
GLYOXAL	0	0	23.7	0	0	0	0	0	0	0	0	0
CH3CHO	0	0	0.6	0	0	0	0	0	0	0	0	0
CH2O	0	0	3	0	0	0	0	0	0	0	0	0
MEOH	0	0	733.5	0	0	0	0	0	0	0	0	0
ETOH	0	0	168	0	0	0	0	0	0	0	0	0
PROPANAL	0	0	67.2	0	0	0	0	0	0	0	0	0
PROPDIAL	0	0	88	0	0	0	0	0	0	0	0	0
GUAIACOL	0	0	5155	0	0	0	0	0	0	0	0	0
COUMARYL	0	0	1187.3	0	0	0	0	0	0	0	0	0
PHENOL	0	0	1992.2	0	0	0	0	0	0	0	0	0
FE2MACR	0	0	1698.8	0	0	0	0	0	0	0	0	0
HMF	0	0	1647.1	0	0	0	0	0	0	0	0	0
FURFURAL	0	0	1674.2	0	0	0	0	0	0	0	0	0
LVG	0	0	369.8	0	0	0	0	0	0	0	0	0
XYL	0	0	13.8	0	0	0	0	0	0	0	0	0
H2O	0	0	12213.6	230.2	0	1019.8	230.2	0	230.2	0	642	642
CO2	0	0	0.8	0	0	0	0	0	0	0	3198.9	3198.9
CO	0	0	0	0	0	0	0	0	0	0	16.8	16.8
CH4	0	0	0	0	0	0	0	0	0	0	0	0
C2H4	0	0	0	0	0	0	0	0	0	0	0	0
H2	0	0	0	0	1.8	0	0	0	0	0	0.2	0.2
NO2	0	0	0	0	0	0	0	0	0	0	0	0
NO	0	0	0	0	0	0	0	0	0	0	3.9	3.9
CELLULOS	0	0	0.3	0	0	0	1029.8	0	422	0	0	0
CELLA	0	0	0.8	0	0	0	0	0	0	0	0	0
HCE	0	0	0.1	0	0	0	493.6	0	202.3	0	0	0
HCEA1	0	0	0.1	0	0	0	0	0	0	0	0	0
HCEA2	0	0	0.2	0	0	0	0	0	0	0	0	0
LIG-C	0	0	0.4	0	0	0	112.6	0	46.1	0	0	0
LIG-O	0	0	0.2	0	0	0	527.2	0	216.1	0	0	0
LIG-H	0	0	0.2	0	0	0	326.9	0	134	0	0	0
LIG-CC	0	0	1.5	0	0	0	0	0	0	0	0	0
LIG-OH	0	0	2.8	0	0	0	0	0	0	0	0	0
LIG	0	0	1.8	0	0	0	0	0	0	0	0	0
C	0	0	96.4	0	366.4	0	0	0	0	0	0	0
G{CO2}	0	0	33	0	119.4	0	0	0	0	0	0	0
G{CO}	0	0	21.4	0	77.4	0	0	0	0	0	0	0
G{COH2}	0	0	12.4	0	44.9	0	0	0	0	0	0	0
DRYBIO	0	0	0	2500	0	0	0	0	0	0	0	0
ASH	0	0	0.3	0	10	0	10	0	0.1	0	10	0

Table B.2: Mass balance for SX simulation using Bio1 sample (Part 2 of 2).

	FLUEGAS3	FLUEGAS4	HEAVYOIL	LIGHTOIL	NCG	PURGE	PYR-CHAR	PYR-GAS	PYR-PROD	PYR-SOL	QCH-COOL	QCH-GAS	WETBIO
Temperature °C	1290.8	986.1	50.2	25	25	25		500	500		25	50.2	25
Pressure bar	1.1	1.1	1	10	10	1.2	1.1	1.1	1.1	1	1.2	1	1
Mass Flow kg/hr	18293.7	18293.7	30053.6	1292.6	7473.7	7541.7	630	8700.2	9330.2	1479.4	30119.9	8766.4	3750
N2	14422.4	14422.4	0.4	0	6600	6600	0	6600	6600	0	0.4	6600	0
O2	9.5	9.5	0	0	0	0	0	0	0	0	0	0	0
HAA	0	0	3881.6	255.6	95.3	78.5	0	232.4	232.4	0	4000.1	350.9	0
GLYOXAL	0	0	19.3	4.4	22.3	12.8	0	14	14	0	31.9	26.7	0
CH3CHO	0	0	0.5	0.1	5.1	4.6	0	4.7	4.7	0	1.1	5.2	0
CH2O	0	0	2.5	0.5	49.2	47	0	47.2	47.2	0	5	49.7	0
MEOH	0	0	655.1	78.3	5.6	15.8	0	42.5	42.5	0	696.5	84	0
ETOH	0	0	141.4	26.6	22.1	12.3	0	18.9	18.9	0	171.3	48.7	0
PROPANAL	0	0	63.3	3.9	386.4	328.5	0	333.2	333.2	0	120.5	390.3	0
PROPDIAL	0	0	87.8	0.2	0	0	0	3.3	3.3	0	84.8	0.2	0
GUAIACOL	0	0	5141.2	13.8	0.3	2.1	0	192.9	192.9	0	4962.4	14.2	0
COUMARYL	0	0	1187.2	0.1	0	0	0	44	44	0	1143.3	0.1	0
PHENOL	0	0	1984.6	7.6	0.1	1.2	0	74.9	74.9	0	1917.4	7.7	0
FE2MACR	0	0	1698.8	0	0	0	0	62.9	62.9	0	1635.9	0	0
HMF	0	0	1647.1	0	0	0	0	61	61	0	1586.1	0	0
FURFURAL	0	0	1641.5	32.8	4.5	7.8	0	69.7	69.7	0	1609	37.2	0
LVG	0	0	369.8	0	0	0	0	13.7	13.7	0	356.1	0	0
XYL	0	0	13.8	0	0	0	0	0.5	0.5	0	13.3	0	0
H2O	642	642	11347.2	866.4	14.6	163.3	0	610.2	610.2	0	11618	881	1250
CO2	3198.9	3198.9	0.7	0.1	199.1	198.7	0	198.7	198.7	0	1.1	199.2	0
CO	16.8	16.8	0	0	15.8	15.8	0	15.8	15.8	0	0	15.8	0
CH4	0	0	0	0	27	27	0	27	27	0	0	27	0
C2H4	0	0	0	0	26.3	26.3	0	26.3	26.3	0	0.1	26.3	0
H2	0.2	0.2	0	0	0	0	0	0	0	0	0	0	0
NO2	0	0	0	0	0	0	0	0	0	0	0	0	0
NO	3.9	3.9	0	0	0	0	0	0	0	0	0	0	0
CELLULOS	0	0	0.3	0	0	0	1	0	1	607.7	0.3	0	0
CELLA	0	0	0.8	0	0	0	2.9	0	3	0	0.8	0	0
HCE	0	0	0.1	0	0	0	0.3	0	0.3	291.3	0.1	0	0
HCEA1	0	0	0.1	0	0	0	0.3	0	0.3	0	0.1	0	0
HCEA2	0	0	0.2	0	0	0	0.6	0	0.6	0	0.2	0	0
LIG-C	0	0	0.4	0	0	0	1.4	0	1.4	66.4	0.4	0	0
LIG-O	0	0	0.2	0	0	0	0.8	0	0.9	311.2	0.2	0	0
LIG-H	0	0	0.2	0	0	0	0.6	0	0.6	192.9	0.2	0	0
LIG-CC	0	0	1.5	0	0	0	5.3	0.1	5.4	0	1.4	0	0
LIG-OH	0	0	2.8	0	0	0	10.2	0.1	10.3	0	2.7	0	0
LIG	0	0	1.8	0	0	0	6.6	0.1	6.6	0	1.7	0	0
C	0	0	95.1	1.3	0	0	348.3	3.6	351.8	0	92.8	1.3	0
G{CO2}	0	0	32.6	0.4	0	0	119.4	1.2	120.6	0	31.8	0.4	0
G{CO}	0	0	21.1	0.3	0	0	77.4	0.8	78.2	0	20.6	0.3	0
G{COH2}	0	0	12.3	0.2	0	0	44.9	0.5	45.4	0	12	0.2	0
DRYBIO	0	0	0	0	0	0	0	0	0	0	0	0	2500
ASH	0	0	0.3	0	0	0	10	0	10	9.9	0.3	0	0

Table B.3: Mass balance for SX simulation using Bio2 sample (Part 1 of 2).

	AIR-COMB	AIR-DRY	BIO-OIL	DRYSOLID	ELEMENTS	EXHAUST	FB-FEED	FB-GASIN	FBGASOUT	FBPG	FLUEGAS1	FLUEGAS2
Temperature °C	25	25	53.5	43	500	95.2	42	810	500.9	20	1368.1	1368.1
Pressure bar	1	1	1	1	1.1	1	1	1.4	1.2	1	1.1	1.1
Mass Flow kg/hr	9100	61250	33082.8	2737.2	629.1	62262.8	2737.3	6900	7812.8	6900	17353.9	17328.9
N2	6980.5	46983.8	0.4	0	0	46983.8	0	6900	6900	6900	13880.4	13880.4
O2	2119.5	14266.2	0	0	4.1	14266.2	0	0	0	0	0	0
HAA	0	0	3699.4	0	0	0	0	0	0	0	0	0
GLYOXAL	0	0	20.3	0	0	0	0	0	0	0	0	0
CH3CHO	0	0	1.9	0	0	0	0	0	0	0	0	0
CH2O	0	0	2.4	0	0	0	0	0	0	0	0	0
MEOH	0	0	905.2	0	0	0	0	0	0	0	0	0
ETOH	0	0	118.7	0	0	0	0	0	0	0	0	0
PROPANAL	0	0	29.9	0	0	0	0	0	0	0	0	0
PROPDIAL	0	0	122.4	0	0	0	0	0	0	0	0	0
GUAIACOL	0	0	4767.5	0	0	0	0	0	0	0	0	0
COUMARYL	0	0	1510.5	0	0	0	0	0	0	0	0	0
PHENOL	0	0	1945.4	0	0	0	0	0	0	0	0	0
FE2MACR	0	0	1772.4	0	0	0	0	0	0	0	0	0
HMF	0	0	1655.5	0	0	0	0	0	0	0	0	0
FURFURAL	0	0	1330.5	0	0	0	0	0	0	0	0	0
LVG	0	0	491.1	0	0	0	0	0	0	0	0	0
XYL	0	0	6.3	0	0	0	0	0	0	0	0	0
H2O	0	0	14530.7	237.2	0	1012.8	237.2	0	237.2	0	474.8	474.8
CO2	0	0	0.7	0	0	0	0	0	0	0	2624	2624
CO	0	0	0	0	0	0	0	0	0	0	346.2	346.2
CH4	0	0	0	0	0	0	0	0	0	0	0	0
C2H4	0	0	0.1	0	0	0	0	0	0	0	0	0
H2	0	0	0	0	0.7	0	0	0	0	0	3.5	3.5
CELLULOS	0	0	0	0	0	0	939.6	0	256.4	0	0	0
CELLA	0	0	0.3	0	0	0	0	0	0	0	0	0
HCE	0	0	0	0	0	0	398.1	0	108.7	0	0	0
HCEA1	0	0	0	0	0	0	0	0	0	0	0	0
HCEA2	0	0	0	0	0	0	0	0	0	0	0	0
LIG-C	0	0	0.1	0	0	0	139.7	0	38.1	0	0	0
LIG-O	0	0	0.1	0	0	0	490.7	0	133.9	0	0	0
LIG-H	0	0	0.1	0	0	0	507	0	138.4	0	0	0
LIG-CC	0	0	0.6	0	0	0	0	0	0	0	0	0
LIG-OH	0	0	1.2	0	0	0	0	0	0	0	0	0
LIG	0	0	1.1	0	0	0	0	0	0	0	0	0
C	0	0	131.1	0	472.7	0	0	0	0	0	0	0
G{CO2}	0	0	12.7	0	45	0	0	0	0	0	0	0
G{CO}	0	0	9.6	0	33.9	0	0	0	0	0	0	0
G{COH2}	0	0	13.4	0	47.7	0	0	0	0	0	0	0
DRYBIO	0	0	0	2500	0	0	0	0	0	0	0	0
ASH	0	0	1.2	0	25	0	25	0	0.1	0	25	0

Table B.4: Mass balance for SX simulation using Bio2 sample (Part 2 of 2).

	FLUEGAS3	FLUEGAS4	HEAVYOIL	LIGHTOIL	NCG	PURGE	PYR-CHAR	PYR-GAS	PYR-PROD	PYR-SOL	QCH-COOL	QCH-GAS	WETBIO
Temperature °C	1114.7	785.5	53.5	25	25	25		550	550		25	53.5	25
Pressure bar	1.1	1.1	1	10	10	1.2	1.1	1.1	1.1	1.2	1.2	1	1
Mass Flow kg/hr	17328.9	17328.9	31426.7	1656	7624.8	7789	629.2	9008	9637.3	1824.4	31699.1	9280.7	3750
N2	13880.4	13880.4	0.3	0.1	6899.9	6900	0	6900	6900	0	0.3	6900	0
O2	0	0	0	0	0	0	0	0	0	0	0	0	0
HAA	0	0	3299.8	399.6	67.7	97.7	0	233.6	233.6	0	3533.6	467.4	0
GLYOXAL	0	0	13	7.3	18.7	13.2	0	14.1	14.1	0	24.8	25.9	0
CH3CHO	0	0	1.4	0.5	21	19.8	0	19.9	19.9	0	3	21.5	0
CH2O	0	0	1.7	0.8	43.3	42.1	0	42.3	42.3	0	3.4	44	0
MEOH	0	0	793.1	112.1	5.9	18.8	0	51.8	51.8	0	859.3	118	0
ETOH	0	0	87.8	30.9	13.4	10.8	0	15.3	15.3	0	116.8	44.3	0
PROPANAL	0	0	23.6	6.3	236.2	216.3	0	218.1	218.1	0	48	242.5	0
PROPDIAL	0	0	122	0.4	0	0	0	4.6	4.6	0	117.8	0.4	0
GUAIACOL	0	0	4742.5	25	0.2	3.3	0	179.7	179.7	0	4587.9	25.2	0
COUMARYL	0	0	1510.3	0.3	0	0	0	56	56	0	1454.5	0.3	0
PHENOL	0	0	1933.8	11.6	0.1	1.5	0	73.5	73.5	0	1872	11.7	0
FE2MACR	0	0	1772.4	0	0	0	0	65.6	65.6	0	1706.7	0	0
HMF	0	0	1655.4	0	0	0	0	61.3	61.3	0	1594.1	0	0
FURFURAL	0	0	1284.8	45.7	2.5	9.4	0	58.4	58.4	0	1274.6	48.2	0
LVG	0	0	491.1	0	0	0	0	18.2	18.2	0	472.9	0	0
XYL	0	0	6.3	0	0	0	0	0.2	0.2	0	6.1	0	0
H2O	474.8	474.8	13515.9	1014.8	15.8	156.2	0	689.2	689.2	0	13857.4	1030.6	1250
CO2	2624	2624	0.5	0.2	193.7	193.5	0	193.5	193.5	0	0.8	193.9	0
CO	346.2	346.2	0	0	36.1	36.1	0	36.1	36.1	0	0	36.1	0
CH4	0	0	0	0	33.4	33.4	0	33.4	33.4	0	0	33.4	0
C2H4	0	0	0	0	36.9	36.9	0	36.9	36.9	0	0.1	36.9	0
H2	3.5	3.5	0	0	0	0	0	0	0	0	0	0	0
CELLULOS	0	0	0	0	0	0	0.2	0	0.2	683.1	0	0	0
CELLA	0	0	0.3	0	0	0	0.9	0	0.9	0	0.2	0	0
HCE	0	0	0	0	0	0	0.1	0	0.1	289.4	0	0	0
HCEA1	0	0	0	0	0	0	0.1	0	0.1	0	0	0	0
HCEA2	0	0	0	0	0	0	0.1	0	0.1	0	0	0	0
LIG-C	0	0	0.1	0	0	0	0.3	0	0.3	101.6	0.1	0	0
LIG-O	0	0	0.1	0	0	0	0.3	0	0.3	356.8	0.1	0	0
LIG-H	0	0	0.1	0	0	0	0.2	0	0.2	368.6	0.1	0	0
LIG-CC	0	0	0.6	0	0	0	2.1	0	2.2	0	0.6	0	0
LIG-OH	0	0	1.2	0	0	0	4.4	0	4.4	0	1.2	0	0
LIG	0	0	1.1	0	0	0	3.9	0	4	0	1.1	0	0
C	0	0	130.7	0.4	0	0	465	4.9	469.8	0	126.2	0.4	0
G{CO2}	0	0	12.7	0	0	0	45	0.5	45.5	0	12.2	0	0
G{CO}	0	0	9.5	0	0	0	33.9	0.4	34.3	0	9.2	0	0
G{COH2}	0	0	13.4	0	0	0	47.7	0.5	48.2	0	12.9	0	0
DRYBIO	0	0	0	0	0	0	0	0	0	0	0	0	2500
ASH	0	0	1.2	0	0	0	25	0	25	24.9	1.1	0	0

Table B.5: Mass balance for SX simulation using Bio3 sample (Part 1 of 2).

	AIR-COMB	AIR-DRY	BIO-OIL	DRYSOLID	ELEMENTS	EXHAUST	FB-FEED	FB-GASIN	FBGASOUT	FBPG	FLUEGAS1	FLUEGAS2
Temperature °C	25	25	49.8	46.4	450	95	46	810	499.8	25	1513.1	1513.1
Pressure bar	1	1	1	1	1.1	1	1	1.4	1.2	1	1.1	1.1
Mass Flow kg/hr	9500	61500	37686.8	2733.2	645.3	62516.8	2733.2	6550	7070.9	6550	17452	17422.1
N2	7287.3	47175.6	0.3	0	0	47175.6	0	6550	6550	6550	13837.1	13837.1
O2	2212.7	14324.4	0	0	12.6	14324.4	0	0	0	0	0.1	0.1
HAA	0	0	1407.1	0	0	0	0	0	0	0	0	0
GLYOXAL	0	0	12.1	0	0	0	0	0	0	0	0	0
CH3CHO	0	0	0.7	0	0	0	0	0	0	0	0	0
CH2O	0	0	1.7	0	0	0	0	0	0	0	0	0
MEOH	0	0	654	0	0	0	0	0	0	0	0	0
ETOH	0	0	102.9	0	0	0	0	0	0	0	0	0
PROPANAL	0	0	19.8	0	0	0	0	0	0	0	0	0
PROPDIAL	0	0	29	0	0	0	0	0	0	0	0	0
GUAIACOL	0	0	5228.6	0	0	0	0	0	0	0	0	0
COUMARYL	0	0	391.6	0	0	0	0	0	0	0	0	0
PHENOL	0	0	1926.5	0	0	0	0	0	0	0	0	0
FE2MACR	0	0	6258.9	0	0	0	0	0	0	0	0	0
HMF	0	0	1073.7	0	0	0	0	0	0	0	0	0
FURFURAL	0	0	875.6	0	0	0	0	0	0	0	0	0
LVG	0	0	3240.7	0	0	0	0	0	0	0	0	0
XYL	0	0	12.3	0	0	0	0	0	0	0	0	0
H2O	0	0	16275.1	233.2	0	1016.8	233.2	0	233.2	0	526.7	526.7
CO2	0	0	0.5	0	0	0	0	0	0	0	2912.1	2912.1
CO	0	0	0	0	0	0	0	0	0	0	144.5	144.5
CH4	0	0	0	0	0	0	0	0	0	0	0	0
C2H4	0	0	0	0	0	0	0	0	0	0	0	0
H2	0	0	0	0	2.1	0	0	0	0	0	1.2	1.2
NO	0	0	0	0	0	0	0	0	0	0	0.4	0.4
CELLULOS	0	0	0.3	0	0	0	1039.5	0	121.1	0	0	0
CELLA	0	0	1.9	0	0	0	0	0	0	0	0	0
HCE	0	0	0.1	0	0	0	439.8	0	51.2	0	0	0
HCEA1	0	0	0.1	0	0	0	0	0	0	0	0	0
HCEA2	0	0	0.2	0	0	0	0	0	0	0	0	0
LIG-C	0	0	0.1	0	0	0	37.2	0	4.3	0	0	0
LIG-O	0	0	0.2	0	0	0	522	0	60.8	0	0	0
LIG-H	0	0	0.2	0	0	0	431.5	0	50.3	0	0	0
LIG-CC	0	0	0.5	0	0	0	0	0	0	0	0	0
LIG-OH	0	0	5.9	0	0	0	0	0	0	0	0	0
LIG	0	0	0	0	0	0	0	0	0	0	0	0
C	0	0	123.1	0	453.9	0	0	0	0	0	0	0
G{CO2}	0	0	28.5	0	100.6	0	0	0	0	0	0	0
G{CO}	0	0	4.3	0	15.3	0	0	0	0	0	0	0
G{COH2}	0	0	8.7	0	30.9	0	0	0	0	0	0	0
DRYBIO	0	0	0	2500	0	0	0	0	0	0	0	0
ASH	0	0	1.6	0	29.9	0	30	0	0	0	29.9	0

Table B.6: Mass balance for SX simulation using Bio3 sample (Part 2 of 2).

	FLUEGAS3	FLUEGAS4	HEAVYOIL	LIGHTOIL	NCG	PURGE	PYR-CHAR	PYR-GAS	PYR-PROD	PYR-SOL	QCH-COOL	QCH-GAS	WETBIO
Temperature °C	1279.3	958.1	49.8	25	25	25		500	500		25	49.8	25
Pressure bar	1.1	1.1	1	10	10	1.2	1.1	1.1	1.1	1.2	1.2	1	1
Mass Flow kg/hr	17422.1	17422.1	36865.3	821.8	7306.8	7239.5	645.3	8638.1	9283.4	2212.3	36355.5	8128.8	3750
N2	13837.1	13837.1	0.3	0	6550	6550	0	6550	6550	0	0.2	6550	0
O2	0.1	0.1	0	0	0	0	0	0	0	0	0	0	0
HAA	0	0	1393	14.1	155.1	44.8	0	101	101	0	1461.2	169.2	0
GLYOXAL	0	0	11.9	0.2	20.3	11.4	0	12.2	12.2	0	20.2	20.5	0
CH3CHO	0	0	0.7	0	9.8	9.2	0	9.3	9.3	0	1.2	9.8	0
CH2O	0	0	1.7	0	40.9	39.5	0	39.6	39.6	0	3	40.9	0
MEOH	0	0	603.3	50.7	12.8	12.7	0	36.9	36.9	0	629.9	63.5	0
ETOH	0	0	99.9	2.9	38.2	12	0	16.8	16.8	0	124.3	41.2	0
PROPANAL	0	0	19.8	0	208.5	192	0	193.4	193.4	0	34.9	208.5	0
PROPDIAL	0	0	29	0.1	0	0	0	1.1	1.1	0	27.9	0.1	0
GUAIACOL	0	0	5222.2	6.4	18.6	4.5	0	198.7	198.7	0	5048.6	25.1	0
COUMARYL	0	0	391.6	0	0.1	0	0	14.5	14.5	0	377.1	0.1	0
PHENOL	0	0	1919.3	7.2	2.1	1.6	0	73	73	0	1855.6	9.2	0
FE2MACR	0	0	6258.9	0	0	0	0	231.8	231.8	0	6027.1	0	0
HMF	0	0	1073.7	0	0	0	0	39.8	39.8	0	1033.9	0	0
FURFURAL	0	0	871.9	3.8	25.2	7.3	0	40.4	40.4	0	860.4	29	0
LVG	0	0	3240.7	0	0	0	0	120	120	0	3120.6	0	0
XYL	0	0	12.3	0	0	0	0	0.5	0.5	0	11.8	0	0
H2O	526.7	526.7	15541.1	734	12.7	142.3	0	740.3	740.3	0	15547.5	746.8	1250
CO2	2912.1	2912.1	0.5	0	167.8	167.5	0	167.5	167.5	0	0.7	167.8	0
CO	144.5	144.5	0	0	2	2	0	2	2	0	0	2	0
CH4	0	0	0	0	27.5	27.5	0	27.5	27.5	0	0	27.5	0
C2H4	0	0	0	0	15.2	15.2	0	15.2	15.2	0	0	15.2	0
H2	1.2	1.2	0	0	0	0	0	0	0	0	0	0	0
NO	0.4	0.4	0	0	0	0	0	0	0	0	0	0	0
CELLULOS	0	0	0.3	0	0	0	1	0	1	918.5	0.3	0	0
CELLA	0	0	1.9	0	0	0	6.8	0.1	6.8	0	1.8	0	0
HCE	0	0	0.1	0	0	0	0.3	0	0.3	388.6	0.1	0	0
HCEA1	0	0	0.1	0	0	0	0.2	0	0.3	0	0.1	0	0
HCEA2	0	0	0.2	0	0	0	0.6	0	0.6	0	0.2	0	0
LIG-C	0	0	0.1	0	0	0	0.5	0	0.5	32.8	0.1	0	0
LIG-O	0	0	0.2	0	0	0	0.8	0	0.8	461.2	0.2	0	0
LIG-H	0	0	0.2	0	0	0	0.8	0	0.9	381.2	0.2	0	0
LIG-CC	0	0	0.5	0	0	0	1.8	0	1.8	0	0.5	0	0
LIG-OH	0	0	5.9	0.1	0	0	21	0.2	21.2	0	5.7	0.1	0
LIG	0	0	0	0	0	0	0.1	0	0.1	0	0	0	0
C	0	0	121.4	1.7	0	0	434.7	4.6	439.3	0	118.6	1.7	0
G{CO2}	0	0	28.1	0.4	0	0	100.6	1.1	101.7	0	27.4	0.4	0
G{CO}	0	0	4.3	0.1	0	0	15.3	0.2	15.4	0	4.2	0.1	0
G{COH2}	0	0	8.6	0.1	0	0	30.9	0.3	31.2	0	8.4	0.1	0
DRYBIO	0	0	0	0	0	0	0	0	0	0	0	0	2500
ASH	0	0	1.6	0	0	0	29.9	0.1	30	30	1.6	0	0

Table B.7: Mass balance for SX simulation using Bio4 sample (Part 1 of 2).

	AIR-COMB	AIR-DRY	BIO-OIL	DRYSOLID	ELEMENTS	EXHAUST	FB-FEED	FB-GASIN	FBGASOUT	FBPG	FLUEGAS1	FLUEGAS2
Temperature °C	25	25	50.6	47	500	95	47	810	500.3	20	1405.3	1405.3
Pressure bar	1	1	1	1	1.1	1	1	1.2	0.9	1	1.1	1.1
Mass Flow kg/hr	9000	61500	35517.3	2733.2	561.4	62516.8	2733.3	6850	8575.4	6850	17377.2	17364.7
N2	6903.7	47175.6	0.4	0	0	47175.6	0	6850	6850	6850	13753.7	13753.7
O2	2096.3	14324.4	0	0	4.6	14324.4	0	0	0	0	0	0
HAA	0	0	1982.9	0	0	0	0	0	0	0	0	0
GLYOXAL	0	0	19.3	0	0	0	0	0	0	0	0	0
CH3CHO	0	0	1.2	0	0	0	0	0	0	0	0	0
CH2O	0	0	2.8	0	0	0	0	0	0	0	0	0
MEOH	0	0	525	0	0	0	0	0	0	0	0	0
ETOH	0	0	164.8	0	0	0	0	0	0	0	0	0
PROPANAL	0	0	38.6	0	0	0	0	0	0	0	0	0
PROPDIAL	0	0	58.9	0	0	0	0	0	0	0	0	0
GUAIACOL	0	0	8856.8	0	0	0	0	0	0	0	0	0
COUMARYL	0	0	794.8	0	0	0	0	0	0	0	0	0
PHENOL	0	0	3277.4	0	0	0	0	0	0	0	0	0
FE2MACR	0	0	396.8	0	0	0	0	0	0	0	0	0
HMF	0	0	1705.2	0	0	0	0	0	0	0	0	0
FURFURAL	0	0	1690.5	0	0	0	0	0	0	0	0	0
LVG	0	0	3140.2	0	0	0	0	0	0	0	0	0
XYL	0	0	16.2	0	0	0	0	0	0	0	0	0
H2O	0	0	12691.4	233.2	0	1016.8	233.2	0	233.2	0	611.5	611.5
CO2	0	0	0.9	0	0	0	0	0	0	0	2808.7	2808.7
CO	0	0	0	0	0	0	0	0	0	0	188.5	188.5
CH4	0	0	0	0	0	0	0	0	0	0	0	0
C2H4	0	0	0	0	0	0	0	0	0	0	0	0
H2	0	0	0	0	0.7	0	0	0	0	0	2.2	2.2
NO	0	0	0	0	0	0	0	0	0	0	0.1	0.1
CELLULOS	0	0	0.3	0	0	0	932.8	0	559.5	0	0	0
CELLA	0	0	0.7	0	0	0	0	0	0	0	0	0
HCE	0	0	0.1	0	0	0	578.3	0	346.8	0	0	0
HCEA1	0	0	0.1	0	0	0	0	0	0	0	0	0
HCEA2	0	0	0.2	0	0	0	0	0	0	0	0	0
LIG-C	0	0	0.3	0	0	0	75.4	0	45.2	0	0	0
LIG-O	0	0	0.4	0	0	0	873.7	0	524	0	0	0
LIG-H	0	0	0	0	0	0	27.4	0	16.4	0	0	0
LIG-CC	0	0	1	0	0	0	0	0	0	0	0	0
LIG-OH	0	0	0.4	0	0	0	0	0	0	0	0	0
LIG	0	0	0	0	0	0	0	0	0	0	0	0
C	0	0	93.2	0	342.3	0	0	0	0	0	0	0
G{CO2}	0	0	43.7	0	157.1	0	0	0	0	0	0	0
G{CO}	0	0	0.8	0	2.7	0	0	0	0	0	0	0
G{COH2}	0	0	11.5	0	41.5	0	0	0	0	0	0	0
DRYBIO	0	0	0	2500	0	0	0	0	0	0	0	0
ASH	0	0	0.5	0	12.5	0	12.5	0	0.3	0	12.5	0

Table B.8: Mass balance for SX simulation using Bio4 sample (Part 2 of 2).

	FLUEGAS3	FLUEGAS4	HEAVYOIL	LIGHTOIL	NCG	PURGE	PYR-CHAR	PYR-GAS	PYR-PROD	PYR-SOL	QCH-COOL	QCH-GAS	WETBIO
Temperature °C	1151.1	825.4	50.7	25	25	25		500	500		25	50.7	25
Pressure bar	1.1	1.1	1	10	10	1.2	1.1	1.1	1.1	1	1.2	1	1
Mass Flow kg/hr	17364.7	17364.7	34542.6	974.5	7815.8	7702.1	561.3	9021.6	9582.8	1007.7	34311.4	8790.6	3750
N2	13753.7	13753.7	0.4	0	6850	6850	0	6850	6850	0	0.4	6850	0
O2	0	0	0	0	0	0	0	0	0	0	0	0	0
HAA	0	0	1967.3	15.7	169.7	42.1	0	120.3	120.3	0	2032.4	185.4	0
GLYOXAL	0	0	19	0.3	26.9	13.3	0	14.5	14.5	0	31.7	27.2	0
CH3CHO	0	0	1.2	0	12.2	10.9	0	11	11	0	2.3	12.2	0
CH2O	0	0	2.8	0	56	53.1	0	53.4	53.4	0	5.4	56	0
MEOH	0	0	473.6	51.3	11.8	11.9	0	31.3	31.3	0	505.4	63.1	0
ETOH	0	0	160.6	4.2	52.9	14.6	0	22.1	22.1	0	195.6	57.1	0
PROPANAL	0	0	38.6	0	252.5	216	0	218.8	218.8	0	72.4	252.6	0
PROPDIAL	0	0	58.8	0.1	0	0	0	2.2	2.2	0	56.7	0.1	0
GUAIACOL	0	0	8850.2	6.5	19.6	3.9	0	332.5	332.5	0	8543.9	26.2	0
COUMARYL	0	0	794.8	0	0	0	0	29.4	29.4	0	765.4	0.1	0
PHENOL	0	0	3267.2	10.2	2.9	2	0	123.4	123.4	0	3156.9	13.1	0
FE2MACR	0	0	396.8	0	0	0	0	14.7	14.7	0	382.1	0	0
HMF	0	0	1705.2	0	0	0	0	63.2	63.2	0	1642.1	0	0
FURFURAL	0	0	1685.3	5.2	34.9	8.6	0	72.2	72.2	0	1653.2	40.1	0
LVG	0	0	3140.2	0	0	0	0	116.3	116.3	0	3023.9	0	0
XYL	0	0	16.2	0	0	0	0	0.6	0.6	0	15.6	0	0
H2O	611.5	611.5	11812.7	878.6	13.6	163.5	0	628	628	0	12076.9	892.2	1250
CO2	2808.7	2808.7	0.9	0	262.1	261.5	0	261.5	261.5	0	1.5	262.1	0
CO	188.5	188.5	0	0	2	2	0	2	2	0	0	2	0
CH4	0	0	0	0	34.7	34.7	0	34.7	34.7	0	0	34.7	0
C2H4	0	0	0	0	14	14	0	14	14	0	0	14	0
H2	2.2	2.2	0	0	0	0	0	0	0	0	0	0	0
NO	0.1	0.1	0	0	0	0	0	0	0	0	0	0	0
CELLULOS	0	0	0.3	0	0	0	1.2	0	1.2	373.3	0.3	0	0
CELLA	0	0	0.7	0	0	0	2.4	0	2.4	0	0.6	0	0
HCE	0	0	0.1	0	0	0	0.3	0	0.3	231.4	0.1	0	0
HCEA1	0	0	0.1	0	0	0	0.3	0	0.3	0	0.1	0	0
HCEA2	0	0	0.2	0	0	0	0.7	0	0.7	0	0.2	0	0
LIG-C	0	0	0.3	0	0	0	0.9	0	0.9	30.2	0.3	0	0
LIG-O	0	0	0.4	0	0	0	1.4	0	1.4	349.7	0.4	0	0
LIG-H	0	0	0	0	0	0	0.1	0	0.1	10.9	0	0	0
LIG-CC	0	0	1	0	0	0	3.6	0	3.6	0	1	0	0
LIG-OH	0	0	0.4	0	0	0	1.3	0	1.3	0	0.4	0	0
LIG	0	0	0	0	0	0	0	0	0	0	0	0	0
C	0	0	91.7	1.5	0	0	335.3	3.5	338.7	0	89.8	1.5	0
G{CO2}	0	0	43	0.7	0	0	157.1	1.6	158.7	0	42.1	0.7	0
G{CO}	0	0	0.7	0	0	0	2.7	0	2.7	0	0.7	0	0
G{COH2}	0	0	11.4	0.2	0	0	41.5	0.4	41.9	0	11.1	0.2	0
DRYBIO	0	0	0	0	0	0	0	0	0	0	0	0	2500
ASH	0	0	0.5	0	0	0	12.5	0	12.5	12.2	0.5	0	0

Table B.9: Mass balance for SX simulation using Bio5 sample (Part 1 of 2).

	AIR-COMB	AIR-DRY	BIO-OIL	DRYSOLID	ELEMENTS	EXHAUST	FB-FEED	FB-GASIN	FBGASOUT	FBPG	FLUEGAS1	FLUEGAS2
Temperature °C	25	25	50.3	42.3	500	95.2	42	810	499.9	20	1474	1474
Pressure bar	1	1	1	1	1.1	1	1	1.4	1.2	1	1.1	1.1
Mass Flow kg/hr	9100	61250	37748.1	2737.4	555.3	62262.6	2737.5	6250	6577	6250	16776	16746.1
N2	6980.5	46983.8	0.3	0	0	46983.8	0	6250	6250	6250	13230	13230
O2	2119.5	14266.2	0	0	9.6	14266.2	0	0	0	0	0.9	0.9
HAA	0	0	1912.8	0	0	0	0	0	0	0	0	0
GLYOXAL	0	0	24.8	0	0	0	0	0	0	0	0	0
CH3CHO	0	0	1.4	0	0	0	0	0	0	0	0	0
CH2O	0	0	2	0	0	0	0	0	0	0	0	0
MEOH	0	0	575.1	0	0	0	0	0	0	0	0	0
ETOH	0	0	131.2	0	0	0	0	0	0	0	0	0
PROPANAL	0	0	32.5	0	0	0	0	0	0	0	0	0
PROPDIAL	0	0	15	0	0	0	0	0	0	0	0	0
GUAIACOL	0	0	6406	0	0	0	0	0	0	0	0	0
COUMARYL	0	0	202.3	0	0	0	0	0	0	0	0	0
PHENOL	0	0	2904.7	0	0	0	0	0	0	0	0	0
FE2MACR	0	0	3637	0	0	0	0	0	0	0	0	0
HMF	0	0	2299.2	0	0	0	0	0	0	0	0	0
FURFURAL	0	0	1481.7	0	0	0	0	0	0	0	0	0
LVG	0	0	2558	0	0	0	0	0	0	0	0	0
XYL	0	0	13.2	0	0	0	0	0	0	0	0	0
H2O	0	0	15401.5	237.4	0	1012.6	237.4	0	237.4	0	564.8	564.8
CO2	0	0	0.7	0	0	0	0	0	0	0	2920.3	2920.3
CO	0	0	0	0	0	0	0	0	0	0	28.8	28.8
CH4	0	0	0	0	0	0	0	0	0	0	0	0
C2H4	0	0	0	0	0	0	0	0	0	0	0	0
H2	0	0	0	0	1.5	0	0	0	0	0	0.3	0.3
NO	0	0	0	0	0	0	0	0	0	0	1	1
CELLULOS	0	0	0.4	0	0	0	1220.4	0	44.3	0	0	0
CELLA	0	0	1.9	0	0	0	0	0	0	0	0	0
HCE	0	0	0.1	0	0	0	480.1	0	17.4	0	0	0
HCEA1	0	0	0.1	0	0	0	0	0	0	0	0	0
HCEA2	0	0	0.2	0	0	0	0	0	0	0	0	0
LIG-C	0	0	0.1	0	0	0	19.6	0	0.7	0	0	0
LIG-O	0	0	0.2	0	0	0	494.5	0	17.9	0	0	0
LIG-H	0	0	0.1	0	0	0	255.5	0	9.3	0	0	0
LIG-CC	0	0	0.3	0	0	0	0	0	0	0	0	0
LIG-OH	0	0	3.5	0	0	0	0	0	0	0	0	0
LIG	0	0	0	0	0	0	0	0	0	0	0	0
C	0	0	95.3	0	353.2	0	0	0	0	0	0	0
G{CO2}	0	0	33.4	0	119.1	0	0	0	0	0	0	0
G{CO}	0	0	2.5	0	9	0	0	0	0	0	0	0
G{COH2}	0	0	9.2	0	33	0	0	0	0	0	0	0
DRYBIO	0	0	0	2500	0	0	0	0	0	0	0	0
ASH	0	0	1.4	0	29.9	0	30	0	0	0	29.9	0

Table B.10: Mass balance for SX simulation using Bio5 sample (Part 2 of 2).

	FLUEGAS3	FLUEGAS4	HEAVYOIL	LIGHTOIL	NCG	PURGE	PYR-CHAR	PYR-GAS	PYR-PROD	PYR-SOL	QCH-COOL	QCH-GAS	WETBIO
Temperature °C	1240.3	906.9	50.3	25	25	25		500	500		25	50.3	25
Pressure bar	1.1	1.1	1	10	10	1.2	1.1	1.1	1.1	1.2	1.2	1	1
Mass Flow kg/hr	16746.1	16746.1	36920.9	827.1	7120.7	7003.4	555.2	8432.3	8987.5	2410.5	36436.6	7948	3750
N2	13230	13230	0.3	0	6250	6250	0	6250	6250	0	0.3	6250	0
O2	0.9	0.9	0	0	0	0	0	0	0	0	0	0	0
HAA	0	0	1895.9	16.9	174.5	47	0	123.9	123.9	0	1963.3	191.4	0
GLYOXAL	0	0	24.4	0.4	35.3	18.4	0	20	20	0	40.2	35.8	0
CH3CHO	0	0	1.4	0	16.4	15.1	0	15.2	15.2	0	2.6	16.4	0
CH2O	0	0	2	0	40.8	39	0	39.2	39.2	0	3.6	40.8	0
MEOH	0	0	530.6	44.5	10.6	10.6	0	32.3	32.3	0	553.4	55.1	0
ETOH	0	0	127.8	3.4	42	12.3	0	18.4	18.4	0	154.9	45.5	0
PROPANAL	0	0	32.4	0	262.1	233.5	0	235.8	235.8	0	58.8	262.1	0
PROPDIAL	0	0	15	0	0	0	0	0.6	0.6	0	14.4	0	0
GUAIACOL	0	0	6399.6	6.3	17.2	3.8	0	246.1	246.1	0	6177.1	23.5	0
COUMARYL	0	0	202.3	0	0	0	0	7.6	7.6	0	194.7	0	0
PHENOL	0	0	2895.3	9.4	2.5	1.9	0	111.6	111.6	0	2795.6	11.9	0
FE2MACR	0	0	3637	0	0	0	0	137.2	137.2	0	3499.8	0	0
HMF	0	0	2299.2	0	0	0	0	86.8	86.8	0	2212.4	0	0
FURFURAL	0	0	1476.3	5.5	34.1	9.3	0	66.1	66.1	0	1449.8	39.6	0
LVG	0	0	2558	0	0	0	0	96.5	96.5	0	2461.5	0	0
XYL	0	0	13.2	0	0	0	0	0.5	0.5	0	12.7	0	0
H2O	564.8	564.8	14661.1	740.4	12.3	140	0	716.3	716.3	0	14697.5	752.7	1250
CO2	2920.3	2920.3	0.7	0	198.6	198.2	0	198.3	198.3	0	1	198.6	0
CO	28.8	28.8	0	0	1.1	1.1	0	1.1	1.1	0	0	1.1	0
CH4	0	0	0	0	9.6	9.6	0	9.6	9.6	0	0	9.6	0
C2H4	0	0	0	0	13.6	13.6	0	13.6	13.6	0	0	13.6	0
H2	0.3	0.3	0	0	0	0	0	0	0	0	0	0	0
NO	1	1	0	0	0	0	0	0	0	0	0	0	0
CELLULOS	0	0	0.4	0	0	0	1.5	0	1.5	1176.2	0.4	0	0
CELLA	0	0	1.9	0	0	0	6.6	0.1	6.7	0	1.8	0	0
HCE	0	0	0.1	0	0	0	0.3	0	0.3	462.7	0.1	0	0
HCEA1	0	0	0.1	0	0	0	0.3	0	0.3	0	0.1	0	0
HCEA2	0	0	0.2	0	0	0	0.6	0	0.6	0	0.2	0	0
LIG-C	0	0	0.1	0	0	0	0.2	0	0.2	18.8	0.1	0	0
LIG-O	0	0	0.2	0	0	0	0.8	0	0.8	476.6	0.2	0	0
LIG-H	0	0	0.1	0	0	0	0.5	0	0.5	246.2	0.1	0	0
LIG-CC	0	0	0.3	0	0	0	0.9	0	0.9	0	0.2	0	0
LIG-OH	0	0	3.5	0	0	0	12.4	0.1	12.6	0	3.4	0	0
LIG	0	0	0	0	0	0	0.1	0	0.1	0	0	0	0
C	0	0	95.1	0.2	0	0	340	3.6	343.6	0	91.7	0.2	0
G{CO2}	0	0	33.3	0.1	0	0	119.1	1.3	120.3	0	32.1	0.1	0
G{CO}	0	0	2.5	0	0	0	9	0.1	9.1	0	2.4	0	0
G{COH2}	0	0	9.2	0	0	0	33	0.3	33.3	0	8.9	0	0
DRYBIO	0	0	0	0	0	0	0	0	0	0	0	0	2500
ASH	0	0	1.4	0	0	0	29.9	0.1	30	30	1.3	0	0